

The Mucosal Barrier in Chronic Rhinosinusitis



JAE VIKTOR MURPHY

MBBS

Submitted for the degree of Doctor of Philosophy

Adelaide Medical School, Discipline of Surgical Specialties

Faculty of Health and Medical Sciences, The University of Adelaide

August, 2018

Table of Contents

TABLE OF CONTENTS	I
ABSTRACT	IV
DECLARATION	V
ACKNOWLEDGEMENTS	VI
PUBLICATIONS ARISING FROM THIS THESIS	VIII
PRESENTATIONS ARISING FROM THIS THESIS	IX
ABBREVIATIONS USED IN THIS THESIS	X
LIST OF TABLES	XII
LIST OF FIGURES	XIII
CHRONIC RHINOSINUSITIS	1
DEFINITION.....	1
EPIDEMIOLOGY	2
PATHOGENESIS	3
Impaired innate immunity.....	4
Dysregulated adaptive immune response	7
Fungal hypothesis	9
Staphylococcal enterotoxins/superantigens	10
Sinonasal microbiome	11
Microbial biofilms	12
MUCOSAL EPITHELIAL BARRIER	16
STRUCTURE AND FUNCTION OF THE INTERCELLULAR JUNCTION COMPLEXES	16
Tight Junctions	17
Adherens Junctions.....	23
Gap Junctions	25
Desmosomes.....	26
ASSESSMENT OF INTERCELLULAR JUNCTION COMPLEXES.....	27
Transepithelial electrical resistance.....	28
Macromolecular permeability	29
Fluorescence microscopy	29
Electron microscopy	30
MUCOSAL BARRIER IN SINONASAL HEALTH AND DISEASE	30
Tight and adherens junctions in sinonasal health and disease	30
Gap junctions in sinonasal health and disease	37
Desmosomes in sinonasal health and disease	40
GASTROINTESTINAL BARRIER FUNCTION AS A PARADIGM	42
Inflammatory bowel disease	42
Enteric bacteria and their extracellular products.....	45
Zinc and barrier function	50

DERMATOLOGICAL BARRIER FUNCTION AS A PARADIGM.....	54
Epidermal bacteria and their extracellular products	54
Inflammatory skin disorders.....	56
PULMONARY BARRIER DYSFUNCTION AS A PARADIGM	59
Bacterial factors altering the lower airway barrier	59
Zinc and the lower airway barrier	62
POTENTIAL MEDIATORS OF MUCOSAL BARRIER DISRUPTION IN CHRONIC RHINOSINUSITIS.....	64
INFLAMMATORY MEDIATORS.....	64
MICROBIAL MEDIATED SINONASAL BARRIER DYSFUNCTION.....	67
STAPHYLOCOCCUS AUREUS TOXINS AND VIRULENCE FACTORS	69
Hemolysins, and cytolysins.....	69
Leukotoxins and Gamma-hemolysin.....	73
Extracellular proteases	75
Staphylococcal enterotoxins/superantigens	79
S. aureus membrane associated products	80
ZINC IN CHRONIC RHINOSINUSITIS.....	82
THESIS	85
IN VITRO CHARACTERISTICS OF AN AIRWAY BARRIER DISRUPTING FACTOR SECRETED BY STAPHYLOCOCCUS AUREUS	87
STATEMENT OF AUTHORSHIP	87
CITATION	89
ABSTRACT	89
INTRODUCTION	91
METHODS	93
RESULTS.....	100
DISCUSSION	107
ACKNOWLEDGEMENTS	111
SUPPLEMENTARY INFORMATION	112
STAPHYLOCOCCUS AUREUS V8 PROTEASE DISRUPTS THE INTEGRITY OF THE AIRWAY EPITHELIAL BARRIER AND IMPAIRS IL-6 PRODUCTION IN-VITRO	120
STATEMENT OF AUTHORSHIP	120
CITATION	122
ABSTRACT	122
INTRODUCTION	124
METHODS	126
RESULTS.....	132
DISCUSSION	140
ACKNOWLEDGEMENTS	143
SUPPLEMENTARY INFORMATION	144

MUCOSAL ZINC DEFICIENCY IN CHRONIC RHINOSINUSITIS WITH NASAL POLYPOSIS CONTRIBUTES TO BARRIER DISRUPTION AND DECREASES ZO-1.....	145
STATEMENT OF AUTHORSHIP	145
CITATION	147
ABSTRACT	147
INTRODUCTION	149
METHODS	151
RESULTS	158
DISCUSSION	167
ACKNOWLEDGEMENTS	169
SUPPLEMENTARY INFORMATION	170
LETTER TO THE EDITOR.....	173
THESIS SYNOPSIS	177
REFERENCES.....	185

Abstract

Chronic rhinosinusitis (CRS) is a heterogeneous disease characterised by inflammation of the nose and paranasal sinuses, which results in nasal obstruction, rhinorrhoea, post-nasal drip, facial pressure, and alterations in smell. The pathophysiology of CRS is complex and involved interactions between the host, microbial flora, and environment. Studies have shown that the mucosa of CRS sufferers demonstrates signs of defective barrier function, although little is known about the contributing factors to this process. Understanding epithelial barrier dysfunction in the gastrointestinal, skin, and pulmonary systems highlights the various contributing factors to this process, which may be paralleled in the paranasal sinuses. It appears that bacterial mediated mechanism, inflammatory surroundings, and the divalent metal zinc are important in these systems. *Staphylococcus aureus* has been implicated in the pathogenesis and persistence of CRS, poorer wound healing, and increased disease severity. Additionally, it is known that *S. aureus* secretes an unknown factor that perturbs the airway barrier *in-vitro*. Previous research has suggested that zinc concentrations may be lower in CRS, particularly in patients with nasal polyposis, however little is known about the consequences of localised zinc deficiency in CRS.

This thesis examines the *S. aureus* secretome to elucidate the factor or factors involved in barrier disruption. Furthermore, the role of zinc in mucosal barrier integrity and CRS has been delineated.

Declaration

I certify that this work contains no material which has been accepted for the award of any other degree or diploma in my name, in any university or other tertiary institution and, to the best of my knowledge and belief, contains no material previously published or written by another person, except where due reference has been made in the text. In addition, I certify that no part of this work will, in the future, be used in a submission in my name, for any other degree or diploma in any university or other tertiary institution without the prior approval of the University of Adelaide and where applicable, any partner institution responsible for the joint-award of this degree.

I acknowledge that copyright of published works contained within this thesis resides with the copyright holder(s) of those works.

I also give permission for the digital version of my thesis to be made available on the web, via the University's digital research repository, the Library Search and also through web search engines, unless permission has been granted by the University to restrict access for a period of time.

I acknowledge the support I have received for my research through the provision of an Australian Government Research Training Program Scholarship.

Jae Viktor Murphy

Acknowledgements

Those who have pursued a doctoral thesis will understand that it can be trying at times, and is rarely a companionless journey.

To my principal supervisor Professor Peter-John Wormald, thank you for accepting me on as a student despite my juniority. Prof's passion for research and improving the lives of patients is exceptional, and those fortunate enough to have worked under his leadership will know how contagious this enthusiasm is. I would also like to thank my co-supervisors Associate Professor Alkis Psaltis and Associate Professor Sarah Vreugde. Alkis has been a wonderful mentor to me throughout the thesis, and his support, honesty, and advice has allowed me to develop both as a researcher and surgeon. Sarah has been vital to the development of my scientific process and helped direct my constant stream of (usually obscure) ideas. Her dedication to science is inspirational, which encourages those around to achieve more.

To the Garnett Passe and Rodney Williams Memorial Foundation and The Hospital Research Foundation for their financial support. This research endeavor would not have been possible without their backing.

I would particularly like to acknowledge Amanda Drilling for all her help and expertise in navigating the lab, and teaching me the absolute basics in good laboratory practice. Amanda mentored my early years in the lab and was always available to give advice. To the ENT scientists Mahnaz Ramezanzpour, Clare Cooksley, Jonathan McGuane, Eugene Roscioli, and Catherine Bennet for their support in the lab and institute.

To the previous surgeon scientists Vikram Padhye, Josh Jarvis-Bardy, Rowan Valentine, and Camille Jardeleza for being exceptional role models and advising me on balancing the dichotomy of training and research. To my friends and colleagues who have shared the peaks and valleys of my PhD, Ahmed Bassiouni, Dijana Miljkovic, Chun Chan, Mian Ooi, Alistair Jukes, Luis Macias, Judy Ou, Sakiko Oue, Daniel Cantero, Stephanie Fong, Rachel Goggin, Sathish Paramasivan, Giri Krishnan, Steven Kao, Zacki Malik, Hilary Dorward, Katharina Richter, Neil Tan, Aaron Rayan, Jake Jarvis-Bardy, Michael Gouzos, Masanobu Suzuki, David Morrissey, Annika Mascarenhas, Irene Frazier, and Lyn Martin.

To my close friends external to the lab and ENT department George Evans, Matthew Roberts, Cheryl Chooi, Rebecca Holst, Bobak Bahrami, and Christian Connolly for their friendship and understanding during my PhD.

I would also like to acknowledge my co-contributors to this research Grzegorz Dubin and Natalia Stach from the Jagiellonian University in Poland for their expert advice and providing several *S. aureus* products.

To my family, my parents Gerald and Vikki Murphy, my sister and brother-in-law Marlee and Jacob Bennett, and to my incredible nephew Addison Jae Bennett. You have provided me with encouragement and reassurance over the years to achieve this goal, which I am sure has not been easy at times. Lastly, to my partner Nikki Burdett whose love and laughter have kept me pushing through the thesis. Her unconditional support and patience has been essential for this undertaking.

Publications arising from this thesis

Murphy J, Ramezanpour M, Stach N, Dubin G, Psaltis AJ, Wormald PJ, Vreugde S. *Staphylococcus aureus* V8 protease disrupts the integrity of the airway epithelial barrier and impairs IL-6 production *in-vitro*. *Laryngoscope*. 2018;128(1):E8-E15. doi:10.1002/lary.26949

Murphy J, Ramezanpour M, Roscioli E, Psaltis A.J, Wormald P.J, Vreugde S. Mucosal Zinc Deficiency in Chronic Rhinosinusitis with Nasal Polyposis Contributes to Barrier Disruption and Decreases ZO-1. *Allergy*. 2018;73(10):2095-2097. doi:10.1111/all.13532

Murphy J, Ramezanpour M, Drilling A, Roscioli E, Psaltis A.J, Wormald P.J, Vreugde S. In vitro characteristics of an airway barrier disrupting factor secreted by *Staphylococcus aureus*. *Int Forum Allergy Rhinol*. Accepted for publication on the 9th October 2018. doi:10.1002/alr.22232

Presentations arising from this thesis

The Mucosal Barrier in Chronic Rhinosinusitis. Basil Hetzel Institute Post Graduate Seminar, Adelaide Australia, August 2014

The Mucosal Barrier in Chronic Rhinosinusitis. Basil Hetzel Institute Post Graduate Seminar, Adelaide Australia, September 2015.

Discovering the *Staphylococcus aureus* product responsible for disruption of the tight junction barrier in sinonasal epithelium. The Queen Elizabeth Hospital Research Day, Adelaide Australia, October 2015.

The Mucosal Barrier in Chronic Rhinosinusitis: progress update. Basil Hetzel Institute Post Graduate Seminar, Adelaide Australia, May 2016.

Discovering the *Staphylococcus aureus* factor responsible for barrier disruption. RACS SA, NT, & WA Annual Scientific Meeting, Adelaide Australia, August 2016.

Discovering the *Staphylococcus aureus* factor responsible for airway barrier disruption. ASOHNS SA Annual Registrar's Presentation Meeting, Adelaide Australia, November 2016.

Mucosal Zinc Deficiency in Chronic Rhinosinusitis. Basil Hetzel Institute Post Graduate Seminar, Adelaide Australia, August 2017.

Mucosal Zinc Deficiency in Chronic Rhinosinusitis. ASOHNS SA Annual Registrar Presentation Meeting, Adelaide Australia, October 2017.

Mucosal Zinc Deficiency in Chronic Rhinosinusitis with Nasal Polyposis Contributes to Barrier Disruption and Decreases ZO-1. American Rhinologic Society Annual Meeting, Atlanta USA, October 2018.

Abbreviations used in this thesis

ABRS	Acute bacterial rhinosinusitis	EPOS	European Position Paper on
AD	Atopic dermatitis		Rhinosinusitis and Nasal
ADAM10	Disintegrin and		Polyps
	metalloproteinase domain-	ESS	Endoscopic sinus surgery
	containing protein 10	ETA	Exfoliative toxin A
AFRS	Allergic fungal rhinosinusitis	EV	Extracellular vesicle
Agr	Accessory gene regulator	FISH	Fluorescent in situ
AJ	Adherens junction		hybridization
ALI	Air-liquid interface	FITC	Fluorescein isothiocyanate
ATCC	American type culture	FnBP	Fibronectin binding protein
	collection	GUK	Guanylate kinase
BAFF	B cell-activating factor	H ₂ O ₂	Hydrogen Peroxide
CBF	Ciliary beat frequency	HLA	Alpha (α) hemolysin
CSLM	Confocal scanning laser	HLB	Beta (β) hemolysin
	microscopy	Hlg	Gamma (γ) hemolysin
CRS	Chronic rhinosinusitis	HNEC	Human nasal epithelial cell
CRSsNP	Chronic rhinosinusitis without	IBD	Inflammatory bowel disease
	nasal polyps	Ig	Immunoglobulin
CRSwNP	Chronic rhinosinusitis with	JAM	Junctional adhesion molecule
	nasal polyps	IBD	Inflammatory bowel disease
CT	Computerised tomography	ILC2	Type 2 innate lymphoid cells
DSS	Dextran sodium sulphate	LPS	Lipopolysaccharide
ECP	Eosinophil cationic protein	LTA	Lipoteichoic acid
eDNA	extracellular DNA		

MAPK	Mitogen associated protein kinase	SP-A	Surfactant protein-A
MLCK	Myosin light chain kinase	TEER	Transepithelial electrical resistance
MRSA	Methicillin-resistant <i>Staphylococcus aureus</i>	TJ	Tight junction
MT	Metallothionein	TLR	Toll-like receptor
PAMPs	Pathogen-associated molecular patterns	TMA	Tissue micro-array
Papp	Apparent permeability	UC	Ultracentrifuged
PAR	Protease activated receptor	UF	Ultrafiltered
PI3K	Phosphoinositide 3-kinase	VE-cadherin	Vascular-endothelial cadherin
PKC	Protein kinase C	ZD	Zinc deplete
PRRs	Pattern recognition receptors	ZIP	Zrt-, Irt-related proteins
qPCR	Quantitative real-time polymerase chain reaction	ZnT	Zinc transporter
RARS	Recurrent acute rhinosinusitis	ZO	Zonula occludens
RFU	Relative fluorescent units		
ROI	Region of interest		
ROS	Reactive oxygen species		
RPM	Revolutions per minute		
ScpA	Staphopain A		
SspB	Staphopain B		
SEA	Staphylococcal superantigen A		
SEB	Staphylococcal superantigen B		
SNP	Single nucleotide polymorphism		

List of Tables

Table 1. Tight junction, Adherens junction, and Desmosome literature summary in Chronic Rhinosinusitis	35
Table 2. Summary of TJ, AJ, and desmosome immunohistochemistry in CRS.....	36
Table 3. Summary of factors products with gastrointestinal mucosal barrier disrupting properties.	53
Table 4. Summary of factors with epidermal barrier disrupting properties.	59
Table 5. Summary of factors with pulmonary barrier altering properties.....	63
Table 6. Summary of inflammatory mediators implicated in airway barrier disruption.....	66
Table 7. ELISA of human IL-6 after exposure to V8 protease.....	138
Table 8. HNEC-ALI cytotoxicity assay.....	139
Table 9. Patient demographics for sinus tissue samples for immunofluorescence and gene expression.	158

Supplemental Tables

Supplemental Table S1. UF-CM 13565 Stationary phase supernatant mascot protein identification with liquid chromatography – electrospray ionization tandem mass spectrometry.	115
Supplemental Table S2. Correlation between zinc transporter gene expression.	170

List of Figures

Figure 1. Schematic diagram of the intercellular junction.	16
Figure 2. Transepithelial electrical resistance (TEER) and paracellular permeability (Papp) are unaffected by Staphylococcal Enterotoxin A (SEA), Alpha Hemolysin (HLA), and Lipoteichoic acid (LTA).....	101
Figure 3. Impact of ultrafiltered conditioned media (UF-CM) derived from different <i>Staphylococcus aureus</i> strains and bacterial growth phases on transepithelial electrical resistance (TEER) and paracellular permeability (Papp).....	102
Figure 4. Impact of heat and proteinase K treatment on barrier disrupting effect of <i>Staphylococcus aureus</i> ultrafiltered conditioned media (UF-CM).....	103
Figure 5. The <i>Staphylococcus aureus</i> barrier disrupting factor is localised to the >30kDa exoproteome fraction.	104
Figure 6. The ultracentrifugated (UC) fraction isolated from the <i>Staphylococcus aureus</i> conditioned media contains the barrier disrupting factor.....	105
Figure 7. Tight junction protein ZO-1 is disrupted by ATCC 13565 ultrafiltered conditioned media (UF-CM) and ultracentrifugated (UC) fraction.	106
Figure 8. V8 protease activity comparison to <i>S. aureus</i> supernatants.	132
Figure 9. V8 protease disrupts the pore pathway of the epithelial barrier with decreases in TEER.	133
Figure 10. V8 protease disruption of the epithelial barrier is time dependent.	134
Figure 11. V8 protease perturbs the leak pathway by increasing macromolecular permeability (Papp).	135
Figure 12. Tight junction proteins Claudin-1 and ZO-1 were discontinuous in V8 exposed cells.	136
Figure 13. Effects of V8 protease on IL-6 production from HNEC-ALI cultures.....	137
Figure 14. MT1a, MT2a, ZIP1, ZIP2, and ZIP14 are downregulated in CRSsNP, while ZnT1 is upregulated. MT3 is downregulated in CRSwNP.	160
Figure 15. Quantification of labile Zn ²⁺ and ZO-1 in the sinonasal epithelium of control, CRSsNP, and CRSwNP patients.	162

Figure 16. Labile Zn ²⁺ and ZO-1 are reduced in sinonasal epithelium of Chronic Rhinosinusitis patients.....	163
Figure 17. Zinc depletion decreased barrier function of human nasal epithelial cell cultures.....	165
Figure 18. Zinc deficiency causes alterations to tight junction ZO-1 localisation and reduction in intracellular labile zinc.....	166

Supplemental Figures

Supplemental Figure S1. Sodium dodecyl sulphate polyacrylamide gel electrophoresis (SDS-PAGE) of <i>S. aureus</i> conditioned media (CM) and ultrafiltered (UF) CM at different growth phases.	118
Supplemental Figure S2. Bacterial growth curve of ATCC strains I3565 and 25923.....	118
Supplemental Figure S3. Lactate dehydrogenase (LDH) assay.....	119
Supplemental Figure S4. HNEC-ALI cultures treated with V8 protease at 10 µg/ml or PBS control for 12 hours (A), and for 24 hours (B).....	144
Supplemental Figure S5. Labile Zn ²⁺ and ZO-1 were quantified in tissue microarray sections.	171
Supplemental Figure S6. Serum zinc concentrations in controls, CRSsNP, and CRSwNP show that systemic zinc is not depleted.	172
Supplemental Figure S7. HNEC-ALI IL-6, IL-8, IL-10, and TNF-α cytokine production show increasing trends with cumulative days in cultured zinc deplete media.	172

Chronic Rhinosinusitis

Definition

The term rhinosinusitis defines a broad group of disorders all characterized by inflammation of the nose and paranasal sinuses. The International Rhinologic Society's European Position Paper on Rhinosinusitis and Nasal Polyps (EPOS) defines rhinosinusitis in adults as inflammation of the nose and paranasal sinuses characterized by two or more symptoms of nasal obstruction, rhinorrhoea, post nasal drip, facial pressure, or loss of smell. This must be accompanied by nasal endoscopic signs of oedema, nasal polyps, and mucopurulent discharge or computerised tomography (CT) scan evidence of sinus mucosa inflammation.¹

Acute rhinosinusitis disorders have a duration of less than 12 weeks and includes common cold/acute viral rhinosinusitis, acute post-viral rhinosinusitis, and acute bacterial rhinosinusitis (ABRS). Chronic rhinosinusitis (CRS) has duration of more than or equal to 12 weeks, and diagnosis can be subdivided into patients without nasal polyposis (CRSsNP) and with nasal polyposis (CRSwNP).¹

Other sub-classifications exist to define different presentations such as aspirin exacerbated respiratory disease (AERD), allergic fungal rhinosinusitis (AFRS), recurrent acute rhinosinusitis (RARS) and recalcitrant CRS (rCRS).^{1,2} There has been recent interest in further inclusion of the underlying pathogenic mechanism as a method of classifying patient endotypes.³ Examples of novel CRS endotypes are:

- Response to treatment (responsive or resistant to: corticosteroids, antibiotics, or newer agents such as anti-IL-5 or anti-IgE)
- Unique inflammatory profiles of nasal polyps
- Presence of circulating biomarkers (blood eosinophils, specific IgE)

The further understanding of CRS and its pathogenesis will contribute to the differentiation of currently used and emerging subtypes, and their applications both clinically and in research.

Epidemiology

There is considerable variation in the prevalence of CRS and its sub-classifications reported in the literature. This is likely an outcome of various methodologies in data collection, difficulties in diagnosis, and nomenclature. The most recent data on the prevalence of CRS in Australia estimates that 1.9 million or 8.7% of the population are affected. This was based on self-reported surveys by the Australian Bureau of Statistics conducted in 2011-12.⁴ The Australian Institute of Health and Welfare has found that sinusitis accounts for 1.4% of all general practitioner encounters, and is listed as among the most frequently managed problems.⁵ In a study of 313 participants conducted in Melbourne, Australia, the rate of self-reported doctor-diagnosed CRS was 10.9%, however symptom criteria based diagnosis only estimated a 2.9% prevalence.⁶

Internationally similar estimates have been reported. The GA²LEN European study collected 57,128 questionnaires across 12 countries, with questions derived from the clinical criteria within EPOS. This identified a self-reported CRS prevalence of 10.9% (range 6.9-27.1%) and a self-reported doctor-diagnosed CRS prevalence of 5% (range 1.1-18.1%).⁷ Given this available data and the inherent problems in diagnosis of CRS the prevalence lies between 2.9–10.9%.

The reliable differentiation between CRSsNP and CRSwNP is only possible with nasal endoscopy, however the task of performing this on a population scale is difficult. Questionnaire based tools have been developed to facilitate this on a large scale at a

lower cost, although these questionnaires rely on a known presence of nasal polyposis to the patient or previous sinus surgery.^{8,9} The incidence of nasal polyposis seen on nasal endoscopy in the general population is between 2.53-2.7%.^{10,11} The proportion of CRS patients with CRSwNP is reported to be 24-36%.^{12,13}

As a chronic disease CRS is associated with significant economic burden, in both direct and indirect costs. The cost of CRS has not been estimated in Australia, however data from North America emphasizes key issues. The most recent estimates of overall direct costs of CRS management were \$9.9 billion USD per annum (adjusted USD, 2014) in the USA.¹⁴ While the indirect costs are an estimated \$12.8 billion USD per annum, which is a result of productivity loss (number of missed work days).¹⁵ The annual direct medical costs per patient with CRS is \$5,560 to \$5,955, while for a non-CRS patient is \$4,743-\$5,008.¹⁶ The indirect costs per person per annum associated with refractory CRS are greater than other chronic diseases such as asthma or diabetes, with an estimated cost of \$8,150 to \$10,077.¹⁵

Pathogenesis

Basic science research in the field of CRS highlights the difficulties in understanding the pathogenesis of this group of disorders. As previously mentioned CRS can be classified as with or without polyps, however within these groups remains significant heterogeneity. This heterogeneity is thought to be due to the complex relationships between the host, microbes, and environmental triggers. Current etiological descriptions include, but are not limited to the impaired innate immunity, dysregulated adaptive immune responses, fungal hypothesis, *Staphylococcus aureus* (*S. aureus*) and superantigen hypothesis, sinonasal microbiome, and microbial biofilms.

Impaired innate immunity

The mucosal barrier and innate immune system of the sinonasal cavity provide the initial interface for interaction between host, environment and microbial organisms. The mucosal barrier defenses include the physical barrier produced by intact sinonasal mucosa, mucociliary clearance, and also secreted antimicrobial products. Beyond the mucosa there is potential for activation of inflammatory cells (neutrophils, macrophages, lymphocytes, eosinophils) along with other cells within the epithelial layers such as dendritic cells, fibroblasts, and innate lymphoid cells.¹⁷

The sinonasal mucosa forms the cellular barrier to incoming pathogens, particles, and allergens. Each cell is in contact with its neighboring cells and bound by intercellular junction complexes, which include tight junction, adherens junction, gap junction and desmosome proteins.¹⁸ Recent interest in this innate barrier has highlighted its potential importance in CRS, with evidence that pathogens can alter barrier integrity and also recognizing the underlying barrier defects in CRS.^{19,20} The subject of epithelial barrier dysfunction is elaborated on below.

Cilia within the sinonasal cavity beat in a coordinated manner to clear overlying mucus, which has trapped particulate matter and pathogens. The mucus layer is composed of a viscous superficial layer “gel phase” and a deeper layer “sol phase” which is mostly water and electrolytes.²¹ Mucus is then propelled to the nasopharynx and swallowed. Several abnormalities of this mechanism have been recognised within CRS. Initial *in-vitro* studies showed that ciliary activity was markedly diminished in the presence of *Haemophilus influenzae* (*H. influenzae*) and *Staphylococcus epidermidis* (*S. epidermidis*) caused loss of coordinated ciliary motion.²² *S. aureus* hemolysin alpha toxin (HLA) can completely abolish ciliary beat within 12 hours of exposure to nasal epithelial cells.²³

Staphylococcal superantigen A (SEA) decreases ciliary beat frequency (CBF) when instilled in rabbit paranasal sinuses, however it also results in rhinosinusitis.²⁴ It is possible that the effects on CBF are due to the inflammatory mediators present rather than SEA itself. Chen et al., (2006) found that CRS patients have a blunted CBF response to external stimuli, and the authors suggested that chronic inflammation within the sinuses leads to down-regulation of receptors that regulate CBF response.²⁵ Interestingly, *ex-vivo* experimentation has shown that once CRS mucosa is removed from the inflammatory environment then the blunted response can be reversed within 12–36 hours.²⁶

Potential threats are recognised by pattern recognition receptors (PRRs), which identify conserved pathogen-associated molecular patterns (PAMPs).¹⁷ The most widely studied PRRs are Toll-like receptors (TLRs), however there is recent interest in novel receptors such as retinoic acid-inducible-like receptors, nucleotide and oligomerization domain-like receptors, protease activated receptors (PARs), and taste receptors.^{17,18} TLRs are transmembrane glycoproteins with extracellular and intracellular domains. Recognition of a PAMP to its reciprocal TLR results in downstream activation of inflammatory processes.¹⁸ TLR expression in CRS is differentially represented. CRSsNP mucosa shows a reduction in TLR4, TLR7, and their downstream protein MyD88, while CRSwNP mucosa shows upregulation of TLR2, TLR4, TLR7, and an increase in IL-4 within nasal polyp tissue.²⁷ Additionally, PAR2 is upregulated in ARS and CRS, which is activated by local serine proteases such as those produced by bacterial and fungal organisms.²⁸ Activation of PAR2 leads to IL-8 and GRO- α chemokine production via NF- κ B signalling.²⁸ Sweet (T1R) and bitter taste (T2R) receptors in relation to CRS have been the focus of recent investigation. It is hypothesised that these taste receptors regulate antimicrobial peptide secretion into nasal mucus. During infection mucosal glucose is

consumed, which then switches on the bitter taste receptor to mount a response against the pathogen.²⁹ A bitter taste receptor polymorphism T2R38 has been recognized as an independent risk factor for failing medical therapy for CRS.³⁰

Type 2 innate lymphoid cells (ILC2) are considered to be particularly important in the inflammatory response in CRSwNP. ILC2 cells have been shown to produce IL-5, IL-9, and IL-13 in the initiation of Th2 type inflammation, and may support switch from a Th1 to Th2 inflammatory environment.³¹ ILC2 are stimulated by IL-25 and IL-33 expression, which are upregulated during activation of PRR.³² Miljkovic et al., (2014) found that ILC2 numbers are significantly increased in nasal polyp tissue from CRSwNP patients, and a positive association with allergy positive patients.³³ They also confirmed that IL-5 and IL-13 were upregulated in CRSwNP patients compared to either CRSsNP or control patients.³³ Furthermore, it has been shown that ILC2s are associated with increased tissue eosinophilia and absence of neutrophilic infiltrate regardless of CRS phenotype.³⁴

Host secreted antimicrobial molecules have been implicated in CRS from several mechanistic classes such as collectins, binding proteins, enzymes, opsonins, and permeabilizing proteins.¹ Surfactant protein-A (SP-A) is a collectin secreted protein found in the upper and lower airways.³⁵ SP-A acts as a mobile PRR and binds to viruses, bacteria and fungi within the airways for immune mediated recognition, however they also regulate local immune activation and support surfactant structures and metabolism.³⁶ SP-A mRNA and protein are both significantly upregulated in CRS patients, however it is not known if this is a local response to inflammation or contributing to a defective innate immunity.³⁵ More recently Uhliarova, et al., (2016) identified that SP-A is augmented in nasal lavage fluid from CRSsNP patients, but not from controls or CRSwNP.³⁷ The increase in SP-A was associated with more severe disease and positive culture of a pathogen.³⁷ Lactoferrin is a binding protein present in

upper airways and is one of the most abundant in sputum.³⁸ CRS patients, in particular those with nasal polyps exhibit reduced mRNA expression and protein production of lactoferrin.³⁹ Other antimicrobial product abnormalities in CRS include higher complement factors C3a and C5a, reduced SPLUNC1 and LPLUNC2 in CRSwNP, increased cathelicidin (LL-37) in eosinophilic CRS, and elevated antimicrobial lipids.⁴⁰⁻⁴³

Dysregulated adaptive immune response

The adaptive immune response is also believed to contribute to the inflammation seen in CRS, with observed abnormalities in T cell representation, naive B cells, plasma cells, and altered immunoglobulin activity.

Research has shown that the total number of T cells are increased in CRSwNP and a larger percentage of Th2 cells, which have a propensity to produce IL-4 and IL-5 cytokines.⁴⁴ This may be partly explained as a downstream consequence of the upregulated innate ILC2 in CRSwNP.³³ Conversely, CRSsNP is associated with a Th1 type polarization, and subsequent high IFN- γ and TGF- β expression.⁴⁵ A flow cytometry study by Miljkovic et al., (2016) identified that Treg and Th17 cells were locally enriched in nasal polyps from CRSwNP patients.⁴⁶ It is known that Treg cells are capable of suppressing the Th1 pathway, and Th17 cells are associated with IL-17 production.^{47,48} Miljkovic and colleagues hypothesized that these two cells are a major driving force in polyp formation.⁴⁶

B cells and their effector functions have been implicated in sinus inflammation. Van Zele et al., (2007) compared the concentrations of immunoglobulin classes in serum and tissue homogenate from CRS and control patients.⁴⁹ This study found that IgE, IgA, and IgG are significantly elevated in nasal polyp tissue, however this was a local tissue finding

with no evidence of elevation in serum. All subclasses of tissue homogenate IgG (IgG1, IgG2, IgG3, IgG4) were increased compared to controls. Interestingly, the percentage of subclass IgG4 was positively associated with total IgE concentrations and specific IgE antibodies to *staphylococcal* enterotoxin.⁴⁹ IgG4 has been associated with several inflammatory and autoimmune diseases, and Th2 cytokines are thought to promote its production.⁵⁰ The exact role of IgG4 in disease modification is still unclear as to whether it acts as a protective response to limit inflammation or is involved in the pathogenesis.⁵⁰ A previous study showed that B cell-activating factor (BAFF) protein and mRNA expression are significantly upregulated in CRSwNP when compared to control and CRSsNP patients.⁵¹ This was observed in polyp tissue, however all CRSsNP comparison tissue was harvested from inferior turbinate mucosa and is likely not representative of the underlying disease process. Nasal lavage showed detectable BAFF in 5 of the 12 CRSwNP patients, which highlights a subset of patients that are capable of BAFF secretion and possibly more local B cell expansion and activation.⁵¹ Other studies have identified increased B cell recruiting chemokines and autoantibodies (anti-dsDNA IgG and IgA) in CRSwNP.^{52,53}

More recently, Yoon et al., (2014) confirmed that BAFF and a proliferation inducing ligand (APRIL) were both increased in the subepithelial layer of non-eosinophilic and eosinophilic polyps.⁵⁴ They also identified correlations in CRSwNP between BAFF, IgA production and B cells using a CD20 marker. BAFF positive cells are co-localized with CD11b positive cells, which includes innate inflammatory cells such as natural killer cells, monocytes, granulocytes, and macrophages.⁵⁴

Psaltis et al., (2013) utilized flow cytometry techniques to identify a statistically significant increase in naive B cells, activated B cells, and memory B cells in both atopic and nonatopic CRSwNP patients when compared against controls.⁵⁵ Additionally,

CRSsNP patients showed an increase in naive B cells, and the atopic CRSwNP patients were the only group to have mucosal plasma cells.⁵⁵ The presence of B cells at all stages of maturation supports the hypothesis that local B cell expansion is occurring in CRS, more so in CRSwNP. The etiology of this is still unknown, although it could be a result of microbial factors or downstream to another dysregulated immune response. Miljkovic et al., (2017) identified that TLR CD180 expression is increased in CRSwNP mucosa, with a reciprocal paucity of CD180 on circulating B cells.⁵⁶ CD180 is a TLR homolog and negatively regulates the binding of microbial ligands and endotoxins to TLR4.⁵⁷ The increase of CD180 in CRSwNP is a potential contributor to the abnormal or dysregulated response against pathogens.

Recent work by Lau et al., (2016) has identified that mucosal tertiary lymphoid organs (TLOs) are formed in patients with CRSwNP.⁵⁸ TLOs are immune cell aggregates that are formed *de novo* in non-lymphoid tissue into a highly organized structure containing follicular dendritic cells, B cells, and surrounded by high endothelial venules.⁵⁹ TLOs form in response to chronic inflammation and are thought to be involved in maintaining balance between the mucosal immune system and commensal organisms.⁵⁹ This novel finding gives further insight into the ongoing inflammation seen in CRSwNP, as once TLOs are formed they will continue to generate an adaptive immune response, at least until the antigen trigger is eliminated.

Fungal hypothesis

The sentinel paper that hypothesized the relationship between CRS and fungus found a high prevalence (>90%) of positive fungal cultures in new cases of CRS, and presence of eosinophilic mucin. It was thought that most CRS presentations may actually be AFRS, and were previously underdiagnosed due to culture technique limitations. Based on

these findings they considered the majority of inflammation in CRS patients to be driven by eosinophilic inflammation aimed at the extramucosal fungal elements.⁶⁰ This was supported by the heavy presence of eosinophils and the eosinophilic toxin (major basic protein) found in CRS mucus.⁶¹ Although, follow up studies failed to show similar culture results achieving only 49% positive fungal cultures compared to positive bacterial cultures in 88% of cases.⁶² In 2003, an European paper utilized newer culture techniques and identified a similar prevalence of fungus in CRS to the initial study, however this was also seen in healthy controls.⁶³ Unfortunately the current literature does not show a positive response to topical or systemic anti-fungal therapy for CRS.^{64,65} Despite this, the evidence suggests that fungus may be important as a disease modifier. *In-vitro* exposure of peripheral blood lymphocytes to fungal extracts of *Aspergillus* and *Alternaria* results in modest increases in the cytokine IFN- γ . Interestingly, when the fungal extracts are combined with staphylococcal superantigen B (SEB) there is a potent synergistic response.⁶⁶

Staphylococcal enterotoxins/superantigens

Staphylococcal superantigens (or enterotoxins) have been a focus in CRS due to their roles in disease modification of atopic dermatitis, and unstable asthma. Superantigens are able to continuously and strongly stimulate T lymphocytes by binding to MHC class II and the T cell receptor outside of the usual peptide binding groove. This in turn leads to massive local cytokine production and inflammatory cell recruitment.⁶⁷ In 2001, a study demonstrated a subset of CRSwNP patients with Staphylococcal Enterotoxin A and B specific IgE in their nasal polyp tissue.⁶⁸ Further to this, superantigens were found in 55-73% of either the mucus of CRSwNP patients or *S. aureus* strains isolated from the sinonasal cavity.^{69,70} *S. aureus* superantigens have been identified within lymphoid

follicle-like structures in nasal polyp tissue. Interestingly, these structures are associated with polyclonal B cell responses, high IgE antibody concentrations, and eosinophilic inflammation.⁷¹ IgG and IgE production is upregulated in CRSwNP patients with IgE antibodies specific for superantigens, and isotype switching from IgG2 to IgG4.⁴⁹ This is particularly noteworthy since IgG4 related diseases have been linked to Th2 phenotype responses, and increased tissue IL-4, IL-5, and IL-13.⁷²

Sinonasal microbiome

The sinonasal microbiome hypothesis has developed upon the idea that in health the native microbial flora of paranasal sinuses is in balance within the host. It is hypothesised that a triggering event (possibly viral infection, or antibiotic overuse) precipitates a shift in the microbiome causing dysbiosis and potential overgrowth of more pathogenic organisms, and then subsequent sinonasal inflammation.⁷³ This has been made possible by the use of culture independent 16s molecular techniques.⁷³ Although paranasal sinus research in this field is relatively new, it has been heavily studied in the gastrointestinal tract.⁷⁴ This led to the development of a gastrointestinal microbiome transplant, which has proven to be a particularly successful treatment for inflammatory bowel disease and associated recurrent *Clostridium difficile* (*C. difficile*) infection.⁷⁵

The studies examining the bacterial microbiome between healthy and CRS afflicted patients have suggested that factors such as an abundance of particular organisms, overall diversity, reduction in probiotic commensals, and presence of anaerobic bacteria play roles in disease inflammation and outcomes.^{73,76,77} There are a handful of fungal microbiome studies utilizing non-culture techniques. One study aimed at 36 species of fungi suggested there may be a subset of CRS patients with a susceptibility to fungal

growth. Following this, expanded techniques using 18S rDNA sequencing found a significantly decreased prevalence of *Malassezia*, an increase in fungal diversity, and dominant *Cryptococcus neoformans* in CRS.⁷⁸ Another 18S rDNA study confirmed a reduction in the abundance of *Malassezia*.⁷⁹ Currently there is no literature on the CRS virome, however recently the human virome of several body sites (nose, skin, mouth, vagina, and stool) has been described, demonstrating complexity and variation between sites.⁸⁰ Future studies may need to incorporate all aspects of microbiome to completely understand the dynamic relationship with the host, and the microbiome effects on disease.

Microbial biofilms

Microbial biofilms are highly organized structures consisting of a community of microbes encased in an extracellular matrix formed by polysaccharides, extracellular nucleic acids, and proteins. Biofilms are irreversibly attached to a surface (mucosa) and the metabolism of microbes in a biofilm state is dramatically slowed.⁸¹ All these features contribute to its ability to withstand host defenses and exogenous antibiotics, with biofilm antibiotic resistance measures ranging from 10 – 1000 fold more than planktonic bacteria.⁸² Furthermore, biofilms present a constant source of viable bacteria and bacterial extracellular products which are released from the biofilm matrix.⁸¹

Initial research identifying biofilm as a possible contributor to CRS comes from Cryer et al., (2004).⁸³ Mucosal samples from patients undergoing revision sinus surgery or office based debridement were examined with scanning electron microscopy. This small series of 16 specimen samples demonstrated structures resembling biofilm in 4 samples, and 1 of the 4 showing visible bacteria on the biofilm surface.⁸³ Even at this preliminary stage it was hypothesized that this may be the link to understanding recalcitrant CRS. Shortly

after this Sanclement et al., (2005) published a small series comparing mucosa from 4 controls and 30 CRS patients, which identified biofilm on 80% of the CRS mucosa while control mucosa remained healthy.⁸⁴ The first attempt at defining biofilm as a prognostic factor in CRS was by Bendouah et al., (2006).⁸⁵ This study cultured sinonasal bacteria from 7 CRSsNP and 12 CRSwNP patients and determined their biofilm forming capacity *in-vitro*. Patient outcomes were only deemed as favorable or unfavorable in terms of disease evolution following surgery at 12 months follow up. They concluded that poor disease evolution was associated with biofilm formation *in-vitro* for both *S. aureus* and *Pseudomonas aeruginosa* (*P. aeruginosa*).⁸⁵

Psaltis et al., (2007) conducted a prospective study comparing mucosal biofilm in CRS and control patients undergoing endoscopic sinus surgery (ESS).⁸⁶ Mucosal specimens were examined with confocal scanning laser microscopy, identifying that biofilms in CRS contained viable microbes, and demonstrated their presence in 44% of CRS patients and absence in all controls. Interestingly, there were no differences in bacterial or fungal culture rates in biofilm positive and negative patients using traditional culture techniques. This was the first study to correlate *in-vivo* biofilm positivity with more severe sinus disease by demonstrating a significant difference in CT scans using the Lund McKay scoring system.⁸⁶

Utilization of fluorescent in situ hybridization (FISH) probes allowed demonstration of fungal elements co-existing within CRS and AFRS bacterial biofilms.⁸⁷ Although this was a preliminary study, it highlighted the potential of bacterial and fungal biofilms to act symbiotically. Foreman et al., (2008) further elucidated the role of poly-microbial biofilms in CRS, confirming biofilm presence in 72% of CRS patients, with over half having two or three organisms per biofilm.⁸⁸ Fungal organisms were identified with a biofilm forming bacteria in 25% of these patients. An *in-vivo* sheep model of sinusitis

displayed that fungal colonization only occurs after destruction of cilia after bacterial biofilm development, giving insight into the pathogenesis of this symbiotic relationship.⁸⁹

Zhang et al., (2009) presented a cohort of CRS patients and reiterated the relationship between biofilm positivity and more severe sinus disease as seen on CT imaging.⁹⁰ In addition to this they found that intraoperative biofilms were associated with worse postoperative endoscopy scores, and if biofilm was present 6 months postoperatively then these patients will report worse symptoms scores and exhibit more severe disease on both endoscopy and CT scoring.⁹⁰ Another study by Singhal et al., (2010) further elaborated on the post-operative effects of biofilm presence over an 18 month period, showing that biofilm positive patients had increased outpatient attendance, poorer symptom scores, and substantially worse endoscopy scores.⁹¹

It is not entirely understood how microbial biofilms influence the underlying mucosa and immune system, conversely biofilm could be an opportunistic occurrence following an initial insult to sinonasal mucosa or abnormal host environment. Psaltis et al., (2008) showed that the antimicrobial protein lactoferrin was significantly reduced at mRNA and protein levels in biofilm positive CRS mucosa.⁹² It is still unclear if this is an innate defect in lactoferrin production or secondary to biofilm colonization/bacterial secreted products. Another study indicated that *S. aureus* biofilms may be a deposition site for superantigens, and that *S. aureus* biofilm is associated with higher levels of IL-5, IL-6, and eosinophil cationic protein (ECP).⁹³ Furthermore, Th₂ skewing has previously been thought to be caused by superantigen, however this study identified biofilm as another independent cause of a Th₂ immune response.⁹³ There is evidence that surface mucosal *S. aureus* biofilm may result in intracellular infection.⁹⁴ Tan et al., (2013) showed that CRS patients with biofilm and intracellular *S. aureus* infection were significantly more

likely to have early and late re-infection of *S. aureus* confirmed with culture techniques, when compared to only biofilm positive.⁹⁵

The current and continuously growing evidence on CRS pathogenesis supports an important focus on both host and external factors. There remains a lack of work identifying and understanding factors that occur in the early development of CRS, however multiple disease modifying factors have been proposed.

Mucosal Epithelial Barrier

Structure and function of the intercellular junction complexes

The intercellular junction complexes are classically divided into tight junctions (TJ), adherens junctions (AJ), gap junctions (GJ), and desmosomes. The TJs form the most apical intercellular connection, followed by AJs, GJs, and desmosomes respectively (Figure 1). The components of the intercellular junction are regulated by several factors, which either interact directly or indirectly via signalling processes that result in dynamic changes of the barrier.

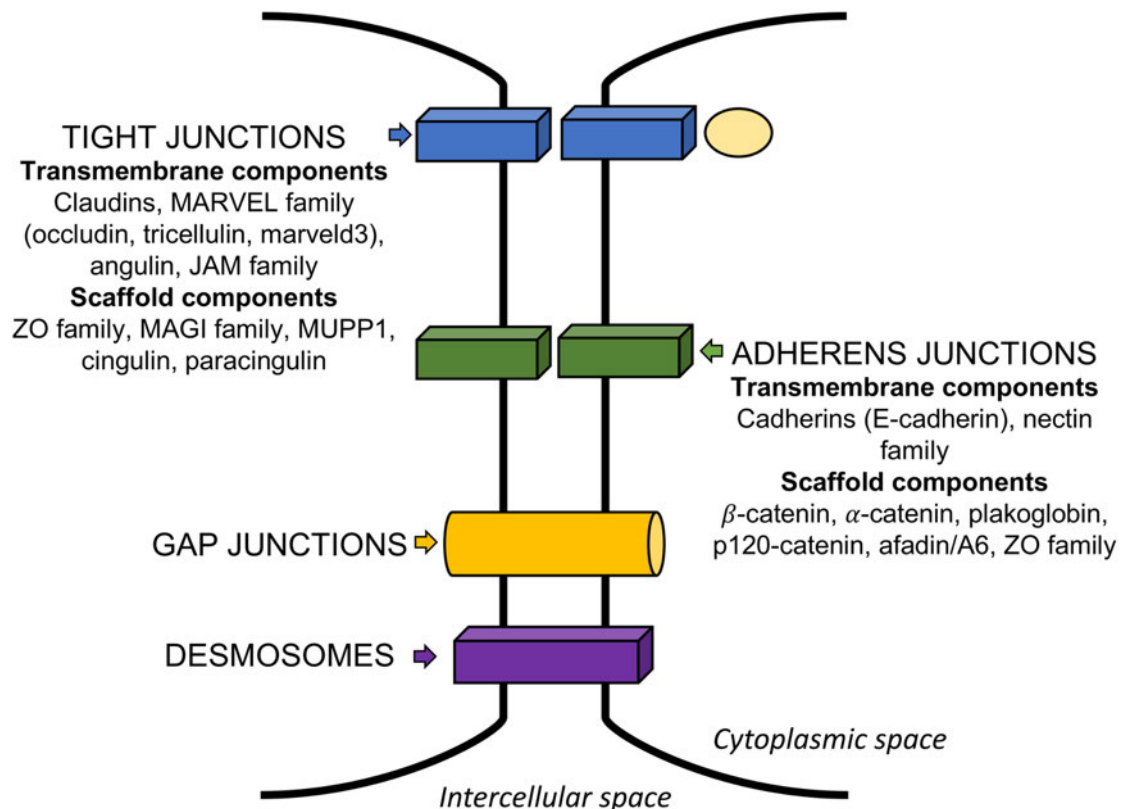


Figure 1. Schematic diagram of the intercellular junction.

Schematic demonstrating the position of TJ, AJ, GJ, and desmosomal complexes at the intercellular junction of neighbouring cells.

Tight Junctions

TJs form intercellular connections with neighbouring cells to create a regulated semipermeable barrier to the paracellular space. Additionally, they also coordinate the orientation of epithelial cells to ensure the apical and basolateral cell interfaces are aligned; known as the fence function. The basic structure of TJs consists of transmembrane components (integral) and scaffolding components (peripheral). The scaffolding components are intimately associated with the cellular actin cytoskeleton and AJ structures. Several authors have demonstrated that the paracellular barrier function can be divided into two separate routes: the pore and the leak pathways.⁹⁶⁻⁹⁸ The high capacity pore pathway primarily allows passage of small ions of less than $\sim 4\text{\AA}$ and is charge selective, while the low capacity leak pathway controls the passage of macromolecules and is not ion selective.⁹⁷

The TJ transmembrane components are comprised of the claudin family, TJ-associated MARVEL protein family (occludin, tricellulin, and marveld3), angulin, and the junctional adhesion molecule (JAM) family.

Claudins are the largest multigene family of TJ proteins with 24 members, and all are between 20-28 kDa in size. Each claudin contains four transmembrane passes, two extracellular loops, and the N- and C-terminal cytoplasmic tails. All the claudin C-terminals end in a binding site with the PDZ domains of zonula occludens (ZO)-1, ZO-2 or ZO-3, except for claudin-12.^{99,100} The first extracellular loop of claudin contains an amino acid motif, which is conserved among claudins. This segment is assumed to be important for maintaining paracellular seal and ion selectivity. The second extracellular loop is involved in homophilic and heterophilic interactions between the different claudins. Claudins primarily regulate pore pathway of barrier function.^{101,102} Claudins can make tight junctions leakier or tighter depending on the claudin type expressed.

Claudin-2 for instance is known to increase the leakiness of the TJ barrier.¹⁰³ Claudin type will determine the size and whether the pore charge is neutral, cationic, or anionic. Additionally, claudin function may differ between epithelial cell types.¹⁰⁰ The function of claudins are regulated by post-translational modifications such as phosphorylation or palmitoylation, and signaling pathways through prostaglandins, cytokines, and hormones. Claudin phosphorylation occurs due to protein kinase C (PKC), protein kinase A, mitogen-activated protein kinase (MAPK), myosin light chain kinase (MLCK), Rho kinase, and the ephrin receptor family. Cytokines, prostaglandins and other factors known to alter claudin function include TGF β , INF- γ , TNF- α , IL-1 β , IL-4, IL-10, IL-13, PGE₂, EGF, FSH, LH, and glucocorticoids.^{99,100,104}

Occludin was the first identified transmembrane protein of the TJ complex.¹⁰⁵ It is a 60 kDa protein that crosses the membrane in four passes with two extracellular loops, and cytoplasmic N- and C-terminal tails. There are multiple phosphorylation sites on occludin, and this is proposed to be related to its regulation and localisation to TJs. The second extracellular segment interacts with claudin and JAM proteins. The cytoplasmic C-terminal binds primarily with ZO-1 and ZO-2, and also with ZO-3 via its interaction with ZO-1.^{99,106} Tricellulin and occludin exhibit some functional redundancy, as occludin null mice showed significant upregulation of tricellulin at the bi-cellular interface where occludin is anticipated.¹⁰⁷ Phosphorylated occludin is localised at the TJ, while non-phosphorylated occludin remains in the basolateral membrane or in cytoplasmic vesicles.¹⁰⁸ Regulation of phosphorylation occurs via several kinases and phosphatases such as non-receptor tyrosine kinase c-Yes, PKC, and protein phosphatase 2A.⁹⁹ Additionally, inhibition of occludin phosphorylation leads to perturbation of the barrier function, and loss of localisation of occludin to the TJ.¹⁰⁹ Cell models of occludin overexpression have shown to promote cell-cell adhesion, and increases the barrier

function. Wong and Gumbiner, (1997) demonstrated that a synthetic peptide corresponding to the second extracellular loop of occludin was able to reversibly disrupt the TJ barrier *in-vitro*. This was coupled with a decrease in occludin protein localisation, but without altering the other TJ proteins.¹¹⁰ It is possible that the synthetic peptide was inhibiting normal assembly and function of occludin across the paracellular gap. Conversely, a previous occludin deficient mouse model showed no change in gastrointestinal barrier function. However, it did exhibit changes in cell morphology and secretory function suggesting a role in epithelial integrity or differentiation.¹¹¹ Considering the previous research, it is unclear how occludin influences the barrier function and whether it is essential in all epithelial barriers.

Marveld3 is a novel four-pass transmembrane 40 kDa protein, that is known to co-localise with occludin. Currently there are two known isoforms, and they are expressed in several cell lines including lung, colon, small intestine, and kidney.^{112,113} Marveld3 may have a primary role in TJ cell signalling; an *in-vitro* study showed it links TJs to the MEKK1/JNK pathway to regulate cell behavior. Depletion of marveld3 leads to prolonged JNK signalling which subsequently leads to TJ disassembly and cell death.

Prior to marveld3, the most recently described transmembrane TJ proteins are tricellulin and angulins (1-3), which are primarily located at the tricellular contacts.¹¹⁴ Tricellulin is a four-pass transmembrane protein, with two extracellular loops and large C- and N-terminal cytoplasmic tails. The tricellulin C-terminal sequence of approximately 130 amino acids is relatively conserved with occludin, although the extracellular loops and N-terminal are unique to each.¹¹⁵ The C-terminal tail interacts with a PDZ region of ZO-1.¹¹⁶ Tricellulin has been identified in skin, nasal, gastrointestinal, pancreas, and kidney epithelium.^{114,117,118} Regulation of tricellulin occurs through phosphorylation, however the specific kinase is yet to be identified. A peroxisome proliferator activated receptor- γ

agonist upregulated several tight junction proteins, including tricellulin; this was shown to be PKC dependent.¹¹⁹ Raleigh et al., (2010) demonstrated that tricellulin and marvel3 are both upregulated by tumor necrosis factor treatment at gene and protein expression levels, while occludin was unaffected. Additionally, claudins may also alter the function and localisation of occludin, marvel3, or tricellulin.¹⁰⁶ Tricellulin appears to be a major contributor to the paracellular leak pathway as the tricellular TJ areas are large enough for passage of macromolecules.¹²⁰

The angulin family (also known as lipolysis stimulated lipoprotein receptor) of proteins are single-pass transmembrane proteins, which is formed by an immunoglobulin (Ig) like extracellular domain (similar to JAM) and a long cytoplasmic tail.¹¹⁴ It is thought that angulin seal the central component of tricellular junctions, with tricellulin arranged around angulin.¹²¹ Expression of angulin isoforms is tissue specific, however expression of at least one isoform is required to maintain proper barrier function. Angulin is necessary to recruit and organize tricellulin at the tricellular TJs, which together are involved in regulating barrier function of the leak pathways. Interestingly, knockdown of angulin affected the pore pathway in MDCK 2 cells showing that it supports the TJ at several regions.¹²²

JAMs are single-pass transmembrane proteins that contains two extracellular Ig-like domains; they belong to the Ig-superfamily. The extracellular domains allow homophilic interactions (i.e. between other JAM proteins), and also heterophilic interactions.^{123,124} Primarily the heterophilic interactions occur between specific integrins on circulating white blood cells, which regulates transmigration of neutrophils and monocytes across the barrier. Additionally, JAM proteins are present on platelets and white blood cells. The cytoplasmic tail of JAM proteins contains the C-terminal and a PDZ domain. Depending on the PDZ class JAM interacts with the scaffolding proteins ZO-1, MAGI-1,

MUPPI.¹²³⁻¹²⁵ Neutralizing anti-JAM-A antibodies were able to prevent repair of the TJ pore pathway after it was disrupted by transient calcium depletion.¹²⁶ It has also been implicated in endothelial migration, and establishing cell polarity by interacting with the cell polarity complex.^{127,128} JAM-A phosphorylation by the atypical protein kinase C PAR3 is required for JAM-A to establish its barrier function and cell adhesion properties.¹²⁹

The scaffolding proteins of TJ structures include PDZ containing and non-PDZ containing proteins. PDZ containing proteins include the ZO family (ZO-1, ZO-2, and ZO-3), membrane associated guanylate kinase with inverted (MAGI) family (MAGI-1, and MAGI-3), and the multi-PDZ domain protein-1 (MUPPI). Non-PDZ containing proteins include examples such as cingulin, paracingulin, signalling proteins (kinases, phosphatases, membrane traffic regulators, and small GTPase regulators).¹³⁰

ZO proteins are amongst the most comprehensively studied TJ proteins, and ZO-1 was the first TJ protein to be identified.¹³¹ Each ZO protein contains three PDZ domains, one SH3 domain, and a guanylate kinase (GUK) domain. The first PDZ domain interacts with the C-terminal tail of claudins. The second PDZ domain interacts with another ZO protein to create a scaffold or with a connexin, while the third PDZ domain interacts with JAM-1. The SH3 domain is required for recruitment of ZO to the TJ and GUK interacts with occludin. Typically, the C-terminal region of the ZO proteins binds to the actin cytoskeleton.^{130,132,133} ZO proteins have been shown to interact with the cadherin based AJs,¹³² and other AJ proteins including the p120 catenin family and alpha catenin.^{134,135} ZO proteins are essential for integrity of the TJ barrier, particularly ZO-1 and ZO-2. Umeda et al., (2006) demonstrated that ZO-1 and ZO-2 are required for TJ strand formation using an epithelial cell model with a combination of knockout and knockdown mutations. ZO-1 and ZO-2 were necessary for recruitment of claudin,

occludin, and JAM to the TJ. Interestingly re-introduction of either ZO-1 or ZO-2 rescued the barrier function, while ZO-3 did not.¹³⁶ ZO-1 knockdown in MDCK II cells results in a disruption of the leak pathway, while the pore pathway remains unaffected. ZO-1 knockdown makes cell monolayers more sensitive to actin polymerization and low calcium concentrations leading to loss of both barrier pathways.¹³⁷ ZO-1 exchange from the cytosolic compartment and the TJ barrier is dependent on MLCK activity.¹³⁸ *In-vitro* TNF- α and IFN- γ treatment of cell monolayers induces MLCK activation resulting in barrier dysfunction.¹³⁹ A study conducted by Raleigh et al., (2011) showed that the kinase CK2 requires ZO-1 to mediate phosphorylation of occludin and subsequent signaling events to claudins.¹⁴⁰ Such studies demonstrate the important role of ZO as a stabilizer and transducer of TJ signaling, which coordinate the regulation of several barrier properties. Additionally, there is evidence to support ZO proteins in supporting GJs, while contributing to their dynamic function and architecture.¹⁴¹

The MAGI family of proteins are known to interact with JAM and several junction signalling molecules such as β -catenin, Rap1, and K-RAS.^{130,142} MUPPI contains 13 PDZ domains and is localised at TJs. It is known to interact with multiple claudins and JAM-1, and is also thought to provide multiple scaffolding supports.^{125,130} The ligands for all the MUPPI PDZ domains are not known, however it is recognized that the G-protein coupled somatostatin receptor-3 is able to interact with MUPPI and influence barrier function.¹⁴³ MAGI is a major degradation target of the human papilloma virus E6 protein, which subsequently leads to TJ disruption.¹⁴⁴ Cleavage of MAGI-1 by endogenous caspases is an important step in initiating cell detachment during apoptosis.¹⁴⁵

Cingulin and paracingulin are non PDZ proteins characterised by a globular head, a coiled rod domain, and a small tail. They are known to bind to JAM, ZO-1, ZO-2, and

ZO-3. Both are thought to contribute to the scaffold structure by cross-linking tight junctions with the actin cytoskeleton.^{146,147}

The multiple core components of TJs, their homophilic and heterophilic interactions, and the regulating factors involved demonstrate that this region is more complex than a simple physical barrier. The pore pathway appears to be primarily regulated by the specific set of claudins present at the time, and is also influenced by the supporting network of TJ proteins. The major contributors to the leak pathway are occludin, tricellulin, angulin, and ZO-1, with likely minor contributions from the other TJ proteins and cytoskeletal components. There has been recent interest in the dynamic properties of TJ protein interactions and barrier regulation, rather than considering the TJ as a static structure.⁹⁸ Although, this field is still in the development of improved molecular and live-imaging techniques that will allow a more detailed understanding of the dynamic properties of the TJ.

Adherens Junctions

The AJ is an intercellular junction that assembles below the TJ region and assists in the integration of cell-cell contacts to form an intact barrier. AJs are involved in several functions including cell-cell adhesion, cell polarity regulation, regulation of the cytoskeleton, cell signalling, and transcriptional pathways.¹⁴⁸ Similar to TJs, the AJs are formed by transmembrane and scaffolding components, which are anchored by the actin cytoskeleton. The two major complexes that form the AJ are the cadherin-catenin complex and the nectin-afadin complex.^{148,149}

AJ cadherins are termed the classic cadherins in the large family of cadherin proteins. Among the numerous types of cadherins, E-cadherin is usually associated with AJs of epithelial barriers. They are a Ca²⁺ dependent single pass transmembrane glycoprotein

and are comprised of five extracellular cadherin repeat domains and the cytoplasmic catenin binding domains.⁹⁹ The extracellular domains engage with homophilic regions of the cadherins in neighbouring cells to form weak connections. However, once Ca^{2+} binds to each domain they undergo a conformational change thereby strengthening the junction.¹⁵⁰ The cytoplasmic tail adjacent the membrane interacts directly with p120-catenin, while the C-terminal interacts with β -catenin or plakoglobin. α -catenin then interacts with β -catenin as an intermediary between the AJ complex and the cytoskeleton.⁹⁹

p120-catenin is proposed to stabilise E-cadherin at the AJ during the formation of its adhesive contact.¹⁵¹ Additionally, p120-catenin regulates cell motility through the cytoskeleton via interaction with Rho GTPases.¹⁵² β -catenin binding is crucial for fully functional AJs, and prevents degradation of E-cadherin.¹⁵³ Several kinases are involved in mediating binding by phosphorylation of the E-cadherin cytoplasmic tail, which significantly increases the binding affinity.^{99,154} β -catenin may also regulate cadherin turnover by preventing clathrin mediated endocytosis.¹⁵⁵ Likewise α -catenin is vital for AJ formation and cadherin localisation at the AJ. α -catenin simultaneously binds to β -catenin and actin, but is thought to require a binding partner to facilitate simultaneous interaction with β -catenin and actin such as ZO-1, afadin, vinculin, or α -actinin.^{156,157}

Nectin is a single pass transmembrane protein that belongs to the Ig-like superfamily of adhesion molecules. There are four known nectins (nectin 1-4) and all consist of an extracellular domain containing three IgG-like loops and a cytoplasmic tail with a PDZ binding region at the C-terminal. The cytoplasmic tail interacts with the PDZ binding domain of afadin/A6.^{99,149} Nectins participate in Ca^{2+} independent homophilic and heterophilic interactions with other nectins and nectin-like receptors. It is proposed that nectin and nectin-like molecules are responsible for the initiation of cell-cell

adhesion.¹⁴⁸ This allows the formation of cadherin-catenin complexes and subsequently the assembly of TJs.¹⁵⁸ Fukuhara et al., (2002) utilised *in-vitro* cell models to demonstrate that nectin is required to recruit ZO-1 and JAM into the TJ. Furthermore, the authors proposed that the nectin induced JAM interaction is responsible for claudin and occludin recruitment to the apical TJ complex.^{159,160}

Afadin/A6 is an actin binding protein that acts as the scaffold for nectin, and also provides connections to the cadherin/catenin complexes through α -catenin and the TJ via ZO-1.^{161,162} Components of afadin include a PDZ domain, two Rap/Ras GTPase binding domains, an actin binding domain, and three proline-rich domains. Afadin knockout mouse embryo models have demonstrated it is crucial in epithelial organisation and the developing TJ and AJ.^{163,164}

Gap Junctions

GJs provide an intercellular communication channel between neighbouring cells, which allows exchange of ions and small molecules (< 1 kDa). Their primary structure is formed by the connexin family of proteins, which are four-pass transmembrane proteins containing two extracellular loops, and N- and C-terminal cytoplasmic tails. Each GJ protein forms a hemi-channel to bridge the intercellular junction to form a channel with a neighbouring hemi-channel.^{165,166} Although GJs are not classically involved in the paracellular barrier, they share the intercellular space with other barrier proteins and are particularly important in the coordination of ciliary function in the sinonasal cavity.¹⁶⁷ There is evidence that ZO-1 enacts an important role in the regulation and turnover of GJs. Dunn and Lampe, (2014) utilized an *in-vitro* wound model which showed that cell injury precipitates Akt phosphorylation of connexin-43 with subsequent increased gap junction communication and junction size due to the partial

uncoupling of ZO-1 and connexin-43.¹⁶⁸ Another study found that additional phosphorylation of connexin-43 leads to a complete dissociation between ZO-1, with subsequent closure of the GJ channel and preparation of GJ endocytosis.¹⁶⁹ Vascular endothelial GJs are negatively altered by TNF treatment, which induces ZO-1 interaction with connexin-37.¹⁷⁰ Palatinus et al., (2010) showed that AJ-associated ZO-1 influences the GJ localisation in cardiac myocytes.¹⁷¹ It seems that GJs share structural components of TJs and AJs, which may have important implications in ciliated airway epithelium.

Desmosomes

Desmosomes are comprised of several components that form the strong connection between neighbouring cells. The basic structure is formed by intercellular links (desmosomal cadherins) and intracellular links (intermediate filaments, desmoplakin, plakoglobin, plankophilin). The desmosomal cadherins include desmoglein and desmocollins, of which there are four and three isoforms respectively. These components cross the extracellular space to create isoform specific crosslinking dimers to provide the adhesive function.^{172,173} Desmosomal cadherins are tissue specific with desmoglein-2 and desmocollins-2 expressed in all desmosomal forming tissues, whereas the remaining desmogleins/desmocollins contribute to various epithelia.^{174,175} Desmoplakin, plakoglobin, and plankophilin form the desmosomal plaques that interact with the desmosomal cadherins at the plasma membrane and the intermediate filaments. The intermediate filaments anchor the desmosomal plaques to the cytoskeleton.^{173,176}

Similar to AJs, the primary function of desmosomes are to maintain integrity and adhesion of cell to cell contacts. As such they are particularly important in epithelial tissues that are subject to mechanical stress. Desmosomes are regulated by calcium concentrations, and protein kinase C (PKC).¹⁷² Whilst desmosomes are developing they

form in a calcium dependent manner, but once matured they are strongly calcium independent and form hyperadhesive connections to neighbouring cells. This is unique to the desmosomal family as other proteins of the intercellular junction are calcium dependent.^{172,173} PKC is known to be localised to in the basal epithelial layers, and during epithelial development and wound healing it is localised with desmosomal plaque proteins. It is currently thought that PKC phosphorylates one of the desmosomal proteins to induce calcium dependence as a means to regulate adhesiveness. During wound healing the wound edge exhibits down-regulation of desmosomes via PKC activation and internalisation of half-desmosomes. However, they are not completely internalised due to their requirement in maintaining the cell-cell adhesion required for coordinated migration.¹⁷⁶ Desmosomes are also involved in intracellular signalling pathways such as Wnt/ β -catenin, and abnormal desmosomal expression has been shown to influence MAPK, STAT3, NF- κ B, and phosphatidylinositol 3-kinase pathways.^{177,178}

Assessment of intercellular junction complexes

Assessment of the intercellular junction complexes typically comprises a combination of functional measurements and structural analysis. This is occasionally supplemented by protein quantification and gene expression methods. Functional measurements include transepithelial electrical resistance (TEER), and macromolecular permeability. In sinonasal barrier research functional assays are usually performed on *in-vitro* cultures derived from healthy primary nasal epithelial cells, CRS derived nasal epithelial cells, and sinonasal secondary cell lines. Structural analysis can be performed by observing cell ultrastructure with electron microscopy, or examining the protein expression of

junctional proteins, and is frequently performed on both *in-vitro* cell models and clinical biopsy specimens.

Transepithelial electrical resistance

TEER is a commonly used technique to assess the real-time status of the intercellular junction of both *in-vitro* and *ex-vivo* barrier models, specifically the pore pathway. TEER provides quantitative information about the ionic conductance across the cell layer by measuring the flux of ions, which is typically Na⁺ and Cl⁻ in physiological solutions. *In-vitro* cell cultures are cultivated on semi-permeable membranes and measurements are generated by placement of two electrodes; one above and below the cell layer. An alternating current is applied across the layer, and the resistance is expressed as Ohm (Ω). Ohm's law states that the current through a conductor is proportional to voltage and inversely proportional to resistance. The TEER of the blank membrane is then subtracted from the experimental TEER measurement. As the TEER is related to the size of the permeable membrane in cm², it is then expressed as Ωcm^2 .¹⁷⁹

TEER measurement is influenced by the specific device used, temperature, apical and basal chamber solutions, cell type, membrane material, membrane size, and also user handling of the device.^{179,180} Initial TEER experiments were performed using Ussing chambers, which require a more complicated setup. It is now more common to perform such measurements using "chopstick" type voltmeters or a chamber voltmeter.¹⁸¹ Additionally, it is possible to assess the integrity of *ex-vivo* mucosa in an Ussing chamber.¹⁸²

Macromolecular permeability

The leak pathway determines the paracellular permeability to macromolecules. This provides information regarding the rate of flux across the cell layer of a selected macromolecule. The permeability rate of a particular molecule is partly determined by the size of the molecule, pH of the solution, charge, hydrophilic vs lipophilic properties, and whether the compound is actively transported transcellularly.¹⁸³⁻¹⁸⁵ This is commonly measured using different sized neutral compounds such as fluorescently tagged dextrans, radiolabeled inulin and mannitol, or horseradish peroxidase. The compound is usually introduced into either the apical or basal cell culture chamber, then samples are taken from the receiving side. The rate of transfer can then be calculated as determined by the starting concentration, receiving concentration, size of the cell layer or membrane, and the time lapsed. The results are expressed as the permeability coefficient or apparent permeability (P_{app} , cm/second) using the following equation:

$$P_{app} = \left(\frac{dQ}{dt} \right) \times \frac{1}{AC_0}$$

Where dQ/dt is the amount of compound over time, A is the area of the membrane, and C_0 the starting concentration of compound.¹⁸⁶

Fluorescence microscopy

Fluorescence microscopy techniques are commonly used to identify the localisation and pattern of intercellular junction proteins and supporting cytoskeletal components. This is usually performed using a laser scanning confocal microscope, allowing assessment of the target proteins in three planes. Localisation and patterns of fluorescent staining differs between each group of intercellular junction proteins (TJs, AJs, GJs, and desmosomes) and is also dependent on the tissue type and experimental conditions.¹⁸⁷

Altered intercellular junctions are observed as redistribution or reorganisation, disrupted or broken staining, relative intensity changes, or lack of staining.^{20,188,189} Additionally, it can be used to determine co-localisation of structures. Live cell fluorescent imaging techniques have been used to further understand the dynamic element of the intercellular junction, however these techniques are still in development and their relevance uncertain given most methods alter the protein structure with a fluorescent tag.^{96,190}

Electron microscopy

Transmission electron microscopy (TEM) on ultrathin sections and freeze fracture replicas allows observation of the intercellular junction ultrastructure.¹⁸⁷ TEM techniques are particularly useful in showing the close contact or “kissing point” between adjacent plasma membranes and lack of paracellular separation.^{187,191} Freeze fracture replica techniques have allowed improved visualization of the individual TJ strands and their complexity at the intercellular interface. The addition of immunolabeling of TJ proteins confirms their presence on the individual strands.^{187,188,192}

Mucosal barrier in sinonasal health and disease

Tight and adherens junctions in sinonasal health and disease

The understanding of TJ and AJ in the sinonasal cavity in both health and CRS is yet to be completely established. The studies that have characterised TJ and AJ associations in CRS are discussed below and summarized in Table 1. Additionally, there are several in-vitro studies investigating potential barrier disrupting mechanisms, which will be addressed in a subsequent section.

Jang, Kim, Koo and Chung (2002) published the earliest research examining TJ and AJ mucosal barrier proteins in nasal polyposis. This study compared immunohistochemical staining of ZO-1 and E-cadherin between nasal polyps from patients undergoing surgery and control mucosa from the ethmoid sinuses of autopsy patients. They found that ZO-1 staining in nasal polyps exhibiting mucous cell hyperplasia was punctate and of lower intensity when compared to the controls, however E-cadherin was significantly more intense. This pattern was also observed in metaplastic nasal polyp epithelium; however, ZO-1 staining was either especially low or absent. Pseudostratified columnar epithelial regions of nasal polyps showed significant similarity to control mucosa.¹⁹³

Zuckerman et al., (2008) conducted an immunofluorescence study of intercellular junctions in patients undergoing ESS for CRSwNP or skullbase surgery as control specimens. Occludin, ZO-1, JAM-A, coxsackievirus and adenovirus receptor (CAR), claudin-1, E-cadherin, desmoglein-2, desmoglein-3, cytokeratin, and plakoglobin were all assessed. There were no differences in the staining intensities or patterns of TJ or AJ proteins between each group. However, all CRSwNP patients were treated with high dose oral corticosteroids prior to specimen collection.¹⁷⁵ Another study elucidated that oral corticosteroid treatment can alter the distribution of TJ proteins in nasal polyp tissue. Occludin, claudin-1, and ZO-1 were examined with qRT-PCR, immunohistochemistry, and western blot in nasal polyp specimens before and after corticosteroid treatment. Corticosteroid treatment produced a significant increase in gene expression, protein localisation, and protein quantification of occludin.¹⁹⁴ *In-vitro* experiments confirmed that the corticosteroid induced upregulation of occludin was due to downregulation of the MAPK via a MKP-1 pathway.¹⁹⁴ MKP-1 expression is a common mediator for the anti-inflammatory effect of corticosteroids.¹⁹⁵ This implies

that CRS inflammatory mediators influence the expression of occludin, and that barrier repair is potentially improved with corticosteroid treatment.

Rogers et al., (2011) assessed the localisation of claudin-1 and occludin in nasal polyposis and control patients, with 3 specimens in each group. Although the study was relatively small it demonstrated a significantly lower expression of each TJ protein in the apical epithelium. Furthermore, the authors demonstrated that treatment of human bronchial epithelial cell line HBE14o⁻ with IFN and TNF cytokines results in significantly reduced occludin and slightly lower claudin-1 protein levels. Barrier changes were observed at 72 hours suggesting that the effects are not a direct effect on TJ proteins, but may be associated with a signaling pathway.¹⁹⁶

Soyka et al., (2012) studied the expression and function of tight junctions in a small cohort of CRS patients.²⁰ Utilising a Ussing chamber, it was shown that the *ex-vivo* mucosal barrier in CRS has reduced trans-tissue electrical resistance compared to controls. This was also supported by irregular immunohistochemistry staining of occludin and ZO-1 proteins in both CRS phenotypes, while western blot techniques confirmed either absent or extremely low levels of occludin in tissue lysates. CRSwNP exhibited a more severe disruption of the TJ barrier. Furthermore, gene expression showed a reduction in claudin-4 in both CRSsNP and CRSwNP, while occludin gene expression was only significantly reduced in CRSwNP. This barrier dysfunction was argued to be due to cytokine induced inflammation. *In-vitro* cell cultures treatments showed that IFN- γ and IL-4 affect both TEER and molecular permeability. Additionally, they demonstrated that IFN- γ has a direct effect on the gene expression of both claudin-4 and ZO-2 mRNA. Interestingly, ALI cultures derived from nasal polyp tissues exhibited significant increases in mRNA expression of claudin-1 and claudin-4.²⁰ This highlights

the potential for nasal polyp ALI cultures to exhibit inherent barrier dysfunction *in-vitro* and for a differential response to treatments with cytokines or other factors.

A study by Meng et al., (2012) examined specimens from a small cohort consisting of 6 controls and 6 CRSwNP patients.¹⁹⁷ An additional group of CRSwNP exhibiting early polyp formation were included, however the epithelial integrity in these specimens was not suitable for assessment of TJ/AJ staining. ZO-1, occludin, and E-cadherin were included in the assessment, and all showed significantly lower staining intensity in the CRSwNP group. Interestingly, this is the only study that showed a lower expression of E-cadherin in CRSwNP. The CRSwNP group also displayed high eosinophil counts, increased staining for macrophage and myofibroblast markers, and lower collagen expression. However, no correlation was made between these factors and TJ/AJ expression.

The largest immunohistochemical study of TJ, AJ, and desmosomes was conducted by Li et al., (2014) consisting of specimens from 19 controls, 20 CRSsNP, and 41 CRSwNP patients undergoing ESS.¹⁹⁸ Claudin-1, ZO-1, and E-cadherin were semi-quantitatively assessed using an ordinal scale. Additionally, the CRSwNP group was separated into eosinophilic and non-eosinophilic subgroups. Similar to previous studies they observed a significant increase in E-cadherin staining, which was seen in both CRSsNP and CRSwNP. CRSsNP exhibited decreased staining of claudin-1, while ZO-1 staining was lower compared to the controls it was not statistically significant. ZO-1, and claudin-1, were reduced in CRSwNP, with no difference between eosinophilic and non-eosinophilic groups. Furthermore, it was demonstrated that tissue levels of IL-5 and IL-6 were negatively correlated with claudin-1. Conversely, IL-8 was positively correlated with E-cadherin expression.

A recent study identified that N-myc downstream-regulated gene 1 (NDRG1) is a positive regulator of the airway epithelial barrier. CRS biopsy specimens exhibited dramatically decreased localisation of NDRG1 protein; specifically, in areas of damaged sinonasal epithelium or goblet cell hyperplasia. NDRG1 knockdown *in-vitro* triggers significant defects in TEER and TJ localisation of occludin and ZO-1. Interestingly, gene expression after NDRG1 knockdown resulted in decreased claudin-9 mRNA and little difference in ZO-1, occludin, and several other claudins.¹⁹⁹

A report by Nguyen et al., (2012) suggested that claudin-1 and tricellulin immunofluorescent staining was increased in nasal polyposis, with an increase in claudin-1 mRNA levels.²⁰⁰ This was observed alongside lower expression of two epidermal growth factor receptors. However, the comparison patient group was composed of specimens from hypertrophic inferior turbinates and is likely not representative of a healthy mucosal interface.

Table 1. Tight junction, Adherens junction, and Desmosome literature summary in Chronic Rhinosinusitis

Tight junction, Adherens junction, and Desmosome literature summary in Chronic Rhinosinusitis		
Authors	Tissue source and method	Key findings
Chen et al., (2014) ¹⁹⁴	Biopsy specimens from CRSwNP patients pre and post treatment with prednisolone (30mg/day for 14 days). Immunohistochemistry staining of occludin. qRT-PCR of occludin, claudin-1, and ZO-1. <i>In-vitro</i> experiments detailed in Table 6.	<ul style="list-style-type: none"> - mRNA of occludin was significantly increased in polyp specimens after prednisolone treatment. No change in ZO-1, or claudin-1 mRNA - Immunoreactivity staining of occludin was increased after treatment
Jang, Kim, Koo & Chung (2002) ¹⁹³	Biopsy specimens from ethmoid mucosa of control autopsy patients (n=5), and 20 patients undergoing ESS for nasal polyposis (n=20). Immunohistochemistry staining of ZO-1, and E-cadherin.	<ul style="list-style-type: none"> - Hyperplastic and metaplastic squamous epithelium of nasal polyps showed decreased ZO-1 and increased E-cadherin staining - Normal areas of pseudostratified ciliated epithelium from nasal polyp patients showed normal ZO-1 and E-cadherin staining
Li et al., (2014) ¹⁹⁸	Biopsy specimens from patients undergoing ESS for CRSwNP (n=41), CRSsNP (n=20), and middle turbinate or uncinata from controls (n=19). Eosinophil count with H&E stain. Immunohistochemical staining of ZO-1, claudin-1, E-cadherin, DSG1, and DSG2. Homogenized tissue ELISA of IL-5, IL-6, and IL-8.	<ul style="list-style-type: none"> - CRSsNP: increased E-cadherin staining. Decreased claudin-1, DSG1, DSG2 staining - CRSwNP: Increased E-cadherin staining. Decreased ZO-1, claudin-1, DSG1, DSG2 staining. - DSG1 significantly lower in CRSwNP than CRSsNP - Negative correlations between (IL-5, IL-6) & claudin-1, (IL-6, IL-8) & DSG2, IL-8 & DSG1. Positive correlation between IL-8 & E-cadherin
Meng et al., (2013) ¹⁹⁷	Biopsy specimen from patients undergoing ESS for CRSwNP (n=6), and control patients (n=6) having a rhinoseptoplasty. An additional group of "immature" or early CRSwNP was included (n=5) Immunohistochemical staining of E-cadherin, ZO-1, and occludin. Other components assessed: eosinophil number, CD-68, mannose receptor, α -SMA, vimentin, pSmad2, fibronectin, and collagen content.	<ul style="list-style-type: none"> - Reductions in E-cadherin, ZO-1, and occludin staining intensity in mature polyps from CRSwNP - Higher eosinophil count in mature CRSwNP - Immature CRSwNP group <ul style="list-style-type: none"> o TJ/AJ not assessed due to epithelial damage o Increased α-SMA, CD-68, mannose receptor, vimentin, pSmad2 - Both mature and immature polyps demonstrated high fibronectin, and low collagen expression
Nguyen et al., (2012) ²⁰⁰	Biopsy specimens from patients undergoing ESS for inferior turbinate hypertrophy (n=10), and nasal polyps (n=10). Immunofluorescent microscopy of ErbB1, ErbB2, claudin-1, and tricellulin. Eosinophil count and % of goblet cells. qRT-PCR of erbB1, erbB2, claudin-1, and tricellulin.	<ul style="list-style-type: none"> - Staining of erbB1 and erbB2 was significantly higher in the inferior turbinate group - Staining of claudin-1 and tricellulin were both increased in nasal polyp specimens - Quantitative mRNA results show erbB1, erbB2, and tricellulin are increased in the inferior turbinate group. Claudin-1 mRNA increased in nasal polyps. - NB: inferior turbinate hypertrophy is not a completely appropriate control group considering the potential association with allergy/rhinitis and TJ/AJ disruption
Rogers et al., (2011) ¹⁹⁶	Biopsy specimens from controls (n=3) and nasal polyps (n=3). Immunofluorescent markers for claudin-1, and occludin. <i>In-vitro</i> experiments detailed in Table 6	<ul style="list-style-type: none"> - Control tissue showed intense staining of both proteins in the apical and basal portions of epithelium - Decreased staining of both claudin-1 and occludin
Soyka et al., (2012) ²⁰	Biopsy specimens from patients undergoing ESS. Nasal polyp from CRSwNP. Maxillary or ethmoid tissue from CRSsNP. Inferior turbinate, middle turbinate, uncinata process from control patients. Ussing chamber TEER, immunofluorescence, gene expression, western blot (n=4 each group). <i>In-vitro</i> experiments detailed in Table 6.	<ul style="list-style-type: none"> - Ussing chamber showed significantly reduced TEER in CRSwNP - Decreased immunofluorescence of occludin and ZO-1 in CRSwNP, and less severe decrease in CRSsNP - CRSwNP: 2.2-fold decrease in claudin-4 mRNA, and 1.6 fold lower occludin mRNA - CRSsNP: 2.1-fold decrease in claudin-4 mRNA - Significant correlation between eosinophil cationic protein and TJ mRNA expression - Western blot confirmed absent occludin in CRSwNP, very low levels in CRSsNP
Zuckerman et al (2008) ¹⁷⁵	Biopsy specimens of nasal polyps and inferior turbinate/septum from patients with nasal polyps (n=11), and control patients (n=6). Adults. Immunofluorescence of occludin, ZO-1, JAM-A, CAR, claudin-1, E-cadherin, desmoglein-2, desmoglein-3, cytokeratin, and plakoglobin <i>In-vitro</i> experiments detailed in Table 6.	<ul style="list-style-type: none"> - No difference in occludin, ZO-1, JAM-A, CAR, claudin-1, E-cadherin, cytokeratin, or plakoglobin between controls and nasal polyps - Decreased immunofluorescence staining of DSG2 and DSG3 in polyps - Normal expression in controls and inferior turbinate tissue from CRSwNP patients

The study of TJ/AJ structures in the pathogenesis of CRS is relatively novel. Considering the findings from these reports it appears that some clinical factors will influence the study findings i.e. pre-operative corticosteroids, inclusion of appropriate control specimens. Additionally, there are incongruous findings between reports. Claudin-1 and occludin appear to be down regulated in CRS. However, most studies only examined one or the other protein. Zuckerman et al., (2008) included claudin-1 and occludin in their study, only to see no difference in staining between control and CRSwNP groups.¹⁷⁵ Patients in this study were taking oral corticosteroids prior to specimen acquisition, which is known to increase occludin expression.¹⁹⁴ Rogers et al., (2011) was the only study to see reductions in both, although this was in a group of 3 control and 3 CRSwNP patients. Furthermore, this report made no mention regarding pre-operative corticosteroid use.¹⁹⁶ Excluding the studies where preoperative corticosteroids were used or use was not explicitly stated, then it seems ZO-1 is consistently decreased in CRSwNP (Table 2). As ZO-1 is involved in multiple interactions with TJ, AJ, GJ and desmosomal proteins it may be a useful indicator of alteration of several barrier components.

Table 2. Summary of TJ, AJ, and desmosome immunohistochemistry in CRS

Immunohistochemistry CRS vs Control	Control	CRSsNP	CRSwNP	Occludin	Claudin-1	ZO-1	JAM-A	CAR	E-Cadherin	DSG1	DSG2	DSG3	Pre-operative corticosteroids
Jang et al , (2002) ¹⁹³	5	n/a	20	n/a	n/a	↓	n/a	n/a	↑	n/a	n/a	n/a	-
Li et al , (2014) ¹⁹⁸	19	20	41	n/a	↓	↓ ^a	n/a	n/a	↑	↓	↓	n/a	-
Meng et al , (2013) ¹⁹⁷	6	n/a	6	↓	n/a	↓	n/a	n/a	↓	n/a	n/a	n/a	-
Rogers et al , (2011) ¹⁹⁶	3	n/a	3	↓	↓	n/a	n/a	n/a	n/a	n/a	n/a	n/a	?
Soyka et al , (2012) ²⁰	4	4	4	↓ ^b	n/a	↓ ^b	n/a	n/a	n/a	n/a	n/a	n/a	-
Zuckerman et al , (2008) ¹⁷⁵	6	n/a	11	↔	↔	↔	↔	↔	↔	n/a	↓	↓	+

Corticosteroid administration (+) or (-) within the 4 weeks prior to specimen collection (a) only significantly decreased in CRSwNP group; (b) qualitatively more disrupted in CRSwNP; (n/a) not assessed

Gap junctions in sinonasal health and disease

There are several comprehensive investigations on GJ distribution and function in CRS emphasizing its importance in cell communication, and relationship to ciliary function. Hama et al., (2001) found connexin 26 at the mucosal cell junctions, while connexin 43 was observed between the stromal cells of the lamina propria and submucosa.¹⁶⁷ However, cultured nasal epithelial cells only stained positive for connexin 43. *In-vitro* functional assays with dye transfer and intercellular calcium waves confirmed that cultured nasal epithelial cells do have capacity for intercellular communication.¹⁶⁷ A separate article also showed connexin 43 in nasal mucosa and cultured nasal epithelial cells, although there was no positive staining for connexin 26 or connexin 32.²⁰¹ Nasal epithelial connexin 43 expression increases with accumulative days of ALI culture.²⁰¹ Yeh et al., (2007) identified that HNEC cultures exhibited optimal gap junction intercellular communication between days 10 and 20 of ALI culture rather than submerged cell culture.²⁰² This coincided with significant increases in connexin 43 and peak ciliogenesis.²⁰² *In-vitro* exposure of nasal epithelial cells to bacterial lipopolysaccharide resulted in a significant release of IL-8 with a dose and time dependent decrease in connexin 43.²⁰³ This may exert an inhibitory effect on ciliary beating by interfering with intercellular communication. Martin and Prince (2007) determined that the human airway cell line IHAEo⁻ communicated TLR2 mediated Ca²⁺ fluxes via gap junctions.²⁰⁴ Ca²⁺ flux was able to generate chemokine secretion in neighboring cells through activation of NF-κB. Furthermore, it was shown that airway cells are able to limit the proinflammatory response by phosphorylation of connexin 43, which effectively closes the gap junction intercellular gate.²⁰⁴ There is a relative deficiency in animal models of airway gap junction research. However, Martin and Prince (2007) did confirm that neutrophil influx into mice lungs secondary to *P.*

aeruginosa inoculation was significantly suppressed by inhibition of gap junction intercellular communication.²⁰⁴

Yeh et al., (2005) investigated the relationship between connexin 43 expression and eosinophil infiltration in nasal polyps.²⁰⁵ Their study identified a significant reduction in connexin 43 with increasing local eosinophils in nasal polyps, although the underlying mechanism was elucidated. The authors hypothesized that the local decrease in connexin 43 could lead to changes in fibroblast differentiation and remodeling in nasal polyposis.²⁰⁵ It is known that gap junction communication contributes to regulation of inflammation, innate and adaptive immune responses, fibrosis, and wound healing.²⁰⁶

BuSaba and Cunningham (2008) conducted a gene sequence study of connexin 26 (*GJB2*) and connexin 30 (*GJB6*) in 46 consecutive patients with CRS or RARS.²⁰⁷ All patients had a normal connexin 30 gene, and two patients with a mutation in connexin 26. Interestingly, one patient had a connexin 26 heterozygotic 35dG mutation and early adulthood onset of sensorineural hearing loss. The connexin 26 35dG mutation has been associated with autosomal recessive non-syndromic hearing loss.²⁰⁸ Another study screened a relatively young cohort of patients (age range 6 – 33 year; n=19) with CRS and RARS for mutations in connexin 32 (*GJB1*) and connexin 43 (*GJA1*) genes.²⁰⁹ 3 patients were identified to have heterozygotic mutations, however all mutations identified were not known to cause protein dysfunction, or associated with a known pathogenic mutation.²⁰⁹ The results of this previous research negates a prevalent genomic mutation of the examined genes as an explanation for mucociliary dysfunction in these cases of CRS.

Connexin 26 has been implicated in the development of allergic rhinitis. Significant down regulation at the mRNA and protein levels was observed in patients with house dust mite sensitized allergic rhinitis.²¹⁰ This was associated with an increase in protease

activated receptor-2 (PAR2), which is activated by house dust mite proteases.²¹⁰ This study proposes that gap junction dysfunction is intimately involved in antigen sensitisation in nasal airways, and that environmental antigens activate mucosal receptors that influence the barrier function.

Kim et al., (2016)²¹¹ have produced the most comprehensive study characterizing connexins in healthy nasal mucosa and CRS mucosa. They identified positive gene expression for 16 connexins, including 9 that had previously not been described in nasal mucosa. Quantitative real-time polymerase chain reaction (qPCR) showed that connexin 26 and connexin 43 gene expression was significantly upregulated in the CRS group. Connexin 30 did not show statistically significant increases, however the individual data points demonstrate potential high expressing CRS patients. The study was limited by a small cohort potentially overlooking gene expression differences between CRSsNP and CRSwNP. Immunohistochemistry exhibited connexin 26 was localized to the basal cell layer, connexin 30 positive staining throughout the epithelium, and connexin 43 primarily in the stroma of CRS patients (2.7 fold higher).²¹¹

The literature supporting the role of gap junctions in CRS and other sinonasal conditions outlined here suggests that the connexin proteins present in the upper airways may be involved in the pathogenesis. Future research will need to further characterize the connexins in healthy sinonasal mucosa and clarify the function of connexin 43, which seems to be conflicting in the current reports. Furthermore, it is unclear if GJ disruption is a feature seen independent of overall barrier disruption or related to TJ or AJ dysfunction.

Desmosomes in sinonasal health and disease

There are little reports regarding the normal characteristics and distribution of desmosomes in the paranasal sinuses and nasal cavity. Currently, this can be extrapolated from the few studies that have investigated upper airway desmosomal patterns.

Zuckerman et al., (2008) examined intercellular junctions in sinonasal tissue from 6 healthy patients and 11 patients with nasal polyposis. Their immunofluorescence study demonstrated strong staining intensity of desmoglein-2, desmoglein-3 and cytokeratin (component of intermediate filaments) throughout healthy mucosa, along with less broad or intense staining of plakoglobin. This was compared with staining patterns in nasal polyps, which exhibited significantly reduced intensity and distribution. Interestingly, non-polyp tissue from nasal polyposis patients showed similar staining of desmosomes to that of the controls.¹⁷⁵ This implies that desmosome dysfunction is a local factor in nasal polyposis. Furthermore, *in-vitro* experiments identified that IL-13 treatment of human bronchial cell line (HBE4-E6/E7) triggers cleavage of desmoglein-2 and an associated loss of immunofluorescent staining. Conversely, IFN- γ induced an increase of staining intensity of desmoglein-2 at 48 and 96 hours, while also promoting cleavage as evidenced by western blot.¹⁷⁵ This suggests that IL-13 associated Th2 inflammation may be involved in the development of nasal polyposis by weakening desmosome adhesion. Analysis of genomic DNA from controls and CRSwNP patients previously revealed no difference in desmoglein-2 and desmoglein-3 genotypes.²¹² This supplements the aforementioned finding that desmosomes are likely to be affected locally. Li et al., (2014) found that desmoglein-1 and desmoglein-2 are significantly reduced in CRSsNP and CRSwNP. Furthermore, tissue levels of IL-6 are negatively

correlated with desmoglein-2, and IL-8 negatively correlated with desmoglein-1 and desmoglein-2.¹⁹⁸

Soyka et al., (2012) investigated the specific mRNA expression patterns of a number of desmosomes in biopsies from a small group of control, CRSsNP, CRSwNP patients using a microfluidic card assay. Their study indicated the presence of mRNA for desmocolin 2-3, desmoglobin 2-4, plankophilin 1-4, plakoglobin, and desmoplakin in sinus mucosa, however there was no difference in CRS cohorts.

An earlier study comparing nasal polyp epithelium between patients with and without asthmatic/allergic symptoms measured the length of desmosomes using electron microscopy.²¹³ It was identified that the columnar and basal cell desmosome lengths were shorter in asthmatic and allergic patients, and it was subsequently suggested that this may represent weakened desmosome junctions. Although, this paper is limited by its methodology in using only electron microscopy to identify and quantify desmosome length.²¹³

A recent case report by Oto et al., (2017) describes an interesting case of IgG4 autoimmunity in a patient with CRSwNP. Immunohistochemical analysis of the sinus tissue showed that IgG4 staining was co-localised with desmoglein-3. Furthermore, ELISA confirmed the presence of anti-desmoglein-3 IgG4 antibodies in the patient's serum.²¹⁴ It is possible that the anti-desmoglein-3 antibodies triggered barrier dysfunction and subsequent development of CRS and nasal polyposis in this particular patient.

The desmosome junctions have briefly been examined in CRS. The key studies to date have identified reductions in one or more of the desmoglein proteins, in particular desmoglein-2.

Gastrointestinal barrier function as a paradigm

The gastrointestinal literature provides the majority of evidence describing barrier function in both health and disease. The gastrointestinal mucosal barrier is indispensable in maintaining separation of the inside of the host from the environment (gastrointestinal lumen). Additionally, the barrier needs to allow transport of necessary nutrients and participate in mucosal immune homeostasis. Below is a summary of the mediating factors of gastrointestinal barrier dysfunction (Table 3).

Inflammatory bowel disease

Mucosal barrier dysfunction is a well described feature of inflammatory bowel diseases (IBD), such as ulcerative colitis and Crohn's disease with clinical research on barrier dysfunction starting in the 1980s.²¹⁵ Both of these conditions provide examples of the interplay between microbial flora and mucosal dysfunction, particularly in susceptible individuals.²¹⁶

It is not understood whether the inflammation in IBD is a consequence or cause of the mucosal barrier dysfunction. However, there are animal models and clinical studies that support the concept that barrier dysfunction precedes the inflammation. Olson et al., (2006) demonstrated that a colitis predisposed mouse strain SAMP have an epithelial barrier defect that precedes the onset of inflammation. Additionally, this was also exhibited in the absence of gastrointestinal bacterial colonisation.²¹⁷ Peeters et al., (1997) examined the epithelial permeability of Crohn's disease patients, their relatives, and their non-Crohn's disease spouses. They identified that 25% of first degree relatives have increased intestinal permeability, although this did not follow any usual genetic pattern. This was coupled with the presence of an increased intestinal permeability in healthy

spouses, suggesting the primary insult may be a common environmental factor on a background predisposition to Crohn's disease.²¹⁸ Increased barrier permeability may be a marker for development of Crohn's disease. One case study described increased epithelial permeability in a first degree relative of a Crohn's affected person, who subsequently presented with the disease 8 years later.²¹⁹ Furthermore, mucosal permeability is a reliable predictor for clinical relapses of Crohn's disease.²²⁰

Immune system mediators are involved in the regulation of barrier integrity in IBD. Th1 cytokines TNF- α and IFN- γ are markedly increased in Crohn's disease, which subsequently disrupt the barrier with alterations in paracellular and transcellular pathways.²²¹ This is mediated by NF- κ B leading to a down regulation of ZO-1 protein expression and disorganised TJ localisation.²²² This concept is supported by the work of Suenart et al., (2002) showing restoration of a normal gut barrier and resolution of inflammation after treatment with an anti-TNF- α antibody in patients with Crohn's disease.²²³ Th2 cytokines are implicated in the barrier dysfunction of ulcerative colitis, particularly IL-13. Subepithelial mononuclear cells in ulcerative colitis produce significantly more IL-13 when compared to controls, and IL-13 has a dose dependent barrier disrupting effect *in-vitro*.²²⁴ This was evidenced by reductions in TEER, increases in Papp, and increased expression of the pore forming claudin-2 TJ protein. Additionally, IL-13 prevents repair of epithelial barrier gaps by reducing cell migration velocity.²²⁴ Unfortunately, two phase 2 clinical trials with the IL-13 antibodies anrukinzumab and tralokinumab have yielded poor results as an effective future treatment option for ulcerative colitis.²²⁵

Gastrointestinal microbes play a central role in the pathophysiology of IBD. Studies suggest that this is underpinned by microbial dysbiosis, and improper immune responses to resident (tolerance) and pathogenic (defence) organisms on a background

of epithelial susceptibility. Sellon et al., (1998) utilised IL-10 deficient germ free (sterile) mice to demonstrate that luminal bacteria are necessary for induction of colitis and immune system activation. Colonisation of these previously germ free mice results in the induction of typical colitis.²²⁶ Experimental mouse models of IBD have been developed to reproduce defects in barrier function, innate immunity, and adaptive immunity. Dextran sodium sulphate (DSS) is commonly used in mouse models to incite barrier dysfunction, which leads to IBD analogous inflammation.²²⁷ More recently it was observed that DSS induced barrier dysfunction has an effect on the gut microbiome. Fazio et al., (2014) conducted a microbiome analysis of DSS induced colitis in mice and found that after 3 days of DSS treatment the microbiome had profoundly shifted. Interestingly, this dysbiosis preceded any inflammatory changes and upon removal of the barrier disrupting factor the microbiome recovered.²²⁸ Another study demonstrated that DSS colitis induces changes in bacterial species richness and alters the community composition in both faecal and colonic samples.²²⁹

The expression and distribution of TJ proteins is altered in IBD gastrointestinal mucosa. Prasad et al., (2005) highlighted that the pore forming claudin-2 was heavily upregulated in both ulcerative colitis and Crohn's disease mucosa, and not in healthy patients. Conversely, claudin-3 and claudin-4 were reduced or showed altered distribution in IBD.²³⁰ Other studies have demonstrated that TJ proteins claudin-5, claudin-8 and occludin may be down regulated in active Crohn's disease, while ulcerative colitis exhibits downregulation of claudin-4 and claudin-7.^{231,232} Furthermore, even in inactive Crohn's disease the TJ proteins occludin and ZO-1 are absent in the apical layers and instead in the basolateral cell layers. This was observed in the absence of inflammation, again emphasizing the role of epithelial barrier function in initiation of IBD.²³³

Enteric bacteria and their extracellular products

The gastrointestinal tract establishes a large mucosal surface area that forms the interface between host and environment. This barrier needs to be able to transport essential nutrients and fluid, prevent uptake of detrimental molecules and waste, while simultaneously participating in immune system regulation. The healthy gastrointestinal tract contains commensal organisms, which live symbiotically together and do not induce disease.²³⁴ Given that the mucosal barrier needs to be breached for entry to the host, it is not unexpected that a variety of bacterial organisms exploit the regulatory and structural components.

Helicobacter pylori (*H. pylori*) is a common chronic bacterial infection associated with the development of gastritis, peptic ulcer disease, and implicated in the pathogenesis of gastric cancer. Literature over the past three decades has described the *H. pylori* mechanisms associated with disruption of the gastric mucosal barrier to facilitate host colonisation.²³⁵ The major barrier disrupting proteins are: cytotoxicity-associated gene A (CagA), vacuolating cytotoxin A (VacA), and high-temperature requirement A (HtrA).²³⁶ CagA is an 120 kDa protein, encoded by the *cag* pathogenicity island seen in highly virulent *H. pylori* strains. The pathogenicity island also encodes a type IV secretion system, which is used to deliver CagA into gastric epithelial cells when *H. pylori* interacts with the basolateral portion of the cell.²³⁷ CagA is known to alter several TJ, AJ and associated support proteins including ZO-1, JAM, E-cadherin, MARK2, and claudins.²³⁶ VacA is secreted as an 88 kDa monomer which oligomerizes in solution, until VacA undergoes proteolytic cleavage into two smaller active molecules. It is unclear how VacA increases epithelial permeability as a specific target has not been identified. However, it is known to cause an influx of extracellular Ca^{2+} and

rearrangement of the F-actin cytoskeleton.²³⁶ HtrA is a soluble serine protease, which specifically cleaves E-cadherin in the AJ complex and allows *H. pylori* to migrate across the cell layer.²³⁸ HtrA is remarkably thermostable, active across extreme pH changes, and resistant to a number of denaturing procedures.²³⁹ Interestingly, all three of *H. pylori* factors have been identified in secreted extracellular vesicles (EVs). CagA is found in associated with both the outer membrane of *H. pylori* and secreted EVs, while VacA is located within the EVs. HtrA is significantly enriched in the EVs, compared to the *H. pylori* outer membrane.²⁴⁰ Beyond the secreted toxins, chronic *H. pylori* infection is associated with significant reductions in mucosal zinc concentrations and a reciprocal increase in neutrophilic inflammation.²⁴¹

The majority of *Escherichia coli* (*E. coli*) are non-pathogenic commensals of the gastrointestinal tract, however specific pathogenic strains have been linked to mucosal barrier disruption. In particular, the enterohaemorrhagic *E. coli* (EHEC), enteropathogenic *E. coli* (EPEC), enterotoxigenic *E. coli* (ETEC), and adherent-invasive *E. coli* (AIEC).²⁴² EHEC is a producer of shiga toxin, which induces a severe haemorrhagic colitis. Murine *in-vivo* experiments have identified EHEC decreases expression of TJ proteins occludin, claudin-3, and increased claudin-2.²⁴³ Additionally, an *in-vitro* EHEC infection model resulted in alteration of ZO-1 via protein kinase C activation of MLCK.²⁴⁴ EPEC induces cytoskeletal contraction and subsequent tight junction dysfunction by phosphorylation of MLCK, and dephosphorylation of occludin.²⁴⁵ EPEC and EHEC produce *E. coli* secreted protein F (EspF), EspG, and EspM, which have been linked to barrier disruption via various mechanisms related to the type 3 secretion system of gram negative bacteria.²⁴⁶ Morampudi et al., (2017) demonstrated that EspG severely disrupts the crucial TJ protein tricellulin, resulting in rapid barrier disruption.²⁴⁷ ETEC produce numerous virulence factors including adhesions and

enterotoxins, such as heat labile toxin (LT), heat resistant toxin-a (STa), and heat resistant toxin-b (STb).²⁴⁸ LT is an 85 kDa protein that has structural similarities with Cholera toxin. *In-vitro* TEER and Papp of cell monolayers are significantly altered by LT, although the cellular target is unknown.²⁴⁹ STa is a small peptide with a molecular weight of 2000 Da, which activates a guanylate cyclase receptor resulting in activation of a G protein second messenger system. Secondary colon cell line T84 showed dramatic decreases in TEER when exposed to STa, however Papp remained unaffected.²⁵⁰ STb is a peptide of 5200 Da size, which is internalised by host endocytosis after binding to glycosphingolipid sulfatide in the gastrointestinal tract.²⁵¹ STb caused reductions in TEER, an increase in Papp, and alterations of F actin, ZO-1, occludin, and claudin-1. Interestingly, an 8-amino acid peptide sequence derived from STb was comparably as active on the TJ barrier as the full-length toxin. This peptide sequence is also shared by Zonula occludens toxin (ZOT) a TJ disrupting toxin of *Vibrio cholerae* (*V. cholerae*).²⁵¹ AIEC strains are known to affect the TJ barrier, with a previous *in-vivo* model demonstrating increased claudin-2 expression and increased permeability.²⁵² Gibold et al., (2016) recently described a novel virulence factor termed Vat-AIEC which contributes to bacterial penetration across the mucosal barrier.²⁵³ Additionally, recent works have identified that *E. coli* also package pathogenic toxins in EVs.²⁵⁴⁻²⁵⁶ Horstman and Kuehn, (2000) identified that LT was significantly augmented on the outside and inside of *E. coli* produced EVs. Furthermore, toxin and EV production was strain and growth condition dependent with increased EV production seen in more virulent strains.²⁵⁵ Cytolethal distending toxin, shiga toxin 2a, and shigella enterotoxin-1 have also been isolated from *E. coli* EVs.^{254,256}

V. cholerae is a highly virulent gram negative bacteria responsible for severe diarrhoea, dehydration, and if untreated can be fatal.²⁵⁷ *V. cholerae* secretes two factors that alter

the gastrointestinal TJ barrier by separate mechanisms. Hemagglutinin/protease (HA/P) is a member of the metalloprotease family, and secreted by pathogenic and non-pathogenic *vibrio* strains. Initial research identified that HA/P efficiently disrupts the TJ barrier as shown by reduction in TEER, disrupts ZO-1, and significantly redistributes F-actin.²⁵⁸ It was subsequently shown that HA/P degrades occludin in a highly specific manner by degrading only its extracellular domains. Redistribution of ZO-1 is thought to be secondary to either occludin degradation or via another indirect mechanism, as it is not degraded by HA/P.²⁵⁹ Fasano et al., (1991) discovered another toxin, which was named zonula occludens toxin (ZOT) after its effect on ZO localisation.²⁶⁰ A follow up study confirmed that the ZOT action is readily reversible, and that it interacts with a surface receptor to activate PKC induced alterations of G- and F-actin.²⁶¹ ZOT targets both leak and pore pathways of the barrier, however preferentially increases the macromolecular leak pathway.²⁶² As mentioned previously the ZOT activity is due to a small peptide (amino acids 288-293 of ZOT), which activates proteinase activated receptor-2 (PAR-2) due to its similarity with host PAR agonists.²⁶³ *V. cholerae* demonstrates various mechanisms by which bacteria utilise to alter the TJ barrier i.e. factors that directly target TJ proteins and those that exploit host signalling events to disrupt TJ proteins.

The majority of gastrointestinal toxin research focuses on gram negative bacteria, however there are notable examples of gram positive induced barrier disruption.

S. aureus has been reported to contribute to gastrointestinal mucosal barrier dysfunction, however the literature is limited. *S. aureus* superantigens SEA and SEB penetrate the mucosa by altering apical endosomal processing to utilise transcytosis to reach the basolateral cell border and lamina propria.^{264,265} Once in the subepithelial layers, superantigen T and B cell activation leads to decreases in TEER and increases in

permeability. Interestingly, the anti-inflammatory cytokine IL-10 significantly attenuated the immune mediated barrier dysfunction by SEB.²⁶⁶ Another study showed that SEB activated peripheral blood mononuclear cells alter the barrier and secretory function of an *in-vitro* colonic cell line. INF- γ and TNF- α were found to be the principal cytokines inducing the response.²⁶⁷ Kwak et al., (2012) established that HLA has barrier disrupting effects on colorectal cell line Caco-2. The target of HLA was noted to be on the basolateral portion of the cell monolayers, and when activated resulted in diminished TEER in a dose and time dependent pattern.²⁶⁸ Additionally, there were observable reductions in ZO-1, ZO-3, occludin and E-cadherin proteins, while mRNA expression levels of ZO-1 and occludin were significantly increased. The barrier changes seem to be secondary to extracellular Ca²⁺ influx, possibly due to HLAs pore forming function.^{268,269}

C. difficile is a spore forming gram positive anaerobic bacteria, that is associated with pseudomembranous colitis. *C. difficile* is known to produce several highly pathogenic toxins such as toxin A and toxin B, both of which target the TJ barrier.^{270,271} Toxin A and B are exceedingly effective at disrupting TEER and Papp barrier function with active concentrations as little as 0.7 $\mu\text{g/ml}$.^{270,271} These toxins inactivate the Rho family of GTPases, which are essential in the maintenance of F-actin. This precipitates F-actin reorganisation and subsequently results in considerable disruption of ZO-1, ZO-2, occludin, and E-cadherin.²⁷² Epithelial and myofibroblast TGF- β is a protective factor against low concentrations of *C. difficile* toxins, and this may partly explain why there are asymptomatic carriers of *C. difficile*.²⁷³

The gastrointestinal literature provides several examples of secreted bacterial factors that alter the mucosal epithelial barrier. These factors illustrate the diversity of bacterial mechanisms to alter the barrier function including direct targeting of intercellular

barrier proteins, targeting the cytoskeleton, or inducing host signals that alter barrier integrity.

Zinc and barrier function

Zinc is an essential trace element required for basic cell functions, immune regulation, and cell survival.²⁷⁴ In addition to these broad processes, zinc has important implications in the maintenance of mucosal barrier function.

Early research by Roy et al., (1992) demonstrated a reversal of intestinal permeability with zinc supplementation in children with acute and chronic diarrhoea. This was evidenced by normalisation of the lactulose mannitol urinary excretion ratio, as an indicator of permeability.²⁷⁵ Zinc's role in maintaining the epithelial barrier is supported by an experimental animal model of barrier dysfunction caused by protein malnutrition. This model demonstrated that high dose dietary zinc reverses reductions in TEER and increases in permeability, although the primary mechanism was unknown.²⁷⁶ Additionally, zinc supplementation in children with Shigellosis improves intestinal barrier function showing significant improvements in permeability and nutritional absorption.²⁷⁷ The mechanism of zinc induced protection from *Shigella* infection was only recently described. Kazi et al., (2014) demonstrated that Shigella infection leads to reductions in claudin-1 and claudin-2 via the second messenger system cAMP, which was readily reversed with zinc treatment.²⁷⁸

The effects of zinc supplementation in IBD were studied on a small cohort of 12 patients with inactive Crohn's disease. Permeability testing revealed inactive patients show increased barrier permeability. After oral zinc supplementation barrier permeability returned to normal in 10 of 12 patients.²⁷⁹ This suggests that zinc is not only effective for

remedying bacterially induced barrier dysfunction, but also for the intrinsic barrier dysfunction seen in Crohn's disease.

In-vitro studies have further emphasised the effects of zinc on the maintenance and enhancement of gastrointestinal barrier function. A study utilising Caco-2 cells that were cultivated in zinc deficient conditions demonstrated a significantly reduced TEER over maturation of the cultures across 18 days. This change was coupled with immunofluorescence defects in TJ proteins occludin and ZO-1, AJ proteins E-cadherin and β -catenin, and cytoskeletal proteins F-actin and β -tubulin. Quantitative protein analysis identified lower levels of occludin, ZO-1, and β -tubulin. Additionally, zinc deficient cultures produced higher chemotactic cytokines and induced the transepithelial migration of polymorphonuclear neutrophils.²⁸⁰ The authors Miyoshi, Tanabe, and Suzuki, (2016) demonstrated that intracellular zinc chelation with TPEN (N,N,N',N'-tetrakis(2-pyridinylmethyl)-1,2-ethanediamine) results in significant alteration of both TEER and permeability with no cell apoptosis or death. Barrier dysfunction was due to down regulation of both occludin by increased proteolysis, and claudin-3 at the transcriptional level.²⁸¹

Interestingly, a previous study showed that even a healthy mucosal barrier is enhanced by zinc supplementation. This was evidenced by an increase in electrical tightness measured by TEER, and a decrease in large molecule permeability. Claudin-2 and claudin-7 were significantly reduced at the protein level by the zinc supplementation.²⁸² Shao et al., (2017) showed that zinc supplementation of Caco-2 cells increased cell proliferation, increased TEER, and enhanced ZO-1 expression. The barrier function alterations were mediated by activation of the intracellular signalling phosphoinositide 3-kinase (PI3K) pathway. PI3K further activates AKT and mTOR pathways, both of which are involved in cell cycle regulation and proliferation.²⁸³ This has potential

implications in the repair of mucosal injury and barrier dysfunction by targeting this pathway with zinc or a novel agent.

Table 3. Summary of factors products with gastrointestinal mucosal barrier disrupting properties.

Factor/toxin/protein	Factor function/family	Mass (kDa)	Cellular compartment	Mechanism of barrier dysfunction
Cytokine - TNF- α ²²²	—	—	—	Decreased TEER, increased Papp—secondary to NF- κ B. ZO-1 disruption.
Cytokine - IFN- γ ²³⁰	—	—	—	Combined with TNF- α : alters claudin 2-4, increases Papp, decreases TEER
Cytokine - IL-13 ^{224(p13)}	—	—	—	Decreases TEER – dose and time dependent. Increases Papp. Upregulates claudin-2.
<i>C. difficile</i> - Toxin A ²⁷³	Cysteine-type peptidase activity/ Glycosyltransferase family 44	308	Secreted, extracellular	Inactivates Rho family of GTPases, causes F-actin reorganisation. Alterations in ZO-1, ZO-2, occludin, & E-cadherin.
<i>C. difficile</i> - Toxin B ²⁷²	Cysteine-type peptidase activity/ Glycosyltransferase family 44	269	Secreted, extracellular	Inactivates Rho family of GTPases, causes F-actin reorganisation. Alterations in ZO-1, ZO-2, occludin, & E-cadherin.
<i>E. coli</i> - EspG ²⁴⁷	Cysteine-type endopeptidase	43	Secreted, extracellular region	Alpha tubulin specific protease, alters tricellulin.
<i>E. coli</i> - LT ²⁴⁹	Enterotoxin	85	Extracellular, EV	Decreases TEER, increases Papp. Structural similarities with cholera toxin. Unknown target
<i>E. coli</i> - STa ²⁵⁰	Enterotoxin	2	Extracellular	Activates guanylate cyclase receptors: decreases TEER.
<i>E. coli</i> - STb ²⁵¹	Enterotoxin	5.2	—	Internalised by cell. Possibly causes Ca ²⁺ influx: alteration of F actin, ZO-1, occludin, & claudin-1. Similar to ZOT toxin.
<i>E. coli</i> - Vat-AIEC ²⁵³	Serine protease/ Autotransporter	—	—	Increases bacterial penetration across mucosa, degrades mucin. Increased claudin-2 expression, & increased Papp.
<i>H. pylori</i> - CagA ^{236,237}	Toxin transmembrane transporter	120	Extracellular, EV	Phosphorylation dependent changes in ZO-1, JAM, & E-cadherin. Inhibits Par1b/MARK2.
<i>H. pylori</i> - VacA ^{236,237}	Toxin/AT-1 family	88	Cell outer membrane, secreted, EV	Ca ²⁺ influx & F-actin rearrangement.
<i>H. pylori</i> - HtrA ²³⁸	Serine-type endopeptidase/ SIC family	51	Periplasm, EV	Cleaves E-cadherin.
<i>S. aureus</i> - HLA ²⁶⁸	Pore forming toxin	35	Extracellular, EV	ZO-1, ZO-3, occludin, & E-cadherin reductions; due to Ca ²⁺ influx.
<i>S. aureus</i> - SEB ²⁶⁶	Enterotoxin	29	Extracellular	INF- γ and TNF- α mediated TEER reduction & Papp increase. Attenuated by IL-10.
<i>V. cholera</i> - HA/P ²⁵⁹	Metalloprotease	65	Secreted, extracellular, EV	Cleaves extracellular occludin, indirectly alters ZO-1 & F-actin.
<i>V. cholera</i> - ZOT ^{261,263}	Enterotoxin	44	Outer membrane, secreted extracellular	Activates PKC: induces G and F-actin changes. PAR2 agonist. Alters TEER & Papp.
Zinc chelator - TPEN ²⁸¹	Intracellular zinc chelator	—	—	TEER reduction, & Papp increase.

Dermatological barrier function as a paradigm

The skin barrier is vitally important as the physical barrier between the host and environment. The components of the barrier function can be divided into the superficial stratum corneum (components include corneocytes, lipid matrix, keratin filaments) and the nucleated epidermis (components include TJs, AJs, GJs, and keratin proteins).²⁸⁴ As the nucleated epidermis is a stratified multilayered epithelium it is formed (from superficial to deep) by the stratum granulosum, stratum spinosum, and stratum basale. Each layer acquires a specific set of intercellular junction proteins, however TJ function and regulation primarily occurs in the stratum granulosum.²⁸⁵ The focus of this section will be on the abnormalities in the nucleated epidermal barrier function, in particular TJ abnormalities due to microbes or relevant host pathologies (Table 4).

Epidermal bacteria and their extracellular products

S. aureus has been implicated in the development and persistence of dermatological pathologies. *S. aureus* produces a family of exfoliative toxins, which are responsible for scalded skin syndrome. Exfoliative toxins A and B are structurally similar to serine proteases; however, they have very specific host targets.²⁸⁶ The targets were identified almost 3 decades after the description of the clinical disease and characterization of the toxin. Amagai et al., (2000) demonstrated that desmosomal cadherin desmoglein-1 was effectively cleaved by exfoliative toxin A (ETA).²⁸⁷ Further studies confirmed that exfoliative toxin B also targeted desmoglein-1.²⁸⁸ In skin, desmoglein-1 is found throughout the epithelium. However, other desmogleins are specific to the site such as desmoglein-3 which is found in the basal layers and in mucosa. This may explain why the effects of this toxin are not seen on mucosa as desmoglein-3 is able to compensate for the loss of desmoglein-1.²⁸⁹

Bukowski et al., (2000) identified that children with atopic dermatitis (AD) were significantly more likely to be colonised with *S. aureus* when compared to healthy controls. Additionally, the *S. aureus* strain was more likely to produce a form of superantigen such as SEA, SEB, SEC, SED, or TSST-1. Children colonised with *S. aureus* had more severe AD disease scores, and those with a superantigen producing strain had the worst severity. A subset of these patients with SEB positive *S. aureus* demonstrated higher percentages of intradermal superantigen responsive T cells²⁹⁰ Currently, it is not known how *S. aureus* superantigens influence epidermal intercellular junction proteins, or whether they gain access across the barrier due to another mechanism. A study by Ohnemus et al., (2008) established that toxin negative *S. aureus* and *Staphylococcus epidermidis* (*S. epidermidis*) strains also alter the intercellular barrier junction in skin. *In-vitro* exposure to superantigen null *S. aureus* causes significant reductions in the staining intensity of claudin-1, occludin, ZO-1, E-cadherin, desmoplakin 1 and 2, and protein kinase C. Comparatively, *S. epidermidis* appears less virulent and only affects ZO-1. The effects of superantigen null *S. aureus* were replicated in an *in-vivo* porcine skin model, showing dramatic reductions in ZO-1, claudin-1, E-cadherin, and desmoplakin localisation.²⁹¹ The molecular mechanism or responsible factor related to these effect has yet to be elucidated.

S. aureus strains isolated from the skin of atopic dermatitis patients exhibited proteolytic activity, which was largely due to the serine protease family.²⁹² The proteolytic activity of isolates from atopic dermatitis patients tended to be moderate to high, while isolates from control patients had essentially nil or weak proteolytic activity.²⁹² Hirasawa et al., (2010) hypothesised that the *S. aureus* protease family may potentiate epidermal barrier dysfunction in AD.²⁹³ Utilising a mouse model the authors demonstrated that skin treatment with increasing doses of *S. aureus* V8 serine protease resulted in significantly

increased epidermal permeability to water and small molecule penetration. Barrier disruption was observed in doses as low as 5 µg/ml, while *S. aureus* production of V8 protease is thought to be in the range of 50 µg/ml.²⁹²

Streptococcus pyogenes (*S. pyogenes*) is a common cause of invasive soft tissue and skin infections. Cywes and Wessels, (2001) showed that *S. pyogenes* binds to keratinocyte CD44 to induce a change in the cellular cytoskeleton. The cytoskeletal rearrangement subsequently opens the intercellular junctions with loss of ZO-1 and E-cadherin on immunofluorescence microscopy. Additionally, intercellular disruption was associated with increased translocation of *S. pyogenes* across the cellular layers. Interestingly, they found that the response was likely due to the hyaluronic acid capsular polysaccharide produced by *S. pyogenes*.²⁹⁴

Inflammatory skin disorders

AD is an inflammatory skin disorder that is characterised by excessive Th2 cell activity, and enhanced immune response to external allergens. Recent studies have identified innate barrier defects in affected and non-affected skin of AD sufferers. De Benedetto et al., (2011) evaluated the TJ localisation and gene expression in AD. They identified that claudin-1 and claudin-23 expression are reduced at the protein and mRNA levels in the epidermis; this was identified even without active disease. Furthermore claudin-1 expression showed an inverse relationship with total IgE and eosinophil counts. Functional barrier tests showed that *ex-vivo* AD epidermis has significantly reduced TEER and increased permeability. In addition, *in-vitro* claudin-1 silencing observed comparable effects on barrier function.²⁹⁵ Hata et al., (2002) demonstrated that non-affected AD skin had increased penetration of hydrophilic and lipophilic dyes.²⁹⁶ Similar

to Crohn's disease, this suggests that the barrier defect exists prior to the initiation of inflammation and injury.

AD patients are known to exhibit higher expression of the cytokines IL-1 β , TNF- α , and IL-12 in the epidermis, and also generate a larger response to allergens when compared to healthy controls.²⁹⁷ IL-1 β and TNF- α treatment of *ex-vivo* porcine and human skin models results in intensified localisation of occludin and ZO-1, and down regulation of claudin-1 protein localisation and gene expression. This was coupled with an initial increase in TEER, followed by a maximal decrease of TEER at 72 hours.²⁹⁸ Ku et al., (2013) demonstrated that TLR2 agonists such as *S. aureus* derived peptidoglycan and synthetic TLR2 agonists tightened the epidermal barrier with increases in TEER. An induction of TJ proteins claudin-1, claudin-23, occludin, and ZO-1 was observed simultaneously with changes in TEER. The authors suggested that this may be a protective event, that could be induced by an organism trying to colonise or invade the epithelium.²⁹⁹ Interestingly, TLR1 and TLR2 are under expressed in patients with AD, and are inversely correlated with increased epithelial permeability.²⁹⁹ Since TLR2 positively regulates TJ proteins this may explain the previous findings that claudin-1 and claudin-23 are more likely to be under expressed in patients with AD.

Furthermore, GJ function appears to be important in maintenance of skin integrity and implicated in AD pathophysiology. Tawdy, Rashed, and Alhanafy, (2011) conducted a small observational study on patients with and without atopic dermatitis, which identified that connexin-43 mRNA was significantly upregulated in atopic dermatitis skin biopsies. ³⁰⁰ De Benedetto et al., (2011) found that connexin-26 and connexin-62 were upregulated in atopic dermatitis, which they confirmed was due to reduction in claudin-1 expression.²⁹⁵

Psoriasis is a chronic inflammatory skin condition with a predominant Th1/Th17 inflammatory profile. The pathophysiology is complex with contributing genetic, immunological, and environmental factors.³⁰¹ A defective stratum corneum is central to psoriasis, however there are studies that outline abnormalities of intercellular junction proteins in the nucleated epidermis. In psoriatic skin, keratinocytes express occludin earlier as they migrate to the most superficial portion of the nucleated epidermis. In comparison, healthy skin only expresses occludin at the apical most intercellular junction or the so called “kissing point”.³⁰² Further research supported these findings, and additionally found that ZO-1 expression was abnormally broad across the epithelium. Kirschner et al., (2009) identified that TJ protein localisation is altered in the early development of psoriasis plaques. Their study found that claudin-1 and claudin-7 staining was significantly decreased, and alteration of JAM-A in the apical most epithelial layers. Interestingly, the loss of TJ expression was detected near CD15+ expressing inflammatory granulocytes.²⁹⁸ It is still unclear whether the TJ response in psoriasis is a primary defect or secondary to another inciting factor. It is possible that the TJ protein expression is initiated earlier in epidermal cell proliferation to compensate for the barrier defects of the stratum corneum.

Table 4. Summary of factors with epidermal barrier disrupting properties.

Factor/toxin/protein	Factor function/family	Mass (kDa)	Cellular compartment	Mechanism of barrier dysfunction
Cytokines - IL-1 β ²⁹⁸	—	—	—	Down regulation of claudin-1 protein/mRNA. Decreased TEER
Cytokines - TNF- α ²⁹⁸	—	—	—	Down regulation of claudin-1 protein/mRNA. Decreased TEER
<i>S. aureus</i> - ETA ²⁸⁶	Serine protease with limited specificity	31	Extracellular/secreted	Cleaves desmoglein-1
<i>S. aureus</i> - ETB ²⁸⁶	Serine protease with limited specificity	30	Extracellular/secreted	Cleaves desmoglein-1
<i>S. aureus</i> - V8 protease ²⁹³	Serine protease	29	Extracellular/secreted	Unknown target. Increased epidermal permeability
<i>S. pyogenes</i> - Hyaluronic acid capsular polysaccharide ²⁹⁴	Repeating units of hyaluronic acid	>10 ⁶	Cell membrane surface/bacterial capsule	Alters ZO-1 & E-cadherin. Increased bacterial translocation

Pulmonary barrier dysfunction as a paradigm

Compared to the study of the gastrointestinal and dermatological barriers, the lower airway barrier is inherently more difficult to access and introducing inflammatory agents, bacteria or bacterial products in animal models is more invasive. The literature presents notable examples of barrier disruption mechanisms, which could be likened to the upper airway barrier (Table 5).

Bacterial factors altering the lower airway barrier

P. aeruginosa toxins such as elastase, exotoxin A, and exoS are known to disrupt TJ structures both *in-vitro* and *in-vivo*.³⁰³⁻³⁰⁶ Treatment of lung epithelial cells with *P. aeruginosa* elastase results in dramatic reductions in TEER, ZO-1, and occludin, within 15 minutes of treatment. *P. aeruginosa* elastase induced barrier dysfunction is dependent on PKC signaling, which subsequently removes ZO-1 and occludin from the perijunctional membrane.³⁰⁴ Aerosolized *P. aeruginosa* elastase increased the rate of

transfer of radiolabeled albumin across the lung barrier in a small animal model in a dose and time dependent manner. Additionally, the increased paracellular permeability in this model was not associated with interstitial oedema, indicating a specific disruption of the leak pathway.³⁰⁷ Another study compared the pulmonary barrier disrupting activities of *P. aeruginosa* elastase and LPS. *P. aeruginosa* elastase exhibited more barrier disrupting effect than LPS, as measured by exchange of aerosolized albumin (air to blood direction) and endogenous albumin (blood to pulmonary air spaces). However, LPS demonstrated some alteration of the barrier integrity, which was associated with increased inflammatory mediators (white blood cells, neutrophils, IL-8).³⁰⁸ This suggests that the barrier disrupting properties of LPS may be indirect, via a proinflammatory response.

There is little *in-vivo* evidence demonstrating the pulmonary barrier disrupting effects of *S. aureus*. McElroy et al., (1999) utilized a rat model of *S. aureus* pulmonary infection including a HLA defective mutant strain, which suggested that HLA is involved in disrupting the pulmonary barrier. However, this was not specific to intercellular junction disruption and may be due to alveolar cell necrosis/apoptosis.³⁰⁹ Another small animal study demonstrated that beta hemolysin (HLB) is necessary to induce inflammation and increase pulmonary leakiness. The sphingomyelinase activity of HLB targets the surface epithelial protein syndecan-1.³¹⁰ Intestinal cell experiments have previously shown that syndecan-1 is vital in maintaining barrier function when stimulated with *S. aureus*.³¹¹

The opportunistic pathogen *Burkholderia cenocepacia* seen in cystic fibrosis has shown TJ altering functions *in-vitro*, showing disrupted occludin staining and a functionally impaired barrier.³¹² Similarly, *Burkholderia thailandensis* and *Francisella tularensis* (*F. tularensis*) decrease TEER, increase permeability, and disrupt occludin localisation. Both

organisms show increasing transepithelial migration and TNF- α release with higher bacterial loads.³¹³ A specific secreted factor from either *Burkholderia* species or *F. tularensis* has not been identified.

Interestingly, treatment of bronchial epithelial cells with the TLR2 ligands peptidoglycans and Pam3CSK4 (P3C) results in an increase in barrier function, evidenced by significant increases in TEER and less permeability. This was associated with increased gene expression of ZO-1 and claudin-1 by 30 and 200 fold respectively, and increases in the TJ localisation of each protein.³¹⁴ Furthermore, there is suggestion that TLR2 may influence GJ protein connexin 43.³¹⁵ These examples could represent a TLR2 dependent epithelial defence mechanism to prevent bacterial penetration or entry of toxins.

There are examples of bacteria and toxin induced pulmonary endothelial barrier disruption. Although, this barrier is different from a mucosal interface it highlights potentially important bacterial invasion mechanisms. Pai et al., (2012) demonstrated that *S. aureus* derived LTA induces barrier dysfunction in pulmonary endothelial cells.³¹⁶ This was shown to be due to TLR2 activation and subsequent generation of ROS and reactive nitrogen species. However, there was no visualisation of the barrier proteins or structures to further understand how LTA or TLR2 activation influences the endothelial TJ/AJ proteins. Another study found that mice challenged with intratracheal heat killed *S. aureus* exhibited prominent pulmonary leakage of labelled albumin.³¹⁷ Gram positive pneumococcal species derived pneumolysin toxin and gram negative bacteria derived LPS treatment of endothelial monolayers leads to a reduction in vascular specific AJ proteins. A mouse model demonstrated that pneumolysin and LPS separately induce pulmonary endothelial barrier dysfunction. Additionally, pneumolysin was shown to increase intracellular calcium flux and increase barrier dysfunction by activating PKC.³¹⁸

Zinc and the lower airway barrier

Zinc's role in the lower airway barrier function is not completely understood. However, there is evidence that zinc contributes to barrier maintenance and protection against inflammatory insults.

Bao and Knoell, (2006) found that zinc depletion enhances barrier disruption and apoptotic responses to IFN- γ and TNF- α in both fully differentiated human lung airway epithelial cells and human alveolar epithelial cells.³¹⁹ Barrier integrity was quantified using TEER and macromolecular permeability, showing dysfunction after 4 hours of treatment with inflammatory cytokines and intracellular zinc chelator TPEN. Interestingly, TPEN or cytokine treatment alone did not alter the barrier function. Combination treatment (TPEN, IFN- γ and TNF- α) leads to cleavage of AJ proteins E-cadherin and β -catenin, which was thought to be due to an increase in caspase 3 activity. Additionally, zinc replacement was more effective at preventing barrier disruption and apoptosis than inhibition of caspase 3, suggesting that AJ cleavage is not entirely mediated by this pathway.

More recent research has shown that *in-vitro* bronchial epithelial cells down regulate TJ proteins claudin-1, ZO-1, and occludin in response to zinc depletion. This was associated with a reduction in TEER and increase in macromolecular paracellular permeability. Additionally, this model demonstrated that cigarette smoke extract produced an additive effect with the local zinc deficiency.³²⁰ These studies imply that zinc deficiency may predispose the epithelial barrier to further disruption when challenged by external or inflammatory factors.

Table 5. Summary of factors with pulmonary barrier altering properties.

Factor/toxin/protein	Factor function/family	Mass (kDa)	Cellular compartment	Mechanism of barrier dysfunction
Bacterial cell wall - Lipopolysaccharide (Pseudomonas derived) ³⁰⁸	Gram negative bacterial cell wall component. Repeating subunits	—	Cell wall, EV	Increase in pulmonary endothelial permeability
Gram positive pneumococci species - Pneumolysin ³¹⁸	Cholesterol binding, pore forming cytolysin	53	Extracellular, cell membrane	Decreased in endothelial/vascular specific VE cadherin. Decreased TEER. Increased intracellular calcium and PKC activity
<i>P. aeruginosa</i> - Elastase ^{303,307,308}	Cleaves elastin, collagen, Ig/ Peptidase M4 family	53	Extracellular	Decreased TEER, ZO-1, and occludin via PKC signaling
<i>P. aeruginosa</i> - Exotoxin A ³⁰⁵	Inhibits elongation factor-2/ Mono-ADP-ribosyltransferase family	66	Extracellular	Decreased TEER when applied to basal cell surface; decrease ZO-1 and ZO-2. Blocks TJ synthesis
<i>S. aureus</i> - HLA ³⁰⁹	Pore forming toxin	35	Extracellular, EV	Alveolar cell apoptosis/necrosis mediated pulmonary barrier dysfunction
<i>S. aureus</i> - HLB ³¹⁰	Neutral sphingomyelinase	33	Extracellular	Increased pulmonary barrier permeability via Syndecan-1 shedding (neutrophil chemotactic factor)
<i>S. aureus</i> derived - LTA ³¹⁶	Membrane associated cell wall component. Repeating subunits	—	Cell wall, EV	Pulmonary endothelial barrier dysfunction: increases permeability to albumin.
TLR2 agonists³¹⁴ - Peptidoglycans - PamC3SK4	—	—	—	Barrier enhancement: increased TEER, decreased Papp. Increased ZO-1 and claudin-1 gene expression
Zinc depletion + Inflammatory cytokines - TPEN + IFN- γ + TNF- α + FasAb ³¹⁹	—	—	—	Decreased TEER, increased Papp. Cleavage of AJ proteins mediated via caspase 3

Potential Mediators of Mucosal Barrier Disruption in Chronic Rhinosinusitis

The above discussion provides a basis for the investigation of mediators that may potentiate mucosal barrier dysfunction in CRS. There are several *in-vitro* reports modelling the effects of inflammatory factors, and bacteria or their products on the TJ/AJ barrier outside of the sinonasal cavity. Previous studies have utilised airway cell models to demonstrate the barrier effects of host inflammatory factors relevant to CRS. Bacteria and bacterial products are a major contributor to barrier dysfunction in epithelial of the intestines, skin, and lower airways.^{242,293,305,315} The capabilities of several bacterial organisms to generate barrier disrupting products and the host factors which alter barrier function are of particular interest to CRS pathophysiology. Additionally, considering the role of zinc in both gastrointestinal and pulmonary barrier dysfunction it would be noteworthy to explore this in CRS as a potential contributor to barrier dysfunction. Thus far, little is known about the role of zinc in CRS, and there are no reports of its influence on mucosal barrier integrity.

Inflammatory mediators

Several studies have examined the effects of various cytokines and proinflammatory mediators on airway barrier integrity (Table 6). IFN- γ and TNF- α combinations have been shown to alter the barrier integrity of bronchial epithelial cells, specifically by disrupting occludin, ZO-1, and JAM in a PKC dependent manner.^{188,196} Another study identified that TNF- α alters TJ and AJ protein localisation of claudin-3, claudin-4, claudin-8, occludin, E-cadherin, and p120-catenin via the non-receptor tyrosine src-kinase family.³²¹ Soyka et al., (2012) demonstrated that IL-4 and IFN- γ alter barrier

function and TJ localisation.²⁰ Furthermore, IFN- γ treatments of HNEC-ALI cultures derived from controls, CRSsNP, and CRSwNP patients results in separation of cellular contacts, evidenced by duplicated peripheral staining of occludin and ZO-1, whereas gene expression of claudin-2 and ZO-2 are upregulated after IFN- γ treatments.²⁰ Zuckerman et al., (2008) observed that IFN- γ increased protein levels and staining intensity of desmoglein-2, while TNF- α and IL-13 had the opposite effect.¹⁷⁵ Additionally, other studies have demonstrated cytokines IL-4, IL-9, IL-13, IL-17, IL-22, and IL-26 are associated with *in-vitro* barrier dysfunction and altered TJ/AJ protein expression and localisation.^{196,322,323}

Table 6. Summary of inflammatory mediators implicated in airway barrier disruption

Cell model	Stimulus	Brief Method	Key findings
I6HBEo- secondary cell line (submerged) ¹⁹⁶	Combination IFN- γ , & TNF- α	IF: occludin WB: claudin-1, & occludin	- Increased levels of claudin-1 at 24 hours. Both claudin-1 and occludin reduced at 72 hours - Disrupted occludin staining at 72 hours
I6HBEo- secondary cell line (submerged) ³²⁴	IL-4, IL-13, IL-25, IL-33, TSLP +/- JAK inhibitors	TEER, & Papp IF: claudin-4, E-cadherin, β -catenin, occludin, ZO-1 WB: claudin (1, 2 & 3), E-cadherin, occludin, ZO-1	- IL-4 decreases TEER and increases Papp in JAK dependent manner - IL-4 altered TJ & AJ protein localisation - TJ & AJ protein levels were not reduced - IL-13 similarly altered TEER and Papp
HBE4-E6/E7 (submerged) ¹⁷⁵	IFN- γ , TNF- α , IL-13	IF & WB: Desmoglein-2	- IFN- γ caused an increase in desmoglein-2 staining; while TNF- α , & IL-13 decreased staining
HNEC (submerged) ³²⁵	TLR ligands: TLR2L, TLR3L (poly I:C), TLR4L, TLR7/8L, TLR8L, TLR9L	TEER WB: JAM-A IF: JAM-A, occludin	- JAM-A levels reduced by poly I:C. JAM-A, & occludin localisation reduced by poly I:C - Mediated via PI3K & p38 MAPK pathways
HNEC-polyp (submerged) ¹⁹⁴	IL-13, IL-17 +/- Dexamethasone; Fluticasone; p38 MAPK inhibitor; MKP-1 siRNA	mRNA: occludin WB: occludin	- IL-13 and IL-17 reduce occludin mRNA and protein expression; attenuated by both dexamethasone and fluticasone - p38 MAPK inhibition increases occludin protein expression.
I6HBEo- secondary cell line (ALI) ³²⁶	LPS & Pam3CSK4. +/- p38 MAPK inhibitor, TGF- β inhibitor	TEER, & Papp mRNA: claudin (7 & 10)	- LPS & Pam3CSK4 decrease claudins 7 & 10 - Barrier disruption requires p38 MAPK and TGF- β signaling
I6HBEo- secondary cell line (ALI) ³²⁷	Pam3Cys, Poly I:C, LPS, flagellin, CpG, +/- PKC inhibitors	TEER, Papp IF: E-cadherin, B-catenin, occludin, ZO-1, & F-actin	- Poly I:C reduced TEER, increased Papp, & altered junctional localisation - Mediated via PKD phosphorylation
HBEC (ALI); plus cystic fibrosis patient derived cells ¹⁸⁸	IFN- γ , IL-1 β , & TNF- α +/- PKC inhibitors	Ussing chamber R_T , & Papp IF & WB: JAM, ZO-1, claudin (1 & 4), & occludin mRNA: JAM, ICAM	- Combination IFN- γ & TNF- α : R_T decreased, increased Papp, disrupted ZO-1 and JAM, decreased ZO-1 and JAM protein levels, decreased JAM mRNA & increased ICAM-1 - PKC inhibitors reduced barrier effect
HBEC (ALI) ³²¹	TNF- α +/- src-family kinase inhibitor	TEER, & Papp IF: claudin (3, 4, & 8), occludin, E-cadherin, p120-catenin	- TNF- α decreased TEER, increased Papp, and altered TJ & AJ localisation - Src-family kinase inhibitor reduced the TNF- α effect on barrier integrity
HBEC (ALI) ³²²	IL-9, & IL-13	TEER	- IL-9, IL-13 & combination all reduced TEER - Exposure over 28 days of culture
HNEC (ALI) – controls, non-eosinophilic & eosinophilic polyp cells ³²⁸	TGF- β 1	TEER, & Papp IF: occludin, & ZO-1	- Decreased TEER, increased Papp, and disrupted TJ localisation in all groups - Baseline barrier functions were affected in both polyp groups
HNEC-polyp (ALI) ³²³	IFN- α , IFN- β , IFN- γ , IL-1 β , TNF- α , IL-4, IL-5, IL-13, IL-17, IL-22, IL-26	TEER, & Papp IF: ZO-1	- Th17 cytokines: IL-17, IL-22, & IL-26 significantly disrupted the airway barrier
HNEC (ALI) – controls, CRSsNP, CRSwNP cells ²⁰	IFN- γ , IL-4 & IL-17	TEER & Papp IF: occludin, & ZO-1 mRNA: claudin (1 & 2), occludin, ZO (1 & 2)	- TEER reduced, Papp increased by IFN- γ & IL-4; similar response between groups. - IFN- γ caused TJ widening, IL-4 caused disruption of TJs - IFN- γ caused upregulation in claudin-2 and ZO-2 gene expression

(AJ) adherens junction; (ALI) air-liquid interface; (EM) electron microscopy; (HBEC) human bronchial epithelial cells; (HNEC)

human nasal epithelial cells; (IF) immunofluorescence; (MAPK) mitogen-associated protein; (PKC) protein kinase C; (PKD)

protein kinase D; (TJ) tight junction; (TSLP) thymic stromal lymphopoietin; (WB) western blot.

Microbial mediated sinonasal barrier dysfunction

When compared to the effects of cytokine and proinflammatory mediators, little is known about the bacterial influence on the airway barrier. Clarke et al., (2011) demonstrated *in-vivo* that *H. influenzae* and *S. pneumoniae* intranasal colonization influenced tight junction regulation.³²⁶ Their research found that claudin-7 and claudin-10 gene expression were significantly downregulated after colonization with either organism. It was confirmed that this was mediated via TLR2 or TLR4 signaling relating to gram positive or gram negative stimulation. Additionally, stimulation of TLR4 (with gram negative derived LPS) can lead to translocation of gram positive bacteria *S. pneumoniae* suggesting synergy between different organisms.³²⁶ An *in-vitro* airway model using the 16HBE14o- bronchial cell line provided evidence that *H. influenzae* and *S. pneumoniae* both alter barrier integrity as measured by TEER and paracellular permeability, via TLR2 or TLR4 downregulation of claudin-7 and claudin-10. This occurred through activation of p38 MAPK and TGF- β , with subsequent expression of the transcription factor SNAIL1.³²⁶ SNAIL1 has previously been shown to suppress the expression of various claudins.³²⁹

There is a plethora of evidence to implicate *S. aureus* in the pathogenesis of CRS. *S. aureus* is associated with the initiation and persistence of CRS, recurrent infection, and poorer postoperative outcomes.^{91,95,330,331} There is however, a paucity of literature regarding the mucosal airway barrier altering effects of *S. aureus*.

Research conducted by Malik et al., (2015) studied the effects of *S. aureus* supernatant products on HNEC-ALI culture barrier function.¹⁹ In this study, bacterial conditioned media from three strains of *S. aureus* (ATCC 13565, 14458, and 25923) was applied to the HNEC-ALI cultures. It was demonstrated that *S. aureus* ATCC 13565 was able to disrupt the TJ barrier, which was evidenced by dose dependent reductions in TEER and

supported by electron microscopy. Furthermore, immunofluorescence microscopy of the TJ protein ZO-1 revealed discontinuous staining after *S. aureus* supernatant exposure compared to the continuous loop ZO-1 staining in an intact barrier. Beyond the mucosal barrier measures it was seen that this strain did not denude the sinonasal cilia, but it did alter the ciliary function.¹⁹ The factor(s) responsible were not elucidated in this study, although it was postulated it could be due to the SEA superantigen.

Steelant et al., (2015) published a conference abstract that described the barrier disrupting effects of SEB on a secondary bronchial epithelial cell line. SEB exposure resulted in decreased TEER, increased permeability, and decreased gene expression of claudin-4, occludin, and ZO-1. Conversely, occludin phosphorylation was increased, which may represent internalization of the protein.³³² Furthermore, Steelant et al., presented further work demonstrating that cells harvested from CRSwNP show more barrier dysfunction when stimulated with SEB compared to control cells. TLR2 and TLR4 were found to be increased in the CRSwNP cell population with TLR4 found to be important in regulating occludin expression in response to SEB.³³³

TLR mediated barrier dysfunction appears to be implicated in airway cell models. The TLR3 ligand polyinosinic:polycytidylic (Poly I:C) alters the localisation of several TJ and AJ proteins via different protein kinases.^{325,327} Both Pam3CSK4 (TLR2) and LPS (TLR4) have demonstrated barrier altering effects *in-vitro*. Airway barrier dysfunction by these pathways is dependent on p38 MAPK and TGF- β signalling.³²⁶ TGF- β directly alters barrier function and TJ localisation of ZO-1 and occludin in HNEC-ALI cultures derived from control, non-eosinophilic and eosinophilic polyp patients. Interestingly, cultures derived from non-eosinophilic and eosinophilic polyp patients exhibit abnormal barrier function phenotypes without a stimulus and generate a larger response to TGF- β stimulation compared to controls.³²⁸

***Staphylococcus aureus* toxins and virulence factors**

The literature demonstrates several mechanisms for microbes to disrupt the intercellular barrier. As discussed there is evidence for airway barrier dysfunction secondary to *S. aureus*. Additionally, there are several *S. aureus* toxins or secreted factors that show barrier disrupting properties in other epithelial barriers, are structurally similar to barrier disrupting toxins of other pathogens, or have important associations with CRS. Review of microbial mediated barrier dysfunction illustrates the role of bacterial cell wall and membrane components. Previous studies have demonstrated that LPS, *S. pyogenes* derived hyaluronic acid capsular polysaccharide, and LTA mediate barrier disruption. Additionally, several of the barrier disrupting bacterial toxins are associated with EVs. The *S. aureus* toxins hemolysins, leukotoxins, cytolysins, extracellular proteases, staphylococcal enterotoxins and membrane associated components are reviewed below.

Hemolysins, and cytolysins

Alpha-hemolysin (HLA)

S. aureus HLA is an extracellular β -barrel pore-forming toxin. The water-soluble toxin is 293 amino acids long and 33 kDa in weight.³³⁴ HLA is encoded by the highly conserved *hla* gene, which is present in over 98% of *S. aureus* isolates.³³⁵ Expression and regulation of the toxin is controlled by several *S. aureus* global regulators under a quorum sensing system.³³⁶ The major regulator is the *accessory gene regulator (agr)* locus which activates secretion via RNAPIII.^{336,337} Other regulators of HLA production include *sar*, *sae*, and *rot* loci.^{338,339} These genes are activated to switch to exoproteome producing phase in late-exponential phase with the highest activity of hemolysis in the immediate post-

exponential phase of bacterial growth.³⁴⁰ HLA monomers bind to lipid bilayer membranes forming aggregated oligomers, which produces a stable heptameric transmembrane pore.²⁶⁹ Pore formation leads to cell lysis and death due to increased permeability to ions, water, and low molecular weight molecules.

Investigation into the relationship between HLA and the integrity of paracellular junctions suggests that it is able to disrupt several innate barriers. Early *in-vivo* work showed that HLA perfused rabbit lungs resulted in severe vascular leakage and capillary filtration coefficients greater than 10-fold of normal, however comparison was not made to human derived cells despite the known sensitivity of rabbit cells to HLA.^{341,342} Cultured porcine endothelial cells exposed to 1 µg/ml of the toxin leads to an increased fluid filtration rate of 75-fold and permeability to albumin, while ultrastructural scanning electron microscopy demonstrated large paracellular gaps.³⁴³ Studies examining the effects on human umbilical vein cells (HUVEC) and *ex-vivo* rat ileum displayed a rapid response (10 minutes) of the endothelial barrier to 1 µg/ml of HLA with disassembly of vascular-endothelial cadherin (VE-cadherin) and occludin, which was related to the activation of MLCK and cell contraction.^{344,345} More recently it was shown that the mechanism for vascular dysfunction in murine sepsis model is due to the binding of HLA to disintegrin and metalloproteinase domain-containing protein 10 (ADAM10) and subsequent cleavage of VE-cadherin and reduction in TEER.³⁴⁶ Interestingly, *in-vitro* human epithelial colorectal adenocarcinoma cells (Caco-2) only showed signs of mucosal barrier dysfunction to HLA when exposed on the basolateral surface of the cell monolayer. This indicates that the receptor is not ubiquitous to the all surfaces of the cell and is highly selective.²⁶⁸

Ex-vivo murine tracheal epithelium had a significant increase in the passage of fluorescent 4 kDa dextran when exposed to either 1 or 10ug/ml of toxin.³⁴⁷ Apically

applied HLA caused rapid reductions in electrical resistance of A549 alveolar cells (Adenocarcinomic human alveolar basal epithelial cells) and 16HBE14o- cells (immortalised human bronchial epithelial cell line) via proteolysis of E-cadherin, mediated via ADAM10.³⁴⁸ Another study observed that 16HBE14o- and S9 cells (immortalised human bronchial cells) showed a significant difference in responses of the cell junction, cell-matrix contacts, and actin cytoskeleton during exposure to the toxin. This differential result was associated with decreased surface expression of ADAM10 and opposite responses of epidermal growth factor receptor (EGFR).³⁴⁹

Ex-vivo explants of paranasal sinus mucosa exposed to 10 µg/ml of HLA initially show an increase in ciliary beat frequency. However, by 12 hours this reduces and completely ceases at 24 hours; 50 µg/ml of toxin resulted in ciliostasis 2 hours after exposure.²³

HLA alters the cell barrier of endothelial, intestinal epithelial, bronchial, and alveolar cells. Given the repertoire of cell barrier interfaces that HLA disrupts—it could be postulated that the sinonasal barrier is also a HLA target.

Beta-hemolysin (HLB)

HLB (sphingomyelinase C) is a 37 kDa neutral sphingomyelinase secreted by *S. aureus*, which hydrolyses the plasma membrane lipid sphingomyelin.³⁵⁰ *S. aureus* strains are able to secrete up to 500 µg/ml of HLB, with secretion beginning in the log phase and extending into the post-exponential growth phase.^{350,351}

HLB has demonstrated cytotoxic activities against erythrocytes and leukocytes. Several leukocytes are affected by HLB such as monocytes, lymphocytes, and neutrophil.³⁵² However, Huseby et al., (2007) demonstrated that HLB is highly cytotoxic to

proliferating T cells.³⁵⁰ Within biofilm, HLB produces a strong insoluble nucleoprotein matrix when in the presence of extracellular DNA (eDNA), which strengthens and stimulates *S. aureus* biofilm.³⁵³ As discussed earlier, HLB has been implicated in enhancing lung injury during *S. aureus* infection.³¹⁰ Kim et al., (2000) studied the effects of HLB on sinonasal cilia.³⁵⁴ HLB was found to significantly reduce ciliary beat frequency within 6 hours of application to *ex-vivo* sinonasal mucosa, and complete cessation of ciliary beat at 12 hours. Additionally, administration of HLB to the maxillary sinuses in a rabbit sinusitis model resulted in ciliary loss, epithelial ulceration, and a subepithelial inflammatory response.

Delta-hemolysin (HLD) and phenol soluble modulins (PSMs)

HLD belongs to the family of phenol-soluble modulins (PSMs), of which *S. aureus* produces 7 different types. Structurally PSMs are amphipathic peptides that in solution exist as a 50% monomeric form, with increasing levels of aggregation in high concentrations.³⁵⁵ Alike to HLA and HLB, the gene encoding HLD is part of the *agr* loci, and expression is regulated by *agr* and RNAIII. Production is maximal during the post-exponential growth phase. HLD and the other PSMs are implicated in erythrocyte lysis.³⁵⁶ Additionally, PSMs have demonstrated ability to lyse neutrophils attempting to phagocytose *S. aureus*. PSMs were previously shown to have antimicrobial effects against other bacteria *in-vitro*.³⁵⁷ Biofilm structures are influenced by PSMs, which facilitate surface attachment and biofilm channel formation. Furthermore, dissemination of bacteria from biofilm relies on PSMs.³⁵⁶ HLD and HLB have demonstrated a synergistic contribution to *S. aureus* evasion of phagosomes in epithelial and endothelial intracellular infection.³⁵⁸

Leukotoxins and Gamma-hemolysin

The *S. aureus* leukotoxin family are bi-component pore forming toxins, that have an affinity for monocytes, macrophages and neutrophils. The two components include a class S and class F protein which forms into a hetero-oligomeric pore; the genes encoding these toxins can be located in the core genome, pathogenicity islands or within the genome of phages. Currently there five class F subunits proteins (HlgB, LukD, LukG, LukF-PV, and LukF'-PV) and six class S subunit proteins (HlgA, HlgC, LukE, LukM, LukH, and LukS-PV) described. It is known that the HlgB can pair with either HlgA or HlgC, the remainder of F and S subunits only pair with their respective protein.³⁵⁹. The most notable toxins in this family are the Panton-Valentine toxin and gamma-hemolysin (HLG).

Panton-Valentine Leucocidin

Panton-Valentine leucocidin (PVL) is one of the most cited leucocidins of the bi-component pore forming family of toxins; formed by the LukF-PV and LukS-PV proteins with sizes of 34 kDa and 33 kDa respectively. The gene encoding PVL is located on temperate phage ϕ Sa2, but has a low prevalence among *S. aureus* isolates between 2-3%.^{360,361} Similar to α -hemolysin the PVL toxin creates a β -barrel pore, but arranged as an octameric structure with alternating S and F subunits.³⁶²

In-vitro investigation of the pathogenic ability of PVL provides evidence for its specificity towards monocytes, macrophages, neutrophils, and the membranes of other polymorphonuclear cell membranes.³⁶³ PVL toxin secreting *S. aureus* displayed increased adherence to ECM components *in-vitro*, particularly collagen type I and IV,

and laminin found in the basement membrane.³⁶⁴ Animal infection models have yielded contradictory results, which may be due to the heterogeneity of the studies and that PVL has shown significantly differing levels of activity between animal species.^{365,366}

Despite not having reliable animal model data of PVL *S. aureus* infection, there are several reports linking the presence of *S. aureus* strains with PVL genes to poorer outcomes, recurrent soft-tissue infection and necrotising pneumonia.³⁶⁷⁻³⁶⁹

Gamma-hemolysin (HLG)

Similar to PVL it is also comprised of two sub units, which when combined together create an octameric pore with 4 of each subunit.³⁷⁰ HLG causes lysis both red blood cells and leucocytes, and includes types HlgAB and HlgCB. The genes for HLG subunits are located on the core genome, and are present in 99% of all *S. aureus* isolates.³⁶¹ The gene for the S-subunit HlgA sits upstream from the operon *hlgCB* which encodes the S-subunit HlgC and F-subunit HlgB.³⁷¹ The proteinaceous receptors for both HLGs were recently described. It was found that HlgAB targets the chemokine receptors CXCR1, CXCR2 and CCR2, while HlgCB targets C5a complement receptors.³⁷² CCR2 is primarily expressed on monocytes and macrophages, while C5a is present on neutrophils.³⁷²

HLG's potential role in disease is less well-studied than the PVL toxin and other *S. aureus* toxins. An *ex vivo* human bloodstream MRSA infection model found that all components of gamma-hemolysin (HlgA, HlgB, and HlgC) were significantly upregulated by the bacteria when it is in the circulatory system.³⁷³ This was also associated with an efficient lysis of circulating neutrophils. Conversely, *hlg*-mutant *S. aureus* has a reduced capacity to form cytolytic pores in neutrophils.³⁷³ Further to this, *in-vivo* the *hlg*-mutant demonstrated less bacterial survival during bacteraemia, yet skin abscess severity and

time to recovery were similar.³⁷³ This demonstrates that HLG may play an important role in survival and immune system evasion during systemic infection. HLG's role in colonisation and establishment of skin or mucosal infection is unknown. Other studies focused on HLG highlight its potential role in ophthalmic infection and inflammation. Initial investigations suggested that the purified toxin was able to disrupt the retinal barrier after being injected into the vitreous chamber of rabbit eyes.³⁷⁴ Following this the strong inflammatory response to a HLG producing *S. aureus* was demonstrated with a similar vitreous model, which was significantly attenuated in a mutant strain.³⁷⁵ Other studies have revealed that HLG contributes to corneal inflammation, oedema, and iritis.³⁷⁶ Additionally, it was shown that HLG and HLA may work synergistically to cause corneal erosions.³⁷⁷

Extracellular proteases

V8 protease (endoproteinase GluC)

V8 protease is a 29 kDa extracellular serine protease produced by *S. aureus*. The activity of V8 protease is specific to peptide bonds on the carbonyl side of glutamate and aspartate residues.³⁷⁸ V8 protease expression is stimulated by the agr system and RNAIII, and repressed by SarA and sigma factor σ^B .^{379,380} Expression is growth phase dependent with the highest levels of activity in the post-exponential phase of bacterial growth with plateauing of activity into stationary phase growth.³⁷⁹ The *sspA* gene for V8 protease is located on the *ssp* operon upstream from *SspB* and *SspC* encoding two other proteases, which are also activated by V8 protease as a part of a post translational cascade of extracellular protease activation.³⁸¹ The cascade of extracellular proteases begins with the metalloprotease aureolysin, which processes the V8 proenzyme to form a mature

serine protease and in turn V8 protease activates the cysteine protease staphopain B.^{381,382}

Since it was first purified in 1972,³⁸³ V8 protease has been implicated in immune system evasion mechanisms and biofilm regulation.³⁸⁴⁻³⁸⁷ The current literature regarding the barrier altering effects of V8 protease is primarily from dermatological research as discussed earlier. Although, *in-vitro* stimulation of nasal epithelial cells with *S. aureus* supernatant with and without serine protease inhibitors has shown that this protease family induces IL-6, IL-8, and CXCL1 production. The cytokine synthesis was due to activation of NF- κ B, however this serine protease response was not inhibited by corticosteroid.³⁸⁸ Given that nasal epithelial cells have a strong inflammatory response to V8 protease, it is plausible that this coincides with airway barrier disruption.

Aureolysin (Zinc metalloproteinase aureolysin)

Aureolysin is a zinc metalloproteinase secreted by *S. aureus*, belonging to the thermolysin family of metalloproteinases. The *aur* gene encoding the protease is highly conserved among *S. aureus* strains.³⁸⁹ Aureolysin has been shown to cleave complement factor C3 with subsequent activation C3a and C3b fragments.³⁹⁰ Additionally, the antimicrobial peptide cathelicidin LL-37 is actively degraded and deactivated by aureolysin. Similarly, V8 protease degrades LL-37, however leaving behind an active antimicrobial peptide.³⁹¹ A murine model of osteomyelitis demonstrated aureolysin is important in induction of *S. aureus* secreted PSMs involved in bone destruction.³⁹² Alike to V8 protease, aureolysin is maximally produced during the post-exponential bacterial growth phase due to the *agr* system.³⁹³

Spl (serine protease-like) proteases

The spl proteases include splA, splB, splC, splD, splE and splF, which were only recently described.³⁹⁴ They are deemed serine protease-like as they showed similar sequences to V8 protease and exfoliative toxins, which contain the serine protease catalytic triad.³⁹⁴ All the spl proteases are similarly sized at 22kDa (range: 21.9 - 22.4 kDa), encoded by a six gene operon.^{394,395}

The spl protease substrate specificities are narrow, similar to the exfoliative toxin family and currently there are no known physiological targets. Screening of the human proteome predicted that potential targets of several spl proteases included olfactory receptors and mucin proteins.³⁹⁶⁻³⁹⁸ There is evidence to suggest that the spls may be involved in invasive infections. One study identified that all spl proteases are upregulated in a murine model of methicillin-resistant *Staphylococcus aureus* (MRSA) bacteremia and from MRSA isolated from cutaneous abscesses.³⁹⁹ The *splA* gene has been associated with a higher vancomycin MIC and inherently poorer bacteremia outcomes.⁴⁰⁰ Antibodies against the spl proteases have been identified in human serum from colonized and acutely infected patients, with higher antibody titers during active infection.⁴⁰¹ Intriguingly, the immune responses towards spl proteases were higher than other proteases such as aureolysin, V8 protease, and the staphopains.⁴⁰¹

In-vitro splA has shown ability to cleave the mucin 16 glycoprotein on the surface of human airway Calu-3 secondary cell line.⁴⁰² Furthermore, spl mutant *S. aureus* are less likely to cause a disseminated bilateral infection.⁴⁰² More recently the spl proteases have been suggested to contribute to the airway allergy. It was seen that T cells stimulated with spls generated a Th2 cytokine response. Spl specific IgE antibodies were found in asthmatic patients, while splD and splF peptides were identified within nasal polyp tissue. Additionally, splD induces expression of IL-5, IL-17 and INF- γ in *ex-vivo* nasal

polyp tissue. Intratracheal instillation of splD results in a strong eosinophilic inflammatory response, increases in splD specific serum IgE, and Th2 cytokine expression upon antigen presentation.⁴⁰³

Cysteine proteases

The *S. aureus* cysteine or thiol proteases include staphopain A and staphopain B. Both proteases are approximately 20kDa in size and very similar in structure, however they demonstrate substantial differences in their substrate specificity.^{404,405} The gene encoding for staphostatin B is located on the same operon and downstream to V8 protease, while the gene for staphostatin A is located on the *scp* operon.^{379,406} They are expressed as prepropeptides, which are folded into an inactive protease in the extracellular environment. Pro-staphopain B is activated by V8 protease and staphopain A is thought to undergo autocatalytic activation, however there are suggestions that the activating protease has not been identified yet.³⁷⁹ Interestingly, *S. aureus* also produces specific staphopain inhibitors called staphostatins, which form stable complexes with the protease and negate proteolytic activity.⁴⁰⁷

The literature regarding staphopains demonstrates that this family of proteases may have a role in invasion, tissue destruction, and immune system evasion. Despite the current *in-vitro* evidence there is a lack of corresponding *in-vivo* experimentation. Initial studies identified that the cysteine proteases are effective at degrading lung elastin, and conversely are inhibited by α_2 -macroglobulin and other unidentified human serum products.⁴⁰⁸ Similar to V8 protease, cysteine proteases also inactivate α 1-antitrypsin.⁴⁰⁹ Additionally cysteine proteases inactivate α 1-antichymotrypsin, a glycoprotein important for limiting proteolytic activity from neutrophil products and other proteases.⁴¹⁰ Inactivated α 1-antichymotrypsin is also strongly chemoattractant and

elimination of the inactivated peptide is slow, hence this could potentiate inflammation during *S. aureus* infection.⁴¹⁰

Staphylococcal enterotoxins/superantigens

Staphylococcal enterotoxins are a family of secreted *S. aureus* toxins of which there are over 20 recognised different isoforms.⁴¹¹ Among the several types, SEA and SEB are well documented in the literature and the most frequently examined staphylococcal enterotoxins in CRS. They range in size from 19.4–28.6 kDa and their genes are usually encoded on the mobile genome such as pathogenicity islands, bacteriophages, and plasmids.⁴¹¹

Bachert et al., (2000) identified the presence of SEA and SEB specific IgE antibodies in tissue specimens from patients with eosinophilic CRSwNP.⁶⁸ The presence of staphylococcal enterotoxin specific IgE in CRSwNP was later correlated with an increased *S. aureus* colonisation.⁴¹² Recently, another study identified that SEA and SEB levels are upregulated in non-eosinophilic and eosinophilic polyps within a Chinese cohort.⁴¹³ Moreover, nasal polyp tissue concentrations of SEA were found to be approximately 7-10 times higher than SEB levels.^{413,414}

As discussed earlier, SEB has demonstrated abilities to disrupt the gastrointestinal and airway barriers. Interestingly, in our previous work we demonstrated that a SEA positive *S. aureus* strain significantly altered the airway barrier *in-vitro*, while conversely this was not observed in the SEB positive strain.¹⁹ The effects of SEA on the airway barrier function is not known. However, Min et al., (2006) conducted a rabbit model of SEA induced sinusitis, which identified that daily instillation of 30 ng/ml SEA causes significant epithelial loss and slowing of ciliary beat frequency. Additionally, *ex vivo* treatment of rabbit sinus tissue with SEA showed complete cessation of ciliary beat at

concentrations of 3 ng/ml.²⁴ Tissue levels of SEA have been found to be up to 96 ng/ml in CRSwNP.

***S. aureus* membrane associated products**

Lipoteichoic acid

LTA is found in the cell wall of gram positive bacteria, which share pathophysiological properties with LPS from gram negative bacteria. LTA is released during bacteriolysis, and known to contribute to proinflammatory cytokine generation, TLR activation, coagulation, complement activation and ROS production.⁴¹⁵ In addition to altering the pulmonary endothelial barrier, LTA has been shown to disrupt the endothelial blood brain barrier.^{416,417} Boveri et al., (2006) demonstrated LTA induces a strong TNF- α and IL-1 response in co-cultured glial cells with subsequent loss of barrier integrity and alteration of TJ localisation in brain capillary endothelial cells.⁴¹⁶ *dltA* encodes the protein responsible for D-alanylation of lipoteichoic acid in *S. aureus*.⁴¹⁸ A previous study showed that a mutant *S. aureus* strain lacking *dltA* was significantly attenuated in its ability to adhere to human nasal epithelial cells and more susceptible to nasal antimicrobial peptides. Additionally, *dltA* mutants were less likely to successfully colonise rat naris.⁴¹⁹ Patou et al., (2008) found that 10 μ g/ml LTA did not stimulate cytokine production when incubated with fragmented *ex-vivo* nasal tissue.⁴²⁰ There is a paucity of experimentation regarding the *in-vitro* effects of LTA on isolated nasal epithelial cells.

Extracellular vesicles

EVs are small spheres comprised of lipid bilayers, and ubiquitously secreted by all living organisms. EVs are found in several sizes ranging from 20 nm to 500 nm, and contain varying proteins, lipids, and nucleic acids. The roles of bacterial secreted EVs are multifaceted, including transfer of pathogenic toxins into host cells, immune system evasion, bacterial cell to cell communication, and incorporation in bacterial biofilms.^{421,422}

Gram positive bacteria EVs were first described in 2009, despite their much earlier discovery in gram negative bacteria. Lee et al., (2009) observed the formation and size distribution of EVs secreted by *S. aureus*. Mass spectrometry protein analysis revealed several noteworthy contents of *S. aureus* EVs including hemolysins, β -lactamase, penicillin-binding proteins, extracellular proteases, IgG binding protein, lipoteichoic acid, and staphylococcal enterotoxins.⁴²³ *S. aureus* EVs are produced *in-vitro* and *in-vivo*, visualised as a budding spherical structure from the bacterial surface. Experimental evidence supports the delivery *S. aureus* bacterial factors into host cells via EVs.⁴²⁴ Additionally, *S. aureus* EVs are necessary to induce host cell death when exposed to HEp-2 cells.⁴²⁴ HLA has been implicated in EV mediated cell cytotoxicity and erythrocyte lysis *in-vitro*.⁴²⁵ Kim et al., (2012) conducted a mouse model of *S. aureus* EV induced pulmonary inflammation, which found EVs induce a strong Th1 and Th17 cytokine response. Furthermore, this was mediated via a TLR2 dependent pathway as TLR2^{-/-} mice exhibited a significantly attenuated response to EVs.⁴²⁶

It is unknown whether *S. aureus* EVs disrupt barrier integrity, however this has been demonstrated in other organisms. *Campylobacter jejuni* (*C. jejuni*) produces EVs, which specifically cleaves junctional proteins occludin and E-cadherin, resulting in disrupted barrier integrity. This is thought to be mediated via serine protease activity.

Furthermore, EV supplementation increases intracellular invasion of *C. jejuni in-vitro*.⁴²⁷ EVs secreted by oral microbial organisms *Treponema denticola* and *Porphyromonas gingivalis* have been associated with epithelial barrier disruption, tight junction protein degradation, and cellular detachment.^{428,429}

Recently, Choi et al., (2014) demonstrated that bacterial EV composition in nasal lavage samples closely reflects the nasal microbiome, while *staphylococcus* species and EVs were increased in CRS patient groups.⁴³⁰ Given the previously known inflammatory effects of EVs, this study suggests EVs may be involved in the pathogenesis of CRS.

Zinc in Chronic Rhinosinusitis

Zinc is an essential trace element required for normal metabolic and protein functions,⁴³¹ immune system regulation, wound healing, and DNA synthesis.⁴³² Additionally, it has important anti-inflammatory and anti-apoptotic properties.^{433,434} As discussed, zinc is vital for maintenance and protection of barrier function in gastrointestinal and pulmonary epithelium, however this has not been addressed in the sinonasal barrier. Furthermore, little is known about the role of zinc in CRS despite its importance across several biological processes.

Önerci and Kus, (1994) examined the serum zinc, magnesium, and copper concentrations in a cohort of CRS and control patients.⁴³⁵ Serum concentrations of the tested trace elements were all within normal range, although copper concentrations were lower in CRS. A decade following this study, Ünal et al., (2004) measured the serum concentrations of several vitamins and trace elements in children with rhinosinusitis against age and sex matched controls.⁴³⁶ Serum concentrations of vitamin E and C, copper, and zinc were all significantly lower in the rhinosinusitis group.

Interpretation of this study is difficult as there was no distinction between acute, chronic, or presence of nasal polyposis. Additionally, there is no reference to clinically factors that influence serum zinc concentrations in children such as diet, biochemical factors, weight and inflammatory markers such as C-reactive protein.⁴³⁷

Rostkowska-Nadolska, Borawska, and Hukalowicz, (2005) conducted atomic absorption spectrometry on digested nasal polyp and control tissue specimens to measure zinc, copper, lead, and selenium levels. All four trace elements were significantly lower in nasal polyp tissue.⁴³⁸ Although, these levels were measurements were taken from whole tissue homogenates rather than epithelium specific levels. More recently, a study by Okur et al., (2012) observed similar findings of low zinc and selenium tissue concentrations in nasal polyp whole tissue specimens.⁴³⁹ Moreover, the antioxidant enzyme superoxide dismutase was significantly lower in nasal polyp tissue, which is involved in regulating ROS and reactive nitrogen species.^{439,440} Extracellular and cytoplasmic forms of superoxide dismutase utilise zinc as a stability co-factor,⁴⁴⁰ hence local zinc deficiency may explain the enzyme reduction. Likewise, Cekin et al., (2009) observed reductions in superoxide dismutase in nasal polyp specimens.⁴⁴¹

Zinc homeostasis is regulated primarily by Zrt-,Irt-related proteins (ZIP), zinc transporters (ZnT), and metallothioneins (MT).^{274,442} ZIP transporters are a family of 14 proteins responsible for transport of zinc into the cytosolic compartment from the extracellular space or other intracellular compartments. Copper, iron, manganese, and cadmium transport can occur through ZIP proteins. The family of ZnT transporters are comprised of 9 isoforms, which mobilise zinc from the cytosolic compartment to the extracellular space or lumens of intracellular compartments.⁴⁴³ ZIP and ZnT transporters have not been evaluated in CRS previously. Metallothioneins (MTs) are a group of small intracellular proteins that have high affinity for binding metals, such as

Zn, Cd, Hg, and Cu.⁴⁴⁴ Along with regulation of intracellular metal regulation, MTs have been associated with protection against apoptosis and reactive oxygen species.⁴⁴⁵ A previous immunohistochemistry study identified that MT expression was more prominent in eosinophilic and lymphocytic nasal polyp epithelium and stromal tissues, compared to healthy mucosa and neutrophilic polyps. The increase in eosinophilic nasal polyp MT was positively associated with M2 type macrophages, however the specific MT isoform was not identified.⁴⁴⁶ The MT3 isoform has been shown to reduce ROS,^{447,448} and absence of MT3 is associated with impaired cellular lysosomal function with potential for intracellular pathogen infection.⁴⁴⁹

Whilst these studies indicate that zinc may be involved in CRS, further research is needed to elucidate how it is distributed in CRSsNP and CRSwNP. Investigation into the regulatory factors may provide more information regarding zinc homeostasis in CRS.

Thesis

CRS is a chronic inflammatory condition with symptoms that impact significantly on quality of life. The public health perspective emphasizes the economic burden that is encompassed by decreased work productivity, increased medicine use, primary care treatment, and use of hospital services. The pathogenesis of CRS is multifaceted involving contributions from host, environment, and microbial factors. Barrier function in CRS is a relatively new concept and the current reports emphasize the importance of this innate immune function. Although, little is understood regarding the potential contributors to CRS barrier dysfunction, review of barrier dysfunction across other epithelial or mucosal interfaces reveals common etiological themes—inflammatory processes (with a bias towards Th2 type inflammation), and bacterial secreted factors. Additionally, trace elemental zinc appears to contribute to mucosal barrier integrity.

Staphylococcus aureus disrupts the sinonasal mucosal barrier

The preliminary research leading into this thesis revealed that *S. aureus* secretes a factor that disrupts the airway barrier. *S. aureus* is known to produce a multitude of toxins, although the majority of evidence associating *S. aureus* toxins and CRS pathogenesis revolves around SEB. Consideration of known barrier disrupting bacterial products emphasizes the role of several proteases, enterotoxins, pore-forming toxins, and cell wall products. Additionally, several bacterial organisms are known to produce more than one barrier disrupting factors. This built-in redundancy points towards barrier disruption as an essential mechanism for certain pathogens, potentially as a means for colonisation, invasion, or enhanced immune system evasion.

Host factors in sinonasal mucosal barrier dysfunction

Several studies have identified host inflammatory factors as potential contributors to sinonasal mucosal barrier dysfunction such as IFN- γ , TNF- α , IL-4, IL-9, IL-13, IL-17, IL-22, and IL-26. It appears that zinc homeostasis is a major contributor to mucosal barrier integrity in the gastrointestinal system. A handful of investigations have recognised that zinc concentrations are depleted in CRS, in particular CRSwNP. However, it is not known whether this is a contributing or predisposing factor to CRS barrier dysfunction.

Thesis aims

Bacterial factors

1. Identify candidate *S. aureus* bacterial products responsible for disruption of tight junctions.
2. Evaluate the sinonasal mucosal barrier altering effects of *S. aureus* toxins with known barrier altering properties observed in other epithelial barriers, such as HLA, SEA, LTA, and *S. aureus* proteases.

Host factors

3. Investigate the role that zinc has in the development and maintenance of the healthy sinonasal mucosal barrier. Determine the relationship between mucosal zinc availability and the mucosal barrier in CRS.

In vitro* Characteristics of an Airway Barrier Disrupting Factor Secreted by *Staphylococcus aureus

Statement of authorship

Title of Paper	In vitro characteristics of an airway barrier disrupting factor secreted by <i>Staphylococcus aureus</i>
Publication Status	Submitted for publication
Publication Details	Murphy J, Ramezanzpour M, Drilling A, Roscioli E, Psaltis A.J, Wormald P.J, Vreugde S. In vitro characteristics of an airway barrier disrupting factor secreted by <i>Staphylococcus aureus</i> . Int Forum Allergy Rhinol. Accepted for publication on the 8 th of October 2018. doi:10.1002/alr.22232

Principal Author

Name of Principal Author (Candidate)	Jae Murphy		
Contribution to the Paper	Experimental design, performed collection of samples, conducted experiments, interpreted and analysed data, preparation of manuscript		
Overall percentage (%)	75%		
Certification	This paper reports on original research I conducted during the period of my Higher Degree by Research candidature and is not subject to any obligations or contractual agreements with a third party that would constrain its inclusion in this thesis. I am the primary author of this paper.		
Signature		Date	6 th July 2018

Co-Author Contributions

By signing the Statement of Authorship, each author certifies that:

- i. the candidate's stated contribution to the publication is accurate;
- ii. permission is granted for the candidate to include the publication in the thesis; and
- iii. the sum of all co-author contributions is equal to 100% less the candidate's stated contribution.

Name of Co-Author	Mahnaz Ramezanpour		
Contribution to the Paper	Assistance with conducting experiments, manuscript editing		
Signature		Date	6 th July 2018
Name of Co-Author	Amanda Drilling		
Contribution to the Paper	Assistance with conducting experiments		
Signature		Date	6 th July 2018
Name of Co-Author	Eugene Roscioli		
Contribution to the Paper	Assistance with conducting experiments, manuscript editing		
Signature		Date	6 th July 2018
Name of Co-Author	Alkis James Psaltis		
Contribution to the Paper	Project supervision, manuscript editing		
Signature		Date	6 th July 2018
Name of Co-Author	Peter-John Wormald		
Contribution to the Paper	Project supervision, manuscript editing		
Signature		Date	6 th July 2018
Name of Co-Author	Sarah Vreugde		
Contribution to the Paper	Assistance with experimental design, project supervision, manuscript editing, corresponding author		
Signature		Date	6 th July 2018

Citation

Murphy J, Ramezanpour M, Drilling A, Roscioli E, Psaltis A.J, Wormald P.J, Vreugde S. *In vitro* characteristics of an airway barrier disrupting factor secreted by *Staphylococcus aureus*. Int Forum Allergy Rhinol. Accepted for publication on the 8th of October 2018. doi:10.1002/alr.22232

Abstract

Introduction: *Staphylococcus aureus* (*S. aureus*) is a major contributor to the pathophysiology of chronic rhinosinusitis (CRS). Previous research has shown that *S. aureus* secreted products disrupt the airway barrier.

Methods: *S. aureus* ATCC 13565 and 25923 strains were grown at exponential, post-exponential, and stationary phases. Microbial conditioned media (CM) was collected from the cultures and ultrafiltered (UF). Liquid chromatography – electrospray ionisation tandem mass spectrometry (LC-ESI-MS/MS) was performed on the UF-CM. UF-CM was subjected to heat and protease treatment, size fractionation, and ultracentrifugation (UC) separation. Human nasal epithelial cell air liquid interface (HNEC-ALI) cultures were exposed to purified alpha hemolysin (HLA), staphylococcal enterotoxin A (SEA), Lipoteichoic acid (LTA), and UF-CM. Barrier function outcomes were measured by transepithelial electrical resistance (TEER) and apparent permeability (Papp). UC fraction exposed cultures were subjected to immunofluorescence microscopy for tight junction protein zonula occludens-1 (ZO-1).

Results: LC-ESI-MS/MS identified 107 protein identities, with HLA being most abundant. HLA, SEA, and LTA did not alter the HNEC-ALI barrier as measured by TEER or Papp. Barrier disruption caused by UF-CM peaked in the post-exponential phase, was sensitive to heat and protease treatment, >30 kDa in size, and enriched in the UC

fraction. Immunofluorescence of HNEC-ALI exposed to UF-CM and UC demonstrated loss of ZO-1 localisation.

Conclusion: These results suggest that the *S. aureus* factor responsible for TJ disruption in HNEC-ALI cultures is either a proteinaceous macromolecule or a combination of secreted factors. The product is enriched in the UC fraction, suggesting it is associated with large structures such as membrane components or vesicles.

Keywords: Chronic rhinosinusitis, epithelial cell, bacteriology, innate immunity and rhinosinusitis

Introduction

Chronic rhinosinusitis (CRS) is characterised by inflammation of the nose and paranasal sinuses, which results in nasal obstruction, rhinorrhoea, post-nasal drip, facial pressure, and alterations in smell. The pathophysiology of CRS is complex and involves pathogenic interactions between host, microbial flora and environment. *S. aureus* has been implicated in the pathogenesis and persistence of CRS, impaired mucosal healing, and is associated with disease severity.^{330,331,450} The contribution of *S. aureus* to CRS is understood to be related to the formation of biofilms, intracellular infection, and its production of Staphylococcal enterotoxins/superantigens.^{88,95,451}

The innate barrier defence of the sinonasal mucosa is essential in preventing entry of external pathogens.⁴⁵² At the cell-to-cell interface are apical junctional complexes, a component of which are tight junction (TJ) proteins. These structures are involved in maintaining the barrier between host and environment, ion and molecular transfer, and cell polarity and organisation.⁴⁵³ Studies have shown that the mucosa of CRS sufferers demonstrate signs of defective barrier function.^{20,454}

Previous research has shown that *S. aureus* supernatants can disrupt the TJs of sinonasal epithelial cells.¹⁹ Although the responsible factor for this remains unknown, previous research has identified other *S. aureus* products that act on cell barriers. Alpha hemolysin (HLA) has been linked to gastrointestinal and vascular barrier disruption.^{268,341} Staphylococcal superantigens contribute to alterations of the mucosal barrier of the gastrointestinal tract, such as staphylococcal enterotoxin A (SEA).⁴⁵⁵ Superantigens have been implicated in the inflammatory drive of CRS with nasal polyposis (CRSwNP).⁴⁵⁶ Lipoteichoic acid (LTA) is a cell wall polymer from gram positive organisms, with known effects on the endothelial barrier function.³¹⁶

This study aims to characterise *S. aureus* factors that disrupt mucosal barrier function and investigate the effects of HLA, LTA, and SEA on airway barrier integrity.

Methods

Microbial conditioned media and bacterial growth phases

Two American Type Culture Collection (ATCC) reference strains of *S. aureus* were used in this study: 13565 and 25923. ATCC 13565 is a known producer of Staphylococcal enterotoxin-A (SEA) and ATCC 25923 is a well documented biofilm forming strain.¹⁹ Planktonic bacterial cultures were initiated from overnight broth cultures in nutrient broth media (Sigma-Aldrich, Castle Hill, Australia) at an OD600 of 0.05. Serial measurements were taken to identify the exponential, post exponential and stationary growth phases of each strain. Cultures were then stopped at each of these points and centrifuged at 3000 revolutions per minute (RPM) to pellet the cells. The conditioned media (CM) was passed through a 0.22 µm syringe filter and a sample taken and pipetted onto a nutrient agar plate to ensure absence of viable bacteria. Following this the CM was concentrated using centrifugal ultrafilters (UF) with a size cut off at 3 kDa (Vivaspin; GE Healthcare, Little Chalfont, UK) to make UF-CM samples. Phosphate buffered saline (PBS) was added to the centrifugal filters during the concentration process. UF-CM samples were subjected to a detergent compatible protein quantification assay (DC™ protein assay; Bio-Rad, Hercules, CA, USA), and experiments were conducted at exoproteome concentrations of 200 µg/ml unless otherwise stated.

Proteomics analysis

ATCC 13565 CM and UF-CM samples were collected from exponential, post-exponential, and stationary growth phases for proteomic analysis with sodium dodecyl sulphate polyacrylamide gel electrophoresis (SDS-PAGE). Stationary phase UF-CM 13565 gel

bands were analysed with liquid chromatography – electrospray ionisation tandem mass spectrometry (LC-ESI-MS/MS) (see Supplementary methods).

***Staphylococcus aureus* toxins**

HLA (ab192009; Abcam, Cambridge, UK) and SEA (Sigma-Aldrich) were obtained and resuspended in PBS to concentrations of 1 µg/ml and 10 µg/ml. LTA (Sigma-Aldrich) was resuspended in PBS to a concentration of 10 µg/ml.

Heat and proteinase K treatment of microbial conditioned media

UF-CM B565 from post-exponential and stationary growth phases were subjected to heat treatment of 80°C for 30 minutes. Stationary growth phase UF-CM B565 was also subjected to 100°C for 30 minutes or incubated with and without 1 mg/ml proteinase K (Sigma-Aldrich) overnight at 37°C. 5 mM PMSF (Phenylmethylsulfonyl fluoride; Sigma-Aldrich) was added to proteinase K digested samples and the PBS control to inhibit the enzyme prior to experimentation.

Size fractionation of microbial conditioned media

Stationary growth phase UF-CM B565 samples were size fractionated using centrifugal ultrafilters (Vivaspin) with size cut offs at 3, and 30 kDa. Initially 30 kDa filters were used to collect proteins >30 kDa in size, followed by 3 kDa filters to collect 3 – 30 kDa size proteins, and then the filtrate containing sizes <3 kDa.

Ultracentrifugation separation

Stationary growth phase UF-CM 13565 samples were ultracentrifuged (UC) to 140,000 x g overnight at 4°C resulting in the pelleted UC and supernatant (SN) fractions. The SN was removed, and the UC pellet resuspended in PBS. The UC suspension, SN, and stationary growth phase UF-CM 13565 were subjected to DC™ protein assay (Bio-Rad) and resuspended to 50 µg/ml in PBS. Samples were then stored at -80°C until use.

Primary human nasal epithelial cell collection

Ethics approval for cytological nasal brushings from healthy volunteers was granted from The Queen Elizabeth Hospital Human Research Ethics Committee. All patients received written participant information and provided informed written consent to be included. Exclusion criteria included active smoking, age less than 18 years, systemic diseases, recent upper respiratory tract infection, topical corticosteroid use, and symptoms/signs of chronic rhinosinusitis or allergic rhinitis.

Nasal brushings were taken from the nasal cavity using sterile cytology brushes and immediately transported in Bronchial Epithelial Cell Growth Medium (BEGM) (Lonza, Basel, Switzerland). Samples were then washed in PBS with centrifugation (1700 RPM for 5 minutes) and resuspended in Clonetics™ B-ALI™ growth medium (Lonza). Cell samples were then depleted of macrophages in a 100 mm diameter culture plate coated with anti-CD68 (Dako, Carpinteria, California, USA) for 20 minutes. Cell samples were removed from the culture plate and seeded directly onto a type I collagen coated T25 flask (Corning, NY, USA). Cells were grown until 80% confluent then harvested for seeding onto collagen coated 6.5 mm permeable transwells with 0.4 µm pores (Corning) at a density of 5×10^4 cells per well.

Air-liquid interface culture

Cell cultures were maintained with B-ALI™ growth medium for 3-4 days in a cell incubator at 37°C with 5% CO₂. The apical and basal media was then removed and only the basal media replaced with B-ALI™ differentiation media, this was changed every alternate day. Human nasal epithelial cultures at air liquid interface (HNEC-ALI) were maintained for a minimum of 14 days for development of tight junctions.⁴⁵⁷

Transepithelial electrical resistance

Transepithelial electrical resistance (TEER) was measured using an EVOM2 epithelial voltohmmeter (World Precision Instruments, Sarasota, FL, USA). TEER values were only taken from cultures more than 14 days maturity and showing >400 ohm x cm² (equivalent to >1200 ohm in a 0.33 cm² transwell membrane). Baseline TEER was initially measured on all HNEC-ALI transwell samples with cell media apically and basally, following this the apical media was removed and replaced with the corresponding treatment. The TEER of cell free collagen coated membranes was subtracted from the experimental measurements and results were expressed relative to baseline. Measurements for HLA, SEA, and LTA were taken at baseline, 6, 12, and 24 hours. Measurements for UF-CM, and size fractionated UF-CM were taken at baseline, 15, 30, 60, and 120 minutes. Heat and proteinase K treated UF-CM TEER measurements were taken at baseline, 60 and 120 minutes. TEER measurements for UC and SN experiments were taken at baseline, 15, 30, 60, 120, 240, and 360 minutes.

Macromolecular paracellular permeability

The macromolecular paracellular permeability (P_{app}) of the air liquid interface differentiated human nasal epithelial cultures was assessed at the defined time points. P_{app} was measured at 2 hours of treatment unless otherwise stated. A neutral 4 kDa fluorescein isothiocyanate (FITC) dextran (Sigma-Aldrich) was added to the apical compartment to a concentration of 3 mg/ml 2 hours prior to measurement. Samples were then taken from the basolateral compartment. The amount of passaged dextran was quantified using a Fluostar Optima 96 well microplate reader using wavelengths 485nm and 520nm for excitation and emission respectively. P_{app} results assumed sink conditions of FITC dextran transfer and calculated according to the following equation:

$$P_{app} = \left(\frac{dQ}{dt} \right) \times \frac{1}{AC_0}$$

P_{app} is the apparent permeability coefficient (cm/s), dQ/dt (mg/s) is the rate of transfer of the FITC dextran to the basolateral compartment, A (cm²) is the surface area of the transwell membrane, and C_0 (mg/ml) is the starting drug concentration of the apical compartment. Fold changes were calculated from P_{app} values by:

$$P_{app} (fold\ change) = \frac{P_{app}(sample)}{P_{app}(control)}$$

Immunofluorescence of ZO-1

Immunofluorescence was performed on HNEC-ALI cultures following treatment with PBS control, UF-CM I3565, UC I3565, and SN I3565 fractions. Samples were PBS washed, and fixed in 2.5% formaldehyde for 10 minutes, followed by four rinses with PBS. Permeabilisation was performed with 1% SDS in PBS and blocked with serum free blocker (SFB; Dako) for 60 minutes. HNEC-ALI cells were incubated with 1:100 mouse monoclonal anti-human zonula occludens-1 (ZO-1) (Invitrogen, Carlsbad, CA, USA) in

TBST (0.5% Tween in tris-buffered saline)-10% SFB overnight. Excess primary antibody was cleared using TBST, followed by 1:200 anti-mouse Alexa Fluor® 488 conjugated secondary antibody (Jackson ImmunoResearch Labs Inc., West Grove, PA, USA) for 1 hour at room temperature. The filters were then rinsed with TBST and 200 ng/ml of 4',6-diamidino-2-phenylindole (DAPI; Sigma-Aldrich) was added after the third wash. Membranes were excised from their supports and mounted on glass slides and anti-fade mounting medium (Dako) was added prior to cover slipping. Samples were imaged using a LSM700 inverted confocal laser scanning microscope (Carl-Zeiss, Oberkochen, Germany).

Cytotoxicity assay

Lactate dehydrogenase (LDH) in the culture medium was measured at 4 and 6 hours after treatment with cell culture media, UF-CM 13565, UC 13565, and SN 13565 using Cytotox Homogenous Membrane Integrity Assay (Promega, Australia). 10% Triton-X was included as a positive control for maximal LDH release. This was performed on a separate cohort from that used to generate TEER, Papp, and immunofluorescence data. Simultaneous TEER was measured during experimentation. 50 µl of media from each well was transferred to a new plate, and 50 µl of LDH reagent was added to the supernatant. The plate was incubated for 30 minutes in the dark at 37°C. OD was measured at 490 nm on a Fluostar Optima 96 well plate reader (BMG Labtech).

Statistical analysis

Statistical differences in TEER were evaluated by 2-way ANOVA followed by Bonferroni's multiple comparisons test with significance set at $p < 0.05$. Papp results were

analysed using ANOVA followed by Holm-Sidak post hoc test and expressed as mean fold change (\pm SD). Statistical analysis was performed using GraphPad Prism version 7 for Apple (GraphPad Software, La Jolla, CA).

Results

Proteomics analysis and candidate factor screening

SDS-PAGE of *S. aureus* conditioned media identified several intense and discrete protein bands that were subject to further analysis (Figure S1), from which a total of 7 gel bands were resolved from the SDS-PAGE for LC-ESI-MS/MS. Proteomic analysis revealed 107 identities, containing 69 unique proteins across all bands analysed (Table S1). HLA was present in all 7 bands, and was the most abundant protein in 4 bands based on exponentially modified protein abundance index value. Other exoproteome factors in gel bands 4 – 7 were gamma-hemolysin component A and B, leucotoxin LukDv, leucotoxin LukEv, leucotoxin Luke, staphopain B, glutamyl endopeptidase (V8 protease), serine like protease family (SplA – SplF). Staphylococcal enterotoxin A was not identified in the resolved gel bands from the SDS-PAGE (Supplemental Figure S1), despite being previously identified in this strain.¹⁹

Transepithelial electrical resistance and paracellular permeability are unaffected by Alpha Hemolysin, Staphylococcal Enterotoxin A, and Lipoteichoic acid

HNEC-ALI cultures exposed to HLA, SEA and LTA did not demonstrate a disrupted barrier function as measured by TEER (Figure 2A) and Papp (Figure 2B). TEER was measured at three time points along 24 hours to recognize any delayed effect. Papp was measured at 24 hours demonstrating a non-significant increase ($p > 0.05$) in permeability for HLA (2.2 (± 2.0) fold change for 1 $\mu\text{g/ml}$ and 3.2 (± 3.3) fold change for 10 $\mu\text{g/ml}$), SEA (1.2 (± 0.2) fold change for 1 $\mu\text{g/ml}$ and 1.5 (± 0.3) fold change for 10 $\mu\text{g/ml}$), and LTA (2.6 (± 1.9) fold change for 10 $\mu\text{g/ml}$) treated cultures.

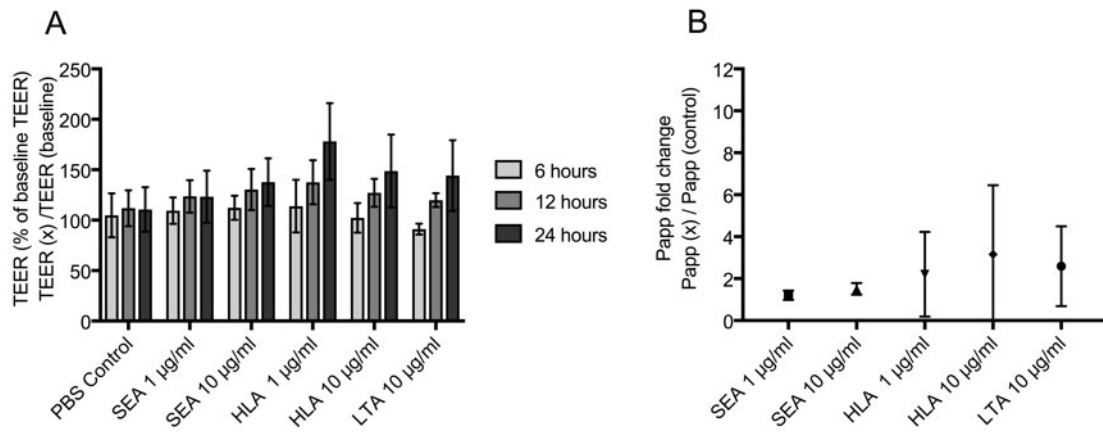


Figure 2. Transepithelial electrical resistance (TEER) and paracellular permeability (Papp) are unaffected by Staphylococcal Enterotoxin A (SEA), Alpha Hemolysin (HLA), and Lipoteichoic acid (LTA).

HNEC-ALI cultures were treated with PBS control, SEA (1 and 10 µg/ml), HLA (1 and 10 µg/ml), and LTA (10 µg/ml). TEER (A) was measured at baseline, 6, 12, and 24 hours, while Papp (B) was measured after 24 hours of exposure to the corresponding factor. TEER measurements are expressed as mean percentage change from the baseline (\pm SD). Alterations in Papp (C) are reported as mean fold change compared to the PBS control (\pm SD). Data from at least 3 biologically independent replicates.

Airway barrier disrupting effects of conditioned media are *Staphylococcus aureus* strain and growth phase dependent

To further elucidate the responsible factor, *S. aureus* CM from two strains (ATCC 13565 and 25923) was collected at different growth phases (Supplemental Figure S2) then subjected to degradation and fractionation techniques. UF-CM 13565 reduced TEER in all phases of growth and statistically significant at all time points ($p < 0.0001$). After 15 minutes of exponential, post-exponential, and stationary phase UF-CM treatment the TEER measurements compared to baseline were 43.2% (± 23.9), 31.3% (± 16.4), and 23.4% (± 6.9) respectively (Figure 3A). Conversely only post-exponential phase UF-CM 25923 demonstrated a reduction in TEER, which was 42.2% (± 24.3) of its baseline after 15 minutes (Figure 3B) ($p < 0.0001$). Exponential and stationary phase UF-CM 25923 did not alter the TEER (Figure 3B). Papp was significantly increased by post-exponential, and stationary growth phase UF-CM 13565 with fold changes of 57.6 (± 13.9 ; $p < 0.001$),

and 45.4 (± 31.8 ; $p < 0.01$) respectively (Figure 3C). Exponential growth phase UF-CM 13565 increased the Papp fold change to 15.17 (± 3.7 ; $p = 0.5929$) and post-exponential growth phase UF-CM 25923 increased the Papp fold change to 16.5 (± 16.2 ; $p = 0.5929$), although these were not statistically significant (Figure 3C).

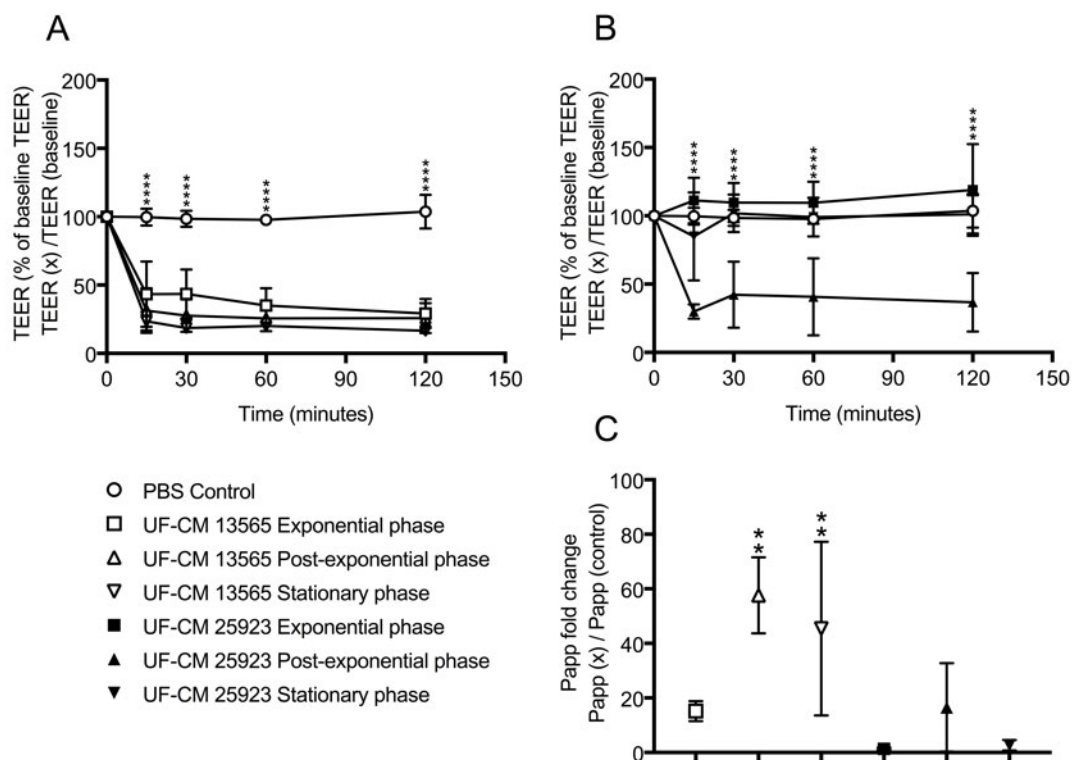


Figure 3. Impact of ultrafiltered conditioned media (UF-CM) derived from different *Staphylococcus aureus* strains and bacterial growth phases on transepithelial electrical resistance (TEER) and paracellular permeability (Papp).

HNEC-ALI cultures were treated with PBS control, exponential, post-exponential or stationary phase UF-CM from ATCC strains 13565 (A) and 25923 (B), with changes in TEER measured over time at 0, 15, 30, 60, and 120 minutes. TEER measurements are expressed as mean percentage change from the baseline (\pm SD). Alterations in Papp (C) are reported as mean fold change compared to the PBS control (\pm SD). Significance is denoted as (*) $p < 0.05$, (**) $p < 0.01$, (****) $p < 0.0001$. Data from at least 3 biologically independent replicates.

Heat and proteinase K treatment limit the barrier disrupting effects of *S. aureus* conditioned media.

Heat treatment to 80°C for 30 minutes abrogated the TEER reducing effects of the post-exponential phase UF-CM 13565, while heat-treated stationary growth phase UF-CM

I3565 retained its activity (Figure 4A). However, heat treatment to 100°C for 30 minutes was able to block the TEER effect from stationary growth phase UF-CM I3565 (Figure 4B). Overnight incubation of stationary growth phase UF-CM I3565 with proteinase K similarly abrogated the TEER reducing effect (Figure 4C).

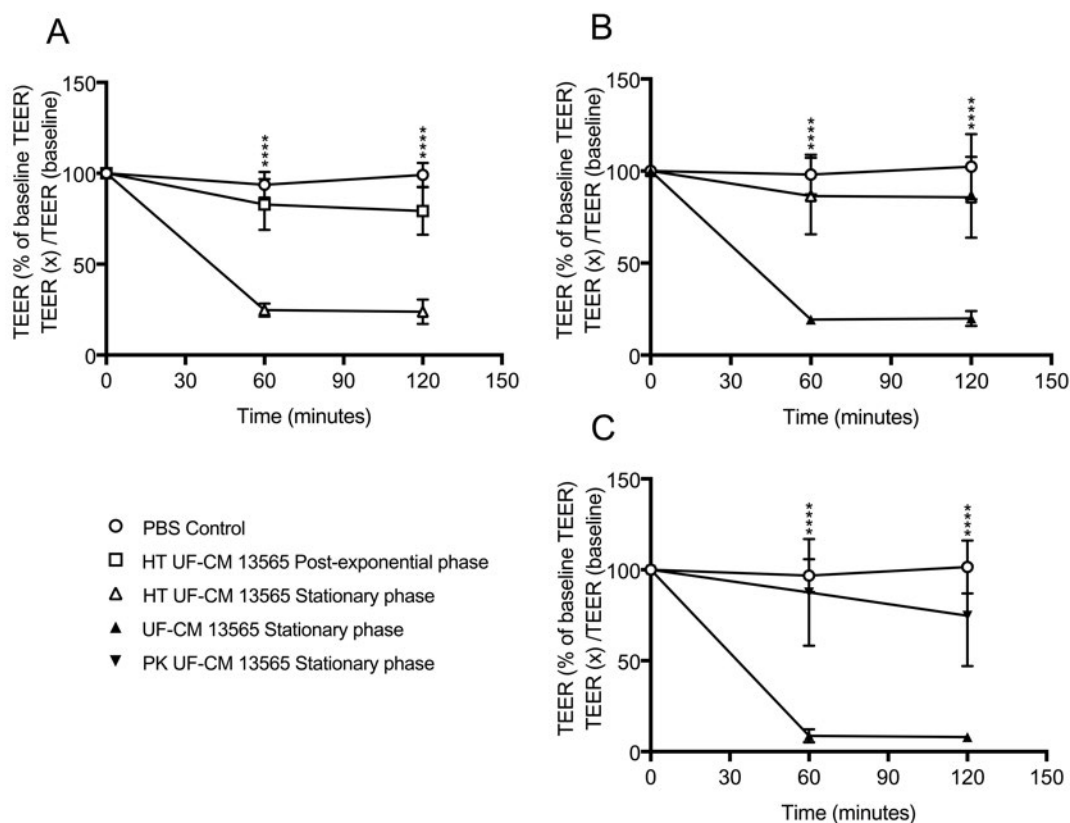


Figure 4. Impact of heat and proteinase K treatment on barrier disrupting effect of *Staphylococcus aureus* ultrafiltered conditioned media (UF-CM).

HNEC-ALI cultures were treated with PBS control, post exponential and stationary phase UF-CM I3565 heat treated to 80°C (A), stationary phase UF-CM I3565 with and without heat treatment (HT) to 100°C (B), and stationary phase UF-CM I3565 with and without proteinase K (PK) (C). Changes in TEER were measured over time at 0, 60, and 120 minutes. Measurements are expressed as mean percentage change from the baseline TEER (\pm SD). Significance is denoted as (****) p<0.0001. Data from at least 3 biologically independent replicates.

The barrier disrupting effect exists in the >30 kDa fraction of the *S. aureus* secretome

HNEC-ALI cultures were exposed to PBS control, and stationary growth phase UF-CM I3565 separated into three fractions: <3 kDa, 3-30 kDa, and >30k Da. Only the >30 kDa

fraction altered both the TEER and Papp (Figure 5). TEER in the >30kDa group was significantly lowered at all time points when compared to either PBS control or the other treatment groups (Figure 5A) ($p < 0.0001$). The >30 kDa Papp was increased to $14.6 (\pm 5.2)$ fold of the PBS control ($p < 0.0001$), while the Papp fold change of <3 kDa and 3-30 kDa groups were $0.8 (\pm 0.5)$ and $1.2 (\pm 1.0)$ respectively (Figure 5B).

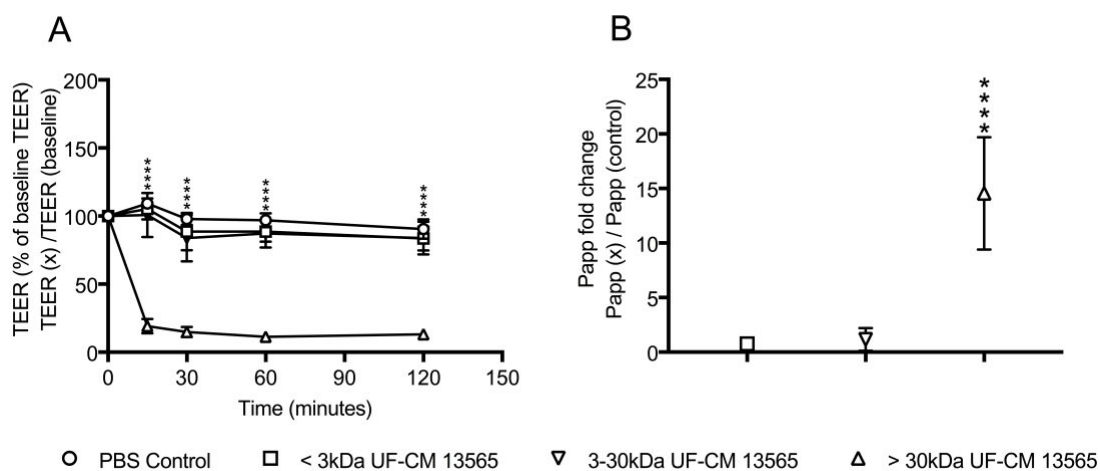


Figure 5. The *Staphylococcus aureus* barrier disrupting factor is localised to the >30kDa exoproteome fraction.

HNEC-ALI cultures were treated with PBS control, <3kDa ultrafiltered conditioned media (UF-CM) 13565, 3-30 kDa UF-CM 13565, and >30kDa UF-CM 13565. Barrier disruption was measured with transepithelial electrical resistance (A) at baseline, 15, 30, 60, and 120 minutes, and with paracellular permeability (Papp) (B). TEER measurements are expressed as mean percentage change from the baseline (\pm SD). Alterations in Papp (C) are reported as mean fold change compared to the PBS control (\pm SD). Significance is denoted as (****) $p < 0.0001$. Data from at least 3 biologically independent replicates.

The barrier disrupting factor is in the ultracentrifuged fraction of the *S. aureus* secretome

The UC fraction, obtained after overnight ultracentrifugation of the stationary growth phase UF-CM 13565 samples, retained the barrier disrupting activity (Figure 6). Disruption of TEER occurred more rapidly in the UC fraction when compared to UF-CM 13565 at the same protein concentration of 50 μ g/ml (Figure 6A) ($p < 0.0001$). The soluble proteins in the SN retained no significant activity on TEER, even when observed

for 360 minutes (Figure 6A). The Papp of the UC fraction was 13.1 (± 4.8 ; $p < 0.01$) fold of the PBS control, while the Papp of UF-CM and SN were 4.5 (± 2.4) and 0.91 (± 0.3) respectively (Figure 6B). The cytotoxicity assay showed no increase in LDH release following any of the treatments at 4 and 6 hours (Supplemental Figure S3). TJ protein ZO-1 immunolocalisation was assessed after treatment with PBS control, UF-CM, UC and SN fractions using confocal scanning laser microscopy (Figure 7). UF-CM and UC (Figures 7B & 7D) produced a discontinuous localisation of ZO-1 at the cell periphery compared to the PBS control and the SN portion (Figures 7A & 7C).

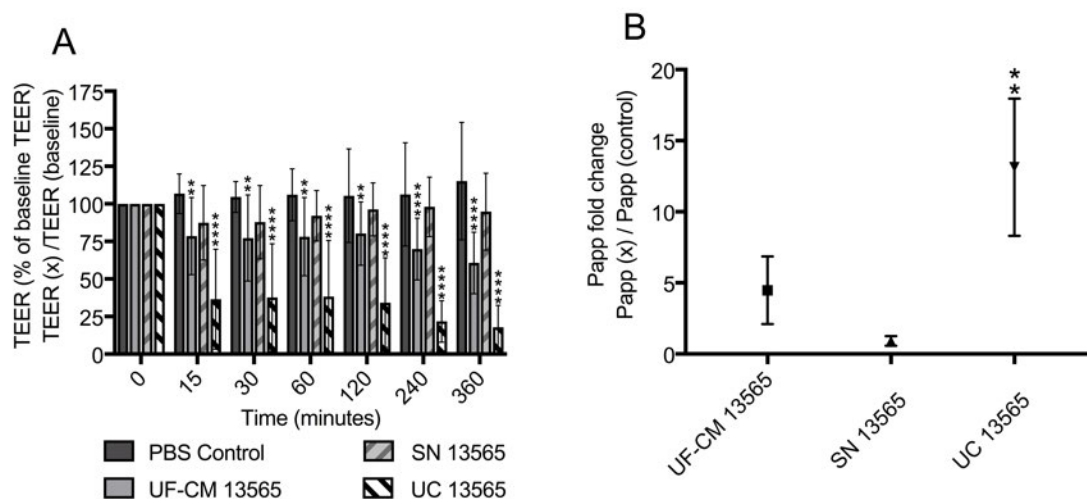


Figure 6. The ultracentrifugated (UC) fraction isolated from the *Staphylococcus aureus* conditioned media contains the barrier disrupting factor.

HNEC-ALI cultures were treated with PBS control, ATCC 13565 ultrafiltered conditioned media (UF-CM), supernatant (SN) fraction, and UC fraction. Barrier disruption was measured with transepithelial electrical resistance (TEER) (A) at baseline, 15, 30, 60, 120, 240, and 360 minutes, and with paracellular permeability (Papp) (B). TEER measurements are expressed as mean percentage change from the baseline (\pm SD). Alterations in Papp (C) are reported as mean fold change compared to the PBS control (\pm SD). Significance is denoted as (*) $p < 0.05$, (**) $p < 0.01$, (****) $p < 0.0001$. Data from 5 biologically independent replicates for TEER data and 3 biologically independent replicates for Papp data.

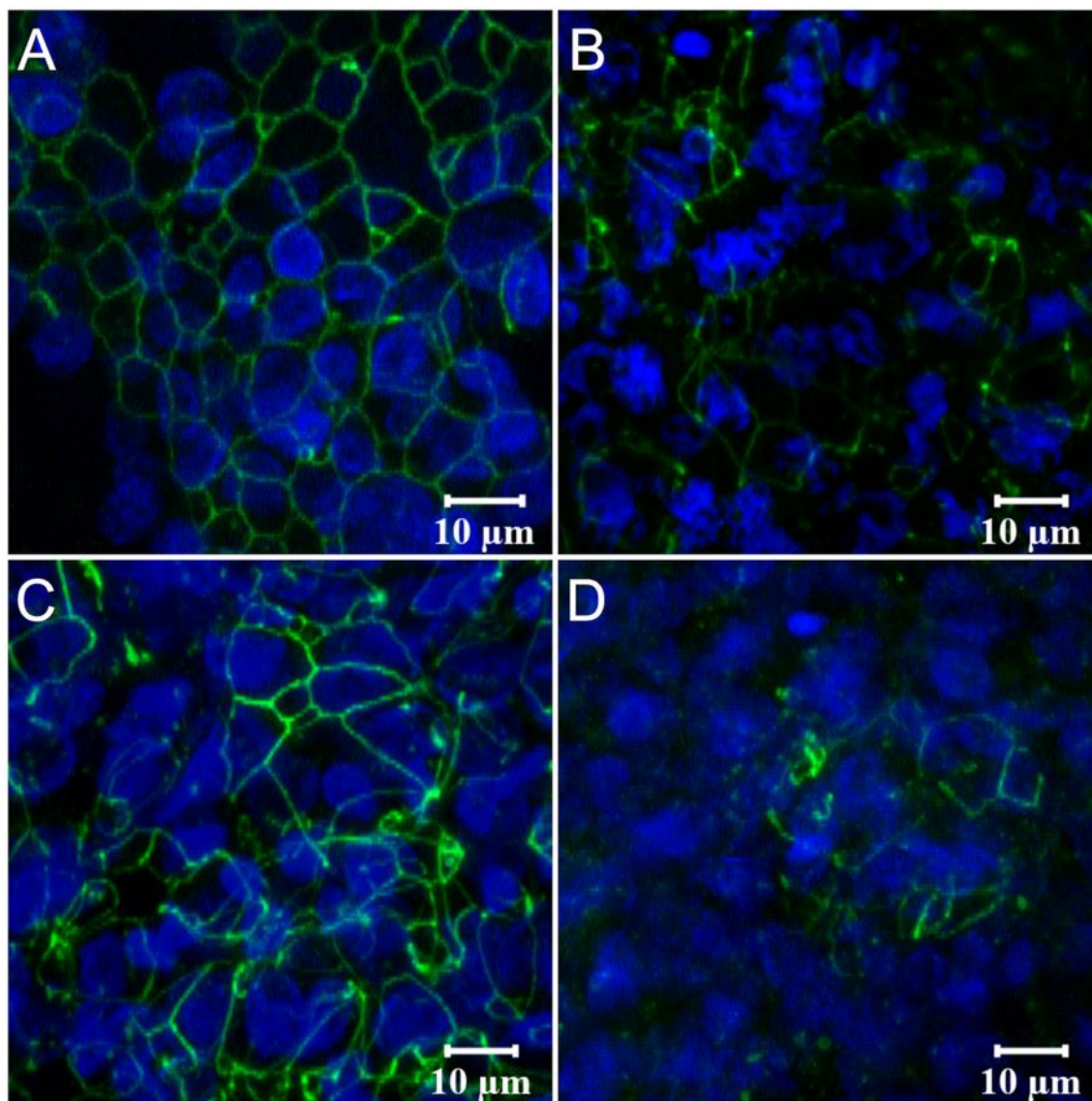


Figure 7. Tight junction protein ZO-1 is disrupted by ATCC 13565 ultrafiltered conditioned media (UF-CM) and ultracentrifuged (UC) fraction.

HNEC-ALI cultures exposed to PBS control (A), ATCC 13565 UF-CM (B), supernatant fraction (C), and UC fraction (D) were assessed for localisation of ZO-1. Immunofluorescence for ZO-1 was performed on two biologically independent samples.

Discussion

S. aureus secretome contains numerous factors and proteins that may explain the detrimental effects seen on the mucosal barrier in our study and the previous work from our department.^{19,458} To approach this unknown factor we have incorporated a top-down and bottom-up design. Our present study excluded purified *S. aureus* toxins/factors HLA, SEA, and LTA as mediators of airway barrier disruption. Additionally, we identified that the *S. aureus* barrier disrupting factor is primarily secreted in the post-exponential growth phase, susceptible to heat and protease treatments, larger than 30 kDa, and enriched in the UC fraction. Taken together, these findings suggest that the secreted factor is a large protein associated structure.

The initial proteomics analysis conducted on the *S. aureus* CM in this study identified 107 proteins; HLA was the most abundant factor found in our analysis. HLA is a soluble secreted protein, which interacts with eukaryotic cell membranes. Monomeric HLA binds to the plasma membrane to create a heptameric transmembrane pore.⁴⁵⁹ It has been reported to decrease the ciliary activity and associated with ultrastructural changes of nasal airway cells *in-vitro*.²³ Hermann et al. (2015) showed that recombinant HLA remodels the actin cytoskeleton of immortalised and primary human airway epithelial cells and prevents formation of cell to cell contacts.⁴⁶⁰ However, this was investigated on less differentiated submerged airway cultures compared to HNEC-ALI cultures. Furthermore, HLA affected each airway cell line differently as I6HBE14o- cells were HLA sensitive, while the bronchial S9 cell line was only transiently altered.⁴⁶⁰ Airway cell specific responses to HLA have previously been reported,⁴⁶¹ and may explain why the barrier in the differentiated ALI cultures in our study were not affected by HLA. Kwak et al., (2012) demonstrated that 0.4 - 1µg/ml HLA treatment of human epithelial colorectal adenocarcinoma (Caco-2) cells *in-vitro* resulted in significant reductions in

TEER and reduced TJ protein localisation. HLA induced TEER reductions were observed after 2 hours, and maximal at 16 hours of treatment. Additionally, they identified that HLA effect on the barrier is mediated through the basolateral side of the cell monolayer.²⁶⁸

Our previous work confirmed that ATCC 13565 carries the SEA gene, however SEA was not identified in our proteomic analysis.¹⁹ This may be due to a sampling issue when identifying the prominent gel spots in the SDS-PAGE. Additionally, the SEA gene is not present in the 25923 strain.¹⁹ *S. aureus* superantigens potentiate chronic inflammation in CRSwNP by activating large numbers of T cells. The detection of superantigens and specific IgE to superantigens are increased in CRSwNP.⁴⁶² It is unclear how these toxins are able to penetrate the sinonasal mucosal barrier. There is literature to support transcytosis of the toxin across a mucosal barrier.⁴⁶³ However, SEA is also thought to disrupt the gastrointestinal mucosal barrier by directly increasing epithelial permeability or via evoking a strong inflammatory and cytopathic response leading to subsequent barrier injury.^{455,464}

Lipoteichoic acid synthase was also identified in the analysis, which is necessary for *S. aureus* growth and LTA synthesis from phosphatidylglycerol.⁴⁶⁵ LTA is a major component of the gram positive cell wall, which is formed by polymers of repeating phosphodiester-linked polyols in the outer plasma membrane.⁴⁶⁵ LTA acts as an adhesion molecule by binding to Toll-like receptor 2 and the CD14 receptor, which results in release of proinflammatory cytokines, reactive oxygen and nitrogen species, and bactericidal peptides.^{316,466} LTA activation of TLR2 in lung endothelial cells mediates an increase in barrier permeability, through generation of reactive oxygen and nitrogen species.³¹⁶ Additionally, LTA has demonstrated effects on the *in-vitro* blood brain barrier in co-cultures of glial and endothelial cell by reductions in TEER and increased Papp.⁴¹⁶

Our findings indicated SEA or LTA purified proteins did not affect the TEER or Papp of HNEC-ALI cultures. These findings indicate that the known effects of these proteins on the mucosal barrier might be indirect and dependent on a third factor that is lacking in our experimental design or is cell type dependent.

From a top-down perspective we conducted further investigations of the CM from *S. aureus* ATCC 13565 and 25923. We have demonstrated that the barrier disrupting effect is secreted ubiquitously by ATCC 13565, however ATCC 25923 only displayed activity during the post-exponential phase. We previously reported that the ATCC 25923 strain had no effect on TEER as CM in this particular study was based on late-stationary phase cultures.¹⁹ The regulation of *S. aureus* extracellular proteins is tightly regulated by *sarA*, *agr* quorum sensing system, and *sigma* factors.^{467,468,379} Extracellular protein secretion differs throughout bacterial growth phases, with some protein expression that reflects absolute cell density and others that are only expressed during exponential and post exponential phases to facilitate host invasion.^{379,469}

Heat treatment of the UF-CM negated the barrier disrupting effects, suggesting that the mechanism of barrier disruption is unlikely due to an immune response to the factor even though previous works have demonstrated that cleaved peptides may still be immunogenic.^{470,471} Also, it reduces the likelihood of the factor being a *S. aureus* superantigen as they are moderately thermostable.^{472,473} To confirm the proteinaceous nature of the factor, UF-CM was incubated overnight with proteinase K at 37°C. This data shows that the factor is altered by the proteinase K treatment, and coupled with the effects of heat treatment and size fractionation suggest the factor is: a large protein (>30 kDa), protein complex, or associated with a larger structure.

The UC fraction demonstrated a rapid (15 minute) TEER disrupting effect coupled with an increase in Papp. Additionally, the staining of TJ protein ZO-1 was dramatically

reduced. Conversely the SN fraction, containing soluble proteins showed no barrier disrupting activity at 6 hours of treatment. Differential ultracentrifugation is a common method for separating soluble proteins from larger microsomal components such as extracellular vesicles (EVs).^{474,475} *S. aureus* EVs have previously been isolated using differential ultracentrifugation.^{426,476,477} A previous proteomics study of *S. aureus* EV contents identified several notable toxins such as staphylococcal enterotoxin Q, HLA, gamma-hemolysin, and staphopain A.⁴²³

Gurung et al., (2011) identified that intact *S. aureus* EVs are necessary to deliver bacterial components into a Hep-2 cell line to induce apoptosis.⁴²⁴ More recently it was shown that EVs are necessary for delivery of active HLA into HeLa cells,⁴²⁵ which may explain why purified HLA had no effect in the current study. *S. aureus* EVs have been implicated in the induction of Th1 and Th17 pulmonary inflammatory responses in a mouse model of EV inhalation.⁴²⁶ Hong et al., (2011) demonstrated that *S. aureus* EVs stimulated atopic dermatitis-like inflammation,⁴⁷⁶ which is associated with an abnormal barrier function.²⁹⁵ Additionally, patients with atopic dermatitis have increased *S. aureus* EVs on their skin and exhibited higher levels of EV-specific IgE.⁴⁷⁶ A follow up study confirmed that *S. aureus* secreted HLA and EV associated HLA both induce skin barrier disruption. The authors established that EV associated HLA stimulated more severe barrier disruption and inflammatory response.⁴⁷⁸

In our study the UC fraction retained the barrier disrupting factor, suggesting that the responsible factor could be related to EVs. However, the UC pellets may have also contained protein aggregates, lipoprotein particles and other contaminants that are artificially increased in the UC fraction. Indeed, further work is needed to continue optimisation, purification, and identification of *S. aureus* EVs to confirm the barrier disrupting mechanism.

In conclusion, we have observed that purified HLA, SEA, and LTA did not mediate airway barrier dysfunction *in-vitro*. These were applied as single toxins, hence additional experiments are needed to definitively exclude any contribution to barrier dysfunction. Furthermore, our characterisation of the *S. aureus* secretome has indicated that the responsible factor is primarily produced in the post-exponential growth phase with differential expression between strains. The UC fraction activity alludes to the possibility that barrier dysfunction is associated with *S. aureus* EVs. The investigation of *S. aureus* EV production and its role in pathogenesis is in its infancy, and clearly further work is warranted.

Acknowledgements

This work is supported by a Garnett Passe and Rodney Williams Memorial Foundation scholarship to JM and a Garnett Passe and Rodney Williams Memorial Foundation Conjoint Grant to PJW and SV.

Supplementary Information

Supplementary methods

Sodium dodecyl sulphate polyacrylamide gel electrophoresis (SDS-PAGE) and Coomassie staining

Conditioned media (CM) and ultrafiltered (UF) CM samples from ATCC B565 at exponential, post-exponential, and stationary phases of growth were prepared for SDS-PAGE separation. Samples were initially mixed with acetone -20°C with a 4:1 ratio and dithiothreitol (DTT) 0.5% w/v, and incubated overnight at -20°C. Following this samples were centrifuged for 60 minutes at 30,000 x g. The acetone was decanted and the protein pellet resuspended in M-PER mammalian protein extraction reagent with HALT protease inhibitor (Thermo Scientific, Waltham, MA). Samples were then subjected to DC protein assay (Bio-Rad, Hercules, CA). 10 µg of protein sample was resolved using NuPAGE Bis-Tris 4-12% gel (Invitrogen, Carlsbad, CA) and MES SDS running buffer (Invitrogen). Briefly, the gel was fixed in 40% ethanol and 10% acetic acid overnight, and then washed with aqua bidest double distilled water. Following this the gel was stained with Coomassie brilliant blue, residual stain was then washed with aqua bidest and the gel stored in 1% acetic acid.

Liquid chromatography – electrospray ionisation tandem mass spectrometry (LC-ESI-MS/MS)

Samples were prepared from the gel bands 1-7 (Supplemental Figure SI). Initially samples were washed in 500 µL of 50 mM ammonium bicarbonate (NH₄HCO₃) and destained with 100 mM NH₄HCO₃ in 30% acetonitrile (ACN). Washed with 50 mM NH₄HCO₃, reduced with 0.5 µmol dithiothreitol (DTT) in 50mM NH₄HCO₃. Alkylated

with 2.75 μmol iodoacetamide (IAA) in 50 mM NH_4HCO_3 , and digested with 100 ng of sequencing grade modified trypsin (Promega, Madison, WI) in 5 mM NH_4HCO_3 in 10% ACN. Peptides were extracted using 3 washes of 1% formic acid (FA) in water, 1% FA in 50% ACN and 100% ACN respectively. The volumes of the resulting peptide extracts were reduced by vacuum centrifugation to approximately 1 μL then resuspended with 0.1% TFA in 2% ACN to a total volume of ~ 10 μL .

LC-ESI-MS/MS was performed using an Ultimate 3000 nan-flow system (Dionex) coupled to an Impact II QTOF mass spectrometer (Bruker Daltonics, Billerica, MA) via an Advance CaptiveSpray source (Bruker Daltonics). 4 μL of each digested sample was loaded onto a trapping column (Acclaim PepMap100, C18, pore size 100 \AA , particle size 3 μm , 75 μm ID x 2 cm length, Thermo Scientific) at 3 $\mu\text{L}/\text{min}$ using 0.1% FA, 5% ACN in water. Peptide separation was then performed on an Acclaim PepMapp RSLC column (C18, pore size 100 \AA , particle size 3 μm , 75 μm ID x 15 cm length, Dionex) at 0.3 $\mu\text{L}/\text{min}$ using a linear gradient of 5-45% ACN in 0.1% FA over 90 minutes. Collision-induced dissociation (CID) spectra were acquired in the 150-2000 m/z range in a data-dependent fashion using Bruker's Shotgun Instant Expertise method. This method uses IDAS (intensity dependent acquisition speed) to adapt the speed of the acquisition depending on the intensity of precursor ions (fixed cycle time), and RT2 (RealTime Re-Think) to exclude previously selected precursor ions from undergoing re-fragmentation unless the chromatographic peak intensity of the ion has increased by a factor of 5.

Proteomic data analysis

Post acquisition, acquired spectra were subjected to peak detection and de-convolution using Compass DataAnalysis for OTOF (version 1.7, Bruker Daltonics). Processed MS/MS spectra were then exported to Mascot generic format (mgf) and submitted to

Mascot (version 2.3.02) for identification. Search parameters were as follows; the SwissProt database was searched, the taxonomy used was Bacteria, the enzyme was specified as trypsin with up to 2 missed cleavages, variable modification of carbamidomethyl of cysteine and oxidation of methionine, MS mass tolerance of 50 ppm, and MS/MS mass tolerance of 0.2 Da. Mascot protein identifications were made if at least two unique peptides were sequenced from a protein and had individual ion scores above the homology threshold. Multiple charge states were not considered as unique. Protein identities, SwissProt accession number, molecular weight, and exponentially modified protein abundance index (emPAI) value are listed in Supplemental Table S1. emPAI is an approximate measure of relative quantification for proteins within each gel spot/band, as previously developed.⁴⁷⁹

Supplementary results

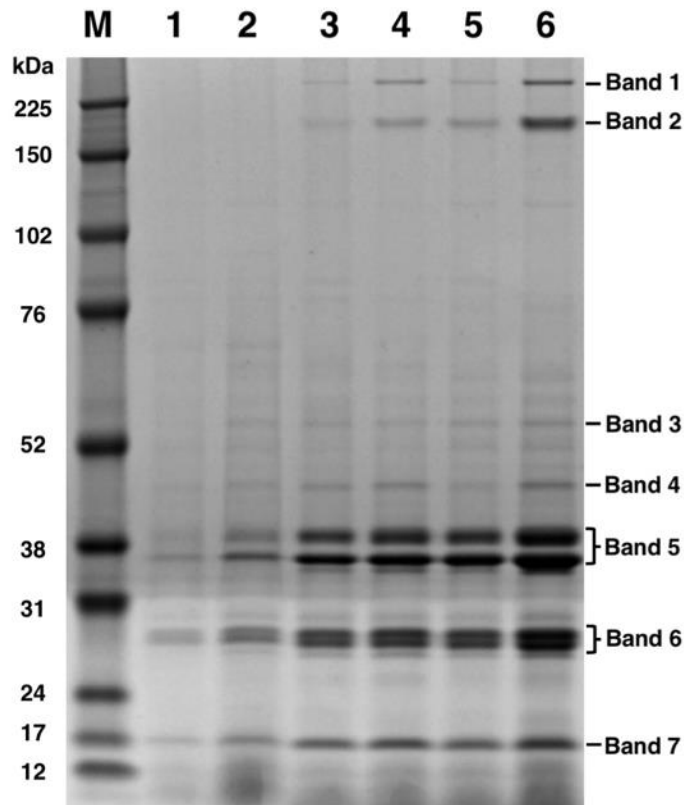
Supplemental Table S1. UF-CM 13565 Stationary phase supernatant mascot protein identification with liquid chromatography – electrospray ionization tandem mass spectrometry.

Accession number of the protein according to SwissProt database. Relative quantification within each band (gel spot) is reported as the exponentially modified protein abundance index (emPAI) value.

Mascot protein identifications	Accession number	MW (kDa)	emPAI
Band 1			
Alpha-hemolysin	HLA_STAAU	35.88	20.82
Extracellular matrix-binding protein ebh	EBH_STAAC	1130.66	-1.0
Extracellular matrix-binding protein EbhA	EBHA_STAAM	721.89	-1.0
Extracellular matrix-binding protein ebh	EBH_STAAR	1156.47	-1.0
DNA gyrase subunit A	GYRA_STAAC	99.29	-1.0
Band 2			
Alpha-hemolysin	HLA_STAAU	35.88	75.38
Extracellular matrix-binding protein ebh	EBH_STAAR	1156.47	-1.0
Band 3			
Lipoteichoic acid synthase	LTAS_STAAC	74.35	6.63
Lipoteichoic acid synthase	LTAS_STAAB	74.35	6.63
Bifunctional autolysin	ATL_STAAM	136.67	0.56
Lipase 1	LIPI_STAA8	76.63	1.79
Lipase 1	LIPI_STAAR	76.56	1.38
Probable glycine dehydrogenase (decarboxylating) subunit 1	GCSPA_STAAM	49.68	1.33
Cysteine-tRNA ligase	SYC_STAAC	53.65	1.46
Alpha-hemolysin	HLA_STAAU	35.88	2.21
Dihydrolipoyl dehydrogenase	DLDH_STAAC	49.42	0.53
N-acetylmuramoyl-L-alanine amidase domain-containing protein SAOUHSC 02979	Y2979_STAA8	69.21	0.36
Elongation factor G	EFG_STAAB	76.56	0.32
Glutamine synthetase	GLNA_STAAC	50.81	0.61
Serine-tRNA ligase	SYS_STAAC	48.61	0.36
Glutamine synthetase	GLNA_STAAR	50.82	0.51
Phosphoenolpyruvate carboxykinase ATP	PCKA_STAAC	59.34	0.29
Glutamate-tRNA ligase	SYE_STAAB	56.31	0.11
Lipase 2	LIP2_STAAR	76.64	0.08
Formate-tetrahydrofolate ligase	FTHS_STAAC	59.88	0.11
Serine-aspartate repeat-containing protein C	SDRC_STAAC	102.85	0.03
Aconitate hydratase	ACON_STAAC	98.91	0.03
Band 4			
Lipase 1	LIPI_STAA8	76.63	3.31
Staphopain B	SSPB_STAAC	44.49	7.67
Staphopain B	SSPB_STAAS	44.58	6.54
Staphopain B	SSPB_STAAU	44.55	5.19
Alanine dehydrogenase 2	DHA2_STAA3	40.08	6.54
Alanine dehydrogenase 2	DHA2_STAAR	40.09	6.54
Enolase	ENO_STAAB	47.09	1.96
Ornithine aminotransferase 2	OAT2_STAAC	43.39	1.0

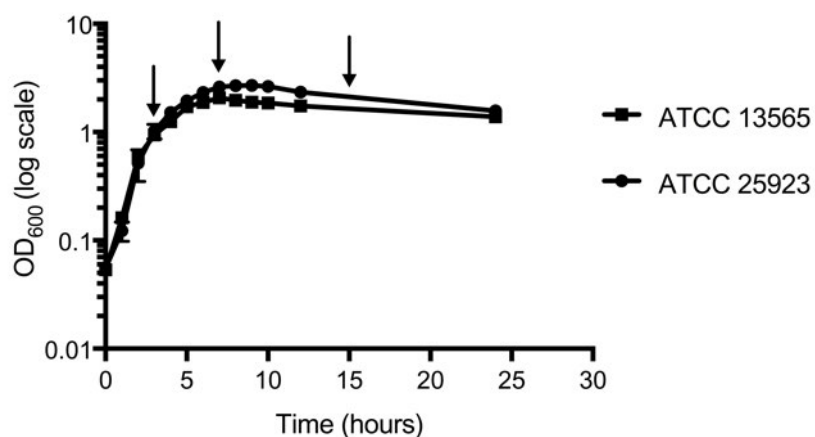
N-acetylmuramoyl-L-alanine amidase domain-containing protein SAOUHSC 02979	Y2979_STAA8	69.21	0.48
Uncharacterized peptidase SA1530	Y1530_STAAN	39.58	0.7
Lipoteichoic acid synthase	LTAS_STAAC	74.35	0.38
Probable acetyl-CoA acyltransferase	THLA_STAAC	41.65	0.54
Phosphoglycerate kinase	PGK_STAAB	42.58	0.64
Alpha-hemolysin	HLA_STAAU	35.88	0.65
Phosphopentomutase	DEOB_STAAB	43.77	0.41
Gamma-hemolysin component B	HLGB_STAAC	36.69	0.39
Lipase 2	HLGB_STAAC	76.34	0.13
6-phosphogluconate dehydrogenase, decarboxylating	6PGD_STAAC	51.77	0.26
NAD-specific glutamate dehydrogenase	DHE2_STAAC	45.73	0.3
Probable uridylyltransferase SACOL2I61	URTF_STAAC	44.87	0.14
Band 5			
Alpha-hemolysin	HLA_STAA8	35.95	133.09
Phospholipase C	PHLC_STAAC	37.21	14.36
Gamma-hemolysin component B	HLGB_STAAC	36.69	6.63
Leucotoxin LukDv	LUKDV_STAAS	36.87	4.49
Gamma-hemolysin component B	HLGB_STAAR	36.79	5.49
Leucotoxin LukEv	LUKEV_STAA8	34.14	3.04
Elongation factor Ts	EFTS_STAAC	32.47	2.29
Gamma-hemolysin component A	HLGA_STAAC	34.93	1.35
Lipase 1	LIPI_STAA8	76.63	0.6
1-phosphatidylinositol phosphodiesterase	PLC_STAAE	35.23	1.15
Leucotoxin LukE	LUKE_STAAU	35.22	0.66
Bifunctional autolysin	ATL_STAAM	136.67	0.14
Foldase protein PrsA	PRSA_STAAB	35.6	0.52
Gamma-hemolysin component C	HLGC_STAAR	35.62	0.52
Glutamyl endopeptidase	SSPA_STAAC	36.29	0.28
Malonyl CoA-acyl carrier protein transacylase	FABD_STAAC	33.61	0.43
Succinyl-CoA ligase ADP-forming subunit alpha	SUCD_STAAC	31.52	0.33
Thioredoxin reductase	TRXB_STAAC	33.59	0.43
Uncharacterized protein MW1862	Y1862_STAAW	38.52	0.17
Alcohol dehydrogenase	ADH_STAAB	36.02	0.18
Band 6			
Serine protease SplB	SPLB_STAAC	26.08	29.27
Serine protease SplB	SPLB_STAAM	26.12	18.21
Serine protease SplA	SPLA_STAAC	25.86	18.69
Serine protease SplD	SPLD_STAAE	25.66	15.02
Serine protease SplF	SPLF_STAA2	25.56	10.45
Serine protease SplF	SPLF_STAAC	25.64	9.09
Alpha-hemolysin	HLA_STAAU	35.88	7.73
Serine protease SplA	SPLA2_STAAU	25.37	2.6
Serine protease SplE	SPLE_STAAC	25.66	2.18
Serine protease SplB	SPLB_STAAB	26.08	1.78
Serine protease SplC	SPLC_STAAC	26.08	1.78
Serine protease SplC	SPLC_STAAS	26.02	1.49
Putative dipeptidase SABI61lc	PEPVL_STAAB	52.75	0.49
Phospholipase C	PHLC_STAAC	37.21	0.38
UPF0447 protein MW0542	Y542_STAAW	29.37	1.03
UPF0447 protein SA0544	Y544_STAAN	29.37	1.03

Serine protease SplE	SPLA_STAAR	25.71	0.78
Adenylate kinase	KAD_STAAC	23.96	1.37
2-C-methyl-D-erythritol 4-phosphate cytidyl transferase 2	ISPD2_STAAC	26.64	1.18
2-C-methyl-D-erythritol 4-phosphate cytidyl transferase 2	ISPD2_STAAB	26.64	1.18
Band 7			
Alpha-hemolysin	HLA_STAAU	35.88	7.05
Serine protease SplB	SPLB_STAAC	26.08	2.92
Serine protease SplF	SPLF_STAAC	25.64	1.52
Serine protease SplF	SPLF_STAA2	25.56	1.53
50S ribosomal protein L17	RL17_STAA1	13.74	1.86
Nucleoside diphosphate kinase	NDK_STAAB	16.56	3.11
50S ribosomal protein L21	RL21_STAA1	11.33	3.56
Serine protease SplA	SPLA_STAAC	25.86	0.99
50S ribosomal protein L25	RL25_STAA3	23.77	1.11
Phospholipase C	PHLC_STAAC	37.21	0.62
50S ribosomal protein L11	RL11_STAA1	14.86	2.93
Serine protease SplD	SPLD_STAAE	25.66	0.59
Staphylokinase	SAK_STAAM	18.48	1.22
50S ribosomal protein L22	RL22_STAA1	12.83	2.07
Gamma-hemolysin component B	HLGB_STAAC	36.69	0.39
Gamma-hemolysin component A	HLGA_STAAC	34.93	0.53
30S ribosomal protein S9	RS9_STAA1	14.61	0.81
77 kDa membrane protein	OMP7_STAAC	77.01	0.12
Uncharacterized protein SAB0704	Y704_STAAB	22.2	0.94
6,7-dimethyl-8-ribityllumazine synthase	RISB_STAAB	16.39	0.7



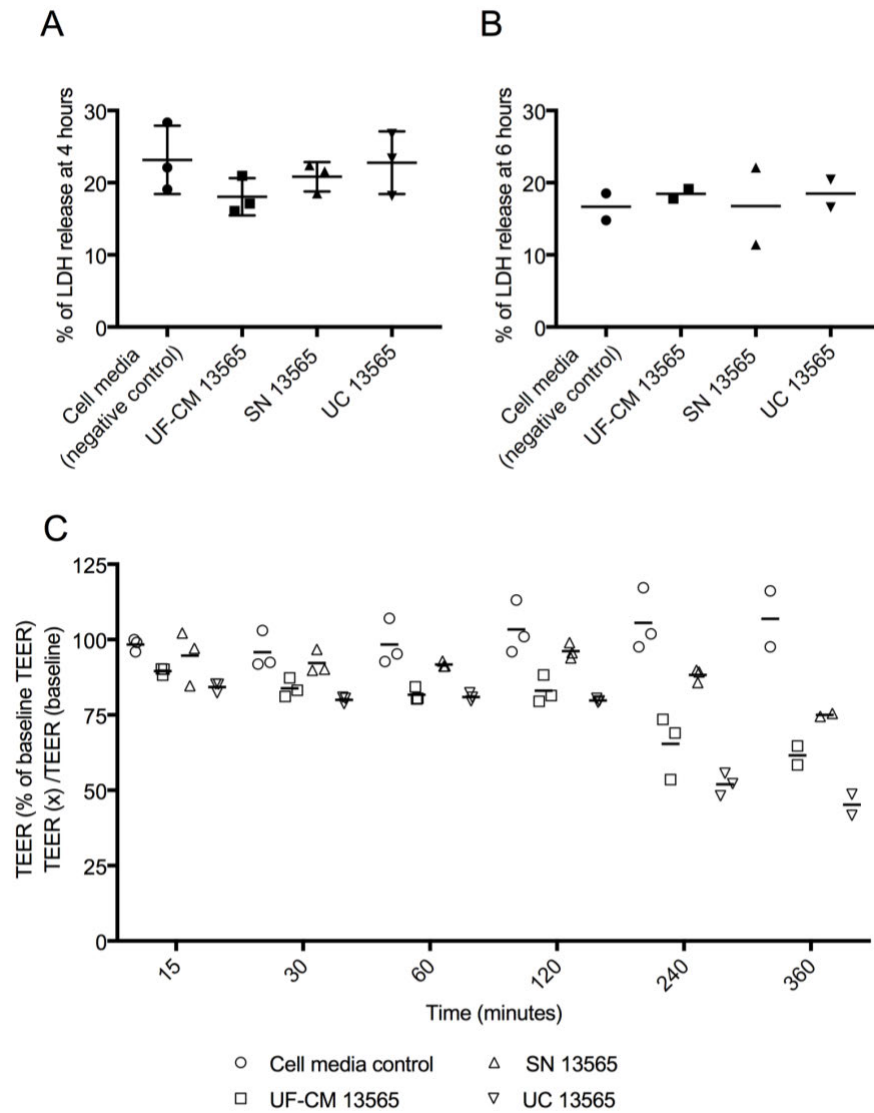
Supplemental Figure S1. Sodium dodecyl sulphate polyacrylamide gel electrophoresis (SDS-PAGE) of *S. aureus* conditioned media (CM) and ultrafiltered (UF) CM at different growth phases.

The lanes depicted are size marker (M), exponential CM ATCC 13565 (1), exponential UF-CM ATCC 13565 (2), post-exponential CM ATCC 13565 (3), post-exponential UF-CM ATCC 13565 (4), stationary CM ATCC 13565 (5), and stationary UF-CM ATCC 13565 (6). SDS-PAGE gel identifies several high intensity stain bands for analysis and demonstrates that UF does not alter the exoproteome.



Supplemental Figure S2. Bacterial growth curve of ATCC strains 13565 and 25923.

Conditioned media collection during the exponential, post-exponential, and stationary growth phases (arrows placed at 3, 7, and 15 hours).



Supplemental Figure S3. Lactate dehydrogenase (LDH) assay

ATCC 13565 UF-CM, supernatant (SN) fraction after ultracentrifugation (UC), and the UC fraction are not cytotoxic at 4 (A) or 6 (B) hours of HNEC-ALI treatment. LDH is expressed as a percentage of total LDH release determined with a Triton-X positive control. (C) Transepithelial electrical resistance (TEER) was measured simultaneously with the LDH assay. Data until 4 hours includes n=3, and data between 4-6 hours includes n=2. The values are shown as single data points, and mean.

Staphylococcus aureus* V8 Protease Disrupts the Integrity of the Airway Epithelial Barrier and Impairs IL-6 Production *in-vitro

Statement of authorship

Title of Paper	Staphylococcus aureus V8 protease disrupts the integrity of the airway epithelial barrier and impairs IL-6 production in vitro
Publication Status	Published
Publication Details	Murphy J , Ramezanpour M, Stach N, Dubin G, Psaltis AJ, Wormald PJ, Vreugde S. <i>Staphylococcus aureus</i> V8 protease disrupts the integrity of the airway epithelial barrier and impairs IL-6 production <i>in-vitro</i> . <i>Laryngoscope</i> . 2018;128(1):E8-E15. doi:10.1002/lary.26949

Principal Author

Name of Principal Author (Candidate)	Jae Murphy		
Contribution to the Paper	Experimental design, performed collection of samples, conducted experiments, interpreted and analysed data, preparation of manuscript		
Overall percentage (%)	75%		
Certification	This paper reports on original research I conducted during the period of my Higher Degree by Research candidature and is not subject to any obligations or contractual agreements with a third party that would constrain its inclusion in this thesis. I am the primary author of this paper.		
Signature		Date	06.07.2018

Co-Author Contributions

By signing the Statement of Authorship, each author certifies that:

- i. the candidate's stated contribution to the publication is accurate;
- ii. permission is granted for the candidate to include the publication in the thesis; and
- iii. the sum of all co-author contributions is equal to 100% less the candidate's stated contribution.

Name of Co-Author	Mahnaz Ramezanpour		
Contribution to the Paper	Assistance with conducting experiments, manuscript editing		
Signature		Date	06.07.2018
Name of Co-Author	Natalia Stach		
Contribution to the Paper	Preparation of experiment materials, manuscript editing		
Signature		Date	06.07.2018
Name of Co-Author	Grzegorz Dubin		
Contribution to the Paper	Preparation of experiment materials, project supervision, manuscript editing		
Signature		Date	06.07.2018
Name of Co-Author	Alkis James Psaltis		
Contribution to the Paper	Project supervision, manuscript editing		
Signature		Date	06.07.2018
Name of Co-Author	Peter-John Wormald		
Contribution to the Paper	Project supervision, manuscript editing		
Signature		Date	06.07.2018
Name of Co-Author	Sarah Vreugde		
Contribution to the Paper	Assistance with experimental design, project supervision, manuscript editing, corresponding author		
Signature		Date	06.07.2018

Citation

Murphy J, Ramezanpour M, Stach N, Dubin G, Psaltis AJ, Wormald PJ, Vreugde S. *Staphylococcus aureus* V8 protease disrupts the integrity of the airway epithelial barrier and impairs IL-6 production *in-vitro*. *Laryngoscope*. 2018;128:E8-E15. doi:10.1002/lary.26949

Abstract

Objectives: *Staphylococcus aureus* (*S. aureus*) infection is known to contribute to the severity and recalcitrance of chronic rhinosinusitis (CRS), and its secreted products have been shown to alter the airway barrier. Extracellular proteases secreted by *S. aureus* are thought to be important in epithelial infection and immune evasion however their effect on airway mucosal barrier function is not known.

Methods: To investigate the impact of extracellular proteases on airway epithelial integrity, the purified *S. aureus* proteases V8 protease, Staphopain A, Staphopain B, Exfoliative Toxin A and Serine protease-like (Spl) A-F were applied to human nasal epithelial cell air-liquid interface (HNEC-ALI) cultures. Transepithelial electrical resistance (TEER), permeability (Papp) measurements and immuno-localisation of the tight junction proteins claudin-1 and ZO-1 were used to assess barrier integrity. Effects of the proteases on inflammation and cell viability were measured using interleukin-6 (IL-6) ELISA and a lactate dehydrogenase (LDH) assay.

Results: Application of V8 protease to HNEC-ALI cultures caused a significant concentration and time dependent decrease in TEER (22.67%, $p < 0.0001$), a reciprocal Papp increase (20.14 fold, $p < 0.05$) and a discontinuous ZO-1 immuno-localisation compared to control. IL-6 production was significantly reduced in V8 protease treated

cells (153.5pg/ml, p=0.0069) compared to control (548.3 pg/ml) while no difference in cell viability was observed.

Conclusion: *S. aureus* V8 protease causes dysfunction of mucosal barrier structure and function indicative of a “leaky” barrier. A reduction in IL-6 levels suggests that the mucosal immunity is impaired by this protease, and hence has the potential to contribute to CRS recalcitrance.

Keywords: *Staphylococcus aureus*, extracellular proteases, Interleukin-6, chronic rhinosinusitis, airway barrier.

Introduction

The sinonasal mucosa presents the first innate barrier defence to external pathogens within the paranasal sinuses. A crucial aspect of which is the function of apical junctional complexes at the cell-to-cell interface. The most superficial of these important structures includes the tight and adherens junctions. These regulate ion and molecular movement between environment and host, and maintain cell polarity, while also coordinating the mucosal response to pathogens, allergens, and other foreign particles.⁴⁵³ Tight junctions (TJ) are formed by the coupling of transmembrane proteins between neighbouring cells and include occludin and the claudin family. Inter-cellular heterodimers such as Zona Occludens-1 (ZO-1), are anchored on their cytoplasmic end by associated proteins and the actin cytoskeleton.⁴⁵²

TJ disruption and a subsequent leaky epithelial barrier have been implicated in several chronic diseases including atopic dermatitis, asthma, and inflammatory bowel disease. Microbial pathogens of the gastrointestinal tract have developed mechanisms to disrupt the TJ barrier and cross the mucosal barrier, reportedly mediated by secreted toxins, proteases, or signalling molecules.⁴⁸⁰

Chronic Rhinosinusitis (CRS) is widely recognised as a heterogeneous disease with a multifactorial pathogenesis involving host, microbial, and environmental influences. Sinonasal mucosa from patients with CRS, particularly those with nasal polyps has recently exhibited properties of a leaky barrier.²⁰ A plethora of evidence implicates *Staphylococcus aureus* (*S. aureus*) in the initiation and persistence of CRS, post-surgical infections and poor wound healing.^{331,450,481,482} *S. aureus* also secretes products that disrupt the sinonasal TJ barrier *in-vitro*.¹⁹ The products responsible for this mechanism in sinonasal epithelium remain unknown.

S. aureus extracellular proteases include cysteine (staphopain A and B), serine (V8 protease) and serine protease-like (spl proteases), and metalloproteases. Such proteases have previously been implicated in enhanced tissue invasion, degradation of immune defences, and regulation of microbial biofilm.^{379,384,483,484} *S. aureus* V8 protease causes epidermal barrier dysfunction, and Exfoliative Toxin A (ETA) cleaves desmoglein resulting in loss of cell-cell adhesion.^{293,485} Furthermore, *S. aureus* induces an interleukin-6 (IL-6) response in cell culture and nasal explant models, confirming IL-6 as an indicator for *S. aureus* related immune responses.^{388,486}

The aim of this study was to investigate the effects of *S. aureus* extracellular proteases on the barrier function of differentiated nasal epithelial cells. Evaluating their ability to alter paracellular junctions, TJ protein localisation, and cytokine expression.

Methods

Ethics statement

Ethics approval for cytological nasal brushings from healthy volunteers was granted by the Queen Elizabeth Hospital Ethics Committee. All participants enrolled were given written informed consent, an information sheet, and participation was voluntary. Exclusion criteria included active smoking, under 18 years old, recent upper respiratory tract infection, and CRS or allergic rhinitis.

Primary nasal epithelial cell air-liquid interface culture

Nasal brushings were taken from the inferior turbinates using cytology brushes (McFarlane Medical Equipment Pty Ltd, VIC, Australia) and transported in Bronchial Epithelial Cell Growth Medium (BEGM) (Lonza, Basel, Switzerland). Samples were centrifuged (1700 RPM; 5 minutes) and resuspended in Clonetics™ B-ALI™ growth medium (Lonza) in a culture plate coated with anti-CD68 (Dako, CA, USA). Cells were then seeded onto a type 1 collagen coated T25 flask (Corning, NY, USA). Cells were harvested when 80% confluent for seeding onto collagen coated 6.5 mm permeable polyester transwell membranes with 0.4 µm pores (Corning) at a density of 7×10^4 cells per well. Human nasal epithelial cell air-liquid interface cultures (HNEC-ALI) were established as reported previously from our department.³²³ In short, cell cultures were maintained with B-ALI™ growth medium for 3-4 days in at 37°C with 5% CO₂. The apical and basal media was then removed and the basal media replaced with B-ALI™ differentiation media. HNEC-ALI cultures were maintained for 14 days for barrier function development.⁴⁵⁷

***Staphylococcus aureus* extracellular proteases**

Staphopains A and B were isolated from the culture supernatants of strain 8325-4, whereas V8 protease was purified from strain V8BC10, as described previously.^{383,487-489} ETA was expressed in *E. coli* and purified as earlier described.^{490,491} SplA, SplB, SplC and SplD were expressed in *E. coli* as described previously.^{396-398,492} SplE was expressed in *E. coli* from pGEX-5T plasmid. The GST fusion was recovered by affinity chromatography and the tag was removed using thrombin. GST was separated by ion-exchange chromatography (SourceS, GE Healthcare, UK) in 50 mM sodium acetate, pH 5.5. SplE was further purified and the buffer exchanged by gel filtration in 5 mM Tris pH 8.0, 100 mM NaCl (Superdex 75 pg, GE Healthcare, UK). SplF was expressed in *E. coli* from pET 20b(+). Secreted SplF was precipitated from the culture medium using ammonium sulphate (85% saturation) and initially purified by nickel affinity chromatography. Further purification was achieved using anion exchange chromatography (MonoQ, GE Healthcare, UK) in 50mM Tris-HCl, pH=7,5. The protein was dialyzed against PBS and stored frozen until further use. The purity of all preparations was at least 95%, as assessed by SDS-PAGE. The enzymes were resuspended in phosphate buffered saline (PBS) and stored at -20 °C. Spl proteases were used separately and as a combined treatment Spl (A-F). All protease was used at 100 µg/ml unless otherwise stated.

Microbial conditioned media and protease activity

Three American Type Culture Collection (ATCC) reference strains of *S. aureus* (13565, 14458, and 25923) were cultured in nutrient broth for 7 hours at 37°C. Supernatant from each strain was collected by centrifugation at 3000 RPM and then 0.22 µm filter sterilized. V8 protease activity of each strain was tested in 90% and 50% supernatant concentrations, and compared to 100, 10, and 1 µg/ml of V8 protease. The fluorescent

substrate (Z-Leu-Leu-Glu-7-amido-4-methylcoumarin; Bachem, Bubendorf, Switzerland) was suspended at 60 μM with the respective protease or supernatant, and incubated for 30 minutes. Excitation 380 nm and emission 460 nm were measured using FLUOstar Optima 96-well microplate reader (BMG Labtech, Ortenberg, Germany). Results are expressed as relative fluorescence units (RFU).

Transepithelial electrical resistance

Transepithelial electrical resistance (TEER) was measured using an EVOM2 voltohmmeter (World Precision Instruments, FL, USA) in Ohms per-square centimeter (Ω/cm^2). TEER of cell free collagen coated membranes was subtracted and results were expressed as a percentage of the baseline. Measurements were only taken from cultures at 14 days maturity showing $>400 \Omega/\text{cm}^2$, while using a 37° stage. TEER was measured with fresh media prior to experimentation. Following this the apical media was replaced with 100 μl of PBS control or protease. Time points included baseline, 2, 4, 6, and 12 hours. Samples exposed to low dose proteases were measured at 24 hours to observe any delayed effect.

Paracellular permeability

The paracellular permeability of HNEC-ALI cultures was assessed after 12 hours. The apical compartment was replaced with 3 mg/ml of a neutral 4 kDa fluorescein isothiocyanate (FITC) dextran (Sigma-Aldrich, MO, USA) in PBS. Samples were then taken from the basolateral compartment after 2 hours of passage to allow sufficient detection. The amount of passaged dextran was measured using a microplate reader (Ex

485 nm, Em 520 nm). Dextran transfer was calculated according to the following equation:

$$P_{app} = \left(\frac{dQ}{dt} \right) \times \frac{1}{AC_0}$$

P_{app} is the apparent permeability coefficient (cm/s), dQ/dt (mg/s) is the transfer rate to the basolateral compartment, A (cm²) is the surface area, and C_0 (mg/ml) is the starting concentration in the apical compartment.¹⁸⁴ Fold changes compared to the control were calculated from P_{app} .

Immunofluorescence of ZO-1 and Claudin-1

Immunofluorescence was performed on HNEC-ALI cultures following 12 hours of treatment. Samples were PBS washed, then fixed in 2% paraformaldehyde for 15 minutes, washed again, and air dried. Fixed samples were permeabilised with 0.1% Triton X-100 in PBS for 15 minutes, PBS washed, blocked for 1 hour with Protein Block (Dako) and incubated with 5 µg/ml monoclonal mouse ZO-1 and 10 µg/ml polyclonal rabbit Claudin-1 antibodies (Invitrogen, CA, USA) in TBS-T plus 10% serum free blocker. Samples were PBS washed before addition of CyTM3 conjugated donkey anti-rabbit and Alexa Fluor® 488 conjugated anti-mouse (Jackson ImmunoResearch Labs, PA, USA) secondary antibodies in blocking buffer for 1 hour followed by application of 4',6-diamidino-2-phenylindole (DAPI) (Sigma-Aldrich). Membranes were mounted on slides with anti-fade mounting medium (Dako), and cover slipped. Slides were imaged using a Zeiss LSM 700 inverted confocal microscope (Carl-Zeiss, Oberkochen, Germany).

Expression of IL-6 in HNEC-ALI supernatants

IL-6 cytokine was measured from the basal supernatant HNEC-ALI cultures. BD Pharmingen™ (BD Biosciences, CA, USA) quantitative IL-6 ELISA was performed according to the manufacturer's instructions. The lower limit of detection was 15 pg/ml, results were expressed in pg/ml.

Degradation of IL-6 by V8 protease

Human IL-6 (BD Biosciences) 400 pg/ml was incubated with V8 protease (10 and 100 µg/ml) for 12 hours at 37°C. Quantitative IL-6 ELISA was performed as above. V8 protease and Human IL-6 alone were used as controls.

Cytotoxicity assay

Cytotoxicity was assessed using a colorimetric assay for lactate dehydrogenase (LDH). Supernatant was collected from HNEC-ALI cultures following 12 hours of exposure and transferred to a 96 well clear bottom plate. CytoTox 96 (Promega, WI, USA) reagent was added to the samples and incubated for 30 minutes at ambient temperature in a dark room. Stop solution was added and the plate read at an absorbance of 490 nm on a microplate reader. Results were expressed as percent of the PBS control by comparing the LDH release in the experimental.

Statistical analysis

TEER experiments were carried out in a minimum of 4 biological replicates. Protease activity, Papp, immunofluorescence and IL-6 measurements were collected from 3

biological replicates, and cytotoxicity from 5 biological replicates. Results are reported as mean (\pm SD). Statistical differences between control and treatment groups were evaluated using unpaired 2-tailed *t* tests using GraphPad Prism version 6 for Apple (GraphPad Software, CA, USA).

Results

S. aureus supernatant protease activity

The relative protease activities of supernatant collected from *S. aureus* ATCC strains 13565, 14458, and 25923 are shown in Figure 8. Relative protease activity of 90% supernatant of ATCC 13565, 14458, and 25923 were 1468 (± 16.26), 1563 (± 3.536), and 1420 (± 0.71) RFU respectively. Relative protease activity of V8 protease at 100, 10, and 1 $\mu\text{g/ml}$ were 1634 (± 147.1), 598.5 (± 70.71), and 34.5 (± 18.38) RFU respectively. This demonstrates that the activity of each strain is similar to 100 $\mu\text{g/ml}$ of V8 protease solution. Previous research has suggested that *S. aureus* protease activity *in-vivo* is equivalent to 50 $\mu\text{g/ml}$, however this varies between isolates and purification techniques.^{292,293}

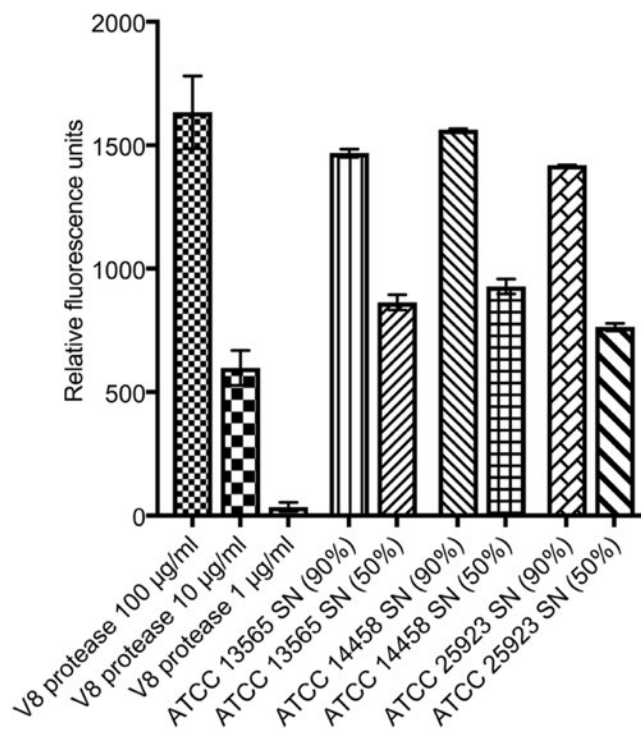


Figure 8. V8 protease activity comparison to *S. aureus* supernatants.

V8 specific protease activity measured in ATCC 13565, 14458, and 25923 supernatants (SN) (90% and 50% concentrations), compared against V8 protease solutions of 100, 10, and 1 $\mu\text{g/ml}$. Measurements are expressed as relative fluorescent units (\pm SD). Data from four biologically independent replicates.

***S. aureus* V8 protease decreases TEER of HNEC-ALI in a time and dose dependent manner**

At 12 hours V8 protease caused a significant decrease in TEER from the baseline to 22.67% (± 7.19) compared to the control 89.36% (± 14.46) ($p < 0.0001$; Figure 9). In contrast, Staphopain A, Staphopain B, ETA, and Spl (A-F) did not result in any significant effect on TEER (Figure 9). SplA, SplB, SplC, SplD, SplE, and SplF were tested separately with no difference in TEER (data not shown). V8 protease's detrimental effect on TEER was time dependent with statistically significant reductions in TEER at 4 hours 41.28% (± 20.83) ($p = 0.029$) and 6 hours 35.05% (± 21.34) ($p = 0.017$; Figure 10). Additionally, a significant decrease in TEER was observed from 2 hours to 12 hours with a 40.06% (± 10.64) reduction ($p = 0.007$; Figure 10). V8 protease at a lower concentration of 10 $\mu\text{g/ml}$ did not decrease TEER (Supplemental Figure S3).

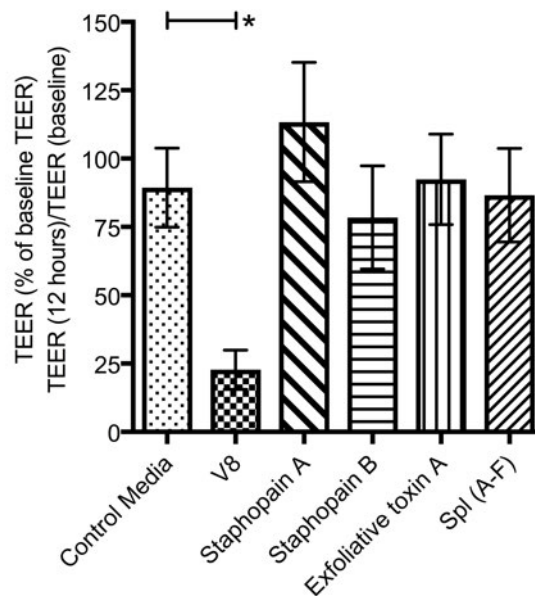


Figure 9. V8 protease disrupts the pore pathway of the epithelial barrier with decreases in TEER.

HNEC-ALI cultures were treated with V8 protease, Staphopain A, Staphopain B, Exfoliative Toxin A, Spl (A-F), or PBS control for 12 hours. TEER measurements were taken at 0 and 12 hours, expressed as a percentage change from the baseline TEER (\pm SD). (*) $p < 0.0001$ as determined by unpaired 2 tailed t tests. Data from four biologically independent replicates.

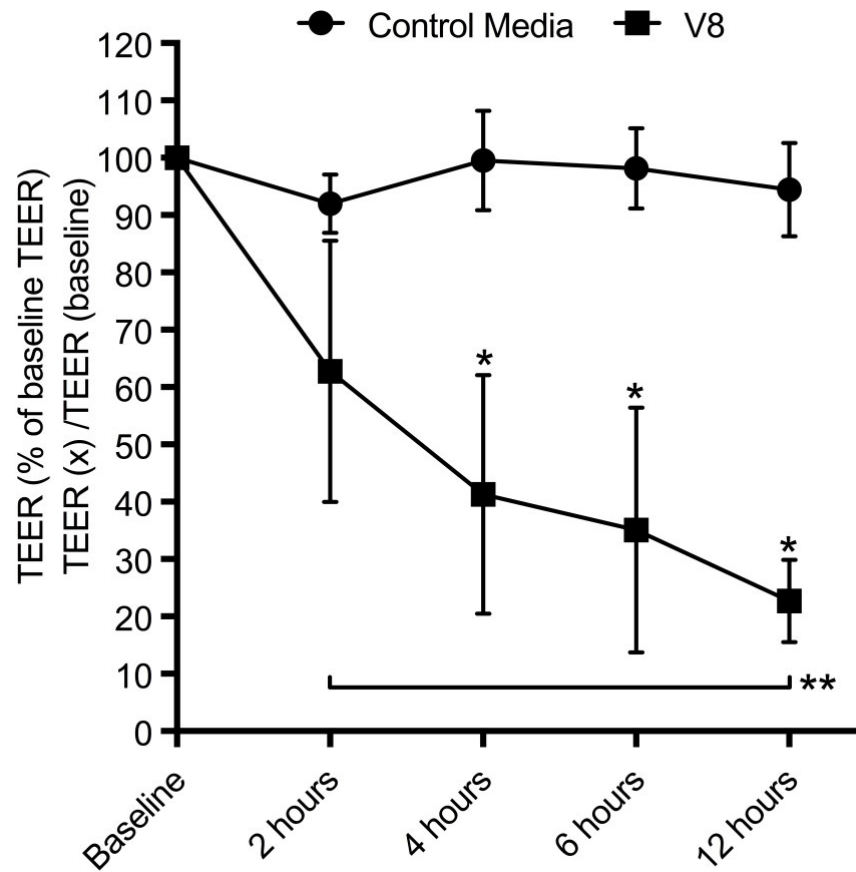


Figure 10. V8 protease disruption of the epithelial barrier is time dependent.

HNEC-ALI cultures were treated with V8 protease or PBS control, changes in TEER were measured over time at 0, 2, 4, 6, and 12 hours. Measurements are expressed as a percentage change from the baseline TEER (\pm SD). (*) comparing to baseline, and (**) comparing between 2 hours and 12 hours, $p < 0.05$ as determined by unpaired 2 tailed t tests. Data from four biologically independent replicates.

S. aureus V8 protease increases the paracellular permeability

V8 protease demonstrated a statistically significant increase in paracellular permeability ($p=0.0476$; Figure II). Fold changes in Papp with each protease were: V8 protease 20.14 (± 11.73), Staphopain A 4.68 (± 4.38), Staphopain B 4.00 (± 3.33), Exfoliative toxin A 1.60 (± 1.26), and Spl (A-F) 3.42 (± 2.63). Exposure to a lower dose did not show a significant change in Papp (Figure II).

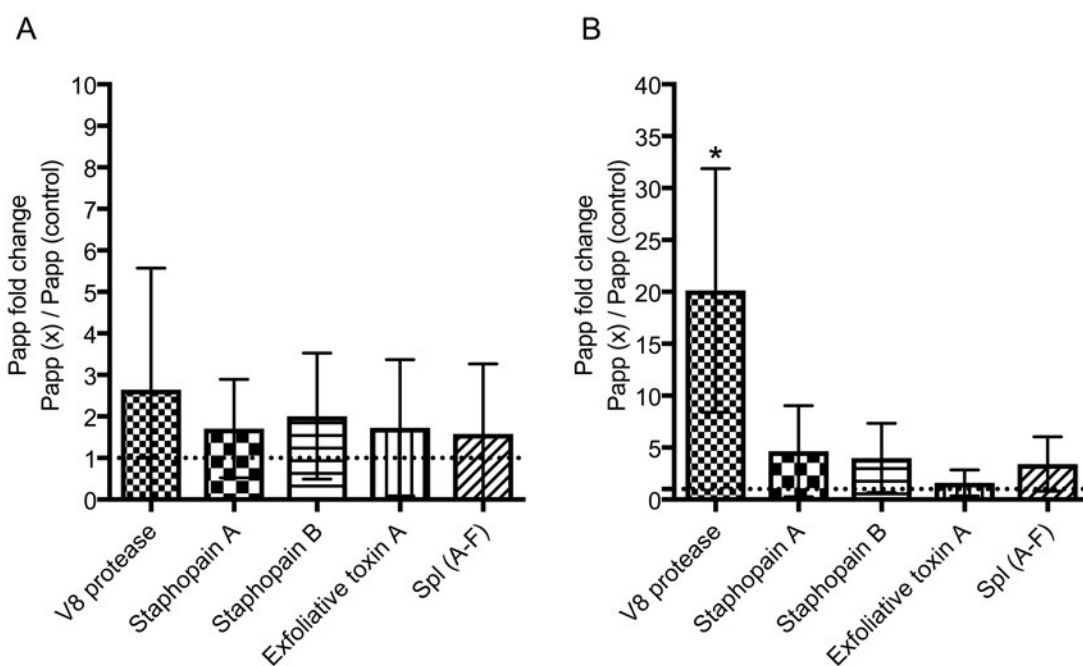


Figure II. V8 protease perturbs the leak pathway by increasing macromolecular permeability (Papp).

HNEC-ALI cultures were exposed to (A) 10 µg/ml or (B) 100 µg/ml of V8 protease, Staphopain A, Staphopain B, Exfoliative Toxin A, Spl (A-F), or PBS control for 12 hours. 4 kDa FITC dextran was added to the apical compartment and basolateral samples were taken after 2 hours of passage. Results are expressed as a fold change Papp compared to the PBS control (\pm SD). * $p < 0.05$ as determined by unpaired 2 tailed t tests. Data from three biologically independent replicates.

Effects on cellular localisation of TJ proteins

TJ proteins ZO-1 and claudin-1 were assessed in HNEC-ALI cultures exposed to V8 protease and the no treatment control using fluorescence microscopy. V8 protease produced a discontinuous and less intense localisation of ZO-1 at the cell periphery compared to the control. Conversely claudin-1 was still localised to the cell periphery, but with an increase in signal intensity (Figure 12).

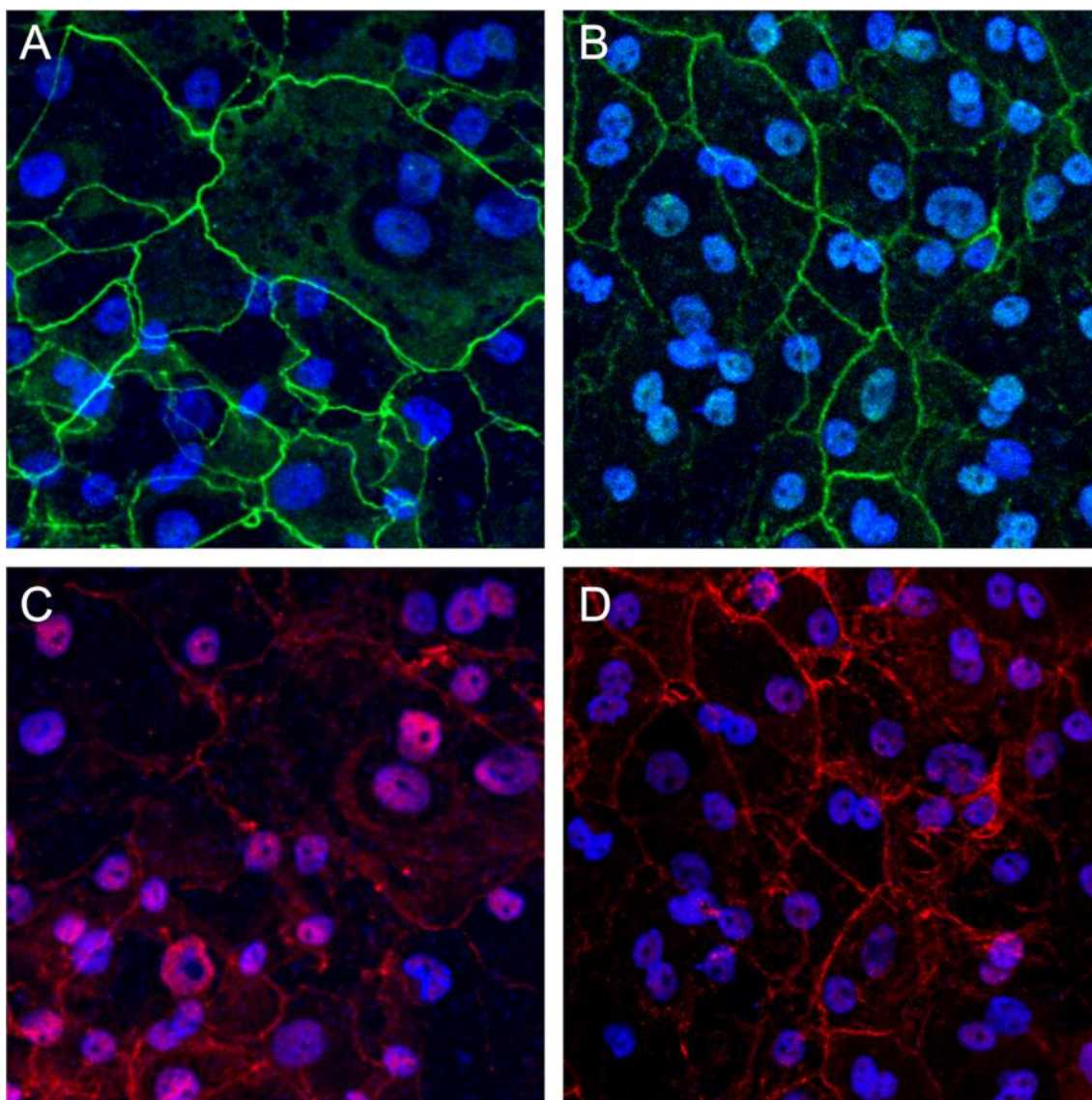


Figure 12. Tight junction proteins Claudin-1 and ZO-1 were discontinuous in V8 exposed cells.

HNEC-ALI cultures exposed to V8 protease or control PBS were simultaneously assessed for Claudin-1 and ZO-1 localisation. Control PBS exposed HNEC-ALI immunolocalisation of ZO-1 (A) and Claudin-1 (C), and V8 protease exposed HNEC-ALI immunolocalisation of ZO-1 (B) and Claudin-1 (D). Immunofluorescence investigation was repeated on three biologically independent samples.

Interleukin-6 production is reduced by V8 protease

Cell culture basal supernatants were analysed after 12 hour of treatment for IL-6 production using ELISA. A significant decrease in IL-6 protein levels were detected following V8 protease compared to the control ($p=0.0069$), 153.5 pg/ml (± 127.6) and 548.3 pg/ml (± 39.97) respectively (Figure 13). The other *S. aureus* proteases did not show a statistically significant difference in IL-6 production.

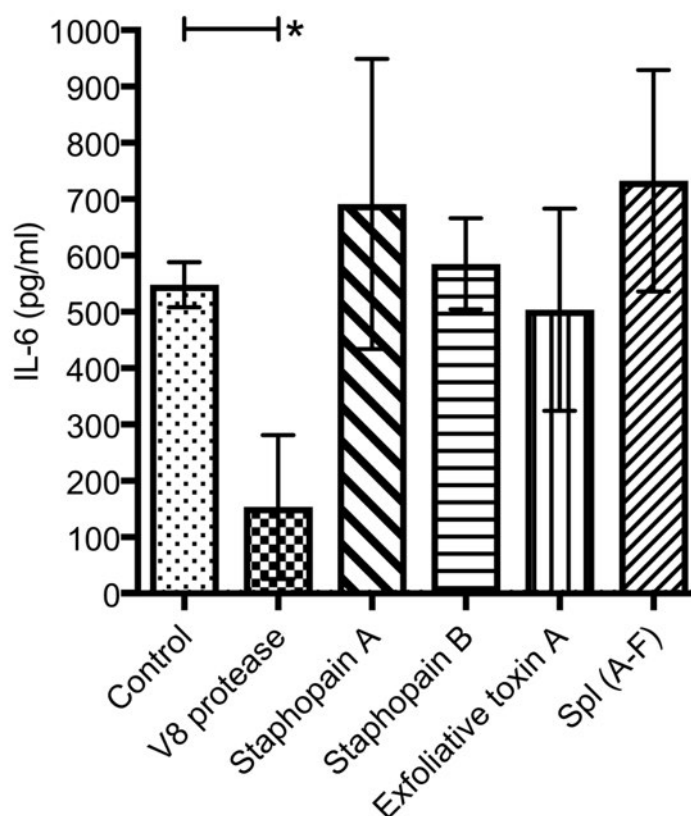


Figure 13. Effects of V8 protease on IL-6 production from HNEC-ALI cultures.

IL-6 production was measured using ELISA after HNEC-ALI cultures were treated with V8 protease, Staphopain A, Staphopain B, Exfoliative Toxin A, Spl (A-F), or PBS control simultaneously for 12 hours. IL-6 is expressed in pg/ml (\pm SD). * $p < 0.05$ as determined by unpaired 2 tailed t tests. Data from three biologically independent replicates.

V8 protease degrades human IL-6 *in-vitro*

IL-6 ELISA following a 12-hour incubation of 400 pg/ml human IL-6 with 10 and 100 µg/ml V8 protease showed a complete loss of detectable IL-6 in the samples. V8 alone showed no background fluorescence or reactivity with the ELISA assay (Table 7).

Table 7. ELISA of human IL-6 after exposure to V8 protease.

IL-6 ELISA of 400 pg/ml human IL-6 incubated for 12 hours with PBS, 10 µg/ml V8 protease, and 100 µg/ml V8 protease. Results are expressed in pg/ml (\pm SD). Undetectable refers to samples below the lower limit of detection of 15 pg/ml.

Sample	IL-6 pg/ml (\pm SD)
400 pg/ml IL-6 + PBS	378.8 (\pm 20.656)
10 µg/ml V8 protease	Undetectable
100 µg/ml V8 protease	Undetectable
400 pg/ml IL-6 + 10 µg/ml V8 protease	Undetectable
400 pg/ml IL-6 + 100 µg/ml V8 protease	Undetectable
PBS	Undetectable

V8 protease induced TJ dysfunction is not secondary to cell cytotoxicity

Measurement of LDH release from HNEC-ALI exposed to the control media and 100 µg/ml of each protease showed no statistically different result in cell cytotoxicity (Table 8).

Table 8. HNEC-ALI cytotoxicity assay.

Cytotoxicity assay of HNEC-ALI cultures exposed to 12 hours of 100 µg/ml V8 protease, Staphopain A, Staphopain B, Exfoliative Toxin A, Spl (A-F). Results are expressed as LDH Optical Density (OD) and LDH % of PBS vehicle control (±SD). Non-significant (NS).

	LDH OD 460 nm (±SD)	LDH % of control (±SD)
Vehicle Control	0.0866 (±0.0053)	N/A
V8 Protease	0.0914 (±0.0078)	105.59 (±7.12)
Staphopain A	0.0909 (±0.0079)	104.90 (±5.07)
Staphopain B	0.0888 (±0.0060)	102.53 (±3.05)
Exfoliative Toxin A	0.0884 (±0.0056)	102.18 (±5.33)
Spl (A-F)	0.0856 (±0.0036)	99.15 (±7.82)

Discussion

This is the first report, to our knowledge that describes the barrier altering effect that *S. aureus* V8 protease has on sinonasal epithelial cells. The function of *S. aureus* extracellular proteases within the sinonasal cavity is not well known and our findings suggest a novel pathogenic mechanism of *S. aureus* extracellular proteases. V8 protease demonstrated a significant effect on the TJ barrier when applied to the sinonasal cell layer by dramatically altering paracellular permeability, and fragmenting protein localisation. V8 protease caused a reduction in TEER that was time and concentration dependent, with maximal effect at 12 hours. This was accompanied by increased molecular permeability to a neutral 4 kDa dextran, which indicates that antigens/proteins up to this size may traverse the mucosa.

The pseudostratified ciliated columnar epithelium lining the paranasal sinuses is a pivotal part of the innate immune system. The complex co-ordination of the barrier function, mucus regulation, mucociliary clearance, cytokine production, and production of antimicrobial molecules all form the first line of defence against pathogens, antigens, or environmental particles.⁴⁹³ CRS is primarily a mucosal disease where by several aspects of the innate immune function are dysregulated.⁴⁹⁴ Recently it has been hypothesised that a defective epithelial barrier is either the cause or the result of mucosal inflammation in CRS. Nasal polyp biopsy specimens showed decreased expression of TJ proteins, which also negatively correlated with disease severity and eosinophilic inflammation. It has been suggested that CRS barrier dysfunction is a result of environmental, microbial and host factors.^{20,193,495} Previous research from our group has shown that the supernatants from *S. aureus* ATCC strain 13565 disrupt the TJs of HNEC-ALI cultures, however the identity of the toxin(s) responsible for this effect has

yet to be identified.¹⁹ This study does not exclude other *S. aureus* products as the responsible factor, but rather highlights the protease family for further investigation.

V8 protease is a 29 kDa serine protease, which is produced by *S. aureus* during the exponential bacterial growth phase.³⁷⁹ This study observed that V8 protease alters the mucosal barrier, however little is known about the bacterial protease activity within the paranasal sinuses. Serine protease activity in severe atopic dermatitis has been correlated to 50 µg/ml, and contributes to dermal injury.²⁹² In addition, V8 protease applied *in-vivo* to murine skin at concentrations of 50–500 µg/ml demonstrated an increase in epidermal permeability and inflammatory infiltration.²⁹³ In our study we have observed decreased staining intensity in the TJ protein ZO-1 with relatively little change in Claudin-1 due to V8 protease. The changes in ZO-1 could be due to protein redistribution or degradation. We have not identified whether this is due to proteolytic degradation or via an indirect mechanism. To date there are no studies examining the specific mucosal barrier effects of *S. aureus* proteases, however other exogenous proteases have been implicated in mucosal barrier dysfunction. Similar effects on barrier function have been seen with pollen derived peptidases.⁴⁹⁶

The effects we have observed on barrier function have potential to increase mucosal bacterial translocation allowing subepithelial infection. *P. aeruginosa* induced barrier dysfunction in human bronchial cell monolayers increases bacterial translocation through the paracellular route.⁴⁹⁷ In addition to the effects on bacterial translocation, protease induced TJ disruption has consequences for antigen sensitisation. The well studied house dust mite derived proteases cause proteolysis of occludin, claudin-1, and ZO-1 in airway epithelium resulting in transepithelial antigen delivery.^{498–500}

Despite these effects on the barrier integrity it should be noted that no significant induction of cell cytotoxicity was evident in our study. Furthermore, barrier dysfunction

was interestingly associated with degradation of the innate pro-inflammatory cytokine IL-6. We observed that production of mucosal IL-6 was diminished in V8 protease treated HNEC-ALI cultures, and this is likely due to a direct effect on IL-6. Incubation of a purified IL-6 with V8 protease resulted in an undetectable IL-6 via ELISA. Indeed, V8 proteases are known to cleave peptide bonds at the carboxyl side of Glutamic acid (Glu) and Aspartic acid (Asp).⁵⁰¹ Analysis of the IL-6 protein sequence shows that IL-6 is rich in Glu and Asp.⁵⁰² IL-6 cytokines are central to monocyte and T cell recruitment, lymphocyte differentiation, mucosal protection against microorganisms, and mucosal IgA responses.⁵⁰³⁻⁵⁰⁶ V8 protease targets the innate immune system by degrading complement factors, and inhibiting complement activators such as collectins.⁵⁰⁷ Furthermore, *S. aureus* derived V8 protease and metalloprotease induce the activation and deposition of complement factor C1q onto *Staphylococcus epidermidis*.⁵⁰⁷ In gastrointestinal mucosa it is known to protect against biofilm colonisation and prevent mucosal apoptosis.⁵⁰⁵ The function of IL-6 specific to sinonasal mucosa is poorly understood. Our findings conflict with the literature, with an article by Cantero et al., (2014) showing that *S. aureus* biofilm grown on nasal explants induces gene and protein expression of IL-6.⁴⁸⁶ We speculate that IL-6 levels might be decreased locally at the bacteria-host interface by V8 protease secreting *S. aureus* strains. This local decrease of IL-6 would alter immune cell recruitment and potentially prevent biofilm eradication, representing a novel immune evasion mechanism.

This study did not observe any change in the mucosal barrier following exposure to the spl proteases. Spl proteases are closely related to V8 protease, but with a very narrow substrate specificity.^{397,492} Recently, spl proteases have been shown to stimulate Th2 cytokine production in airway tissue and T cells, implicating spl proteases in airway allergy.⁴⁰³ We reason that the V8 protease could potentially act as a complement to the

spl proteases, allowing penetration through the nasal mucosa so the spl proteases can exert effects on the submucosal immune structures. In view of these previous observations and our results, V8 protease plays a role in the initial invasion of *S. aureus* by perturbing the innate barrier, and disrupting the immune system. It is likely that the *S. aureus* extracellular proteases act synergistically, each possessing site-specific targets between host and bacteria to promote survival.

Future studies may reveal the interplay between numerous virulence factors within the *S. aureus* exoproteome, and how this contributes to disease. In particular, how *S. aureus* proteases modulate the sinonasal mucosal immune response individually and in concert, and whether their presence enhances the occurrence of opportunistic bacterial or fungal infection.

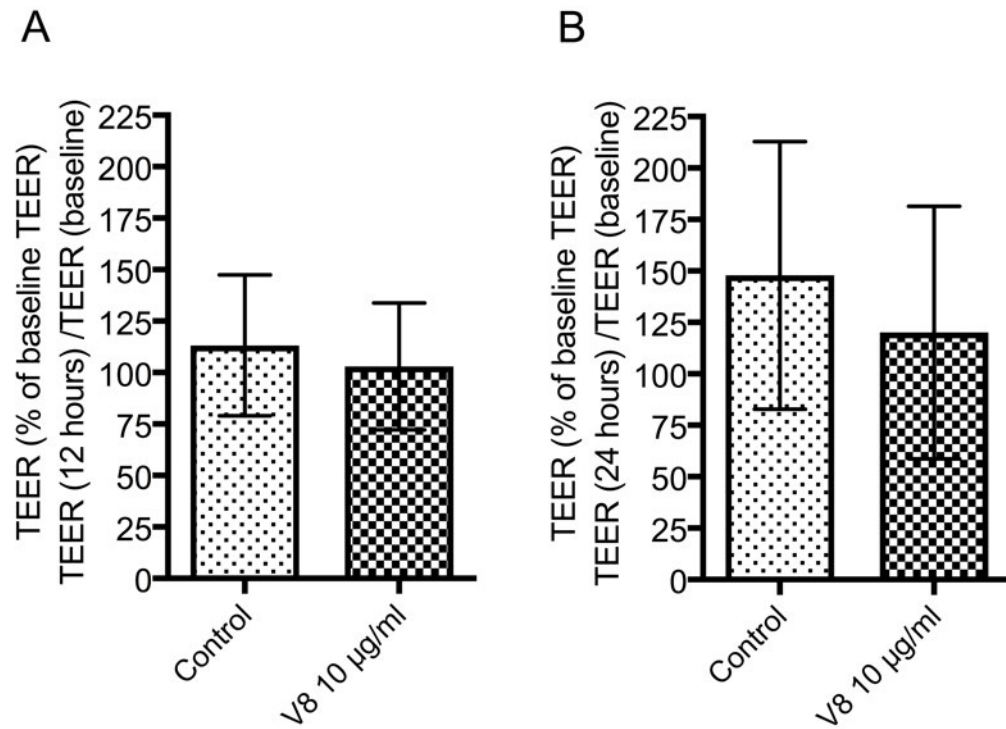
We have identified a novel mechanism of barrier dysfunction in sinonasal epithelium caused by the *S. aureus* V8 protease. This has the potential to impair the innate barrier, alter mucus secretion, increase antigen exposure, and initiate subepithelial infection. V8 protease is a highly conserved gene among *S. aureus* clinical isolates, and its importance may only become evident in clinical studies observing the pathogen, host, and environment—or as a target for medical therapy.

Acknowledgements

This work is supported by a Garnett Passe and Rodney Williams Memorial Foundation scholarship to JM and a Garnett Passe and Rodney Williams Memorial Foundation Conjoint Grant to PJW and SV.

Supplementary Information

Supplementary results



Supplemental Figure S4. HNEC-ALI cultures treated with V8 protease at 10 µg/ml or PBS control for 12 hours (A), and for 24 hours (B).

TEER measurements were taken at 0, 12 and 24 hours, expressed as a percentage change from the baseline TEER (\pm SD). Data from three biologically independent replicates.

Mucosal Zinc Deficiency in Chronic Rhinosinusitis with Nasal Polyposis Contributes to Barrier Disruption and Decreases ZO-1

Statement of authorship

Title of Paper	Mucosal Zinc Deficiency in Chronic Rhinosinusitis with Nasal Polyposis Contributes to Barrier Disruption and Decreases ZO-1
Publication Status	Published
Publication Details	Murphy J, Ramezanzpour M, Roscioli E, Psaltis A.J, Wormald P.J, Vreugde S. Mucosal Zinc Deficiency in Chronic Rhinosinusitis with Nasal Polyposis Contributes to Barrier Disruption and Decreases ZO-1. Allergy. 2018;73(10):2095-2097. doi:10.1111/all.13532

Principal Author

Name of Principal Author (Candidate)	Jae Murphy		
Contribution to the Paper	Experimental design, performed collection of samples, conducted experiments, interpreted and analysed data, preparation of manuscript		
Overall percentage (%)	75%		
Certification	This paper reports on original research I conducted during the period of my Higher Degree by Research candidature and is not subject to any obligations or contractual agreements with a third party that would constrain its inclusion in this thesis. I am the primary author of this paper.		
Signature		Date	06.07.2018

Co-Author Contributions

By signing the Statement of Authorship, each author certifies that:

- iv. the candidate's stated contribution to the publication is accurate;
- v. permission is granted for the candidate to include the publication in the thesis; and
- vi. the sum of all co-author contributions is equal to 100% less the candidate's stated contribution.

Name of Co-Author	Mahnaz Ramezanpour		
Contribution to the Paper	Assistance with conducting experiments, manuscript editing		
Signature		Date	06.07.2018
Name of Co-Author	Eugene Roscioli		
Contribution to the Paper	Assistance with conducting experiments, manuscript editing		
Signature		Date	06.07.2018
Name of Co-Author	Alkis James Psaltis		
Contribution to the Paper	Project supervision, manuscript editing		
Signature		Date	06.07.2018
Name of Co-Author	Peter-John Wormald		
Contribution to the Paper	Project supervision, manuscript editing		
Signature		Date	06.07.2018
Name of Co-Author	Sarah Vreugde		
Contribution to the Paper	Assistance with experimental design, project supervision, manuscript editing, corresponding author		
Signature		Date	06.07.2018

Citation

Murphy J, Ramezanpour M, Roscioli E, Psaltis A.J, Wormald P.J, Vreugde S. Mucosal Zinc Deficiency in Chronic Rhinosinusitis with Nasal Polyposis Contributes to Barrier Disruption and Decreases ZO-1. *Allergy*. 2018;73:2095-2097. doi:10.1111/all.13532

Abstract

Background: Zinc is an essential trace element that influences the integrity of the epithelial barrier, immune system, and other cellular functions. Previous studies have suggested that zinc levels are decreased in chronic rhinosinusitis (CRS), however the role of zinc in barrier function is not known. The objective of this study was to estimate labile zinc levels within CRS patient tissues compared to controls and to determine the effect of zinc depletion (ZD) on the sinonasal epithelial barrier.

Methods: Samples were collected from 56 patients undergoing endoscopic sinus surgery (CRSsNP n=18, and CRSwNP n=38) and 17 control patients undergoing skullbase surgery. Dual labelling immunofluorescence was used to examine labile zinc levels and Zonula occludens-1 (ZO-1) expression in sinonasal tissue and nasal epithelial cells at air liquid interface (ALI). The effects of ZD on barrier function of ALI cultures was measured using transepithelial electrical resistance (TEER) and dextran flux. qPCR was used to compare zinc transporter gene expression between patient groups.

Results: Immunohistofluorescence of sinonasal tissue showed that labile zinc and apical ZO-1 were both significantly decreased in CRSwNP. *In-vitro* ZD resulted in barrier dysfunction evidenced by decreased TEER by days 10 and 15 of ALI culture. This was paired with loss of ZO-1 protein expression and cellular labile ZD. Zinc transporter gene expression identified MT1a, MT2a, ZIP1, ZIP2, ZIP14 were down regulated and ZnT1 up regulated in CRSsNP, while MT3 was down regulated in CRSwNP.

Conclusion: These results suggest that zinc directly contributes to barrier function and integrity in chronic rhinosinusitis. Furthermore, zinc transporter gene expression is differentially regulated between CRSsNP and CRSwNP.

Keywords: Zinc; airway barrier; chronic rhinosinusitis; zinc transporters; tight junction.

Introduction

Chronic rhinosinusitis (CRS) is an inflammatory disease of the paranasal sinuses with a heterogeneous clinical presentation and a multifaceted pathogenesis.¹ The clinical spectrum of CRS is subdivided into the broad phenotypes of CRS without nasal polyps (CRSsNP) and CRS with nasal polyps (CRSwNP). The sinonasal mucosa forms the physical barrier against allergens, microbes, and particulate matter. The physical barrier is formed by epithelial cells and the junctional complexes connecting neighbouring cells. Junctional complexes are composed of tight junctions (TJs), adherens junctions and desmosome proteins, descending apical to basal.⁴⁵² Recent investigation into the CRS barrier function has shown that TJ genes/proteins are down regulated, particularly in nasal polyps.^{20,196,495} Little is known about the contributing and mechanistic factors leading to a dysfunctional barrier in CRS. *Staphylococcus aureus* secreted factors¹⁹ and host inflammatory cytokines^{20,323,454} have been implicated in causing *in-vitro* barrier dysfunction.

Zinc is an essential trace element involved in aspects of immune system regulation,⁵⁰⁸ cell membrane stabilisation,⁴³¹ barrier function,²⁷⁹ wound healing, and cellular functions.⁵⁰⁹ In the gastrointestinal mucosal barrier zinc homeostasis can regulate TJ development.²⁸² Zinc homeostasis is coordinated by the zinc transporter families ZIP (SLC39) and ZnT (SLC30), complemented by metallothioneins as intracellular zinc binders and donors.⁴⁴² Local zinc deficiency along with barrier dysfunction have been implicated in chronic inflammatory disorders such as *Helicobacter pylori* induced gastritis²⁴¹ and inflammatory bowel disease.^{279,510} Furthermore, research in CRS identified that zinc abundance was significantly lower in nasal polyp tissue,⁴³⁸ while serum zinc concentrations are unaffected in CRS.⁴³⁵

Based on this previous work we hypothesised that local zinc deficiency in sinonasal mucosa may affect the development of appropriate barrier function hence contributing to the pathogenesis of chronic rhinosinusitis. This study aims to evaluate the effect of zinc deficiency on airway barrier integrity and investigated the gene expression of zinc transporters in CRS patients.

Methods

Patients and tissue collection

Institutional ethics approval was obtained and all participants were given written informed consent, and an approved participant information sheet. All consecutive unselected patients undergoing endoscopic sinus surgery (ESS) in a tertiary referral rhinology practice were recruited into the study, and were defined as controls, CRSsNP or CRSwNP. Control patients were undergoing ESS for skull base tumor resection, and were only included in the absence of radiographic or endoscopic evidence of sinusitis. CRS patients were divided into CRSsNP and CRSwNP depending on the absence or presence of nasal polyps respectively, as defined by the European Position Paper.¹ Exclusion criteria included immunosuppression and treatments with oral antibiotics, nasal or parenteral corticosteroids in the week prior to study inclusion, and limited or unavailable tissue samples. Demographic and clinical data including past medical history, previous sinus surgery, and SNOT22 was recorded (Table 9).⁵¹¹ Tissue samples were collected at the time of ESS and stored in RNeasy later at -80°C until analysis. A separate cohort of samples was stored in 10% neutral buffered formalin and then paraffin embedded for immunofluorescence.

RNA extraction and real-time polymerase chain reaction

Total RNA was extracted from RNeasy later stored samples using the Qiagen RNeasy Mini kit (Qiagen GmbH, Germany) according to the manufacturer's instructions followed by DNase treatment with RNase-Free DNase set (Qiagen). Extracted RNA was assessed for quality using the Experion RNA StdSens analysis kit (Bio-Rad Laboratories, CA, USA) and total quantification using the Nanodrop 1000 spectrophotometer (Thermo Fisher

Scientific, MA, USA). Reverse transcription (RT) was performed using the M-MLV Reverse Transcriptase system (Invitrogen, CA, USA) performed at 37°C for 90 minutes, and 72°C for 10 minutes. All RT reactions were performed with a no-RT control and no-RNA control. Real-time PCR (RT-PCR) was performed on an Applied Biosciences ViiA7 Real Time PCR system and TaqMan primer/probes (Thermo Fisher Scientific) to beta-2 microglobulin (B2M) (Hs4326319E), hypoxanthine-guanine phosphoribosyltransferase 1 (HRPT) (Hs99999909_ml), metallothionein 1A (MT1a) (Hs00831826_sl), metallothionein 2A (MT2a) (Hs02379661_g1), metallothionein 3 (MT3) (Hs01921768_sl), zinc transporter ZIP1 (ZIP1) (Hs00205358_ml), zinc transporter ZIP2 (ZIP2) (Hs001113548_g1), zinc transporter ZIP14 (ZIP14) (Hs00299262_ml), zinc transporter 1 (ZnT1) (Hs00253602_ml), and zinc transporter 4 (ZnT4) (Hs00203308_ml). Gene expression levels were normalised relative to the housekeeping genes B2M and HRPT1, and calculated using the $\Delta\Delta\text{CT}$ method. Results are expressed as the normalised gene expression and fold change between groups.

Immunofluorescence of labile zinc and Zonula occludens-1 (ZO-1) protein in tissue samples

Tissue samples were formalin fixed and paraffin embedded. Cylindrical cores (2 or 3 mm) were taken from epithelial sections of samples, and then embedded in a fresh paraffin block to produce a tissue microarray (TMA). The TMA was sectioned at 4 μm and mounted on glass slides for immunofluorescence. Slides were deparaffinised and subjected to heat induced antigen retrieval, followed by incubation with Protein Block, Serum Free (Dako, CA, USA). Slides were then incubated with mouse anti-ZO-1 antibodies (Invitrogen) at 1:100 dilution in TBS-T plus 10% fetal bovine serum overnight at 4°C. Negative control tissue slides were incubated with TBS-T plus 10% fetal bovine

serum overnight at 4°C. The slides were then incubated with Alexa Fluor 488 anti-mouse (Jackson ImmunoResearch Labs Inc, PA, USA) 1:200 dilution in blocking buffer for 1 hour at room temperature followed by incubation with the labile zinc fluorophore Zinquin [20] (gift from Dr P Zalewski, The University of Adelaide, Australia) 25 µM in phosphate buffered saline (PBS) for 30 minutes at 37°C, and mounted with fluorescent mounting medium (Dako). Slides were imaged using a Zeiss LSM 700 confocal microscope (Carl Zeiss AG, Oberkochen, Germany) using the 20x objective. Images were taken sequentially to minimise cross-talk between fluorophores. Excitation and emission values for ZO-1 and Zinquin were 488/525nm and 405/460nm respectively. All images were acquired with identical microscopy parameters. Processing was performed using ZEN Imaging Software (Carl Zeiss AG). The threshold of each image was adjusted for each channel to remove background fluorescence, and performed in a blinded fashion. Quantification of labile zinc was performed by selecting the epithelium as a region of interest (ROI) (Supplemental Figure S4). Quantification of TJ protein ZO-1 was acquired by selecting the apical third of the epithelium within the previous ROI. Results are expressed as a mean fluorescence intensity (\pm SD).

Serum zinc concentration

Serum was collected from 11 patients (2 controls, 5 CRSsNP, and 4 CRSwNP) with matching tissue samples that were included in the TMA. 3 additional serum samples from control patients were included. 100 µL of serum was measured for zinc concentrations using an inductively coupled plasma mass spectrometer (ICP-MS)(Elan DRC; Perkin Elmer, MA, USA)

Zinc deplete media

Zinc deplete (ZD) media was prepared by adding Chelex 100 (Sigma-Aldrich, MO, USA) 10% wt:v to B-ALI™ differentiation media (Lonza, Basel, Switzerland) for 1 hour at 4°C, then decanted and Chelex 100 added again overnight at 4°C followed by filter sterilisation. B-ALI™ differentiation media and chelated media were analysed for zinc, magnesium, and copper concentrations using inductively coupled mass spectrometry. Sodium, chloride, and potassium concentrations were analysed using ion selective electrode potentiometry (Roche Cobras Integra 400, Rotkreuz, Switzerland). Calcium, Iron and Phosphorus were analysed using substrate specific absorbance photometry (Roche Cobras Integra 400). MgSO₄, MgCl₂, and CaCl₂ were re-added to the chelated media to that of the B-ALI™ differentiation media (MgSO₄ 0.2 mM, MgCl₂ 0.45 mM, CaCl₂ 2.0 mM). Zinc concentrations in the B-ALI™ differentiation media were 2.72 µM (2.67 – 2.79 µM) and in the zinc deplete media were 0.3 µM (0.1-0.6 µM). Zinc concentrations were measured from three independent preparations of ZD media.

Nasal epithelial cell collection and culture

Ethics approval for cytological nasal brushings from healthy volunteers was granted from The Queen Elizabeth Hospital Human Ethics Committee. Cytological nasal brushings were collected from participants having signed written informed consent. Exclusion criteria included active smoking, age less than 18 years, systemic diseases, recent upper respiratory tract infection, and evidence of chronic rhinosinusitis or allergic rhinitis. Human nasal epithelial cell cultures (HNEC) were established as reported previously from our department.^{19,323}

Air-liquid interface (ALI) culture in ZD media

HNEC cultures were maintained with B-ALI™ growth medium (Lonza) for 3-4 days in a cell incubator at 37°C with 5% CO₂. The apical and basal media was then removed and the basal media replaced with B-ALI™ differentiation media (Lonza) as a negative control or ZD media and changed every alternate day. HNEC cultures were maintained at ALI for 15 days for development of TJs and normal barrier function.

Transepithelial electrical resistance and paracellular permeability

Transepithelial electrical resistance (TEER) was measured using an EVOM2 epithelial volt-ohmmeter (World Precision Instruments, FL, USA) at 5, 10, and 15 days on a 37°C stage. Fresh B-ALI™ differentiation media (Lonza) or ZD media was added to the apical and basal compartments before measurement. The TEER of a cell free transwell membrane was subtracted from the measurement. Data are expressed as a mean percentage of control TEER (±SD) at the corresponding day of HNEC culture. The paracellular permeability of the HNEC-ALI cultures was assessed by addition of a neutral 4 kDa fluorescein isothiocyanate (FITC) dextran (Sigma-Aldrich) apically to a concentration of 3 mg/ml, permeability samples were then taken from the basolateral compartment after 2 hours of passage to allow sufficient 4kDa FITC for detection. The amount of passaged dextran was measured using a FLUOstar Optima 96 well microplate reader (BMG Labtech, Offenburg, Germany) using wavelengths 485 nm and 520 nm for excitation and emission respectively. Results assumed sink conditions of FITC dextran transfer and calculated according to the following equation as the apparent permeability (P_{app}):

$$P_{app} = \left(\frac{dQ}{dt} \right) \times \frac{1}{AC_0}$$

P_{app} is the apparent permeability coefficient (cm/s), dQ/dt (mg/s) is the rate of transfer of the FITC dextran to the basolateral compartment, A (cm²) is the surface area of the transwell membrane, and C_0 (mg/ml) is the starting drug concentration of the apical compartment.¹⁸⁴ The paracellular permeability of ALI cultures was assessed on days 5, 10, and 15 of ZD and control conditions. Measurements were performed as previously described.³²³ Data are expressed as the mean fold change (\pm SD) compared to the control at the corresponding day.

$$P_{app}(\text{fold change}) = \frac{P_{app}(\text{sample})}{P_{app}(\text{control})}$$

Immunofluorescence of ZD cultures

ALI cultures from control and ZD conditions were prepared for immunofluorescence at 5, 10, and 15 days. Staining for ZO-1 was conducted as previously described.¹⁹ Following application of the secondary antibody, samples were then washed five times in PBS and incubated with the Zinquin fluorophore 25 μ M in PBS for 30 minutes at 37°C. Samples were washed three times in PBS, and mounted with fluorescent mounting medium (Dako) before cover slipping. Slides were imaged using a Zeiss LSM 700 confocal microscope (Carl Zeiss AG).

Bio-Plex cytokine assay on HNEC-ALI supernatants

Cytokine levels of IL-1 β , IL-2, IL-4, IL-5, IL-6, IL-8, IL-10, IL-13, IFN- γ , and TNF- α were quantified from the HNEC-ALI supernatant via a Bio-Plex 10 cytokine assay (Bio-Rad, CA, USA). The assays were conducted as per the manufacturer's instructions. Concentrations were determined using Bio-Plex manager software with five parameter logistic regression (5PL) curve fitting and reported in pg/ml.

Statistical analysis

All analysis was performed using PRISM 6 software (GraphPad Software, CA, USA). Immunofluorescence intensity values and normalised gene expression data were statistically analysed between patient groups using a non-parametric Kruskal-Wallis analysis followed by Dunn's test for multiple comparisons with $p < 0.05$ considered statistically significant. Differences for TEER and Papp data between control and ZD groups were evaluated using unpaired 2-tailed t tests. All correlation tests were non-parametric Spearman rank correlations. Differences in cytokine production were statistically tested using multiple t tests with correction for multiple comparisons using the Holm-Sidak method.

Results

Patient demographics

Samples for immunofluorescence and gene expression were collected from in total 73 patients that underwent endoscopic sinus surgery, this included 17 control patients without sinus disease undergoing sinus surgery for skull base surgery. Demographic and phenotypic data are tabulated in Table 9.

Table 9. Patient demographics for sinus tissue samples for immunofluorescence and gene expression.

Clinical Features	Control (n=17)	CRSsNP (n=18)	CRSwNP (n=38)
Age mean years (range)	52.5 (26,73)	51.7 (20, 75)	53.4 (18, 82)
Gender (male/female)	5/12	9/9	23/15
Asthma (%)*	0 (0%)	9 (50%)	22 (57.9%)
Aspirin Sensitivity (%)	0 (0%)	0 (0%)	9 (23.7%)
Allergy (%)†	1 (5.8%)	6 (33.3%)	16 (42.1%)
SNOT 22 (±SD)	n/a	47.9 (±18.1)	54.8 (±18.3)
Previous sinus surgery (%)	n/a	3 (16.7%)	22 (57.9%)

* 31 patients reported a history of physician diagnosed asthma. † Defined as a previous positive skin prick test or RAST to at least 1 allergen.

Genes involved in zinc homeostasis are differentially expressed in CRSsNP and CRSwNP

We first wanted to evaluate whether expression of zinc homeostasis genes was altered in CRS. mRNA extracted from 10 controls, 10 CRSsNP, and 19 CRSwNP patients was assessed for expression of MT1a, MT2a, MT3, ZIP1, ZIP2, ZIP14, ZnT1, ZnT4 (Figure 14). Metallothionein (MT1a, MT2a, and MT3) mRNA expression was differentially down

regulated in CRS patients. MT1a and MT2a were down regulated in CRSsNP patients compared to controls (fold changes of 0.179 ($p<0.05$) and 0.316 ($p<0.05$) for MT1a and MT2a respectively). MT3 was down regulated in CRSwNP compared to controls (fold change 0.269; $p<0.05$). MT2a expression in CRSsNP patients was 0.165 fold lower than in CRSwNP patients ($p<0.001$). Zinc uptake transporter (ZIP1, ZIP2, and ZIP14) gene expression was significantly reduced in CRSsNP patients compared to controls. Fold change values for ZIP1, ZIP2, and ZIP14 were 0.420 ($p<0.05$), 0.438 ($p<0.05$), and 0.583 ($p<0.05$) respectively. Fold change values for CRSsNP compared to CRSwNP were significant for ZIP1 of 0.357 ($p<0.001$), and ZIP14 of 0.475 ($p<0.001$). Zinc efflux transporter ZnT1 was significantly up regulated in CRSsNP patients compared to both controls and CRSwNP, with fold changes of 2.281 ($p<0.001$) and 1.687 ($p<0.05$). No difference was observed in the relative gene expression of ZnT4. Correlations between zinc transporter gene expressions were analysed by patient phenotype and overall using the nonparametric Spearman rank correlation test. Results show some genes such as (ZIP14 and MT1a) and (ZIP14 and ZnT4) to significantly correlate across all CRS phenotypes whilst others such as (MT2a and MT3) and (MT3 and ZnT4) to correlate only in CRSwNP patients (Supplemental Table S2).

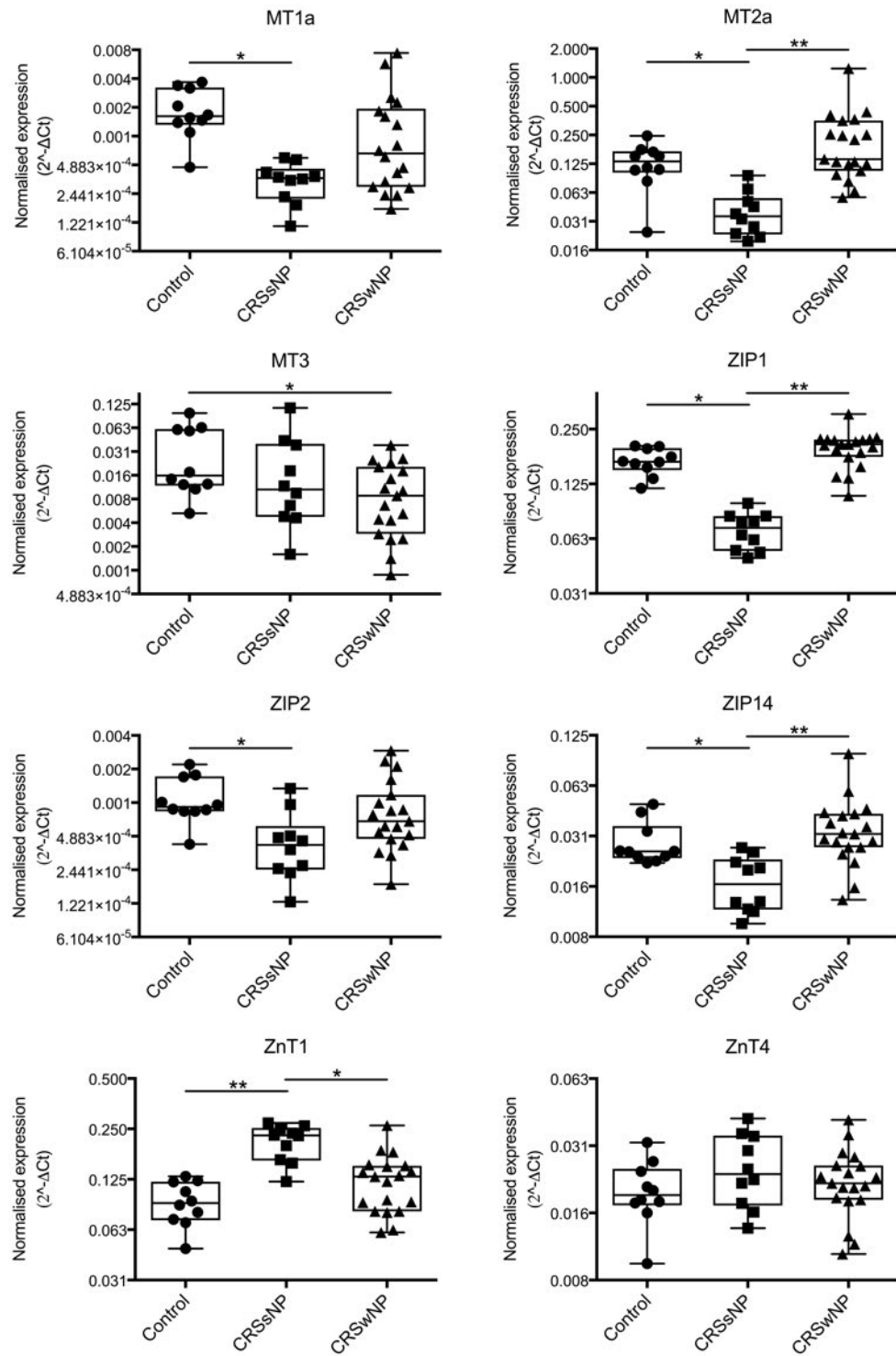


Figure 14. MT1a, MT2a, ZIP1, ZIP2, and ZIP14 are downregulated in CRSsNP, while ZnT1 is upregulated. MT3 is downregulated in CRSwNP.

qPCR analysis of sinus samples from controls (n=10), CRSsNP (n=10), and CRSwNP (n=19) patients. The box represents the median (2^{-ΔCt}) and the interquartile range, the whiskers represent minimum and maximum values. (*) P<0.05; (**) P<0.001; (Kruskal-Wallis analysis with Dunn's test for multiple comparisons).

Labile zinc and apical tight junction protein ZO-1 expression were diminished in CRSwNP tissue

We next wanted to identify whether levels of epithelial labile zinc and apically located ZO-1 were different between controls, CRSsNP and CRSwNP, using a tissue microarray including samples from 35 patients (7 controls, 9 CRSsNP, and 19 CRSwNP). Reductions in the epithelial labile zinc and ZO-1 distribution were seen in tissue samples from CRSwNP patients (Figure 15). CRSsNP tissue samples appeared to retain uniform ZO-1 protein expression linearly across the apical border with intermittent interruptions (Figure 16E). CRSwNP patients showed similar ZO-1 immunolocalisation albeit lower intensity throughout the epithelium (Figure 16H). Zinquin staining, assessing labile zinc levels, appeared less intense in CRSwNP compared to controls (Figures 16D & 16G). In the image channel overlay, in control patients, there appeared to be co-localisation of labile zinc and ZO-1, however zinc levels were high throughout the entire epithelium, evidenced by intense Zinquin staining (Figure 16C). To identify relative differences between the patient groups we quantified the fluorescence intensity of each channel in the epithelial samples (Supplemental Figure S4). Consistent with previous research identifying decreased total zinc concentrations in CRSwNP polyp tissue,⁴³⁸ we found that loosely bound labile zinc levels were decreased in CRSwNP epithelium ($p < 0.05$) (Figure 15A). In addition, apical ZO-1 protein expression was diminished in CRSwNP compared to both controls ($p < 0.01$) and CRSsNP ($p < 0.05$) (Figure 15B). Furthermore, relative intensities from labile zinc and apical ZO-1 were significantly correlated ($R = 0.44$, $p < 0.01$) (Figure 15C).

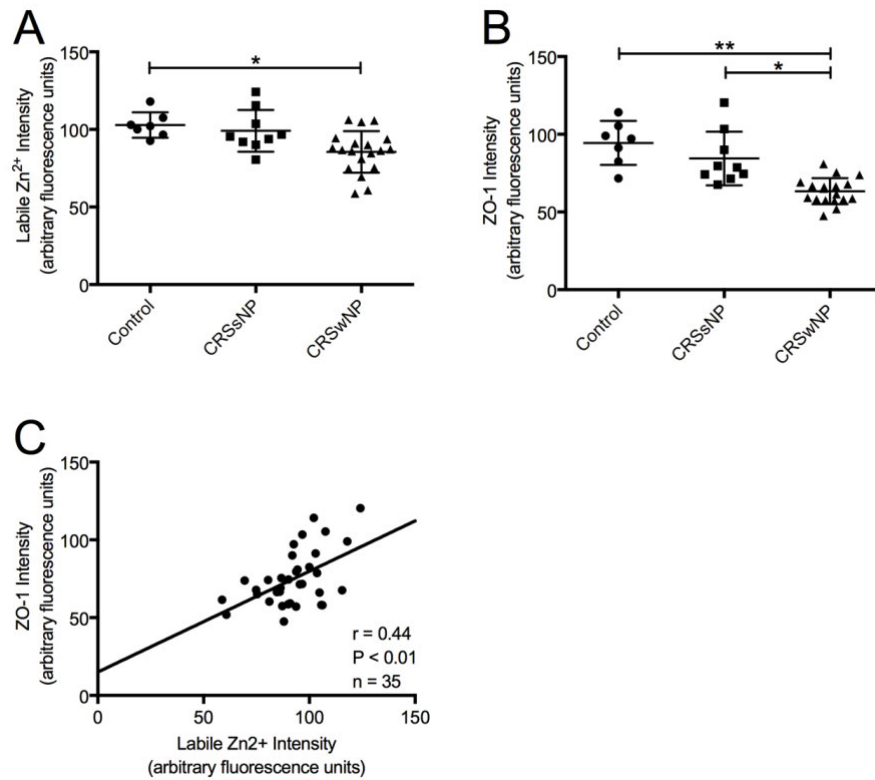


Figure 15. Quantification of labile Zn²⁺ and ZO-1 in the sinonasal epithelium of control, CRSsNP, and CRSwNP patients.

(A) Zn²⁺ fluorescent mean intensities were calculated from an epithelial region of interest (ROI) of each sample; the apical third of this ROI was measured for ZO-1 fluorescent mean intensities (B). Data represents means (n=35) (\pm SD), (*) $p < 0.05$, (**) $p < 0.01$, (Kruskal-Wallis analysis with Dunn's test for multiple comparisons). (C) Correlations between labile Zn²⁺ and apical ZO-1 were evaluated using the nonparametric Spearman rank correlation coefficient.

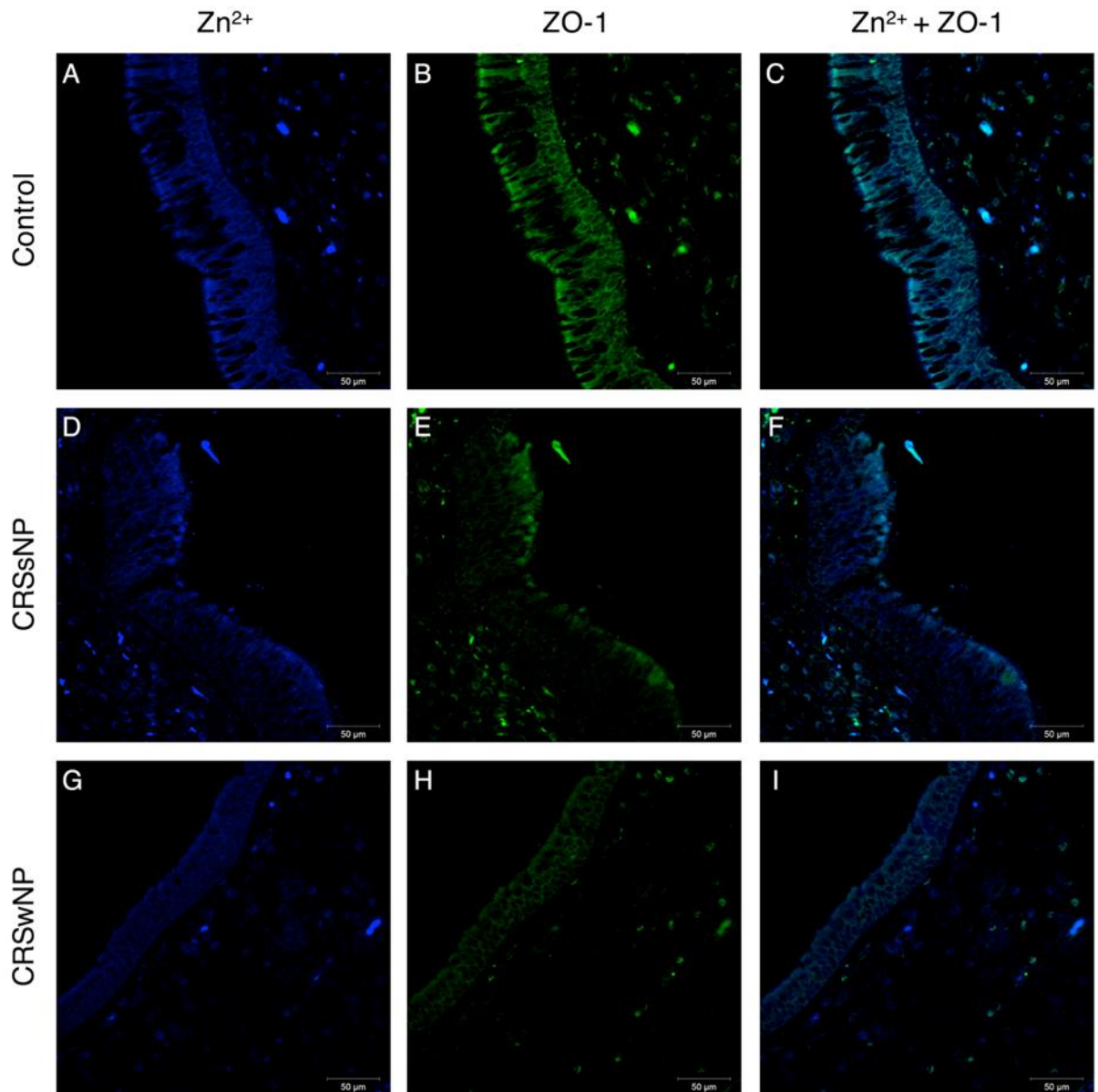


Figure 16. Labile Zn²⁺ and ZO-1 are reduced in sinonasal epithelium of Chronic Rhinosinusitis patients.

Tissue microarray sections were stained for labile Zn²⁺ in blue (A, D, G) and ZO-1 in green (B, E, H). An overlay image was generated (C, F, I). Representative images of control (A, B, C), CRSsNP (D, E, F), and CRSwNP (G, H, I) patient tissue samples.

Serum zinc concentrations are not reduced in CRSsNP or CRSwNP

To assess whether the local reductions in mucosal zinc are a result of systemic deficiency we analysed serum from controls, CRSsNP, and CRSwNP. Mean zinc concentrations of for controls, CRSsNP, and CRSwNP were 13.1 (5.4), 11.6 (2.5), and 13.31 (5.4) µmol/L

respectively and not statistically significant (Supplemental Figure S5). Additionally, there was no correlation between matched serum zinc and labile tissue zinc measurements; $r=0.36$ ($p>0.05$).

Zinc depletion impairs barrier function in developing primary HNEC-ALI cultures

To model the effect of local zinc deprivation on the sinonasal mucosal barrier we used HNEC-ALI cultures that were grown in zinc depleted media for 2 weeks. TEER and Papp were measured at 3 time points over 15 days. Zinc depletion *in-vitro* caused a statistically significant reduction in TEER compared to the control at 10 and 15 days (approximately 45% of the control at 15 days) (Figure 17A). TEER in ZD HNEC-ALI cultures compared to the matched control at 5, 10, and 15 days were 125.5% (± 27.13 ; $p=0.1783$), 70.07% (± 2.173 ; $p<0.0001$), and 44.72% (± 21.08 , $p=0.0105$) respectively. The difference in ZD HNEC-ALI culture TEER between days 5, 10, and 15 showed a significant reduction from day 5 to 10 (mean reduction 55.48%; $p=0.0242$), and day 5 to 15 (mean reduction 80.83%, $p=0.0152$). To assess the effects on Papp a fluorescein-conjugated 4kDa dextran was used to assess flux across the barrier. The comparative fold change means in Papp at days 5, 10, and 15 were 1.052 (± 0.4505), 3.522 (± 2.942), and 4.163 (± 2.622 ; $p=0.0524$) respectively. Whilst an increase in mean Papp in ZD samples was seen at days 10 and 15, the difference with controls was not statistically significant (Figure 17B). The reduction in TEER coupled with a trend to increased molecular flux suggests that paracellular permeability of ALI cultures is increased when intracellular zinc levels are depleted.

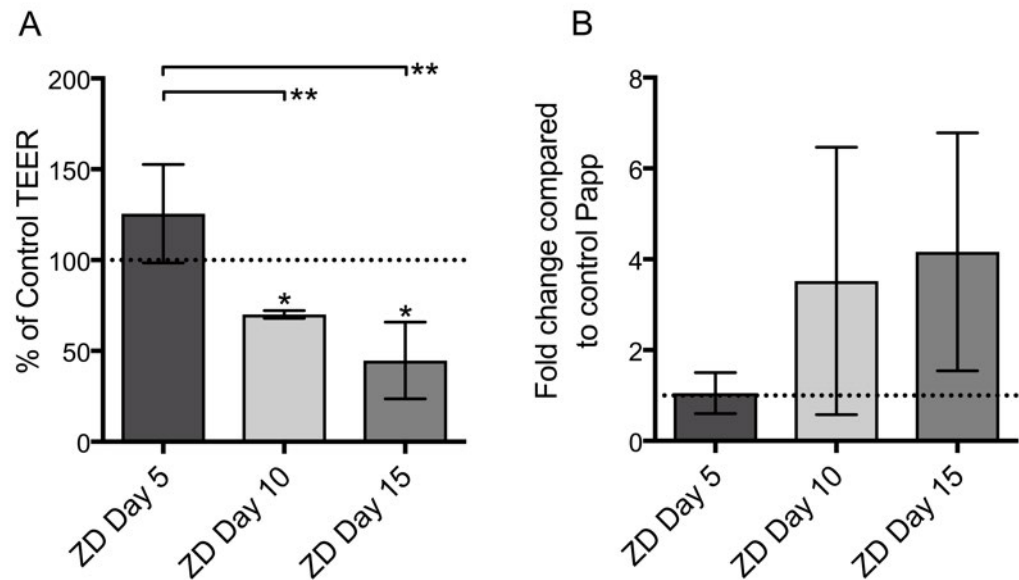


Figure 17. Zinc depletion decreased barrier function of human nasal epithelial cell cultures.

ALI cultures were grown with control cell media or zinc deplete (ZD) media for 15 days. Measurements of TEER (A) and Papp (B) were taken at 5, 10, and 15 days after initiation of air liquid interface culture. (A) Zinc depletion resulted in a time dependent decrease in TEER. Results are expressed as a percentage change compared to the control (ZD TEER/ Control TEER) * 100 (mean ±SD) (n=3; p<0.05, unpaired t-test). (*) comparison between control and ZD groups, and (**) comparison between days 5, 10 and 15 of ZD conditions. (B) FITC Dextran permeability shows an increase in mean flux across the cell barrier, however not statistically significant.

Zinc deficiency induces alterations in tight junction formation and intracellular labile zinc in HNEC- ALI cultures

To assess the effect of zinc depletion in the medium on intracellular zinc levels and TJ structures we performed immunofluorescence staining of the tight junction protein ZO-1 and determined intracellular labile zinc levels in control and ZD HNEC-ALI cultures (Figure 18). At day 5, there was a subtle reduction in intracellular zinc in ZD samples compared to controls, however TJ proteins remained localised to the cell peripheries (Figure 18D). ZD cultures at day 10 showed a faint intracellular zinc signal (Figure 18E). ZO-1 staining at day 10 was still localised to the periphery of the cell, however there was a diffuse cytoplasmic ZO-1 signal and widening at the cell peripheries. At day 15, the ZD

cultures were completely depleted of labile zinc with profound disruption of ZO-1 continuity at the cell peripheries (Figure 18F).

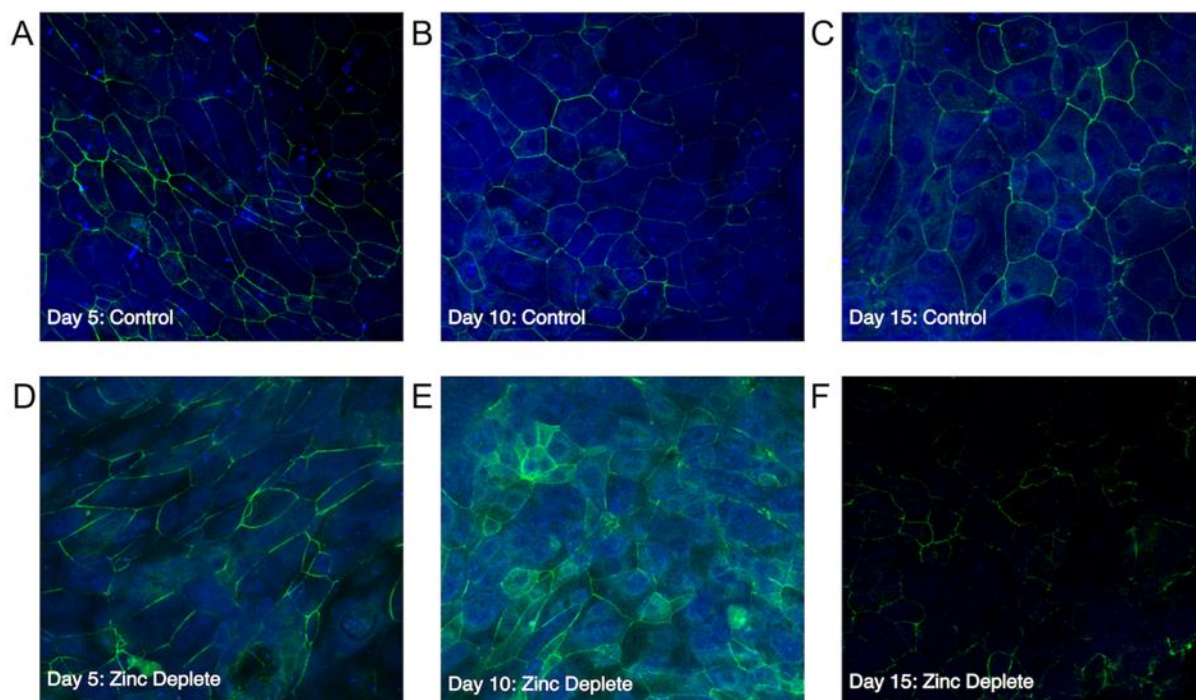


Figure 18. Zinc deficiency causes alterations to tight junction ZO-1 localisation and reduction in intracellular labile zinc.

Immunofluorescence of ZO-1 (green) localisation and labile zinc (blue) was assessed in control (A, B, and C) and zinc deplete (D, E, and F) ALI cultures at 5 (A, D), 10 (B, E), and 15 (C, F) days. Images taken with 20x objective power using a confocal laser scanning microscope (ALI, n=3).

Inflammatory cytokine production in ZD HNEC-ALI cultures

Cytokine production was measured in the cell culture supernatant at days 5, 10, and 15 of exposure to either zinc deplete media or control media. IL-1 β , IL-2, IL-4, IL-5, IL-13, and IFN- γ were all below the lower limit of assay quantitation. IL-6, IL-8, IL-10 and TNF- α were within the limits of quantitation. Zinc depleted cells increased the mean production of IL-8 and TNF- α at day 15, compared to control, however, this was not statistically significant (Supplemental Figure S6).

Discussion

Our present work showed that zinc homeostasis is altered in chronic rhinosinusitis mucosa and that intramucosal zinc depletion negatively affects mucosal barrier structure and function. Prior work has focused on how zinc regulates airway epithelial apoptosis and allergic inflammation^{512,513} however, whether zinc homeostasis is changed in CRS and how this affects barrier function is unknown. We found that the sinonasal epithelium from CRSwNP patients showed decreased labile zinc levels in correlation with low apical ZO-1 levels. Moreover, *in-vitro* depletion of zinc in HNEC-ALI cultures identified zinc as an essential requirement for normal functioning of the TJ complex via ZO-1. Together, these findings suggest that mucosal zinc deficiency may contribute to the defective epithelial barrier in CRSwNP. The role of zinc in barrier function is well recognised in the gastrointestinal (GI) mucosa where zinc deprivation and supplementation affects the GI barrier by modifying TJ proteins.⁵¹⁴ ZD CACO-2 cells exhibit significant barrier defects,²⁸² and ZD conditions increased the susceptibility to bacteria induced barrier dysfunction.^{241,515} In agreement with our finding of a decreased ZO-1 immunoreactivity in CRSwNP patients compared to controls, previous studies have likewise observed that the CRSwNP barrier is disrupted, and have suggested that Th2 and Th17 cytokines are contributing factors.^{20,323,454} Zinc availability has important implications on the regulation of cytokine production in different cell types. In particular zinc deprivation has been shown to reduce IFN- γ and IL-2 production from Th0/Th1 polarised T cell lines, whilst TNF- α , IL-1 β , and IL-8 are increased in a ZD monocyte-macrophage cell line.⁵¹⁶ Whilst not significant, our findings also support an increased secretion of IL-8 and TNF- α in ZD HNECs.

To elucidate the role of zinc transporter genes in CRS phenotypes we conducted a gene expression panel of ZIP, ZnT, and MT families in CRS patients and controls. ZIP, MT,

and ZnT transporters have been identified in airway epithelium, however there is no previous description of their expression in sinonasal epithelium.^{517,518} The coordination of zinc homeostasis and the physiological consequences of zinc transporter alterations are seemingly complex and not entirely understood. The ZIP family is implicated in zinc transport into the cytoplasmic compartment.⁵¹⁹ ZIP1 and ZIP2, showing decreased expression in CRSsNP patients compared to controls, facilitate zinc uptake through the plasma membrane and ZIP14 may also play a role in cellular uptake of iron and manganese.^{519,520} ZnT1, overexpressed in CRSsNP patients compared to controls, localises to the plasma membrane regulating cellular zinc efflux and detoxification. ZnT1 is also highly inducible during an over supply of zinc.⁵²¹ MTs, also differentially expressed in CRS patients compared to controls, have a broad range of functions including regulation of intracellular metals (zinc, copper, cadmium), anti-oxidant properties, and cellular apoptosis.^{444,522} In this study, whilst zinc transporter genes and MTs were differentially expressed in CRSsNP patient tissue samples, labile zinc levels within the epithelium layer did not appear to be altered in CRSsNP compared to controls. The aetiology and specific cell types involved in these gene expression alterations are unclear, but indicate an imbalance in the zinc homeostasis mechanisms in these patients.

Expression of MT3 was significantly downregulated in CRSwNP patients. Similar to MT1 and MT2, MT3 has metal binding properties.⁵²³ In addition, MT3 has potential antioxidant activities by scavenging Reactive Oxygen Species (ROS) during inflammatory processes.⁴⁴⁸ Deficiency of MT3 may impair the function of intracellular lysosomes and the autophagy process.⁴⁴⁹ This could be particularly detrimental in CRSwNP where intracellular pathogens are found more frequently.^{95,524} Future studies

will be needed to identify how local zinc supply alters zinc transporter protein expression and how Th1 and Th2 inflammatory states influence zinc homeostasis.

Acknowledgements

Dr Peter Zalewski from the University of Adelaide, South Australia, Australia for supplying the Zinquin fluorophore. This work is supported by a Garnett Passe and Rodney Williams Memorial Foundation scholarship to JM and a Garnett Passe and Rodney Williams Memorial Foundation Conjoint Grant to PJW and SV.

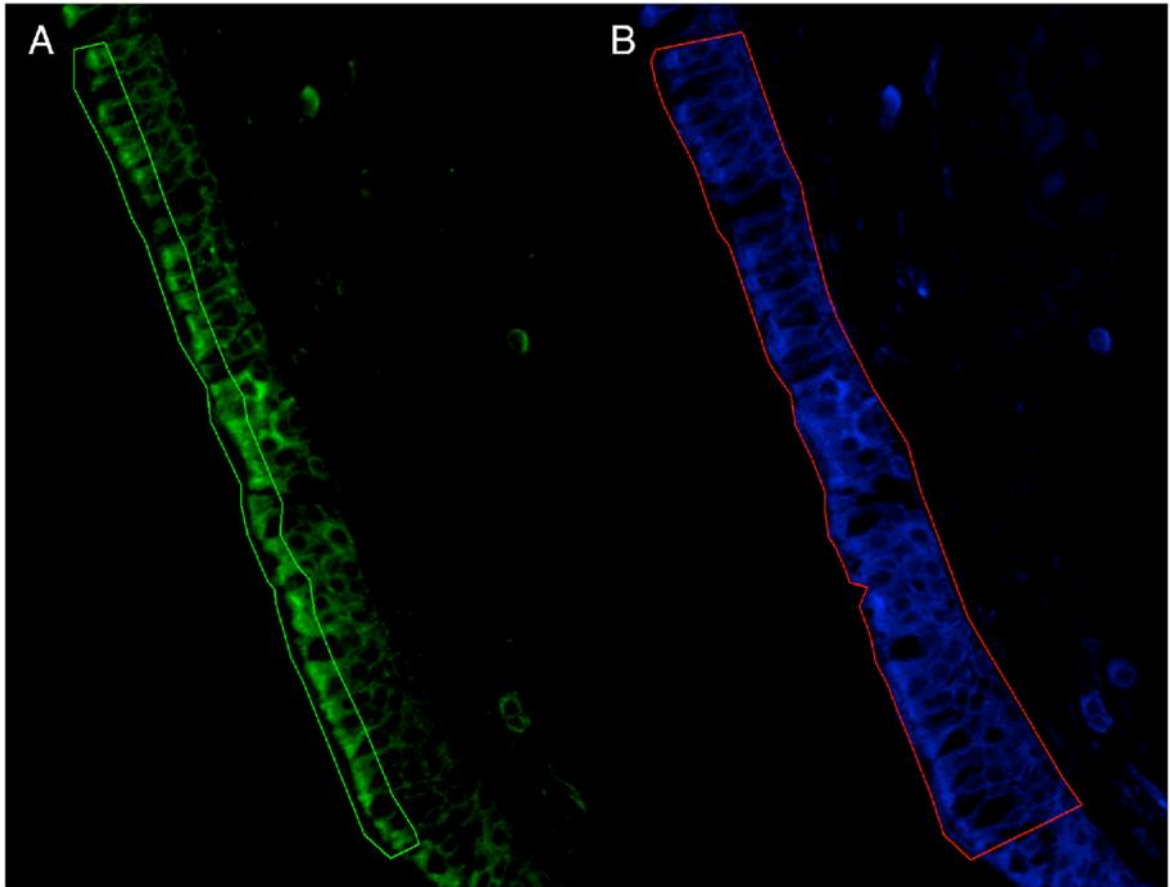
Supplementary Information

Supplementary results

Supplemental Table S2. Correlation between zinc transporter gene expression.

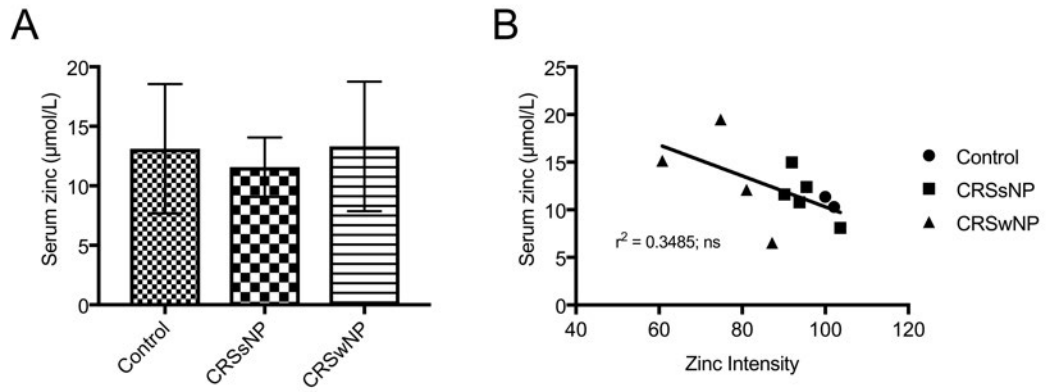
Correlations between zinc transporter gene expressions. Analysed by patient phenotype and overall. Correlations were evaluated using the nonparametric Spearman rank correlation coefficient, reported as the (r) value. (*) p<0.05, (**) p<0.01, (***) p<0.001, (****) p<0.0001.

Group (n)	MT2a	MT3	ZIP1	ZIP2	ZIP14	ZnT1	ZnT4
MT1a (39)	0.738****	0.108	0.423**	0.2	0.725****	-0.198	0.344*
Control (10)	0.054	-7.28x10 ⁻⁵	0.675*	0.682*	0.833**	0.436	0.870**
CRSsNP (10)	0.063	-0.035	0.581	0.180	0.679*	0.434	0.277
CRSwNP (19)	0.831****	0.394	0.214	-0.073	0.727***	0.102	0.566
MT2a (39)		0.059	0.455**	0.127	0.509***	-0.078	0.332*
Control (10)		0.282	0.074	-0.053	-0.065	0.243	0.128
CRSsNP (10)		0.269	-0.363	-0.268	-0.301	-0.163	-0.264
CRSwNP (19)		0.608**	0.258	0.046	0.431	0.234	0.656**
MT3 (39)			-0.056	0.001	-0.156	0.114	-0.085
Control (10)			0.502	0.154	-0.237	0.827**	0.0228
CRSsNP (10)			-0.137	-0.438	-0.564	-0.0107	-0.440
CRSwNP (19)			0.303	0.146	0.288	0.211	0.522*
ZIP1 (39)				0.451**	0.649****	-0.292	0.040
Control (10)				0.615	0.553	0.818**	0.818**
CRSsNP (10)				0.745*	0.749*	0.725*	0.587
CRSwNP (19)				0.271	0.485*	0.605**	0.294
ZIP2 (39)					0.189	0.031	0.27
Control (10)					0.325	0.424	0.64*
CRSsNP (10)					-0.034	0.362	0.366
CRSwNP (19)					0.520	0.516*	0.386
ZIP14 (39)						-0.165	0.346*
Control (10)						0.146	0.848**
CRSsNP (10)						0.721*	0.782**
CRSwNP (19)						0.113	0.461*
ZnT1 (39)							0.526***
Control (10)							0.462
CRSsNP (10)							0.795**
CRSwNP (19)							0.359



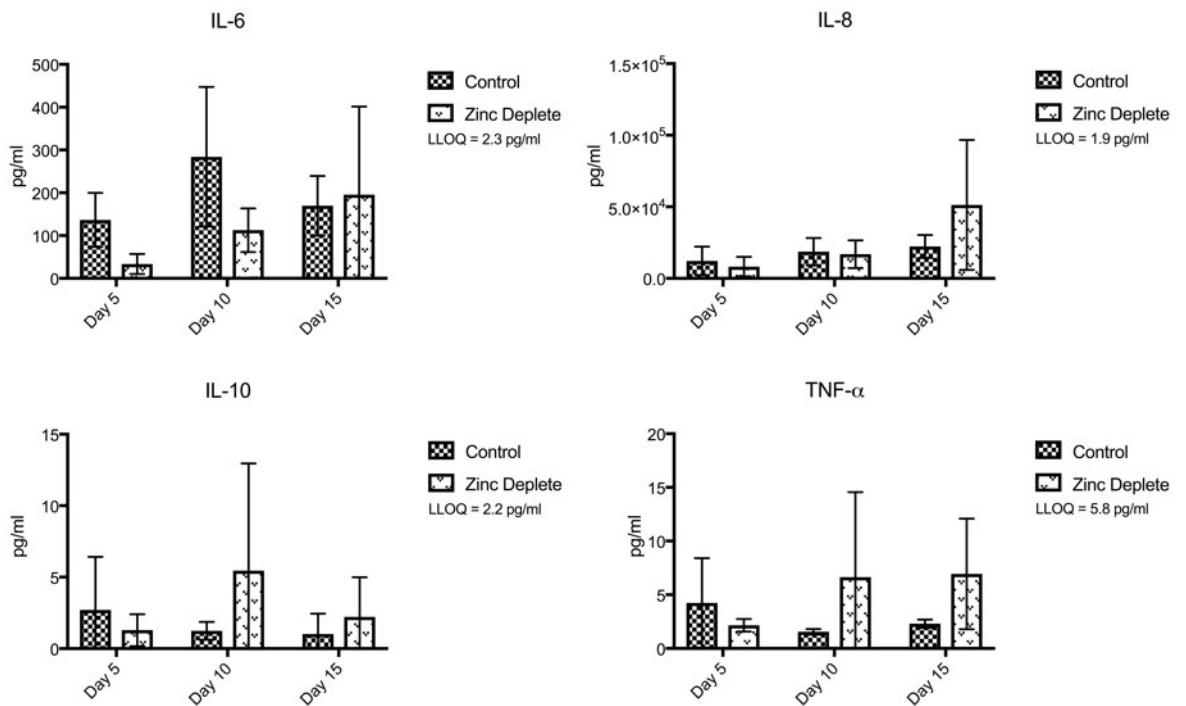
Supplemental Figure S5. Labile Zn²⁺ and ZO-1 were quantified in tissue microarray sections.

Example of a region of interest (ROI) made around the epithelium for labile Zn²⁺ relative quantification, and a second ROI identifying the apical third of the epithelium was added for ZO-1 relative quantification.



Supplemental Figure S6. Serum zinc concentrations in controls, CRSsNP, and CRSwNP show that systemic zinc is not depleted.

Serum analysis from serum collected at the time of tissue samples during endoscopic sinus surgery. Results are expressed in $\mu\text{mol/L}$ (SD). $n=14$ (Controls 5, CRSsNP 5, CRSwNP 4).



Supplemental Figure S7. HNEC-ALI IL-6, IL-8, IL-10, and TNF- α cytokine production show increasing trends with cumulative days in cultured zinc deplete media.

Bio-Plex assay results from cell culture supernatant at day 5, 10, and 15 grown with zinc deplete media or control media. Results are expressed in pg/ml . Lower limit of quantitation (LLOQ).

Letter to the Editor

To the Editor:

Recent investigation into the mucosal barrier function in CRS has shown that TJ genes/proteins are down regulated, particularly in CRSwNP.^{20,198} Whilst some cytokines and bacterial products have been shown to disrupt mucosal barrier structure and function,^{19,454} little is known about the contributing and mechanistic factors leading to a dysfunctional barrier in CRS. Zinc is an essential trace element involved in aspects of immune system regulation, barrier function, healing, and cellular functions.^{432,514} Local zinc deficiency induced barrier dysfunction has been implicated in chronic inflammatory disorders such as gastritis and inflammatory bowel disease.⁵¹⁴ Previous studies have indicated that zinc levels are lower in CRSwNP tissue than control mucosa.^{438,439} However, both reports utilised spectrophotometry on homogenised specimens, which does not allow for analysis of mucosal zinc distribution. It remains unclear whether zinc homeostasis is altered in CRS patients and whether zinc levels may influence the TJ barrier function in CRS.

To identify cell types exhibiting altered labile zinc levels in relation to markers of mucosal barrier structure we used a tissue microarray comprising tissue cores from 35 patients, including 7 controls, 9 CRSsNP, and 19 CRSwNP. Specimens were stained with anti-ZO-1 antibodies and the zinc fluorophore Zinquin (Figure 16). Details of materials and methods, and patient demographic data (Table 9) are found in this article's Online Repository. Zinc levels and ZO-1 staining were high and uniform throughout the entire epithelium in controls. To identify relative differences between the patient groups we quantified the fluorescence intensity of each channel in the epithelial samples (Supplemental Figure S4). Consistent with previous research,^{438,439} we found that labile zinc levels were significantly decreased in CRSwNP epithelium compared to controls

($p < 0.05$) (Figure 15). Apical ZO-1 protein expression was diminished in CRSwNP compared to both controls and CRSsNP ($p < 0.05$) (Figure 15). Furthermore, relative intensities from labile zinc and apical ZO-1 were significantly correlated ($r = 0.44$, $p < 0.01$) (Figure 15). Patient serum zinc concentrations were also measured and showed no significant difference between controls and CRS groups (Supplemental Figure S5).

To model the effect of local zinc deprivation on the sinonasal mucosal barrier we used HNEC-ALI cultures that were grown in zinc deplete media for 2 weeks. TEER and Papp were measured at 5, 10, and 15 days (Figure 17). Zinc deficient (ZD) *in-vitro* conditions caused a statistically significant reduction in TEER compared to the control at 10 and 15 days (approximately 45% of the control at 15 days) (Figure 17). TEER in ZD HNEC-ALI cultures compared to the matched control at 5, 10, and 15 days were 125.5% (± 27.13 ; $p = 0.1783$), 70.07% (± 2.173 ; $p < 0.0001$), and 44.72% (± 21.08 , $p < 0.05$) respectively. The TEER difference in ZD cultures between days 5, 10, and 15 showed a significant reduction from day 5 to 10 (mean reduction 55.48%; $p < 0.05$), and day 5 to 15 (mean reduction 80.83%, $p < 0.05$). To assess the effects on Papp a fluorescein-conjugated 4kDa dextran was used to assess flux across the barrier. The comparative fold change means in Papp at days 5, 10, and 15 were 1.052 (± 0.4505), 3.522 (± 2.942), and 4.163 (± 2.622 ; $p = 0.0524$) respectively. Whilst an increase in mean Papp in ZD samples was seen at days 10 and 15, the difference with controls was not statistically significant. The reduction in TEER coupled with a trend to increased molecular flux suggests that paracellular permeability of ALI cultures is increased when intracellular zinc levels are depleted. To assess the effect of ZD on intracellular zinc and TJ structures we performed immunofluorescence staining of ZO-1 and intracellular labile zinc in HNEC-ALI cultures (Figure 18). Results showed a gradual decrease in intracellular zinc levels in ZD samples compared to controls accompanied by a redistribution of the ZO-1 immunolocalisation. At day 15, the

ZD cultures were completely depleted of labile zinc with profound disruption of ZO-1 continuity at the cell peripheries. Additionally, cytokine production (see supporting information) was measured in the cell culture supernatant showing a non-significant mean increase in IL-8 and TNF- α at day 15 in the ZD cultures (Supplemental Figure S6). These *in-vitro* findings suggest that zinc is essential for the maintenance of sinonasal TJ barrier function and ZO-1 localisation as it is in gastrointestinal cell lines.²⁸⁰

To investigate the role of zinc in CRS, we evaluated the expression of zinc homeostasis genes in tissue harvested from 10 CRSsNP patients, 19 CRSwNP patients and 10 controls. Relative expression was determined by normalizing to the housekeeping genes beta-2 microglobulin (B2M) and hypoxanthine-guanine phosphoribosyltransferase 1 (HRPT), expressed as fold change between groups. Metallothioneins MT1a and MT2a were down regulated in CRSsNP ($p < 0.05$), while MT3 was down regulated in CRSwNP compared to controls ($p < 0.05$). Zinc uptake transporter (ZIP1, ZIP2, and ZIP4) gene expression was significantly reduced in CRSsNP patients compared to controls ($p < 0.05$). Zinc efflux transporter ZnT1 was significantly up regulated in CRSsNP patients compared to controls ($p < 0.001$) (Figure 14). Correlations between zinc transporter gene expressions were analysed by patient phenotype and overall using the nonparametric Spearman rank correlation test. Results show some genes such as (ZIP14 and MT1a) and (ZIP14 and ZnT4) to significantly correlate across all CRS phenotypes whilst others such as (MT2a and MT3) and (MT3 and ZnT4) to correlate only in CRSwNP patients (Supplemental Table S2). The coordination of zinc homeostasis and the physiological consequences of zinc transporter alterations are seemingly complex and not entirely understood. The finding of a differential expression of zinc transporter genes in CRSsNP and CRSwNP compared to control indicates an imbalance or change in zinc homeostasis within the sinonasal mucosa in the context of CRS.

In conclusion, our present work showed that zinc homeostasis is altered in CRSwNP patient tissue, which is associated with decreased ZO-1 expression. *In-vitro* experimentation indicates that intramucosal zinc depletion negatively affects mucosal barrier structure and function.

Thesis Synopsis

This thesis was started to investigate the potential airway barrier disrupting factors secreted by *S. aureus*. After review of the literature it became clear that although local bacterial factors are capable of mediating epithelial and mucosal barrier disruption, there are additional host factors that support barrier integrity. Thereafter, the study expanded to examine the mucosal barrier in CRS with a focus on zinc homeostasis.

The first study was comprised of two major aims: proteomic analysis to identify and investigate candidate toxins and then a combination of several techniques to further characterise the barrier disrupting effects of a crude *S. aureus* supernatant (cell-free). Our prior work observed *S. aureus* barrier disruption in a HNEC-ALI culture model, hence this model was utilised in testing of the candidate toxins. A limitation of this model is that it does not lend itself to high throughput testing of toxins due to extended culturing times, needing TEER to measure barrier function, and a finite number of cell divisions in primary cultures.

Analysis of protein identities in the crude supernatant revealed several candidate toxins for further investigation. Candidate toxins were selected based on: known barrier disrupting properties in non-sinonasal epithelial barriers, or significance to CRS. Considering this, we decided to firstly investigate HLA, SEA, and LTA.

Our results showed that the purified toxins HLA, SEA, and LTA had no effect on HNEC-ALI barrier function. This is interesting as the literature regarding other epithelial barriers found that HLA and LTA contribute to barrier disruption. SEA on the other hand is known to be produced by *S. aureus* strain ATCC 13565 used in our prior work,¹⁹ and shares conserved regions with other staphylococcal enterotoxins including

SEB.^{525,526} As discussed in the literature review there is emerging evidence that SEB mediates airway barrier disruption *in-vitro*.

We can only speculate on why the HNEC-ALI culture was unaffected by HLA. The purified HLA was obtained commercially, and hemolysis activity checked prior to experimentation. However, it is known that HLA binding affinities and cell cytotoxicity is known to differ between cell types and species. Previous studies demonstrated that rabbit erythrocytes are over 100 times more sensitive to HLA when compared to human erythrocytes.⁴⁵⁹ Further investigation on other human and murine cell lines showed cytotoxicity of several epithelial derived cells, however fibroblasts, neuroblasts, and granulocytes are intrinsically resistant.^{459,527} Recently host ADAM10 was shown to be necessary for cell binding cytotoxicity, and that cell lines expressing differential amounts of ADAM10 showed a correlation between receptor expression and binding.⁵²⁸ Additionally, ADAM10 is essential for HLA mediated vascular endothelial cadherin disruption.³⁴⁶ Crombruggen et al., (2012) found that ADAM10 concentrations in CRSwNP tissue trended to be higher, although this was not statistically significant.⁵²⁹ We did not confirm the expression of ADAM10 in the HNEC-ALI model, although this should be considered for future investigation of HLA. Furthermore, EV-associated HLA has been shown to be more pathogenic *in-vitro* and *in-vivo*.^{425,478} Intracellular EV delivery of HLA may represent a mechanism to bypass binding of surface proteins such as ADAM10.

The second component of the initial paper further characterised the crude supernatant. We showed that both *S. aureus* ATTC strains 13565 and 25923 alter barrier function. ATCC 13565 ubiquitously produces the unknown factor, with the highest activity during the post-exponential phase. While barrier disrupting activity was only detectable from ATCC 25923 when supernatant was collected during the post-exponential phase. The

post-exponential bacterial growth phase is known to be a crucial point of toxin production.^{379,469} We next employed size fractionation using centrifugal size filters, which avoid the use of chemical precipitation/separation methods, as this may have introduced impurities or contamination not suitable for use in the HNEC-ALI model. This identified the barrier activity was confined to the >30 kDa fraction. Following this we observed heat and proteinase K treatment attenuated the barrier effect, which is highly suggestive of a protein mediated mechanism.

The supernatant was further separated with differential ultracentrifugation, which is known to sediment/pellet EVs while leaving soluble protein suspended in the supernatant.^{474,530,531} Screening of the UC pelleted and supernatant fractions revealed the activity was restricted to the UC pellet fraction. Additionally, it seemed that barrier disrupting activity was enriched in the UC pellet fraction compared to whole supernatant (non-ultracentrifuged) when used in the same total protein concentration. Similar to our results, previous works have demonstrated that bacterial EVs can be degraded with heat and proteinase K, particularly if the targeted protein is incorporated in the EV membrane.^{254,429,477} It is possible that the responsible barrier factor is associated with the EV membrane. Ultimately further work needs to be completed to demonstrate the barrier disrupting factor is indeed due to EVs, and if so may represent a novel mechanism of *S. aureus* virulence for consideration in the context of CRS.

With the knowledge that the initially tested toxins had no effect on barrier function, we next evaluated the activity of *S. aureus* extracellular proteases. Several extracellular proteases were identified in the proteomics analysis from the first study including V8 protease, staphopain B, and the family of spl-like proteases (splA, splB, splC, splD, splE, splF). V8 protease has shown previous barrier altering properties in the epidermal literature, and the staphopain family were known to degrade lung elastin and α 1-

antichymotrypsin. Very little was known about the spl-like protease family when this study was conducted, however predicted protein targets included mucin proteins and olfactory receptors. Fortunately, we were able to collaborate with the research group responsible for the initial purification, and structural analysis of the spl-like proteases. We decided to add staphopain A to the evaluation due to its similarity with staphopain B, and exfoliative toxin A as it has potent epidermal barrier disruption properties.

Our results showed that V8 protease is produced by the three *S. aureus* strains used in our previous work, and that V8 protease has a barrier disrupting effect. We observed a time and dose dependent effect on TEER and Papp when V8 was applied apically to HNEC-ALI cultures. This was coupled with a disruption of ZO-1 fluorescence staining and apparent increase in claudin-1 intensity. Staphopain A, staphopain B, exfoliative toxin A, and the spl-like proteases had no effect on barrier function. Unexpectedly, we also observed that V8 protease reduces IL-6 in HNEC-ALI supernatant.

Early research recognised that V8 protease inactivates α 1-antitrypsin by proteolytic cleavage.³⁸⁵ The cleaved α 1-antitrypsin product was also seen to be a potent neutrophil chemoattractant, hence potentiating inflammation at the site of the V8 protease.³⁸⁵ A handful of studies have linked heterozygotic α 1-antitrypsin deficiency with a higher risk of developing nasal polyposis, and single nucleotide polymorphisms (SNP) increasing susceptibility to severe CRSwNP.⁵³²⁻⁵³⁴ It is possible that colonisation with a V8 producing *S. aureus* is an epigenetic contributor to CRS in susceptible people. V8 protease cleaves the immunoglobulins IgG, IgM, IgA1 and IgA2 (secretory IgA), thus may impair antibody mediated phagocytosis.³⁸⁶ Additionally, the complement system is affected by *S. aureus* proteases (V8 protease, aureolysin, staphopain A, and staphopain B) by altering activation of both the classical and alternative complement pathways. V8 protease inhibits the classical and alternative pathways at least by 70% and 50%

respectively, with aureolysin being even more effective. Conversely it was seen that both V8 protease and aureolysin non-specifically activate the C1 component and caused increased deposition of C1q on the commensal bacteria *S. epidermidis*.⁵⁰⁷ *In-vivo* murine infection with wild type, aureolysin, and V8 protease producing *S. aureus* strains was able to induce both a strong polyclonal B cell activation and a specific V8 neutralising antibody response.⁵³⁵ In a clinic setting V8 specific antibodies have been identified more frequently in persistent *S. aureus* nasal carriers, compared to non-carriers.⁵³⁶ Extracellular V8 protease can alter the fibronectin binding phenotype of *S. aureus* by proteolytically cleaving cell surface fibronectin binding protein (FnBP).³⁸⁷ *S. aureus* adheres to host fibronectin through FnBP, which is maximally expressed during exponential growth phases and required for biofilm formation.⁵³⁷ The extracellular proteases are thought to precipitate release of bacteria from biofilm,³⁸⁷ which is induced by locally high cell density.^{379,384,387} Although we did not observe any barrier effect due to the spl-like proteases, it is possible that they may potentiate barrier dysfunction *in vivo*. Stenzel et al., (2016) demonstrated *in-vivo* induction of a Th2 inflammatory response due to SplD. Additionally, splD treatment of *ex-vivo* nasal polyp tissue leads to a strong IL-5, IL-17, and INF- γ response;⁴⁰³ IL-17, and INF- γ are both known to disrupt the airway barrier.^{20,323}

Our results showed V8 protease caused a reduction of IL-6 in the HNEC-ALI supernatant. Furthermore, incubation of V8 protease with purified IL-6 demonstrated a direct effect on IL-6 levels, as quantified by ELISA. Little is understood about the function of IL-6 in the sinonasal mucosa, although it appears to be essential in protection of gastrointestinal mucosa against microbial adhesion. Dann et al., (2008) found that IL-6 deficient mice were unable to control growth of gastrointestinal pathogens, and lead to increased bacterial attachment to mucosa.⁵⁰⁵

The combination of immune system alteration, biofilm regulation, and barrier disruption caused by V8 protease and the other *S. aureus* extracellular proteases highlights pathogenic mechanisms that could be implicated in CRS.

It is unlikely that the barrier disrupting activity seen in the first study is entirely a result of V8 protease. We identified similar protease activity in three *S. aureus* strains, which have shown differential effects on barrier integrity (ATCC 13565 is seemingly the most potent). V8 protease is a 29 kDa, which may have passed through the 30 kDa centrifugal filters placing it in the 3-30 kDa fraction or extended across both fractions. V8 protease undergoes autodigestion when heated to temperatures between 40 – 65°C, and other *S. aureus* glutamyl endopeptidases lose activity when heated above 55°C.^{538,539} Whereas the first study identified that heating to 100°C was necessary to diminish barrier disruption. Additionally, V8 protease is a highly conserved *S. aureus* protein and was not associated with *S. aureus* EVs in previous studies.^{423,424} There are no known inhibitors for V8 protease, hence this cannot be exploited to remove V8 activity from the crude supernatant. However, neutralizing antibodies are produced *in-vivo* and could be used in future work to isolate V8 activity from the remaining *S. aureus* supernatant.⁵³⁵

The third study has revealed an important contribution to understanding the mucosal barrier integrity in CRS. Initially the gene expression of several zinc transporters was evaluated in tissue samples from control, CRSsNP, and CRSwNP patients. We found that zinc transporters were differentially expressed between CRSsNP and CRSwNP. This suggested that zinc homeostasis was indeed altered in CRS, however the complexities of zinc transporter functions in setting are still unknown. Future research will therefore expand this investigation to assess the protein expression and functional consequences of individual transporters.

Utilisation of an intracellular zinc fluorophore and TMA allowed us to examine mucosal zinc concentrations in a cohort of control, CRSsNP, and CRSwNP patients, and combine this with ZO-1 immunofluorescence. We reported that labile zinc and apically located ZO-1 were both significantly reduced in the mucosa of CRSwNP. ZO-1 is one of the most commonly studied TJ proteins in the CRS literature,^{20,193,197,198} with results consistent with our own. Other studies have found that zinc levels are reduced in nasal polyp specimens, however this is the first to demonstrate this is localised to the epithelial layer. Additionally, the reduction in ZO-1 showed a significant correlation with mucosal zinc deficiency. Serum zinc levels were normal in the CRS cohort, suggesting that zinc deficiency is a local phenomenon. Furthermore, we confirmed that zinc is necessary for formation and function of TJs in HNEC-ALI cultures. It is unknown exactly how zinc supports barrier function, however the gastrointestinal literature suggests it may increase TJ phosphorylation, increase TJ protein expression, and simultaneously increase MT and reduce ZnT levels.²⁸⁰⁻²⁸² The etiological factors in CRS local zinc deficiency is unknown. Interestingly, the *S. aureus* zinc acquisition systems were only recently discovered.⁵⁴⁰ Perhaps future work will elucidate the effects of Th1 and Th2 inflammatory responses, and the role of *S. aureus* in mucosal zinc deficiency.

The pathogenesis of CRS is complex and multifactorial, embracing a range of host, environment, and microbial factors. This thesis has provided novel insights into the role of the mucosal barrier in CRS. Firstly, we have identified *S. aureus* secreted factors that may have implications in mucosal barrier dysfunction. We have isolated a particularly potent barrier disrupting product using ultracentrifugation, implying that it may be incorporated into a *S. aureus* EV. Additionally, our work has demonstrated the role of zinc in CRS mucosal barrier integrity. With further investigation there is potential to elucidate the EV-associated proteins of *S. aureus*, with an aim to identify the causative

barrier disrupting product. Perhaps continued research will clarify the role of *S. aureus* V8 protease and EVs in the clinical setting of CRS. Optimistically, an improvement of the understanding of contributors to mucosal barrier disruption could result in targeted therapeutic options for CRS sufferers.

References

1. Fokkens WJ, Lund VJ, Mullol J, et al. European position paper on rhinosinusitis and nasal polyps 2012. *Rhinol Suppl.* 2012;(23):3 p preceding table of contents, 1-298.
2. Bachert C, Akdis CA. Phenotypes and Emerging Endotypes of Chronic Rhinosinusitis. *J Allergy Clin Immunol Pract.* 2016;4(4):621-628. doi:10.1016/j.jaip.2016.05.004
3. Akdis CA, Bachert C, Cingi C, et al. Endotypes and phenotypes of chronic rhinosinusitis: A PRACTALL document of the European Academy of Allergy and Clinical Immunology and the American Academy of Allergy, Asthma & Immunology. *J Allergy Clin Immunol.* 2013;131(6):1479-1490. doi:10.1016/j.jaci.2013.02.036
4. Australian Bureau of Statistics. Australian Health Survey: First results, 2011-12. Cat. no. 4364.0.55.001. <http://www.abs.gov.au/AUSSTATS/abs@.nsf/DetailsPage/4364.0.55.0012011-12?OpenDocument>. Published 2012. Accessed February 3, 2017.
5. Britt H, Miller C, Henderson B, et al. General Practice Activity in Australia 1998-99 to 2007-08: 10 Year Data Tables. Australian Institute of Health and Welfare; 2008.
6. Ferreira DS, Kaushik S, Dharmage S, Thompson B, Benke G, Abramson MJ. Rhinitis and chronic rhinosinusitis in Melbourne, Australia. *Eur Respir J.* 2015;46(suppl 59). doi:10.1183/13993003.congress-2015.PA1141
7. Hastan D, Fokkens WJ, Bachert C, et al. Chronic rhinosinusitis in Europe - an underestimated disease. A GA2LEN study: Chronic rhinosinusitis in Europe. *Allergy.* 2011;66(9):1216-1223. doi:10.1111/j.1398-9995.2011.02646.x
8. Hedman J, Kaprio J, Poussa T, Nieminen MM. Prevalence of asthma, aspirin intolerance, nasal polyposis and chronic obstructive pulmonary disease in a population-based study. *Int J Epidemiol.* 1999;28(4):717-722.
9. Klossek J, Neukirch F, Pribil C, et al. Prevalence of nasal polyposis in France: a cross-sectional, case-control study. *Allergy.* 2005;60(2):233-237. doi:10.1111/j.1398-9995.2005.00688.x
10. Johansson L, Akerlund A, Melén I, Holmberg K, Bende M. Prevalence of nasal polyps in adults: the Skovde population-based study. *Ann Otol Rhinol Laryngol.* 2003;112(7):625-629.
11. We J, Lee WH, Tan KL, et al. Prevalence of nasal polyps and its risk factors: Korean National Health and Nutrition Examination Survey 2009-2011. *Am J Rhinol Allergy.* 2015;29(1):e24-e28.
12. Bhattacharyya N. Clinical and Symptom Criteria for the Accurate Diagnosis of Chronic Rhinosinusitis. *The Laryngoscope.* 2006;116(S110):1-22. doi:10.1097/01.mlg.0000224508.59725.19
13. Smith TL, Mendolia-Loffredo S, Loehrl TA, Sparapani R, Laud PW, Nattinger AB. Predictive Factors and Outcomes in Endoscopic Sinus Surgery for Chronic Rhinosinusitis: The Laryngoscope. 2005;115(12):2199-2205. doi:10.1097/01.mlg.0000182825.82910.80

14. Smith KA, Orlandi RR, Rudmik L. Cost of adult chronic rhinosinusitis: A systematic review: Cost of Adult Chronic Rhinosinusitis. *The Laryngoscope*. 2015;125(7):1547-1556. doi:10.1002/lary.25180
15. Rudmik L, Smith TL, Schlosser RJ, Hwang PH, Mace JC, Soler ZM. Productivity costs in patients with refractory chronic rhinosinusitis: Productivity Costs in Patients with Refractory CRS. *The Laryngoscope*. 2014;124(9):2007-2012. doi:10.1002/lary.24630
16. Caulley L, Thavorn K, Rudmik L, Cameron C, Kilty SJ. Direct costs of adult chronic rhinosinusitis by using 4 methods of estimation: Results of the US Medical Expenditure Panel Survey. *J Allergy Clin Immunol*. 2015;136(6):1517-1522. doi:10.1016/j.jaci.2015.08.037
17. Ooi EH, Psaltis AJ, Witterick IJ, Wormald P-J. Innate Immunity. *Otolaryngol Clin North Am*. 2010;43(3):473-487. doi:10.1016/j.otc.2010.02.020
18. Hariri BM, Cohen NA. New insights into upper airway innate immunity. *Am J Rhinol Allergy*. 2016;30(5):319.
19. Malik Z, Roscioli E, Murphy J, et al. Staphylococcus aureus impairs the airway epithelial barrier in vitro: S. aureus impairs airway epithelial barrier. *Int Forum Allergy Rhinol*. 2015;5(6):551-556. doi:10.1002/alr.21517
20. Soyka MB, Wawrzyniak P, Eiwegger T, et al. Defective epithelial barrier in chronic rhinosinusitis: The regulation of tight junctions by IFN- γ and IL-4. *J Allergy Clin Immunol*. 2012;130(5):1087-1096.e10. doi:10.1016/j.jaci.2012.05.052
21. Cohen NA. Sinonasal mucociliary clearance in health and disease. *Ann Otol Rhinol Laryngol*. 2006;115(9_suppl):20-26.
22. Ferguson JL, McCaffrey TV, Kern EB, Martin WJ. The effects of sinus bacteria on human ciliated nasal epithelium in vitro. *Otolaryngol Neck Surg*. 1988;98(4):299-304.
23. Yun Y-S, Min Y-G, Rhee C-S, et al. Effects of alpha-toxin of Staphylococcus aureus on the ciliary activity and ultrastructure of human nasal ciliated epithelial cells. *The Laryngoscope*. 1999;109(12):2021-2024.
24. Min Y-G, Jun Oh S, Won T-B, et al. Effects of staphylococcal enterotoxin on ciliary activity and histology of the sinus mucosa. *Acta Otolaryngol (Stockh)*. 2006;126(9):941-947. doi:10.1080/00016480500469016
25. Chen B, Shaari J, Claire SE, et al. Altered sinonasal ciliary dynamics in chronic rhinosinusitis. *Am J Rhinol*. 2006;20(3).
26. Chen B, Antunes MB, Palmer JN, Chiu AG, Kennedy DW, Cohen NA. Reversal of chronic rhinosinusitis-associated sinonasal ciliary dysfunction. *Am J Rhinol*. 2007;21(3):346-353.
27. Zhang Q, Wang C-S, Han D-M, et al. Differential expression of Toll-like receptor pathway genes in chronic rhinosinusitis with or without nasal polyps. *Acta Otolaryngol (Stockh)*. 2013;133(2):165-173. doi:10.3109/00016489.2012.717713
28. Rudack C, Steinhoff M, Mooren F, et al. PAR-2 activation regulates IL-8 and GRO- α synthesis by NF- κ B, but not RANTES, IL-6, eotaxin or TARC

- expression in nasal epithelium. *Clin Exp Allergy*. 2007;37(7):1009-1022. doi:10.1111/j.1365-2222.2007.02686.x
29. Lee RJ, Cohen NA. Bitter and sweet taste receptors in the respiratory epithelium in health and disease. *J Mol Med*. 2014;92(12):1235-1244. doi:10.1007/s00109-014-1222-6
 30. Adappa ND, Zhang Z, Palmer JN, et al. The bitter taste receptor T2R38 is an independent risk factor for chronic rhinosinusitis requiring sinus surgery: T2R38: independent factor for rhinosinusitis. *Int Forum Allergy Rhinol*. 2014;4(1):3-7. doi:10.1002/alr.21253
 31. Licona-Limón P, Kim LK, Palm NW, Flavell RA. TH2, allergy and group 2 innate lymphoid cells. *Nat Immunol*. 2013;14(6):536-542. doi:10.1038/ni.2617
 32. Mjösberg JM, Trifari S, Crellin NK, et al. Human IL-25- and IL-33-responsive type 2 innate lymphoid cells are defined by expression of CCR4 and CD161. *Nat Immunol*. 2011;12(11):1055-1062. doi:10.1038/ni.2104
 33. Miljkovic D, Bassiouni A, Cooksley C, et al. Association between Group 2 Innate Lymphoid Cells enrichment, nasal polyps and allergy in Chronic Rhinosinusitis. *Allergy*. 2014;69(9):1154-1161. doi:10.1111/all.12440
 34. Ho J, Bailey M, Zaunders J, et al. Group 2 innate lymphoid cells (ILC2s) are increased in chronic rhinosinusitis with nasal polyps or eosinophilia. *Clin Exp Allergy*. 2015;45(2):394-403. doi:10.1111/cea.12462
 35. Lee H-M, Kang HJ, Woo J-S, Chae SW, Lee SH, Hwang SJ. Upregulation of Surfactant Protein A in Chronic Rhinosinusitis: The Laryngoscope. 2006;116(2):328-330. doi:10.1097/01.mlg.0000194223.22763.5f
 36. Kingma PS, Whitsett JA. In defense of the lung: surfactant protein A and surfactant protein D. *Curr Opin Pharmacol*. 2006;6(3):277-283. doi:10.1016/j.coph.2006.02.003
 37. Uhliarova B, Kopincova J, Adamkov M, Svec M, Calkovska A. Surfactant proteins A and D are related to severity of the disease, pathogenic bacteria and comorbidity in patients with chronic rhinosinusitis with and without nasal polyps. *Clin Otolaryngol*. 2016;41(3):249-258.
 38. Harbitz O, Jenssen AO, Smidsrød O. Lysozyme and lactoferrin in sputum from patients with chronic obstructive lung disease. *Eur J Respir Dis*. 1984;65(7):512-520.
 39. Psaltis AJ, Bruhn MA, Ooi EH, Tan LW, Wormald P-J. Nasal Mucosa Expression of Lactoferrin in Patients With Chronic Rhinosinusitis: The Laryngoscope. 2007;117(11):2030-2035. doi:10.1097/MLG.0b013e31812e01ab
 40. Schlosser RJ, Mulligan RM, Casey SE, Varela JC, Harvey RJ, Atkinson C. Alterations in gene expression of complement components in chronic rhinosinusitis. *Am J Rhinol Allergy*. 2010;24(1):21-25. doi:10.2500/ajra.2010.24.3399
 41. Seshadri S, Lin DC, Rosati M, et al. Reduced expression of antimicrobial PLUNC proteins in nasal polyp tissues of patients with chronic rhinosinusitis. *Allergy*. 2012;67(7):920-928. doi:10.1111/j.1398-9995.2012.02848.x

42. Ooi EH, Wormald P-J, Carney AS, James CL, Tan LW. Human cathelicidin antimicrobial peptide is up-regulated in the eosinophilic mucus subgroup of chronic rhinosinusitis patients. *Am J Rhinol*. 2007;21(4):395–401.
43. Lee JT, Jansen M, Yilma AN, Nguyen A, Desharnais R, Porter E. Antimicrobial lipids: Novel innate defense molecules are elevated in sinus secretions of patients with chronic rhinosinusitis. *Am J Rhinol Allergy*. 2010;24(2):99-104. doi:10.2500/ajra.2010.24.3444
44. Derycke L, Eyerich S, Van Crombruggen K, et al. Mixed T Helper Cell Signatures In Chronic Rhinosinusitis with and without Polyps. Zhang L, ed. *PLoS One*. 2014;9(6):e97581. doi:10.1371/journal.pone.0097581
45. Van Zele T, Claeys S, Gevaert P, et al. Differentiation of chronic sinus diseases by measurement of inflammatory mediators. *Allergy*. 2006;61(11):1280-1289. doi:10.1111/j.1398-9995.2006.01225.x
46. Miljkovic D, Psaltis A, Wormald P-J, Vreugde S. T regulatory and Th17 cells in chronic rhinosinusitis with polyps: Treg and Th17 cells in CRS. *Int Forum Allergy Rhinol*. 2016;6(8):826-834. doi:10.1002/alr.21742
47. Nie CQ, Bernard NJ, Schofield L, Hansen DS. CD4+ CD25+ Regulatory T Cells Suppress CD4+ T-Cell Function and Inhibit the Development of Plasmodium berghei-Specific TH1 Responses Involved in Cerebral Malaria Pathogenesis. *Infect Immun*. 2007;75(5):2275-2282. doi:10.1128/IAI.01783-06
48. Weaver CT, Hatton RD. Interplay between the TH17 and TReg cell lineages: a (co-) evolutionary perspective. *Nat Rev Immunol*. 2009;9(12):883.
49. Van Zele T, Gevaert P, Holtappels G, van Cauwenberge P, Bachert C. Local immunoglobulin production in nasal polyposis is modulated by superantigens. *Clin Exp Allergy*. 2007;37(12):1840-1847. doi:10.1111/j.1365-2222.2007.02838.x
50. Nirula A, Glaser SM, Kalled SL, Taylor FR. What is IgG4? A review of the biology of a unique immunoglobulin subtype: *Curr Opin Rheumatol*. 2011;23(1):119-124. doi:10.1097/BOR.0b013e3283412fd4
51. Kato A, Peters A, Suh L, et al. Evidence of a role for B cell-activating factor of the TNF family in the pathogenesis of chronic rhinosinusitis with nasal polyps. *J Allergy Clin Immunol*. 2008;121(6):1385-1392.e2. doi:10.1016/j.jaci.2008.03.002
52. Patadia M, Dixon J, Conley D, et al. Evaluation of the presence of B-cell attractant chemokines in chronic rhinosinusitis. *Am J Rhinol Allergy*. 2010;24(1):11.
53. Tan BK, Li Q-Z, Suh L, et al. Evidence for intranasal antinuclear autoantibodies in patients with chronic rhinosinusitis with nasal polyps. *J Allergy Clin Immunol*. 2011;128(6):1198-1206.e1. doi:10.1016/j.jaci.2011.08.037
54. Yoon YH, Jin J, Kwon KR, Kim SH, Rha K-S, Kim YM. The role of B cell Activating Factor (BAFF) expression on pathogenesis of nasal polyp in chronic rhinosinusitis with nasal polyposis. *Rhinology*. 2014;52(4):390-396.
55. Psaltis AJ, Schlosser RJ, Yawn JR, Henriquez O, Mulligan JK. Characterization of B-cell subpopulations in patients with chronic rhinosinusitis: B-cell subpopulations in CRS patients. *Int Forum Allergy Rhinol*. 2013;3(8):621-629. doi:10.1002/alr.21173

56. Miljkovic D, Ou J, Kirana C, et al. Discordant frequencies of tissue-resident and circulating CD180-negative B cells in chronic rhinosinusitis: CD180 B cells in CRS. *Int Forum Allergy Rhinol.* 2017;7(6):609-614. doi:10.1002/alr.21924
57. Divanovic S, Trompette A, Atabani SF, et al. Negative regulation of Toll-like receptor 4 signaling by the Toll-like receptor homolog RPI05. *Nat Immunol.* 2005;6(6):571.
58. Lau A, Lester S, Moraitis S, et al. Tertiary lymphoid organs in recalcitrant chronic rhinosinusitis. *J Allergy Clin Immunol.* 2017;139(4):1371-1373. e6.
59. Neyt K, Perros F, GeurtsvanKessel CH, Hammad H, Lambrecht BN. Tertiary lymphoid organs in infection and autoimmunity. *Trends Immunol.* 2012;33(6):297-305. doi:10.1016/j.it.2012.04.006
60. Ponikau JU, Sherris DA, Kern EB, et al. The diagnosis and incidence of allergic fungal sinusitis. In: *Mayo Clinic Proceedings.* Vol 74. Elsevier; 1999:877-884.
61. Ponikau JU, Sherris DA, Kephart GM, et al. Striking deposition of toxic eosinophil major basic protein in mucus: Implications for chronic rhinosinusitis. *J Allergy Clin Immunol.* 2005;116(2):362-369. doi:10.1016/j.jaci.2005.03.049
62. Jiang R-S, Su M-C, Lin J-F. Nasal mycology of chronic rhinosinusitis. *Am J Rhinol.* 2005;19(2):131-133.
63. Braun H, Buzina W, Freudenschuss K, Beham A, Stammberger H. 'Eosinophilic fungal rhinosinusitis': a common disorder in Europe? *The Laryngoscope.* 2003;113(2):264-269.
64. Ebbens F, Scadding G, Badia L, et al. Amphotericin B nasal lavages: Not a solution for patients with chronic rhinosinusitis. *J Allergy Clin Immunol.* 2006;118(5):1149-1156. doi:10.1016/j.jaci.2006.07.058
65. Kennedy DW, Kuhn FA, Hamilos DL, et al. Treatment of Chronic Rhinosinusitis with High-Dose Oral Terbinafine: A Double Blind, Placebo-Controlled Study: *The Laryngoscope.* 2005;115(10):1793-1799. doi:10.1097/01.mlg.0000175683.81260.26
66. Douglas R, Bruhn M, Tan L-W, Ooi E, Psaltis A, Wormald P-J. Response of Peripheral Blood Lymphocytes to Fungal Extracts and Staphylococcal Superantigen B in Chronic Rhinosinusitis: *The Laryngoscope.* 2007;117(3):411-414. doi:10.1097/MLG.0b013e31802c0707
67. Li H, Llera A, Malchiodi EL, Mariuzza RA. The structural basis of T cell activation by superantigens. *Annu Rev Immunol.* 1999;17(1):435-466.
68. Bachert C, Gevaert P, Holtappels G, Johansson SGO, van Cauwenberge P. Total and specific IgE in nasal polyps is related to local eosinophilic inflammation. *J Allergy Clin Immunol.* 2001;107(4):607-614. doi:10.1067/mai.2001.112374
69. Bernstein JM, Ballou M, Schlievert PM, Rich G, Allen C, Dryja D. A superantigen hypothesis for the pathogenesis of chronic hyperplastic sinusitis with massive nasal polyposis. *Am J Rhinol.* 2003;17(6):321-326.
70. Van Zele T, Vanechoutte M, Holtappels G, Gevaert P, Van Cauwenberge P, Bachert C. Detection of enterotoxin DNA in *Staphylococcus aureus* strains obtained from the middle meatus in controls and nasal polyp patients. *Am J Rhinol.* 2008;22(3):223-227.

71. Gevaert P, Holtappels G, Johansson SGO, Cuvelier C, Cauwenberge P, Bachert C. Organization of secondary lymphoid tissue and local IgE formation to *Staphylococcus aureus* enterotoxins in nasal polyp tissue. *Allergy*. 2005;60(1):71-79. doi:10.1111/j.1398-9995.2004.00621.x
72. Pieringer H, Parzer I, Wöhrer A, Reis P, Oppl B, Zwerina J. IgG4-related disease: an orphan disease with many faces. *Orphanet J Rare Dis*. 2014;9(1):110.
73. Lee JT, Frank DN, Ramakrishnan V. Microbiome of the paranasal sinuses: update and literature review. *Am J Rhinol Allergy*. 2016;30(1):3-16.
74. Bäckhed F, Fraser CM, Ringel Y, et al. Defining a Healthy Human Gut Microbiome: Current Concepts, Future Directions, and Clinical Applications. *Cell Host Microbe*. 2012;12(5):611-622. doi:10.1016/j.chom.2012.10.012
75. Ianiro G, Bibbò S, Scaldaferrri F, Gasbarrini A, Cammarota G. Fecal Microbiota Transplantation in Inflammatory Bowel Disease: Beyond the Excitement. *Medicine (Baltimore)*. 2014;93(19):e97. doi:10.1097/MD.0000000000000097
76. Cleland EJ, Drilling A, Bassiouni A, James C, Vreugde S, Wormald P-J. Probiotic manipulation of the chronic rhinosinusitis microbiome: Probiotic manipulation of the CRS microbiome. *Int Forum Allergy Rhinol*. 2014;4(4):309-314. doi:10.1002/alr.21279
77. Cleland EJ, Bassiouni A, Vreugde S, Wormald P-J. The bacterial microbiome in chronic rhinosinusitis: richness, diversity, postoperative changes, and patient outcomes. *Am J Rhinol Allergy*. 2016;30(1):37-43.
78. Aurora R, Chatterjee D, Hentzleman J, Prasad G, Sindwani R, Sanford T. Contrasting the Microbiomes From Healthy Volunteers and Patients With Chronic Rhinosinusitis. *JAMA Otolaryngol Neck Surg*. 2013;139(12):1328. doi:10.1001/jamaoto.2013.5465
79. Cleland EJ, Bassiouni A, Boase S, Dowd S, Vreugde S, Wormald P-J. The fungal microbiome in chronic rhinosinusitis: richness, diversity, postoperative changes and patient outcomes: Fungal microbiome in CRS. *Int Forum Allergy Rhinol*. 2014;4(4):259-265. doi:10.1002/alr.21297
80. Wylie KM, Mihindukulasuriya KA, Zhou Y, Sodergren E, Storch GA, Weinstock GM. Metagenomic analysis of double-stranded DNA viruses in healthy adults. *BMC Biol*. 2014;12(1):71.
81. Costerton JW. Bacterial Biofilms: A Common Cause of Persistent Infections. *Science*. 1999;284(5418):1318-1322. doi:10.1126/science.284.5418.1318
82. Ha KR, Psaltis AJ, Butcher AR, Wormald P-J, Tan LW. In Vitro Activity of Mupirocin on Clinical Isolates of *Staphylococcus aureus* and its Potential Implications in Chronic Rhinosinusitis. *The Laryngoscope*. 2008;118(3):535-540. doi:10.1097/MLG.0b013e31815bf2e3
83. Cryer J, Schipor I, Perloff JR, Palmer JN. Evidence of Bacterial Biofilms in Human Chronic Sinusitis. *ORL*. 2004;66(3):155-158. doi:10.1159/000079994
84. Sanclement JA, Webster P, Thomas J, Ramadan HH. Bacterial Biofilms in Surgical Specimens of Patients with Chronic Rhinosinusitis. *The Laryngoscope*. 2005;115(4):578-582. doi:10.1097/01.mlg.0000161346.30752.18
85. Bendouah Z, Barbeau J, Hamad W, Desrosiers M. Biofilm formation by *Staphylococcus aureus* and *Pseudomonas aeruginosa* is associated with an

- unfavorable evolution after surgery for chronic sinusitis and nasal polyposis. *Otolaryngol Head Neck Surg.* 2006;134(6):991-996. doi:10.1016/j.otohns.2006.03.001
86. Psaltis AJ, Ha KR, Beule AG, Tan LW, Wormald P-J. Confocal Scanning Laser Microscopy Evidence of Biofilms in Patients With Chronic Rhinosinusitis: The Laryngoscope. 2007;117(7):1302-1306. doi:10.1097/MLG.0b013e31806009b0
 87. Healy D, Leid J, Sanderson A, Hunsaker D. Biofilms with fungi in chronic rhinosinusitis. *Otolaryngol Head Neck Surg.* 2008;138(5):641-647. doi:10.1016/j.otohns.2008.02.002
 88. Foreman A, Psaltis AJ, Tan LW, Wormald P-J. Characterization of bacterial and fungal biofilms in chronic rhinosinusitis. *Am J Rhinol Allergy.* 2009;23(6):556-561.
 89. Boase S, Jervis-Bardy J, Cleland E, Pant H, Tan L, Wormald P-J. Bacterial-induced epithelial damage promotes fungal biofilm formation in a sheep model of sinusitis: Induced epithelial injury promotes fungal biofilm. *Int Forum Allergy Rhinol.* 2013;3(5):341-348. doi:10.1002/alr.21138
 90. Zhang Z, Han D, Zhang S, et al. Biofilms and mucosal healing in postsurgical patients with chronic rhinosinusitis. *Am J Rhinol Allergy.* 2009;23(5):506-511.
 91. Singhal D, Psaltis AJ, Foreman A, Wormald P-J. The impact of biofilms on outcomes after endoscopic sinus surgery. *Am J Rhinol Allergy.* 2010;24(3):169-174.
 92. Psaltis AJ, Wormald P-J, Ha KR, Tan LW. Reduced Levels of Lactoferrin in Biofilm-Associated Chronic Rhinosinusitis: The Laryngoscope. 2008;118(5):895-901. doi:10.1097/MLG.0b013e31816381d4
 93. Foreman A, Holtappels G, Psaltis AJ, et al. Adaptive immune responses in *Staphylococcus aureus* biofilm-associated chronic rhinosinusitis: Immune responses in *S. aureus* biofilm-associated CRS. *Allergy.* 2011;66(11):1449-1456. doi:10.1111/j.1398-9995.2011.02678.x
 94. Tan NC-W, Foreman A, Jardeleza C, Douglas R, Tran H, Wormald PJ. The multiplicity of *Staphylococcus aureus* in chronic rhinosinusitis: Correlating surface biofilm and intracellular residence. *The Laryngoscope.* 2012;122(8):1655-1660. doi:10.1002/lary.23317
 95. Tan NC-W, Foreman A, Jardeleza C, Douglas R, Vreugde S, Wormald P-J. Intracellular *Staphylococcus aureus* : the Trojan horse of recalcitrant chronic rhinosinusitis?. *Int Forum Allergy Rhinol.* 2013;3(4):261-266. doi:10.1002/alr.21154
 96. Steed E, Balda MS, Matter K. Dynamics and functions of tight junctions. *Trends Cell Biol.* 2010;20(3):142-149. doi:10.1016/j.tcb.2009.12.002
 97. Shen L, Weber CR, Raleigh DR, Yu D, Turner JR. Tight Junction Pore and Leak Pathways: A Dynamic Duo. *Annu Rev Physiol.* 2011;73(1):283-309. doi:10.1146/annurev-physiol-012110-142150
 98. Weber CR. Dynamic properties of the tight junction barrier: Dynamic properties of the tight junction barrier. *Ann N Y Acad Sci.* 2012;1257(1):77-84. doi:10.1111/j.1749-6632.2012.06528.x

99. Hartsock A, Nelson WJ. Adherens and tight junctions: Structure, function and connections to the actin cytoskeleton. *Biochim Biophys Acta BBA - Biomembr.* 2008;1778(3):660-669. doi:10.1016/j.bbamem.2007.07.012
100. Chiba H, Osanai M, Murata M, Kojima T, Sawada N. Transmembrane proteins of tight junctions. *Biochim Biophys Acta BBA - Biomembr.* 2008;1778(3):588-600. doi:10.1016/j.bbamem.2007.08.017
101. Krug SM, Günzel D, Conrad MP, et al. Charge-selective claudin channels: Charge-selective claudin channels. *Ann N Y Acad Sci.* 2012;1257(1):20-28. doi:10.1111/j.1749-6632.2012.06555.x
102. Van Itallie CM. The Role of Claudins in Determining Paracellular Charge Selectivity. *Proc Am Thorac Soc.* 2004;1(1):38-41. doi:10.1513/pats.2306013
103. Van Itallie CM, Holmes J, Bridges A, et al. The density of small tight junction pores varies among cell types and is increased by expression of claudin-2. *J Cell Sci.* 2008;121(3):298-305. doi:10.1242/jcs.021485
104. González-Mariscal L, Garay E, Quirós M. Regulation of claudins by posttranslational modifications and cell-signaling cascades. In: *Current Topics in Membranes.* Vol 65. Elsevier; 2010:113-150.
105. Furuse M, Hirase T, Itoh M, Nagafuchi A, Yonemura S, Tsukita S. Occludin: a novel integral membrane protein localizing at tight junctions. *J Cell Biol.* 1993;123(6):1777-1788.
106. Cording J, Berg J, Kading N, et al. In tight junctions, claudins regulate the interactions between occludin, tricellulin and marvelD3, which, inversely, modulate claudin oligomerization. *J Cell Sci.* 2013;126(2):554-564. doi:10.1242/jcs.114306
107. Ikenouchi J, Sasaki H, Tsukita S, Furuse M, Tsukita S. Loss of Occludin Affects Tricellular Localization of Tricellulin. *Mol Biol Cell.* 2008;19(11):4687-4693. doi:10.1091/mbc.E08-05-0530
108. Sakakibara A, Furuse M, Saitou M, Ando-Akatsuka Y, Tsukita S. Possible involvement of phosphorylation of occludin in tight junction formation. *J Cell Biol.* 1997;137(6):1393-1401.
109. Chen Y-H, Lu Q, Goodenough DA, Jeanson B. Nonreceptor tyrosine kinase c-Yes interacts with occludin during tight junction formation in canine kidney epithelial cells. *Mol Biol Cell.* 2002;13(4):1227-1237.
110. Wong V, Gumbiner BM. A Synthetic Peptide Corresponding to the Extracellular Domain of Occludin Perturbs the Tight Junction Permeability Barrier. *J Cell Biol.* 1997;136(2):399-409. doi:10.1083/jcb.136.2.399
111. Schulzke JD, Gitter AH, Mankertz J, et al. Epithelial transport and barrier function in occludin-deficient mice. *Biochim Biophys Acta BBA-Biomembr.* 2005;1669(1):34-42.
112. Raleigh DR, Marchiando AM, Zhang Y, et al. Tight Junction-associated MARVEL Proteins MarvelD3, Tricellulin, and Occludin Have Distinct but Overlapping Functions. *Mol Biol Cell.* 2010;21(7):1200-1213. doi:10.1091/mbc.E09-08-0734

113. Steed E, Rodrigues NT, Balda MS, Matter K. Identification of MarvelD3 as a tight junction-associated transmembrane protein of the occludin family. *BMC Cell Biol.* 2009;10(1):95. doi:10.1186/1471-2121-10-95
114. Higashi T, Miller AL. Tricellular junctions: how to build junctions at the TRICKiest points of epithelial cells. Bement W, ed. *Mol Biol Cell.* 2017;28(15):2023-2034. doi:10.1091/mbc.E16-10-0697
115. Ikenouchi J. Tricellulin constitutes a novel barrier at tricellular contacts of epithelial cells. *J Cell Biol.* 2005;171(6):939-945. doi:10.1083/jcb.200510043
116. Schuetz A, Radusheva V, Krug SM, Heinemann U. Crystal structure of the tricellulin C-terminal coiled-coil domain reveals a unique mode of dimerization: Crystal structure of the coiled-coil domain of human tricellulin. *Ann N Y Acad Sci.* 2017;1405(1):147-159. doi:10.1111/nyas.13408
117. Mariano C, Sasaki H, Brites D, Brito MA. A look at tricellulin and its role in tight junction formation and maintenance. *Eur J Cell Biol.* 2011;90(10):787-796. doi:10.1016/j.ejcb.2011.06.005
118. Ohkuni T, Kojima T, Ogasawara N, et al. Expression and localization of tricellulin in human nasal epithelial cells in vivo and in vitro. *Med Mol Morphol.* 2009;42(4):204-211. doi:10.1007/s00795-009-0470-y
119. Ogasawara N, Kojima T, Go M, et al. PPAR γ agonists upregulate the barrier function of tight junctions via a PKC pathway in human nasal epithelial cells. *Pharmacol Res.* 2010;61(6):489-498. doi:10.1016/j.phrs.2010.03.002
120. Krug SM, Amasheh S, Richter JF, et al. Tricellulin Forms a Barrier to Macromolecules in Tricellular Tight Junctions without Affecting Ion Permeability. *Mol Biol Cell.* 2009;20(16):3713-3724. doi:10.1091/mbc.E09-01-0080
121. Masuda S, Oda Y, Sasaki H, et al. LSR defines cell corners for tricellular tight junction formation in epithelial cells. *J Cell Sci.* 2011;124(4):548-555. doi:10.1242/jcs.072058
122. Higashi T, Tokuda S, Kitajiri S -i., et al. Analysis of the “angulin” proteins LSR, ILDR1 and ILDR2 - tricellulin recruitment, epithelial barrier function and implication in deafness pathogenesis. *J Cell Sci.* 2013;126(16):3797-3797. doi:10.1242/jcs.138271
123. Bazzoni G. The JAM family of junctional adhesion molecules. *Curr Opin Cell Biol.* 2003;15(5):525-530.
124. Ebnet K, Suzuki A, Ohno S, Vestweber D. Junctional adhesion molecules (JAMs): more molecules with dual functions? *J Cell Sci.* 2004;117(1):19-29.
125. Hamazaki Y, Itoh M, Sasaki H, Furuse M, Tsukita S. Multi-PDZ domain protein 1 (MUPPI) is concentrated at tight junctions through its possible interaction with claudin-1 and junctional adhesion molecule. *J Biol Chem.* 2002;277(1):455-461.
126. Liu Y, Nusrat A, Schnell FJ, et al. Human junction adhesion molecule regulates tight junction resealing in epithelia. *J Cell Sci.* 2000;113(13):2363-2374.
127. Van Itallie CM, Anderson JM. Architecture of tight junctions and principles of molecular composition. *Semin Cell Dev Biol.* 2014;36:157-165. doi:10.1016/j.semcdb.2014.08.011

128. Ebnet K, Suzuki A, Horikoshi Y, et al. The cell polarity protein ASIP/PAR-3 directly associates with junctional adhesion molecule (JAM). *EMBO J.* 2001;20(14):3738-3748.
129. Iden S, Misselwitz S, Peddibhotla SS, et al. aPKC phosphorylates JAM-A at Ser285 to promote cell contact maturation and tight junction formation. *J Cell Biol.* 2012;196(5):623-639.
130. Guillemot L, Paschoud S, Pulimeno P, Foglia A, Citi S. The cytoplasmic plaque of tight junctions: A scaffolding and signalling center. *Biochim Biophys Acta BBA - Biomembr.* 2008;1778(3):601-613. doi:10.1016/j.bbamem.2007.09.032
131. Stevenson BR, Siliciano JD, Mooseker MS, Goodenough DA. Identification of ZO-1: a high molecular weight polypeptide associated with the tight junction (zonula occludens) in a variety of epithelia. *J Cell Biol.* 1986;103(3):755-766.
132. Bauer H, Zweimueller-Mayer J, Steinbacher P, Lametschwandtner A, Bauer HC. The Dual Role of Zonula Occludens (ZO) Proteins. *J Biomed Biotechnol.* 2010;2010:1-II. doi:10.1155/2010/402593
133. Rodgers LS, Beam MT, Anderson JM, Fanning AS. Epithelial barrier assembly requires coordinated activity of multiple domains of the tight junction protein ZO-1. *J Cell Sci.* 2013;126(7):1565-1575. doi:10.1242/jcs.113399
134. Itoh M, Morita K, Tsukita S. Characterization of ZO-2 as a MAGUK family member associated with tight as well as adherens junctions with a binding affinity to occludin and α catenin. *J Biol Chem.* 1999;274(9):5981-5986.
135. Itoh M, Nagafuchi A, Moroi S, Tsukita S. Involvement of ZO-1 in cadherin-based cell adhesion through its direct binding to α catenin and actin filaments. *J Cell Biol.* 1997;138(1):181-192.
136. Umeda K, Ikenouchi J, Katahira-Tayama S, et al. ZO-1 and ZO-2 Independently Determine Where Claudins Are Polymerized in Tight-Junction Strand Formation. *Cell.* 2006;126(4):741-754. doi:10.1016/j.cell.2006.06.043
137. Van Itallie CM, Fanning AS, Bridges A, Anderson JM. ZO-1 stabilizes the tight junction solute barrier through coupling to the perijunctional cytoskeleton. *Mol Biol Cell.* 2009;20(17):3930-3940.
138. Yu D, Marchiando AM, Weber CR, et al. MLCK-dependent exchange and actin binding region-dependent anchoring of ZO-1 regulate tight junction barrier function. *Proc Natl Acad Sci.* 2010;107(18):8237-8241. doi:10.1073/pnas.0908869107
139. Zolotarevsky Y, Hecht G, Koutsouris A, et al. A membrane-permeant peptide that inhibits MLC kinase restores barrier function in in vitro models of intestinal disease. *Gastroenterology.* 2002;123(1):163-172.
140. Raleigh DR, Boe DM, Yu D, et al. Occludin S408 phosphorylation regulates tight junction protein interactions and barrier function. *J Cell Biol.* 2011;193(3):565-582.
141. Hervé J-C, Derangeon M, Sarrouilhe D, Bourmeyster N. Influence of the scaffolding protein Zonula Occludens (ZOs) on membrane channels. *Biochim Biophys Acta BBA - Biomembr.* 2014;1838(2):595-604. doi:10.1016/j.bbamem.2013.07.006

142. Sakurai A, Fukuhara S, Yamagishi A, et al. MAGI-1 is required for Rap1 activation upon cell-cell contact and for enhancement of vascular endothelial cadherin-mediated cell adhesion. *Mol Biol Cell*. 2006;17(2):966-976.
143. Liew CW, Vockel M, Glassmeier G, et al. Interaction of the human somatostatin receptor 3 with the multiple PDZ domain protein MUPPI enables somatostatin to control permeability of epithelial tight junctions. *FEBS Lett*. 2009;583(1):49-54.
144. Kranjec C, Banks L. A systematic analysis of human papillomavirus (HPV) E6 PDZ substrates identifies MAGI-1 as a major target of HPV type 16 (HPV-16) and HPV-18 whose loss accompanies disruption of tight junctions. *J Virol*. 2011;85(4):1757-1764.
145. Gregorc U, Ivanova S, Thomas M, et al. Cleavage of MAGI-1, a tight junction PDZ protein, by caspases is an important step for cell-cell detachment in apoptosis. *Apoptosis*. 2007;12(2):343-354.
146. Cordenonsi M, D'atri F, Hammar E, et al. Cingulin contains globular and coiled-coil domains and interacts with ZO-1, ZO-2, ZO-3, and myosin. *J Cell Biol*. 1999;147(7):1569-1582.
147. Citi S, Pulimeno P, Paschoud S. Cingulin, paracingulin, and PLEKHA7: signaling and cytoskeletal adaptors at the apical junctional complex: Cingulin, paracingulin, and PLEKHA7. *Ann N Y Acad Sci*. 2012;1257(1):125-132. doi:10.1111/j.1749-6632.2012.06506.x
148. Meng W, Takeichi M. Adherens Junction: Molecular Architecture and Regulation. *Cold Spring Harb Perspect Biol*. 2009;1(6):a002899-a002899. doi:10.1101/cshperspect.a002899
149. Niessen CM, Gottardi CJ. Molecular components of the adherens junction. *Biochim Biophys Acta BBA - Biomembr*. 2008;1778(3):562-571. doi:10.1016/j.bbamem.2007.12.015
150. Pokutta S, Herrenknecht K, Kemler R, ENGEL J. Conformational changes of the recombinant extracellular domain of E-cadherin upon calcium binding. *FEBS J*. 1994;223(3):1019-1026.
151. Niessen CM, Gumbiner BM. The juxtamembrane region of the cadherin cytoplasmic tail supports lateral clustering, adhesive strengthening, and interaction with p120ctn. *J Cell Biol*. 1998;141(3):779-789.
152. Noren NK, Liu BP, Burrige K, Kreft B. p120 catenin regulates the actin cytoskeleton via Rho family GTPases. *J Cell Biol*. 2000;150(3):567-580.
153. Huber AH, Stewart DB, Laurents DV, Nelson WJ, Weis WI. The Cadherin Cytoplasmic Domain Is Unstructured in the Absence of β -Catenin: a possible mechanism for regulating cadherin turnover. *J Biol Chem*. 2001;276(15):12301-12309.
154. Lickert H, Bauer A, Kemler R, Stappert J. Casein kinase II phosphorylation of E-cadherin increases E-cadherin/ β -catenin interaction and strengthens cell-cell adhesion. *J Biol Chem*. 2000;275(7):5090-5095.
155. Delva E, Kowalczyk AP. Regulation of cadherin trafficking. *Traffic*. 2009;10(3):259-267.

156. Harris TJC, Tepass U. Adherens junctions: from molecules to morphogenesis. *Nat Rev Mol Cell Biol.* 2010;11(7):502-514. doi:10.1038/nrm2927
157. Desai R, Sarpal R, Ishiyama N, Pellikka M, Ikura M, Tepass U. Monomeric α -catenin links cadherin to the actin cytoskeleton. *Nat Cell Biol.* 2013;15(3):261.
158. Takai Y, Irie K, Shimizu K, Sakisaka T, Ikeda W. Nectins and nectin-like molecules: Roles in cell adhesion, migration, and polarization. *Cancer Sci.* 2003;94(8):655-667. doi:10.1111/j.1349-7006.2003.tb01499.x
159. Fukuhara A, Irie K, Yamada A, et al. Role of nectin in organization of tight junctions in epithelial cells. *Genes Cells.* 2002;7(10):1059-1072.
160. Fukuhara A, Irie K, Nakanishi H, et al. Involvement of nectin in the localization of junctional adhesion molecule at tight junctions. *Oncogene.* 2002;21(50):7642.
161. Takai Y. Nectin and afadin: novel organizers of intercellular junctions. *J Cell Sci.* 2003;116(1):17-27. doi:10.1242/jcs.00167
162. Yokoyama S, Tachibana K, Nakanishi H, et al. α -Catenin-independent recruitment of ZO-1 to nectin-based cell-cell adhesion sites through afadin. *Mol Biol Cell.* 2001;12(6):1595-1609.
163. Ikeda W, Nakanishi H, Miyoshi J, et al. Afadin: A Key Molecule Essential for Structural Organization of Cell-Cell Junctions of Polarized Epithelia during Embryogenesis. *J Cell Biol.* 1999;146(5):1117-1132. doi:10.1083/jcb.146.5.1117
164. Zhadanov AB, Provance DW, Speer CA, et al. Absence of the tight junctional protein AF-6 disrupts epithelial cell-cell junctions and cell polarity during mouse development. *Curr Biol.* 1999;9(16):880-S2. doi:10.1016/S0960-9822(99)80392-3
165. Hervé J-C, Derangeon M. Gap-junction-mediated cell-to-cell communication. *Cell Tissue Res.* 2013;352(1):21-31. doi:10.1007/s00441-012-1485-6
166. Nicholson BJ. Gap junctions - from cell to molecule. *J Cell Sci.* 2003;116(22):4479-4481. doi:10.1242/jcs.00821
167. Hama T, Oyamada M, Dejima K, Takenaka H, Takamatsu T. Expression of gap junctional protein connexins in human nasal epithelium, and its contribution to intercellular calcium signalling. *Acta Histochem Cytochem.* 2001;33(1):23-30.
168. Dunn CA, Lampe PD. Injury-triggered Akt phosphorylation of Cx43: a ZO-1-driven molecular switch that regulates gap junction size. *J Cell Sci.* 2014;127(2):455-464. doi:10.1242/jcs.142497
169. Thévenin AF, Margraf RA, Fisher CG, Kells-Andrews RM, Falk MM. Phosphorylation regulates connexin43/ZO-1 binding and release, an important step in gap junction turnover. Yap A, ed. *Mol Biol Cell.* 2017;28(25):3595-3608. doi:10.1091/mbc.E16-07-0496
170. Ouellette Y, Ermilov LG, Sieck GC. Vascular Gap Junction Cx37 Uncoupling By Tumor Necrosis Factor Is Dependent On ZO-1. *FASEB J.* 2010;24(1 Supplement):776.3-776.3.
171. Palatinus JA, O'Quinn MP, Barker RJ, Harris BS, Jourdan J, Gourdie RG. ZO-1 determines adherens and gap junction localization at intercalated disks. *Am J Physiol-Heart Circ Physiol.* 2010;300(2):H583-H594.

172. Garrod D. Desmosomes in vivo. *Dermatol Res Pract.* 2010;2010.
173. Garrod D, Chidgey M. Desmosome structure, composition and function. *Biochim Biophys Acta BBA-Biomembr.* 2008;1778(3):572-587.
174. Nuber UA, Schäfer S, Stehr S, Rackwitz HR, Franke WW. Patterns of desmocollin synthesis in human epithelia: immunolocalization of desmocollins 1 and 3 in special epithelia and in cultured cells. *Eur J Cell Biol.* 1996;71(1):1-13.
175. Zuckerman JD, Lee WY, DelGaudio JM, et al. Pathophysiology of nasal polyposis: the role of desmosomal junctions. *Am J Rhinol.* 2008;22(6):589-597.
176. Danjo Y, Gipson IK. Actin 'purse string' filaments are anchored by E-cadherin-mediated adherens junctions at the leading edge of the epithelial wound, providing coordinated cell movement. *J Cell Sci.* 1998;111(22):3323-3332.
177. Brennan D, Hu Y, Joubert S, et al. Suprabasal Dsg2 expression in transgenic mouse skin confers a hyperproliferative and apoptosis-resistant phenotype to keratinocytes. *J Cell Sci.* 2007;120(5):758-771.
178. Zhurinsky J, Shtutman M, Ben-Ze'ev A. Plakoglobin and beta-catenin: protein interactions, regulation and biological roles. *J Cell Sci.* 2000;113(18):3127-3139.
179. Srinivasan B, Kolli AR, Esch MB, Abaci HE, Shuler ML, Hickman JJ. TEER Measurement Techniques for In Vitro Barrier Model Systems. *J Lab Autom.* 2015;20(2):107-126. doi:10.1177/2211068214561025
180. Blume L-F, Denker M, Gieseler F, Kunze T. Temperature corrected transepithelial electrical resistance (TEER) measurement to quantify rapid changes in paracellular permeability. *Pharm- Int J Pharm Sci.* 2010;65(1):19-24.
181. Sheller RA, Cuevas ME, Todd MC. Comparison of transepithelial resistance measurement techniques: Chopsticks vs. Endohm. *Biol Proced Online.* 2017;19(1). doi:10.1186/s12575-017-0053-6
182. Li H, Sheppard DN, Hug MJ. Transepithelial electrical measurements with the Ussing chamber. *J Cyst Fibros.* 2004;3:123-126. doi:10.1016/j.jcf.2004.05.026
183. Hubatsch I, Ragnarsson EGE, Artursson P. Determination of drug permeability and prediction of drug absorption in Caco-2 monolayers. *Nat Protoc.* 2007;2(9):2111-2119. doi:10.1038/nprot.2007.303
184. Lee M-K, Yoo J-W, Lin H, et al. Air-Liquid Interface Culture of Serially Passaged Human Nasal Epithelial Cell Monolayer for In Vitro Drug Transport Studies. *Drug Deliv.* 2005;12(5):305-311. doi:10.1080/10717540500177009
185. Youdim KA, Avdeef A, Abbott NJ. In vitro trans-monolayer permeability calculations: often forgotten assumptions. *Drug Discov Today.* 2003;8(21):997-1003.
186. Wook-Jin Y. Serially Passaged Human Nasal Epithelial Cell Monolayer for In Vitro Drug Transport Studies. 2003.
187. Johnson L. Applications of imaging techniques to studies of epithelial tight junctions. *Adv Drug Deliv Rev.* 2005;57(1):111-121. doi:10.1016/j.addr.2004.08.004

188. Coyne CB, Vanhook MK, Gambling TM, Carson JL, Boucher RC, Johnson LG. Regulation of airway tight junctions by proinflammatory cytokines. *Mol Biol Cell*. 2002;13(9):3218–3234.
189. Buckley AG, Looi K, Iosifidis T, et al. Visualisation of Multiple Tight Junctional Complexes in Human Airway Epithelial Cells. *Biol Proced Online*. 2018;20(1). doi:10.1186/s12575-018-0070-0
190. Shen L, Weber CR, Turner JR. The tight junction protein complex undergoes rapid and continuous molecular remodeling at steady state. *J Cell Biol*. 2008;181(4):683–695. doi:10.1083/jcb.200711165
191. Staehelin LA. Further observations on the fine structure of freeze-cleaved tight junctions. *J Cell Sci*. 1973;13(3):763–786.
192. Colegio OR, Itallie CV, Rahner C, Anderson JM. Claudin extracellular domains determine paracellular charge selectivity and resistance but not tight junction fibril architecture. *Am J Physiol-Cell Physiol*. 2003;284(6):C1346–C1354.
193. Jang Y, Kim H-G, Koo T, Chung P. Localization of ZO-1 and E-cadherin in the nasal polyp epithelium. *Eur Arch Otorhinolaryngol*. 2002;259(9):465–469.
194. Chen X, Luo X, Han M, et al. Corticosteroid Regulates Epithelial Occludin Expression in Nasal Polyps through a MKP-1-Dependent Pathway. *ORL*. 2014;76(5):248–256. doi:10.1159/000368652
195. Moosavi SM, Prabhala P, Ammit AJ. Role and regulation of MKP-1 in airway inflammation. *Respir Res*. 2017;18(1):154.
196. Rogers GA, Beste KD, Parkos CA, Nusrat A, DelGaudio JM, Wise SK. Epithelial tight junction alterations in nasal polyposis. *Int Forum Allergy Rhinol*. 2011;1(1):50–54. doi:10.1002/alr.20014
197. Meng J, Zhou P, Liu Y, et al. The Development of Nasal Polyp Disease Involves Early Nasal Mucosal Inflammation and Remodelling. Cohen NA, ed. *PLoS One*. 2013;8(12):e82373. doi:10.1371/journal.pone.0082373
198. Li Y, Wang X, Wang R, et al. The Expression of Epithelial Intercellular Junctional Proteins in the Sinonasal Tissue of Subjects with Chronic Rhinosinusitis: A Histopathologic Study. *ORL*. 2014;76(2):110–119. doi:10.1159/000362246
199. Gon Y, Maruoka S, Kishi H, et al. NDRG1 is important to maintain the integrity of airway epithelial barrier through claudin-9 expression: NDRG1 maintains epithelial barrier integrity. *Cell Biol Int*. 2017;41(7):716–725. doi:10.1002/cbin.10741
200. Nguyen K-H, Suzuki H, Wakasugi T, Hohchi N, Hashida K, Ohbuchi T. Different expressions of erbB1/2 and tight junction proteins in hypertrophic inferior turbinates and nasal polyps. *Eur Arch Otorhinolaryngol*. 2012;270(3):945–951. doi:10.1007/s00405-012-2166-5
201. Yeh T, Su M, Hsu C, Chen Y, Lee S. Epithelial Cells of Nasal Mucosa Express Functional Gap Junctions of Connexin 43. *Acta Otolaryngol (Stockh)*. 2003;123(2):314–320. doi:10.1080/0036554021000028104
202. Yeh T-H, Tsai C-H, Chen Y-S, et al. Increased Communication Among Nasal Epithelial Cells in Air-Liquid Interface Culture. *The Laryngoscope*. 2007;117(8):1439–1444. doi:10.1097/MLG.0b013e318063e84f

203. Yeh T-H, Hsu W-C, Chen Y-S, Hsu C-J, Lee S-Y. Lipopolysaccharide decreases connexin 43 expression on nasal epithelial cells in vitro. *Acta Otolaryngol (Stockh)*. 2005;125(10):1091-1096. doi:10.1080/00016480510037906
204. Martin FJ, Prince AS. TLR2 Regulates Gap Junction Intercellular Communication in Airway Cells. *J Immunol*. 2008;180(7):4986-4993. doi:10.4049/jimmunol.180.7.4986
205. Yeh T-H, Hsu W-C, Chen Y-S, Hsu C-J, Lee S-Y. Decreased connexin 43 expression correlated with eosinophil infiltration in nasal polyps. *Am J Rhinol*. 2005;19(1):59-64.
206. Chanson M, Derouette J-P, Roth I, et al. Gap junctional communication in tissue inflammation and repair. *Biochim Biophys Acta BBA - Biomembr*. 2005;1711(2):197-207. doi:10.1016/j.bbamem.2004.10.005
207. BuSaba NY, Cunningham MJ. Connexin 26 and 30 Genes Mutations in Patients with Chronic Rhinosinusitis. *The Laryngoscope*. 2008;118(2):310-313. doi:10.1097/MLG.0b013e31815744b6
208. Jun AI, McGuirt WT, Hinojosa R, Green GE, Fischel-Ghodsian N, Smith RJ. Temporal bone histopathology in connexin 26-related hearing loss. *The Laryngoscope*. 2000;110(2):269-269.
209. Sedaghat AR, Cunningham MJ, Busaba NY. Connexin 32 and 43 mutations: Do they play a role in chronic rhinosinusitis? *Am J Otolaryngol*. 2014;35(1):33-36. doi:10.1016/j.amjoto.2013.08.008
210. Zheng J, Liu W, Fan Y, et al. Suppression of connexin 26 is related to protease-activated receptor 2-mediated pathway in patients with allergic rhinitis. *Am J Rhinol Allergy*. 2012;26(1):e5-e9.
211. Kim R, Chang G, Hu R, Phillips A, Douglas R. Connexin gap junction channels and chronic rhinosinusitis: Connexion gap junction channels and CRS. *Int Forum Allergy Rhinol*. 2016;6(6):611-617. doi:10.1002/alr.21717
212. Apuhan T, Gepdiremen S, Arslan AO, Aktas G. Evaluation of patients with nasal polyps about the possible association of desmosomal junctions, RORA and PDE4D gene. *Eur Rev Med Pharmacol Sci*. 2013;17(19):2680-2683.
213. Shahana S, Jaunmuktane Z, Stenkvist Asplund M, Roomans GM. Ultrastructural investigation of epithelial damage in asthmatic and non-asthmatic nasal polyps. *Respir Med*. 2006;100(11):2018-2028. doi:10.1016/j.rmed.2006.02.012
214. Ota Y, Ishikawa F, Sato T, et al. A case of refractory chronic rhinosinusitis with anti-desmoglein 3 IgG4 autoantibody. *Allergol Int*. 2017;66(4):634-636. doi:10.1016/j.alit.2017.04.009
215. Pearson AD, Eastham EJ, Laker MF, Craft AW, Nelson R. Intestinal permeability in children with Crohn's disease and coeliac disease. *Br Med J Clin Res Ed*. 1982;285(6334):20-21.
216. Bouma G, Strober W. The immunological and genetic basis of inflammatory bowel disease. *Nat Rev Immunol*. 2003;3(7):521.
217. Olson TS, Reuter BK, Scott KG-E, et al. The primary defect in experimental ileitis originates from a nonhematopoietic source. *J Exp Med*. 2006;203(3):541-552. doi:10.1084/jem.20050407

218. Peeters M, Geypens B, Claus D, et al. Clustering of increased small intestinal permeability in families with Crohn's disease. *Gastroenterology*. 1997;113(3):802–807.
219. Irvine EJ, Marshall JK. Increased intestinal permeability precedes the onset of Crohn's disease in a subject with familial risk. *Gastroenterology*. 2000;119(6):1740-1744. doi:10.1053/gast.2000.20231
220. Wyatt J, Vogelsang H, Hübl W, Waldhoer T, Lochs H. Intestinal permeability and the prediction of relapse in Crohn's disease. *The Lancet*. 1993;341(8858):1437–1439.
221. Schulzke JD, Ploeger S, Amasheh M, et al. Epithelial Tight Junctions in Intestinal Inflammation. *Ann N Y Acad Sci*. 2009;1165(1):294-300. doi:10.1111/j.1749-6632.2009.04062.x
222. Ma TY, Iwamoto GK, Hoa NT, et al. TNF- α -induced increase in intestinal epithelial tight junction permeability requires NF- κ B activation. *Am J Physiol-Gastrointest Liver Physiol*. 2004;286(3):G367-G376. doi:10.1152/ajpgi.00173.2003
223. Suenart P, Bulteel V, Lemmens L, et al. Anti-tumor necrosis factor treatment restores the gut barrier in Crohn's disease. *Am J Gastroenterol*. 2002;97(8):2000.
224. Heller F, Florian P, Bojarski C, et al. Interleukin-13 Is the Key Effector Th2 Cytokine in Ulcerative Colitis That Affects Epithelial Tight Junctions, Apoptosis, and Cell Restitution. *Gastroenterology*. 2005;129(2):550-564. doi:10.1053/j.gastro.2005.05.002
225. Tilg H, Kaser A. Failure of interleukin 13 blockade in ulcerative colitis. *Gut*. 2015;(0):1-2. doi:10.1136/gutjnl-2015-309464
226. Sellon RK, Tonkonogy S, Schultz M, et al. Resident Enteric Bacteria Are Necessary for Development of Spontaneous Colitis and Immune System Activation in Interleukin-10-Deficient Mice. *Infect Immun*. 1998;66(11):5224-5231.
227. Solomon L, Mansor S, Mallon P, et al. The dextran sulphate sodium (DSS) model of colitis: an overview. *Comp Clin Pathol*. 2010;19(3):235-239. doi:10.1007/s00580-010-0979-4
228. Fazio LD. Longitudinal analysis of inflammation and microbiota dynamics in a model of mild chronic dextran sulfate sodium-induced colitis in mice. *World J Gastroenterol*. 2014;20(8):2051. doi:10.3748/wjg.v20.i8.2051
229. Munyaka PM, Rabbi MF, Khafipour E, Ghia J-E. Acute dextran sulfate sodium (DSS)-induced colitis promotes gut microbial dysbiosis in mice: Dextran sulfate sodium and mice gut microbiota. *J Basic Microbiol*. 2016;56(9):986-998. doi:10.1002/jobm.201500726
230. Prasad S, Mingrino R, Kaukinen K, et al. Inflammatory processes have differential effects on claudins 2, 3 and 4 in colonic epithelial cells. *Lab Invest*. 2005;85(9):1139.
231. Zeissig S, Burgel N, Gunzel D, et al. Changes in expression and distribution of claudin 2, 5 and 8 lead to discontinuous tight junctions and barrier

- dysfunction in active Crohn's disease. *Gut*. 2007;56(1):61-72.
doi:10.1136/gut.2006.094375
232. Oshima T, Miwa H, Joh T. Changes in the expression of claudins in active ulcerative colitis. *J Gastroenterol Hepatol*. 2008;23:S146-S150.
doi:10.1111/j.1440-1746.2008.05405.x
233. Oshitani N, Watanabe K, Nakamura S, Fujiwara Y, Higuchi K, Arakawa T. Dislocation of tight junction proteins without F-actin disruption in inactive Crohn's disease. *Int J Mol Med*. 2005;15(3):407-410.
234. Hollister EB, Gao C, Versalovic J. Compositional and functional features of the gastrointestinal microbiome and their effects on human health. *Gastroenterology*. 2014;146(6):1449-1458.
235. Caron TJ. Tight junction disruption: *Helicobacter pylori* and dysregulation of the gastric mucosal barrier. *World J Gastroenterol*. 2015;21(40):11411.
doi:10.3748/wjg.v21.i40.11411
236. Backert S, Schmidt TP, Harrer A, Wessler S. Exploiting the gastric epithelial barrier: *Helicobacter pylori*'s attack on tight and adherens junctions. In: *Molecular Pathogenesis and Signal Transduction by Helicobacter Pylori*. Springer; 2017:195-226.
237. Jones KR, Whitmire JM, Merrell DS. A Tale of Two Toxins: *Helicobacter Pylori* CagA and VacA Modulate Host Pathways that Impact Disease. *Front Microbiol*. 2010;1. doi:10.3389/fmicb.2010.00115
238. Hoy B, Löwer M, Weydig C, et al. *Helicobacter pylori* HtrA is a new secreted virulence factor that cleaves E-cadherin to disrupt intercellular adhesion. *EMBO Rep*. 2010;11(10):798-804. doi:10.1038/embor.2010.114
239. Hoy B, Brandstetter H, Wessler S. The stability and activity of recombinant *Helicobacter pylori* HtrA under stress conditions: The stability and activity of recombinant. *J Basic Microbiol*. 2013;53(5):402-409.
doi:10.1002/jobm.201200074
240. Olofsson A, Vallström A, Petzold K, et al. Biochemical and functional characterization of *Helicobacter pylori* vesicles: *H. pylori* vesicles and properties for adhesion. *Mol Microbiol*. 2010;77(6):1539-1555. doi:10.1111/j.1365-2958.2010.07307.x
241. Sempertegui F, Diaz M, Mejia R, et al. Low Concentrations of Zinc in Gastric Mucosa are Associated with Increased Severity of *Helicobacter pylori*-Induced Inflammation. *Helicobacter*. 2007;12(1):43-48.
242. Barreau F, Hugot J. Intestinal barrier dysfunction triggered by invasive bacteria. *Curr Opin Microbiol*. 2014;17:91-98. doi:10.1016/j.mib.2013.12.003
243. Roxas JL, Koutsouris A, Bellmeyer A, et al. Enterohemorrhagic *E. coli* alters murine intestinal epithelial tight junction protein expression and barrier function in a Shiga toxin independent manner. *Lab Invest*. 2010;90(8):1152.
244. Philpott DJ, McKay DM, Mak W, Perdue MH, Sherman PM. Signal transduction pathways involved in enterohemorrhagic *Escherichia coli*-induced alterations in T84 epithelial permeability. *Infect Immun*. 1998;66(4):1680-1687.

245. Simonovic I, Rosenberg J, Koutsouris A, Hecht G. Enteropathogenic *Escherichia coli* dephosphorylates and dissociates occludin from intestinal epithelial tight junctions. *Cell Microbiol.* 2000;2(4):305-315.
246. Ugalde-Silva P, Gonzalez-Lugo O, Navarro-Garcia F. Tight junction disruption induced by type 3 secretion system effectors injected by enteropathogenic and enterohemorrhagic *Escherichia coli*. *Front Cell Infect Microbiol.* 2016;6:87.
247. Morampudi V, Graef FA, Stahl M, et al. Tricellular tight junction protein tricellulin is targeted by the enteropathogenic *Escherichia coli* effector EspGI, leading to epithelial barrier disruption. *Infect Immun.* 2017;85(1):e00700-16.
248. Dubreuil JD. Enterotoxigenic *Escherichia coli* targeting intestinal epithelial tight junctions: An effective way to alter the barrier integrity. *Microb Pathog.* 2017;113:129-134. doi:10.1016/j.micpath.2017.10.037
249. Kreisberg RB, Harper J, Strauman MC, Marohn M, Clements JD, Nataro JP. Induction of increased permeability of polarized enterocyte monolayers by enterotoxigenic *Escherichia coli* heat-labile enterotoxin. *Am J Trop Med Hyg.* 2011;84(3):451-455.
250. Nakashima R, Kamata Y, Nishikawa Y. Effects of *Escherichia coli* heat-stable enterotoxin and guanylin on the barrier integrity of intestinal epithelial T84 cells. *Vet Immunol Immunopathol.* 2013;152(1-2):78-81. doi:10.1016/j.vetimm.2012.09.026
251. Ngendahayo Mukiza C, Dubreuil JD. *Escherichia coli* Heat-Stable Toxin b Impairs Intestinal Epithelial Barrier Function by Altering Tight Junction Proteins. Blanke SR, ed. *Infect Immun.* 2013;81(8):2819-2827. doi:10.1128/IAI.00455-13
252. Denizot J, Sivignon A, Barreau F, et al. Adherent-invasive *Escherichia coli* induce claudin-2 expression and barrier defect in CEABAC10 mice and Crohn's disease patients. *Inflamm Bowel Dis.* 2011;18(2):294-304.
253. Gibold L, Garenaux E, Dalmaso G, et al. The Vat-AIEC protease promotes crossing of the intestinal mucus layer by Crohn's disease-associated *Escherichia coli*. *Cell Microbiol.* 2016;18(5):617-631.
254. Kunsmann L, Rüter C, Bauwens A, et al. Virulence from vesicles: Novel mechanisms of host cell injury by *Escherichia coli* O104:H4 outbreak strain. *Sci Rep.* 2015;5:13252. doi:10.1038/srep13252
255. Horstman AL, Kuehn MJ. Enterotoxigenic *Escherichia coli* secretes active heat-labile enterotoxin via outer membrane vesicles. *J Biol Chem.* 2000;275(17):12489-12496.
256. Scorza FB, Doro F, Rodríguez-Ortega MJ, et al. Proteomics characterization of outer membrane vesicles from the extraintestinal pathogenic *Escherichia coli* Δ tolR IHE3034 mutant. *Mol Cell Proteomics.* 2008;7(3):473-485.
257. Cholera WHO. Fact Sheet No. 107. Geneva; 2012.
258. Wu Z, Milton D, Nybom P, Sjö A, Magnusson K-E. *Vibrio cholerae* hemagglutinin/protease (HA/protease) causes morphological changes in cultured epithelial cells and perturbs their paracellular barrier function. *Microb Pathog.* 1996;21(2):111-123.

259. Wu Z, Nybom P, Magnusson K-E. Distinct effects of *Vibrio cholerae* haemagglutinin/protease on the structure and localization of the tight junction-associated proteins occludin and ZO-1. *Cell Microbiol.* 2000;2(1):11-17.
260. Fasano A, Baudry B, Pumplun DW, et al. *Vibrio cholerae* produces a second enterotoxin, which affects intestinal tight junctions. *Proc Natl Acad Sci.* 1991;88(12):5242-5246.
261. Fasano A, Fiorentini C, Donelli G, et al. Zonula occludens toxin modulates tight junctions through protein kinase C-dependent actin reorganization, in vitro. *J Clin Invest.* 1995;96(2):710-720. doi:10.1172/JCI118114
262. Fasano A, Uzzau S, Fiore C, Margareten K. The enterotoxic effect of zonula occludens toxin on rabbit small intestine involves the paracellular pathway. *Gastroenterology.* 1997;112(3):839-846.
263. Goldblum SE, Rai U, Tripathi A, et al. The active Zot domain (aa 288-293) increases ZO-1 and myosin 1C serine/threonine phosphorylation, alters interaction between ZO-1 and its binding partners, and induces tight junction disassembly through proteinase activated receptor 2 activation. *FASEB J.* 2011;25(1):144-158. doi:10.1096/fj.10-158972
264. Hamad ARA, Marrack P, Kappler JW. Transcytosis of staphylococcal superantigen toxins. *J Exp Med.* 1997;185(8):1447-1454.
265. Danielsen EM, Hansen GH, Karlsdóttir E. *Staphylococcus aureus* enterotoxins A- and B: binding to the enterocyte brush border and uptake by perturbation of the apical endocytic membrane traffic. *Histochem Cell Biol.* 2013;139(4):513-524. doi:10.1007/s00418-012-1055-8
266. Lu J, Philpott DJ, Saunders PR, Perdue MH, Yang P-C, McKay DM. Epithelial ion transport and barrier abnormalities evoked by superantigen-activated immune cells are inhibited by interleukin-10 but not interleukin-4. *J Pharmacol Exp Ther.* 1998;287(1):128-136.
267. McKay DM, Singh PK. Superantigen activation of immune cells evokes epithelial (T84) transport and barrier abnormalities via IFN-gamma and TNF alpha: inhibition of increased permeability, but not diminished secretory responses by TGF-beta2. *J Immunol.* 1997;159(5):2382-2390.
268. Kwak Y-K, Vikstrom E, Magnusson K-E, Vecsey-Semjen B, Colque-Navarro P, Mollby R. The *Staphylococcus aureus* Alpha-Toxin Perturbs the Barrier Function in Caco-2 Epithelial Cell Monolayers by Altering Junctional Integrity. *Infect Immun.* 2012;80(5):1670-1680. doi:10.1128/IAI.00001-12
269. Song L, Hobaugh MR, Shustak C, Cheley S, Bayley H, Gouaux JE. Structure of staphylococcal α -hemolysin, a heptameric transmembrane pore. *Science.* 1996;274(5294):1859-1865.
270. Hecht G, Pothoulakis C, LaMont JT, Madara JL. *Clostridium difficile* toxin A perturbs cytoskeletal structure and tight junction permeability of cultured human intestinal epithelial monolayers. *J Clin Invest.* 1988;82(5):1516.
271. Hecht G, Koutsouris A, Pothoulakis C, LaMont JT, Madara JL. *Clostridium difficile* toxin B disrupts the barrier function of T84 monolayers. *Gastroenterology.* 1992;102(2):416-423.

272. Nusrat A, von Eichel-Streiber C, Turner JR, Verkade P, Madara JL, Parkos CA. Clostridium difficile Toxins Disrupt Epithelial Barrier Function by Altering Membrane Microdomain Localization of Tight Junction Proteins. *Infect Immun*. 2001;69(3):1329-1336. doi:10.1128/IAI.69.3.1329-1336.2001
273. Johal SS, Solomon K, Dodson S, Borriello SP, Mahida YR. Differential effects of varying concentrations of Clostridium difficile toxin A on epithelial barrier function and expression of cytokines. *J Infect Dis*. 2004;189(11):2110-2119.
274. Fukada T, Yamasaki S, Nishida K, Murakami M, Hirano T. Zinc homeostasis and signaling in health and diseases: Zinc signaling. *JBIC J Biol Inorg Chem*. 2011;16(7):1123-1134. doi:10.1007/s00775-011-0797-4
275. Roy SK, Behrens RH, Haider R, et al. Impact of zinc supplementation on intestinal permeability in Bangladeshi children with acute diarrhoea and persistent diarrhoea syndrome. *J Pediatr Gastroenterol Nutr*. 1992;15(3):289-296.
276. Rodriguez P, Darmon N, Chappuis P, et al. Intestinal paracellular permeability during malnutrition in guinea pigs: effect of high dietary zinc. *Gut*. 1996;39(3):416-422.
277. Alam AN, Sarker SA, Wahed MA, Khatun M, Rahaman MM. Enteric protein loss and intestinal permeability changes in children during acute shigellosis and after recovery: effect of zinc supplementation. *Gut*. 1994;35(12):1707-1711.
278. Kazi M, Paramita S, Sheikh I, Chakraborty S. Zinc recovers altered intestinal ion-transport and barrier function caused by Shigella infection in T84 cells (902.9). *FASEB J*. 2014;28(1 Supplement):902.9.
279. Sturniolo GC, Di Leo V, Ferronato A, D'Odorico A, D'Inca R. Zinc Supplementation Tightens "Leaky Gut" in Crohn's Disease: *Inflamm Bowel Dis*. 2001;7(2):94-98. doi:10.1097/00054725-200105000-00003
280. Finamore A, Massimi M, Devirgiliis LC, Mengheri E. Zinc deficiency induces membrane barrier damage and increases neutrophil transmigration in Caco-2 cells. *J Nutr*. 2008;138(9):1664-1670.
281. Miyoshi Y, Tanabe S, Suzuki T. Cellular zinc is required for intestinal epithelial barrier maintenance via the regulation of claudin-3 and occludin expression. *Am J Physiol-Gastrointest Liver Physiol*. 2016;311(1):G105-G116. doi:10.1152/ajpgi.00405.2015
282. Wang X, Valenzano MC, Mercado JM, Zurbach EP, Mullin JM. Zinc Supplementation Modifies Tight Junctions and Alters Barrier Function of CACO-2 Human Intestinal Epithelial Layers. *Dig Dis Sci*. 2013;58(1):77-87. doi:10.1007/s10620-012-2328-8
283. Shao Y, Wolf PG, Guo S, Guo Y, Gaskins HR, Zhang B. Zinc enhances intestinal epithelial barrier function through the PI3K/AKT/mTOR signaling pathway in Caco-2 cells. *J Nutr Biochem*. 2017;43:18-26. doi:10.1016/j.jnutbio.2017.01.013
284. Proksch E, Brandner JM, Jensen J-M. The skin: an indispensable barrier. *Exp Dermatol*. 2008;17(12):1063-1072. doi:10.1111/j.1600-0625.2008.00786.x
285. Brandner J, Zorn-Kruppa M, Yoshida T, Moll I, Beck L, De Benedetto A. Epidermal tight junctions in health and disease. *Tissue Barriers*. 2015;3(1-2):e974451. doi:10.4161/21688370.2014.974451

286. Bukowski M, Wladyka B, Dubin G. Exfoliative Toxins of *Staphylococcus aureus*. *Toxins*. 2010;2(5):1148-1165. doi:10.3390/toxins2051148
287. Amagai M, Matsuyoshi N, Wang ZH, Andl C, Stanley JR. Toxin in bullous impetigo and staphylococcal scalded-skin syndrome targets desmoglein 1. *Nat Med*. 2000;6(11):1275-1277.
288. Amagai M, Nishifuji K, Yamaguchi T, Hanakawa Y, Sugai M, Stanley JR. Staphylococcal exfoliative toxin B specifically cleaves desmoglein 1. *J Invest Dermatol*. 2002;118(5):845-850.
289. Payne AS, Hanakawa Y, Amagai M, Stanley JR. Desmosomes and disease: pemphigus and bullous impetigo. *Curr Opin Cell Biol*. 2004;16(5):536-543.
290. Bunikowski R, Mielke MEA, Skarabis H, et al. Evidence for a disease-promoting effect of *Staphylococcus aureus*-derived exotoxins in atopic dermatitis. *J Allergy Clin Immunol*. 2000;105(4):814-819. doi:10.1067/mai.2000.105528
291. Ohnemus U, Kohrmeyer K, Houdek P, et al. Regulation of epidermal tight-junctions (TJ) during infection with exfoliative toxin-negative *Staphylococcus* strains. *J Invest Dermatol*. 2008;128(4):906-916.
292. Miedzobrodzki J, Kaszycki P, Bialecka A, Kasprowicz A. Proteolytic Activity of *Staphylococcus aureus* Strains Isolated from the Colonized Skin of Patients with Acute-Phase Atopic Dermatitis. *Eur J Clin Microbiol Infect Dis*. 2002;21(4):269-276. doi:10.1007/s10096-002-0706-4
293. Hirasawa Y, Takai T, Nakamura T, et al. *Staphylococcus aureus* extracellular protease causes epidermal barrier dysfunction. *J Invest Dermatol*. 2010;130(2):614-617.
294. Cywes C, Wessels MR. Group A *Streptococcus* tissue invasion by CD44-mediated cell signalling. *Nature*. 2001;414(6864):648.
295. De Benedetto A, Rafaels NM, McGirt LY, et al. Tight junction defects in patients with atopic dermatitis. *J Allergy Clin Immunol*. 2011;127(3):773-786.e7. doi:10.1016/j.jaci.2010.10.018
296. Hata M, Tokura Y, Takigawa M, et al. Assessment of Epidermal Barrier Function by Photoacoustic Spectrometry in Relation to Its Importance in the Pathogenesis of Atopic Dermatitis. *Lab Invest*. 2002;82(11):1451-1461. doi:10.1097/01.LAB.0000036874.83540.2B
297. Junghans V, Gutgesell C, Jung T, Neumann C. Epidermal Cytokines IL-1 β , TNF- α , and IL-12 in Patients with Atopic Dermatitis: Response to Application of House Dust Mite Antigen. *J Invest Dermatol*. 1998;111(6):1184-1188.
298. Kirschner N, Poetzl C, von den Driesch P, et al. Alteration of tight junction proteins is an early event in psoriasis: putative involvement of proinflammatory cytokines. *Am J Pathol*. 2009;175(3):1095-1106.
299. Kuo I-H, Carpenter-Mendini A, Yoshida T, et al. Activation of epidermal toll-like receptor 2 enhances tight junction function: implications for atopic dermatitis and skin barrier repair. *J Invest Dermatol*. 2013;133(4):988-998.
300. El Tawdy AM, Rashed LM, Alhanafy HM. Gap junction and atopic dermatitis: a study of connexin 43 mRNA expression in atopic skin lesions. *J Egypt Women's Dermatol Soc*. 2011;8(2):78-83.

301. Perera GK, Di Meglio P, Nestle FO. Psoriasis. *Annu Rev Pathol Mech Dis.* 2012;7(1):385-422. doi:10.1146/annurev-pathol-011811-132448
302. Yoshida Y, Morita K, Mizoguchi A, Ide C, Miyachi Y. Altered expression of occludin and tight junction formation in psoriasis. *Arch Dermatol Res.* 2001;293(5):239-244.
303. Azghani AO, Gray LD, Johnson AR. A bacterial protease perturbs the paracellular barrier function of transporting epithelial monolayers in culture. *Infect Immun.* 1993;61(6):2681-2686.
304. Clark CA, Thomas LK, Azghani AO. Inhibition of Protein Kinase C Attenuates *Pseudomonas aeruginosa* Elastase-Induced Epithelial Barrier Disruption. *Am J Respir Cell Mol Biol.* 2011;45(6):1263-1271. doi:10.1165/rcmb.2010-0459OC
305. Azghani AO. *Pseudomonas aeruginosa* and epithelial permeability: role of virulence factors elastase and exotoxin A. *Am J Respir Cell Mol Biol.* 1996;15(1):132-140.
306. Soong G, Parker D, Magargee M, Prince AS. The Type III Toxins of *Pseudomonas aeruginosa* Disrupt Epithelial Barrier Function. *J Bacteriol.* 2008;190(8):2814-2821. doi:10.1128/JB.01567-07
307. Azghani AO, Connelly JC, Peterson BT, Gray LD, Collins ML, Johnson AR. Effects of *Pseudomonas aeruginosa* elastase on alveolar epithelial permeability in guinea pigs. *Infect Immun.* 1990;58(2):433-438.
308. Azghani AO, Miller EJ, Peterson BT. Virulence Factors from *Pseudomonas aeruginosa* Increase Lung Epithelial Permeability. *Lung.* 2000;178(5):261-269. doi:10.1007/s004080000031
309. McElroy MC, Harty HR, Hosford GE, Boylan GM, Pittet J-F, Foster TJ. Alpha-toxin damages the air-blood barrier of the lung in a rat model of *Staphylococcus aureus*-induced pneumonia. *Infect Immun.* 1999;67(10):5541-5544.
310. Hayashida A, Bartlett AH, Foster TJ, Park PW. *Staphylococcus aureus* Beta-Toxin Induces Lung Injury through Syndecan-1. *Am J Pathol.* 2009;174(2):509-518. doi:10.2353/ajpath.2009.080394
311. Wang Z, Li R, Tan J, et al. Syndecan-1 Acts in Synergy with Tight Junction Through Stat3 Signaling to Maintain Intestinal Mucosal Barrier and Prevent Bacterial Translocation: *Inflamm Bowel Dis.* 2015;21(8):1894-1907. doi:10.1097/MIB.0000000000000421
312. Kim JY, Sajjan US, Krasan GP, LiPuma JJ. Disruption of Tight Junctions during Traversal of the Respiratory Epithelium by *Burkholderia cenocepacia*. *Infect Immun.* 2005;73(11):7107-7112. doi:10.1128/IAI.73.11.7107-7112.2005
313. Blume C, David J, Bell R, et al. Modulation of Human Airway Barrier Functions during *Burkholderia thailandensis* and *Francisella tularensis* Infection
Running Title: Airway Barrier Functions during Bacterial Infections. *Pathogens.* 2016;5(3):53. doi:10.3390/pathogens5030053
314. Ragupathy S, Esmaeili F, Paschoud S, Sublet E, Citi S, Borchard G. Toll-like receptor 2 regulates the barrier function of human bronchial epithelial monolayers through atypical protein kinase C zeta, and an increase in

- expression of claudin-1. *Tissue Barriers*. 2014;2(2):e29166. doi:10.4161/tisb.29166
315. Martin FJ, Soong G, Prince A. Modulation of airway epithelial barrier function in response to bacterial ligands. *FASEB J*. 2006;20(4):A200-A200.
316. Pai AB, Patel H, Prokopienko AJ, et al. Lipoteichoic Acid from *Staphylococcus aureus* Induces Lung Endothelial Cell Barrier Dysfunction: Role of Reactive Oxygen and Nitrogen Species. James LR, ed. *PLoS One*. 2012;7(11):e49209. doi:10.1371/journal.pone.0049209
317. Meliton AY, Meng F, Tian Y, et al. Oxidized phospholipids protect against lung injury and endothelial barrier dysfunction caused by heat-inactivated *Staphylococcus aureus*. *Am J Physiol-Lung Cell Mol Physiol*. 2015;308(6):L550-L562. doi:10.1152/ajplung.00248.2014
318. Czikora I, Sridhar S, Gorshkov B, et al. Protective effect of Growth Hormone-Releasing Hormone agonist in bacterial toxin-induced pulmonary barrier dysfunction. *Front Physiol*. 2014;5. doi:10.3389/fphys.2014.00259
319. Bao S, Knoell DL. Zinc modulates cytokine-induced lung epithelial cell barrier permeability. *AJP Lung Cell Mol Physiol*. 2006;291(6):L1132-L1141. doi:10.1152/ajplung.00207.2006
320. Roscioli E, Jersmann H, Lester S, et al. Zinc deficiency as a codeterminant for airway epithelial barrier dysfunction in an ex vivo model of COPD. *Int J Chron Obstruct Pulmon Dis*. 2017;Volume 12:3503-3510. doi:10.2147/COPD.S149589
321. Hardyman MA, Wilkinson E, Martin E, et al. TNF- α -mediated bronchial barrier disruption and regulation by src-family kinase activation. *J Allergy Clin Immunol*. 2013;132(3):665-675.e8. doi:10.1016/j.jaci.2013.03.005
322. Parker JC, Thavagnanam S, Skibinski G, et al. Chronic IL9 and IL-13 Exposure Leads to an Altered Differentiation of Ciliated Cells in a Well-Differentiated Paediatric Bronchial Epithelial Cell Model. Semple MG, ed. *PLoS One*. 2013;8(5):e61023. doi:10.1371/journal.pone.0061023
323. Ramezanpour M, Moraitis S, Smith JLP, Wormald PJ, Vreugde S. Th17 Cytokines Disrupt the Airway Mucosal Barrier in Chronic Rhinosinusitis. *Mediators Inflamm*. 2016;2016:1-7. doi:10.1155/2016/9798206
324. Saatian B, Rezaee F, Desando S, et al. Interleukin-4 and interleukin-13 cause barrier dysfunction in human airway epithelial cells. *Tissue Barriers*. 2013;1(2):e24333. doi:10.4161/tisb.24333
325. Ohkuni T, Kojima T, Ogasawara N, et al. Poly(I:C) reduces expression of JAM-A and induces secretion of IL-8 and TNF- α via distinct NF- κ B pathways in human nasal epithelial cells. *Toxicol Appl Pharmacol*. 2011;250(1):29-38. doi:10.1016/j.taap.2010.09.023
326. Clarke TB, Francella N, Huegel A, Weiser JN. Invasive Bacterial Pathogens Exploit TLR-Mediated Downregulation of Tight Junction Components to Facilitate Translocation across the Epithelium. *Cell Host Microbe*. 2011;9(5):404-414. doi:10.1016/j.chom.2011.04.012
327. Rezaee F, Meednu N, Emo JA, et al. Polyinosinic:polycytidylic acid induces protein kinase D-dependent disassembly of apical junctions and barrier

- dysfunction in airway epithelial cells. *J Allergy Clin Immunol*. 2011;128(6):1216-1224.e11. doi:10.1016/j.jaci.2011.08.035
328. Jiao J, Wang M, Duan S, et al. Transforming growth factor- β 1 decreases epithelial tight junction integrity in chronic rhinosinusitis with nasal polyps. *J Allergy Clin Immunol*. 2017.
 329. Carrozzino F. Inducible expression of Snail selectively increases paracellular ion permeability and differentially modulates tight junction proteins. *AJP Cell Physiol*. 2005;289(4):C1002-C1014. doi:10.1152/ajpcell.00175.2005
 330. Cleland EJ, Bassiouni A, Wormald P-J. The bacteriology of chronic rhinosinusitis and the pre-eminence of *Staphylococcus aureus* in revision patients: CRS bacteriology and *S. aureus* in revision patients. *Int Forum Allergy Rhinol*. 2013;3(8):642-646. doi:10.1002/alr.21159
 331. Jervis-Bardy J, Foreman A, Field J, Wormald PJ. Impaired mucosal healing and infection associated with *Staphylococcus aureus* after endoscopic sinus surgery. *Am J Rhinol Allergy*. 2009;23(5):549-552.
 332. Steelant B, Lan F, Zhang N, et al. *Staphylococcus aureus* enterotoxin B induces airway epithelial barrier dysfunction in vitro. In: *Allergy: European Journal of Allergy and Clinical Immunology*. Vol 70. ; 2015:537.
 333. Steelant B, Martens K, Boeckxstaens G, Seys SF, Hellings PW. TLR4 mediates epithelial barrier dysfunction by *Staphylococcus aureus* Enterotoxin B in CRSwNP. In: *Clinical and Translational Allergy*. Vol 7:3. Dusseldorf, Germany: BioMed Central; 2017:8.
 334. Tweten RK, Christianson KK, Iandolo JJ. Transport and processing of staphylococcal alpha-toxin. *J Bacteriol*. 1983;156(2):524-528.
 335. Sharma-Kuinkel BK, Wu Y, Tabor DE, et al. Characterization of Alpha-Toxin hla Gene Variants, Alpha-Toxin Expression Levels, and Levels of Antibody to Alpha-Toxin in Hemodialysis and Postsurgical Patients with *Staphylococcus aureus* Bacteremia. Diekema DJ, ed. *J Clin Microbiol*. 2015;53(1):227-236. doi:10.1128/JCM.02023-14
 336. Arvidson S, Tegmark K. Regulation of virulence determinants in *Staphylococcus aureus*. *Int J Med Microbiol*. 2001;291(2):159-170.
 337. Recsei P, Kreiswirth B, O'reilly M, Schlievert PM, Gruss A, Novick RP. Regulation of exoprotein gene expression in *Staphylococcus aureus* by agr. *Mol Gen Genet MGG*. 1986;202(1):58-61.
 338. Xiong YQ, Willard J, Yeaman MR, Cheung AL, Bayer AS. Regulation of *Staphylococcus aureus* α -Toxin Gene (hla) Expression by agr, sarA and sae In Vitro and in Experimental Infective Endocarditis. *J Infect Dis*. 2006;194(9):1267-1275.
 339. McNamara PJ, Milligan-Monroe KC, Khalili S, Proctor RA. Identification, cloning, and initial characterization of rot, a locus encoding a regulator of virulence factor expression in *Staphylococcus aureus*. *J Bacteriol*. 2000;182(11):3197-3203.
 340. Fairweather N, Kennedy S, Foster TJ, Kehoe M, Dougan G. Expression of a cloned *Staphylococcus aureus* alpha-hemolysin determinant in *Bacillus subtilis* and *Staphylococcus aureus*. *Infect Immun*. 1983;41(3):1112-1117.

341. Seeger W, Birkemeyer RG, Ermert L, Suttorp N, Bhakdi S, Duncker HR. Staphylococcal alpha-toxin-induced vascular leakage in isolated perfused rabbit lungs. *Lab Investig J Tech Methods Pathol.* 1990;63(3):341-349.
342. Walmrath D, Scharmman M, Konig R, Pilch J, Grimminger F, Seeger W. Staphylococcal alpha-toxin induced ventilation-perfusion mismatch in isolated blood-free perfused rabbit lungs. *J Appl Physiol.* 1993;74(4):1972-1980.
343. Suttorp N, Hessz T, Seeger W, et al. Bacterial exotoxins and endothelial permeability for water and albumin in vitro. *Am J Physiol-Cell Physiol.* 1988;255(3):C368-C376.
344. Brell B, Temmesfeld-Wollbruck B, Altschner I, et al. Adrenomedullin reduces Staphylococcus aureus alpha-toxin induced rat ileum microcirculatory damage. *Crit Care Med.* 2005;33(4):819-826. doi:10.1097/01.CCM.0000159194.53695.7A
345. Hocke AC, Temmesfeld-Wollbrueck B, Schmeck B, et al. Perturbation of endothelial junction proteins by Staphylococcus aureus α -toxin: inhibition of endothelial gap formation by adrenomedullin. *Histochem Cell Biol.* 2006;126(3):305-316. doi:10.1007/s00418-006-0174-5
346. Powers ME, Kim HK, Wang Y, Bubeck Wardenburg J. ADAM10 Mediates Vascular Injury Induced by Staphylococcus aureus -Hemolysin. *J Infect Dis.* 2012;206(3):352-356. doi:10.1093/infdis/jis192
347. Phillips JR, Tripp TJ, Regelman WE, Schlievert PM, Wangenstein OD. Staphylococcal α -toxin causes increased tracheal epithelial permeability. *Pediatr Pulmonol.* 2006;41(12):1146-1152. doi:10.1002/ppul.20501
348. Inoshima I, Inoshima N, Wilke GA, et al. A Staphylococcus aureus pore-forming toxin subverts the activity of ADAM10 to cause lethal infection in mice. *Nat Med.* 2011;17(10):1310-1314. doi:10.1038/nm.2451
349. Richter E, Harms M, Ventz K, et al. A Multi-Omics Approach Identifies Key Hubs Associated with Cell Type-Specific Responses of Airway Epithelial Cells to Staphylococcal Alpha-Toxin. Passaniti A, ed. *PLoS One.* 2015;10(3):e0122089. doi:10.1371/journal.pone.0122089
350. Huseby M, Shi K, Brown CK, et al. Structure and Biological Activities of Beta Toxin from Staphylococcus aureus. *J Bacteriol.* 2007;189(23):8719-8726. doi:10.1128/JB.00741-07
351. Cheung AL, Ying P. Regulation of alpha-and beta-hemolysins by the sar locus of Staphylococcus aureus. *J Bacteriol.* 1994;176(3):580-585.
352. Walev I, Weller U, Strauch S, Foster T, Bhakdi S. Selective Killing of Human Monocytes and Cytokine Release Provoked by Sphingomyelinase (Beta-Toxin) of. *Infect Immun.* 2018;64:6.
353. Huseby MJ, Kruse AC, Digre J, et al. Beta toxin catalyzes formation of nucleoprotein matrix in staphylococcal biofilms. *Proc Natl Acad Sci.* 2010;107(32):14407-14412. doi:10.1073/pnas.0911032107
354. Seop Kim C, Jeon S-Y, Min Y-G, et al. Effects of β -Toxin of Staphylococcus aureus on Ciliary Activity of Nasal Epithelial Cells. *The Laryngoscope.* 2000;110(12):2085-2088.

355. Verdon J, Girardin N, Lacombe C, Berjeaud J-M, Héchard Y. δ -hemolysin, an update on a membrane-interacting peptide. *Peptides*. 2009;30(4):817-823. doi:10.1016/j.peptides.2008.12.017
356. Otto M. Phenol-soluble modulins. *Int J Med Microbiol*. 2014;304(2):164-169. doi:10.1016/j.ijmm.2013.11.019
357. Joo H-S, Cheung GYC, Otto M. Antimicrobial Activity of Community-associated Methicillin-resistant *Staphylococcus aureus* Is Caused by Phenol-soluble Modulin Derivatives. *J Biol Chem*. 2011;286(11):8933-8940. doi:10.1074/jbc.M111.221382
358. Giese B, Glowinski F, Paprotka K, et al. Expression of δ -toxin by *Staphylococcus aureus* mediates escape from phago-endosomes of human epithelial and endothelial cells in the presence of β -toxin: Toxins mediating *S. aureus* phagosomal escape. *Cell Microbiol*. 2011;13(2):316-329. doi:10.1111/j.1462-5822.2010.01538.x
359. Grumann D, Nübel U, Bröker BM. *Staphylococcus aureus* toxins – Their functions and genetics. *Infect Genet Evol*. 2014;21:583-592. doi:10.1016/j.meegid.2013.03.013
360. Kaneko J, Kamio Y. Bacterial Two-component and Hetero-heptameric Pore-forming Cytolytic Toxins: Structures, Pore-forming Mechanism, and Organization of the Genes. *Biosci Biotechnol Biochem*. 2004;68(5):981-1003. doi:10.1271/bbb.68.981
361. von Eiff C, Friedrich AW, Peters G, Becker K. Prevalence of genes encoding for members of the staphylococcal leukotoxin family among clinical isolates of *Staphylococcus aureus*. *Diagn Microbiol Infect Dis*. 2004;49(3):157-162. doi:10.1016/j.diagmicrobio.2004.03.009
362. Pédelacq J-D, Maveyraud L, Prévost G, et al. The structure of a *Staphylococcus aureus* leucocidin component (LukF-PV) reveals the fold of the water-soluble species of a family of transmembrane pore-forming toxins. *Structure*. 1999;7(3):277-287.
363. Löffler B, Hussain M, Grundmeier M, et al. *Staphylococcus aureus* Panton-Valentine Leukocidin Is a Very Potent Cytotoxic Factor for Human Neutrophils. Cheung A, ed. *PLoS Pathog*. 2010;6(1):e1000715. doi:10.1371/journal.ppat.1000715
364. de Bentzmann S, Tristan A, Etienne J, Brousse N, Vandenesch F, Lina G. *Staphylococcus aureus* isolates associated with necrotizing pneumonia bind to basement membrane type I and IV collagens and laminin. *J Infect Dis*. 2004;190(8):1506-1515.
365. Diep BA, Chan L, Tattevin P, et al. Polymorphonuclear leukocytes mediate *Staphylococcus aureus* Panton-Valentine leukocidin-induced lung inflammation and injury. *Proc Natl Acad Sci*. 2010;107(12):5587-5592. doi:10.1073/pnas.0912403107
366. Wardenburg JB, Palazzolo-Ballance AM, Otto M, Schneewind O, DeLeo FR. Panton-Valentine Leukocidin Is Not a Virulence Determinant in Murine Models of Community-Associated Methicillin-Resistant *Staphylococcus aureus* Disease. *J Infect Dis*. 2008;198(8):1166-1170. doi:10.1086/592053

367. Mesrati I, Saïdani M, Ennigrou S, Zouari B, Ben Redjeb S. Clinical isolates of Panton–Valentine leucocidin- and γ -haemolysin-producing *Staphylococcus aureus*: prevalence and association with clinical infections. *J Hosp Infect.* 2010;75(4):265-268. doi:10.1016/j.jhin.2010.03.015
368. Cupane L, Pugacova N, Berzina D, Cauce V, Gardovska D, Miklaševics E. Patients with Panton-Valentine leukocidin positive *Staphylococcus aureus* infections run an increased risk of longer hospitalisation. *Int J Mol Epidemiol Genet.* 2012;3(1):48.
369. Hamilton SM, Bryant AE, Carroll KC, et al. In Vitro Production of Panton-Valentine Leukocidin among Strains of Methicillin-Resistant *Staphylococcus aureus* Causing Diverse Infections. *Clin Infect Dis.* 2007;45(12):1550-1558. doi:10.1086/523581
370. Alonzo F, Torres VJ. The Bicomponent Pore-Forming Leucocidins of *Staphylococcus aureus*. *Microbiol Mol Biol Rev.* 2014;78(2):199-230. doi:10.1128/MMBR.00055-13
371. Cooney J, Kienle Z, Foster TJ, O'toole PW. The gamma-hemolysin locus of *Staphylococcus aureus* comprises three linked genes, two of which are identical to the genes for the F and S components of leukocidin. *Infect Immun.* 1993;61(2):768–771.
372. Spaan AN, Vrieling M, Wallet P, et al. The staphylococcal toxins γ -haemolysin AB and CB differentially target phagocytes by employing specific chemokine receptors. *Nat Commun.* 2014;5:5438. doi:10.1038/ncomms6438
373. Malachowa N, Whitney AR, Kobayashi SD, et al. Global Changes in *Staphylococcus aureus* Gene Expression in Human Blood. Chakravorty D, ed. *PLoS One.* 2011;6(4):e18617. doi:10.1371/journal.pone.0018617
374. Siqueira JA, Speeg-Schatz C, Freitas FIS, Sahel J, Monteil H, Prevost G. Channel-forming leucotoxins from *Staphylococcus aureus* cause severe inflammatory reactions in a rabbit eye model. *J Med Microbiol.* 1997;46(6):486–494.
375. Supersac G, Piemont Y, Kubina M, Prevost G, Foster TJ. Assessment of the role of gamma-toxin in experimental endophthalmitis using a hlg-deficient mutant of *Staphylococcus aureus*. *Microb Pathog.* 1998;24(4):241-251.
376. Dajcs JJ, Thibodeaux BA, Girgis DO, O'Callaghan RJ. Corneal virulence of *Staphylococcus aureus* in an experimental model of keratitis. *DNA Cell Biol.* 2002;21(5-6):375–382.
377. Dajcs JJ, Austin MS, Sloop GD, et al. Corneal pathogenesis of *Staphylococcus aureus* strain Newman. *Invest Ophthalmol Vis Sci.* 2002;43(4):1109-1115.
378. Chobert JM, Sitohy MZ, Whitaker JR. Solubility and emulsifying properties of caseins modified enzymatically by *Staphylococcus aureus* V8 protease. *J Agric Food Chem.* 1988;36(1):220–224.
379. Shaw L. The role and regulation of the extracellular proteases of *Staphylococcus aureus*. *Microbiology.* 2004;150(1):217-228. doi:10.1099/mic.0.26634-0
380. Horsburgh MJ, Aish JL, White IJ, Shaw L, Lithgow JK, Foster SJ. B Modulates Virulence Determinant Expression and Stress Resistance: Characterization of a

- Functional rsbU Strain Derived from *Staphylococcus aureus* 8325-4. *J Bacteriol.* 2002;184(19):5457-5467. doi:10.1128/JB.184.19.5457-5467.2002
381. Rice K, Peralta R, Bast D, de Azavedo J, McGavin MJ. Description of *Staphylococcus* Serine Protease (ssp) Operon in *Staphylococcus aureus* and Nonpolar Inactivation of sspA-Encoded Serine Protease. *Infect Immun.* 2001;69(1):159-169. doi:10.1128/IAI.69.1.159-169.2001
382. Nickerson N, Ip J, Passos DT, McGavin MJ. Comparison of Staphopain A (ScpA) and B (SspB) precursor activation mechanisms reveals unique secretion kinetics of proSspB (Staphopain B), and a different interaction with its cognate Staphostatin, SspC. *Mol Microbiol.* 2010;75(1):161-177. doi:10.1111/j.1365-2958.2009.06974.x
383. Drapeau GR, Boily Y, Houmard J. Purification and properties of an extracellular protease of *Staphylococcus aureus*. *J Biol Chem.* 1972;247(20):6720-6726.
384. Loughran AJ, Atwood DN, Anthony AC, et al. Impact of individual extracellular proteases on *Staphylococcus aureus* biofilm formation in diverse clinical isolates and their isogenic sarA mutants. *MicrobiologyOpen.* 2014;3(6):897-909. doi:10.1002/mbo3.214
385. Baran K, Górka M, Potempa J, Porwit-Bóbr Z. Chemoattractant activity of *Staphylococcus aureus* serine proteinase modified human plasma α -1-proteinase inhibitor. *Antonie Van Leeuwenhoek.* 1989;56(4):361-365.
386. Prokešová L, Potužníková B, Potempa J, et al. Cleavage of human immunoglobulins by serine proteinase from *Staphylococcus aureus*. *Immunol Lett.* 1992;31(3):259-265.
387. McGavin MJ, Zahradka C, Rice K, Scott JE. Modification of the *Staphylococcus aureus* fibronectin binding phenotype by V8 protease. *Infect Immun.* 1997;65(7):2621-2628.
388. Rudack C, Sachse F, Albert N, Becker K, von Eiff C. Immunomodulation of Nasal Epithelial Cells by *Staphylococcus aureus*-Derived Serine Proteases. *J Immunol.* 2009;183(11):7592-7601. doi:10.4049/jimmunol.0803902
389. Sabat A, Kosowska K, Poulsen K, et al. Two Allelic Forms of the Aureolysin Gene (aur) within *Staphylococcus aureus*. *Infect Immun.* 2000;68(2):973-976. doi:10.1128/IAI.68.2.973-976.2000
390. Laarman AJ, Ruyken M, Malone CL, van Strijp JAG, Horswill AR, Rooijackers SHM. *Staphylococcus aureus* Metalloprotease Aureolysin Cleaves Complement C3 To Mediate Immune Evasion. *J Immunol.* 2011;186(11):6445-6453. doi:10.4049/jimmunol.1002948
391. Sieprawska-Lupa M, Mydel P, Krawczyk K, et al. Degradation of Human Antimicrobial Peptide LL-37 by *Staphylococcus aureus*-Derived Proteinases. *Antimicrob Agents Chemother.* 2004;48(12):4673-4679. doi:10.1128/AAC.48.12.4673-4679.2004
392. Cassat JE, Hammer ND, Campbell JP, et al. A Secreted Bacterial Protease Tailors the *Staphylococcus aureus* Virulence Repertoire to Modulate Bone Remodeling during Osteomyelitis. *Cell Host Microbe.* 2013;13(6):759-772. doi:10.1016/j.chom.2013.05.003

393. Gustafsson E, Oscarsson J. Maximal transcription of *aur* (aureolysin) and *sspA* (serine protease) in *Staphylococcus aureus* requires staphylococcal accessory regulator *R* (*sarR*) activity. *FEMS Microbiol Lett.* 2008;284(2):158-164. doi:10.1111/j.1574-6968.2008.01198.x
394. Reed SB, Wesson CA, Liou LE, et al. Molecular Characterization of a Novel *Staphylococcus aureus* Serine Protease Operon. *Infect Immun.* 2001;69(3):1521-1527. doi:10.1128/IAI.69.3.1521-1527.2001
395. Baba T, Bae T, Schneewind O, Takeuchi F, Hiramatsu K. Genome Sequence of *Staphylococcus aureus* Strain Newman and Comparative Analysis of Staphylococcal Genomes: Polymorphism and Evolution of Two Major Pathogenicity Islands. *J Bacteriol.* 2008;190(1):300-310. doi:10.1128/JB.01000-07
396. Dubin G, Stec-Niemczyk J, Kisielewska M, et al. Enzymatic Activity of the *Staphylococcus aureus* SplB Serine Protease is Induced by Substrates Containing the Sequence Trp-Glu-Leu-Gln. *J Mol Biol.* 2008;379(2):343-356. doi:10.1016/j.jmb.2008.03.059
397. Stec-Niemczyk J, Pustelny K, Kisielewska M, et al. Structural and functional characterization of SplA, an exclusively specific protease of *Staphylococcus aureus*. *Biochem J.* 2009;419(3):555. doi:10.1042/BJ20081351
398. Zdzalik M, Kalinska M, Wysocka M, et al. Biochemical and Structural Characterization of SplD Protease from *Staphylococcus aureus*. Khan AU, ed. *PLoS One.* 2013;8(10):e76812. doi:10.1371/journal.pone.0076812
399. Date SV, Modrusan Z, Lawrence M, et al. Global Gene Expression of Methicillin-resistant *Staphylococcus aureus* USA300 During Human and Mouse Infection. *J Infect Dis.* 2014;209(10):1542-1550. doi:10.1093/infdis/jit668
400. Holmes NE, Turnidge JD, Munckhof WJ, et al. Genetic and Molecular Predictors of High Vancomycin MIC in *Staphylococcus aureus* Bacteremia Isolates. *J Clin Microbiol.* 2014;52(9):3384-3393. doi:10.1128/JCM.01320-14
401. Zdzalik M, Karim AY, Wolski K, et al. Prevalence of genes encoding extracellular proteases in *Staphylococcus aureus* - important targets triggering immune response in vivo. *FEMS Immunol Med Microbiol.* 2012;66(2):220-229. doi:10.1111/j.1574-695X.2012.01005.x
402. Paharik AE, Salgado-Pabon W, Meyerholz DK, White MJ, Schlievert PM, Horswill AR. The Spl Serine Proteases Modulate *Staphylococcus aureus* Protein Production and Virulence in a Rabbit Model of Pneumonia. D'Orazio SEF, ed. *mSphere.* 2016;1(5):e00208-16. doi:10.1128/mSphere.00208-16
403. Stentzel S, Teufelberger A, Nordengrün M, et al. Staphylococcal serine protease-like proteins are pacemakers of allergic airway reactions to *Staphylococcus aureus*. *J Allergy Clin Immunol.* May 2016. doi:10.1016/j.jaci.2016.03.045
404. Hofmann B, Schomburg D, Hecht HJ. Crystal structure of a thiol proteinase from *Staphylococcus aureus* V-8 in the E-64 inhibitor complex. *Acta Crystallogr.* 1993;49(Suppl):102.
405. Filipek R. The Staphostatin-Staphopain Complex: A FORWARD BINDING INHIBITOR IN COMPLEX WITH ITS TARGET CYSTEINE PROTEASE. *J Biol Chem.* 2003;278(42):40959-40966. doi:10.1074/jbc.M302926200

406. Rzychon M, Sabat A, Kosowska K, Potempa J, Dubin A. Staphostatins: an expanding new group of proteinase inhibitors with a unique specificity for the regulation of staphopains, *Staphylococcus* spp. cysteine proteinases: Staphostatins - *S. aureus* cysteine proteinase inhibitors. *Mol Microbiol.* 2003;49(4):1051-1066. doi:10.1046/j.1365-2958.2003.03613.x
407. Dubin G. Defense against own arms: staphylococcal cysteine proteases and their inhibitors. *Acta Biochim Pol.* 2003;50:715–724.
408. Potempa J, Dubin A, Korzus G, Travis J. Degradation of elastin by a cysteine proteinase from *Staphylococcus aureus*. *J Biol Chem.* 1988;263(6):2664–2667.
409. Potempa J, Watorek W, Travis J. The inactivation of human plasma alpha 1-proteinase inhibitor by proteinases from *Staphylococcus aureus*. *J Biol Chem.* 1986;261(30):14330-14334.
410. Potempa J, Fedak D, Dubin A, Mast A, Travis J. Proteolytic inactivation of alpha-1-anti-chymotrypsin. Sites of cleavage and generation of chemotactic activity. *J Biol Chem.* 1991;266(32):21482-21487.
411. Benkerroum N. Staphylococcal enterotoxins and enterotoxin-like toxins with special reference to dairy products: An overview. *Crit Rev Food Sci Nutr.* June 2017;1-28. doi:10.1080/10408398.2017.1289149
412. Van Zele T, Gevaert P, Watelet J-B, et al. *Staphylococcus aureus* colonization and IgE antibody formation to enterotoxins is increased in nasal polyposis. *J Allergy Clin Immunol.* 2004;114(4):981-983. doi:10.1016/j.jaci.2004.07.013
413. Cheng K-J, Wang S-Q, Xu Y-Y. Different roles of *Staphylococcus aureus* enterotoxin in different subtypes of nasal polyps. *Exp Ther Med.* 2017;13(1):321-326. doi:10.3892/etm.2016.3951
414. Cheng K-J, Xu Y-Y, Zhou M-L, Zhou S-H, Wang S-Q. Role of local allergic inflammation and *Staphylococcus aureus* enterotoxins in Chinese patients with chronic rhinosinusitis with nasal polyps. *J Laryngol Otol.* 2017;131(08):707-713. doi:10.1017/S0022215117001335
415. Ginsburg I. Role of lipoteichoic acid in infection and inflammation. *Lancet Infect Dis.* 2002;2(3):171-179.
416. Boveri M, Kinsner A, Berezowski V, et al. Highly purified lipoteichoic acid from gram-positive bacteria induces in vitro blood–brain barrier disruption through glia activation: Role of pro-inflammatory cytokines and nitric oxide. *Neuroscience.* 2006;137(4):1193-1209. doi:10.1016/j.neuroscience.2005.10.011
417. Sheen TR, Ebrahimi CM, Hiemstra IH, Barlow SB, Peschel A, Doran KS. Penetration of the blood–brain barrier by *Staphylococcus aureus*: contribution of membrane-anchored lipoteichoic acid. *J Mol Med.* 2010;88(6):633–639. doi:10.1007/s00109-010-0630-5
418. Peschel A, Otto M, Jack RW, Kalbacher H, Jung G, Götz F. Inactivation of the *dlt* Operon in *Staphylococcus aureus* Confers Sensitivity to Defensins, Protegrins, and Other Antimicrobial Peptides. *J Biol Chem.* 1999;274(13):8405-8410. doi:10.1074/jbc.274.13.8405
419. Weidenmaier C, Kokai-Kun JF, Kristian SA, et al. Role of teichoic acids in *Staphylococcus aureus* nasal colonization, a major risk factor in nosocomial infections. *Nat Med.* 2004;10(3):243-245. doi:10.1038/nm991

420. Patou J, Gevaert P, Van Zele T, Holtappels G, van Cauwenberge P, Bachert C. Staphylococcus aureus enterotoxin B, protein A, and lipoteichoic acid stimulations in nasal polyps. *J Allergy Clin Immunol.* 2008;121(1):110-115. doi:10.1016/j.jaci.2007.08.059
421. Brown L, Wolf JM, Prados-Rosales R, Casadevall A. Through the wall: extracellular vesicles in Gram-positive bacteria, mycobacteria and fungi. *Nat Rev Microbiol.* 2015;13(10):620-630. doi:10.1038/nrmicro3480
422. György B, Szabó TG, Pásztói M, et al. Membrane vesicles, current state-of-the-art: emerging role of extracellular vesicles. *Cell Mol Life Sci.* 2011;68(16):2667-2688. doi:10.1007/s00018-011-0689-3
423. Lee E-Y, Choi D-Y, Kim D-K, et al. Gram-positive bacteria produce membrane vesicles: Proteomics-based characterization of Staphylococcus aureus-derived membrane vesicles. *PROTEOMICS.* 2009;9(24):5425-5436. doi:10.1002/pmic.200900338
424. Gurung M, Moon DC, Choi CW, et al. Staphylococcus aureus Produces Membrane-Derived Vesicles That Induce Host Cell Death. Bereswill S, ed. *PLoS One.* 2011;6(11):e27958. doi:10.1371/journal.pone.0027958
425. Thay B, Wai SN, Oscarsson J. Staphylococcus aureus α -Toxin-Dependent Induction of Host Cell Death by Membrane-Derived Vesicles. Otto M, ed. *PLoS One.* 2013;8(1):e54661. doi:10.1371/journal.pone.0054661
426. Kim M-R, Hong S-W, Choi E-B, et al. Staphylococcus aureus -derived extracellular vesicles induce neutrophilic pulmonary inflammation via both Th1 and Th17 cell responses. *Allergy.* 2012;67(10):1271-1281. doi:10.1111/all.12001
427. Elmi A, Nasher F, Jagatia H, et al. Campylobacter jejuni outer membrane vesicle-associated proteolytic activity promotes bacterial invasion by mediating cleavage of intestinal epithelial cell E-cadherin and occludin: Campylobacter jejuni OMV-associated proteolytic activity. *Cell Microbiol.* 2016;18(4):561-572. doi:10.1111/cmi.12534
428. Chi B, Qi M, Kuramitsu HK. Role of dentilisin in Treponema denticola epithelial cell layer penetration. *Res Microbiol.* 2003;154(9):637-643. doi:10.1016/j.resmic.2003.08.001
429. Nakao R, Takashiba S, Kosono S, et al. Effect of Porphyromonas gingivalis outer membrane vesicles on gingipain-mediated detachment of cultured oral epithelial cells and immune responses. *Microbes Infect.* 2014;16(1):6-16. doi:10.1016/j.micinf.2013.10.005
430. Choi E-B, Hong S-W, Kim D-K, et al. Decreased diversity of nasal microbiota and their secreted extracellular vesicles in patients with chronic rhinosinusitis based on a metagenomic analysis. *Allergy.* 2014;69(4):517-526. doi:10.1111/all.12374
431. Maret W, Li Y. Coordination Dynamics of Zinc in Proteins. *Chem Rev.* 2009;109(10):4682-4707. doi:10.1021/cr800556u
432. Bonaventura P, Benedetti G, Albarède F, Miossec P. Zinc and its role in immunity and inflammation. *Autoimmun Rev.* 2015;14(4):277-285. doi:10.1016/j.autrev.2014.11.008

433. Bao S. Zinc modulates airway epithelium susceptibility to death receptor-mediated apoptosis. *AJP Lung Cell Mol Physiol*. 2005;290(3):L433-L441. doi:10.1152/ajplung.00341.2005
434. Zalewski PD, Truong-Tran AQ, Grosser D, Jayaram L, Murgia C, Ruffin RE. Zinc metabolism in airway epithelium and airway inflammation: basic mechanisms and clinical targets. A review. *Pharmacol Ther*. 2005;105(2):127-149. doi:10.1016/j.pharmthera.2004.09.004
435. Önerci M, Kus S. Trace elements in chronic sinusitis. *Eur Arch Otorhinolaryngol*. 1995;252(6):374-375.
436. Ünal M, Tamer L, Pata YS, et al. Serum levels of antioxidant vitamins, copper, zinc and magnesium in children with chronic rhinosinusitis. *J Trace Elem Med Biol*. 2004;18(2):189-192. doi:10.1016/j.jtemb.2004.07.005
437. Alves CX, Brito NJN de, Vermeulen KM, et al. Serum zinc reference intervals and its relationship with dietary, functional, and biochemical indicators in 6- to 9-year-old healthy children. *Food Nutr Res*. 2016;60(1):30157. doi:10.3402/fnr.v60.30157
438. Rostkowska-Nadolska B, Borawska M, Hukalowicz K. Trace elements in nasal polyps. *Biol Trace Elem Res*. 2005;106(2):117-121.
439. Okur E, Gul A, Kilinc M, et al. Trace elements in nasal polyps. *Eur Arch Otorhinolaryngol*. 2013;270(8):2245-2248.
440. Fukai T, Ushio-Fukai M. Superoxide Dismutases: Role in Redox Signaling, Vascular Function, and Diseases. *Antioxid Redox Signal*. 2011;15(6):1583-1606. doi:10.1089/ars.2011.3999
441. Çekin E, Ipcioglu O, Erkul B, et al. The Association of Oxidative Stress and Nasal Polyposis. *J Int Med Res*. 2009;37(2):325-330. doi:10.1177/147323000903700206
442. Kambe T, Hashimoto A, Fujimoto S. Current understanding of ZIP and ZnT zinc transporters in human health and diseases. *Cell Mol Life Sci*. 2014;71(17):3281-3295. doi:10.1007/s00018-014-1617-0
443. Kambe T, Tsuji T, Hashimoto A, Itsumura N. The Physiological, Biochemical, and Molecular Roles of Zinc Transporters in Zinc Homeostasis and Metabolism. *Physiol Rev*. 2015;95(3):749-784. doi:10.1152/physrev.00035.2014
444. Coyle P, Philcox JC, Carey LC, Rofe AM. Metallothionein: the multipurpose protein. *Cell Mol Life Sci CmLS*. 2002;59(4):627-647.
445. Ruttkay-Nedecky B, Nejdil L, Gumulec J, et al. The Role of Metallothionein in Oxidative Stress. *Int J Mol Sci*. 2013;14(3):6044-6066. doi:10.3390/ijms14036044
446. Dutsch-Wicherek M, Tomaszewska R, Lazar A, et al. The evaluation of metallothionein expression in nasal polyps with respect to immune cell presence and activity. *BMC Immunol*. 2010;11(1):10.
447. Dziegiel P, Pula B, Kobierzycki C, Stasiolek M, Podhorska-Okolow M. Metallothionein-3. In: *Metallothioneins in Normal and Cancer Cells*. Springer; 2016:21-27.

448. You HJ, Lee KJ, Jeong HG. Overexpression of human metallothionein-III prevents hydrogen peroxide-induced oxidative stress in human fibroblasts. *FEBS Lett.* 2002;521(1-3):175-179.
449. Lee S-J, Koh J-Y. Roles of zinc and metallothionein-3 in oxidative stress-induced lysosomal dysfunction, cell death, and autophagy in neurons and astrocytes. *Mol Brain.* 2010;3:30-30. doi:10.1186/1756-6606-3-30
450. Zhang Z, Adappa ND, Doghramji LJ, Chiu AG, Cohen NA, Palmer JN. Different clinical factors associated with *Staphylococcus aureus* and *Pseudomonas aeruginosa* in chronic rhinosinusitis: *S. aureus* and *P. aeruginosa* in CRS. *Int Forum Allergy Rhinol.* 2015;5(8):724-733. doi:10.1002/alr.21532
451. Seiberling KA, Grammer L, Kern RC. Chronic Rhinosinusitis and Superantigens. *Otolaryngol Clin North Am.* 2005;38(6):1215-1236. doi:10.1016/j.otc.2005.08.006
452. Kojima T, Go M, Takano K, et al. Regulation of Tight Junctions in Upper Airway Epithelium. *BioMed Res Int.* 2013;2013:1-11. doi:10.1155/2013/947072
453. Sawada N. Tight junction-related human diseases: Tight junction-related human diseases. *Pathol Int.* 2013;63(1):1-12. doi:10.1111/pin.12021
454. Wise SK, Laury AM, Katz EH, Den Beste KA, Parkos CA, Nusrat A. Interleukin-4 and interleukin-13 compromise the sinonasal epithelial barrier and perturb intercellular junction protein expression: IL-4 and IL-13 Effect on Sinus Epithelial Barrier. *Int Forum Allergy Rhinol.* February 2014:n/a-n/a. doi:10.1002/alr.21298
455. Yang P-C, Wang C-S, An Z-Y. A murine model of ulcerative colitis: induced with sinusitis-derived superantigen and food allergen. *BMC Gastroenterol.* 2005;5(1). doi:10.1186/1471-230X-5-6
456. Huvenne W, Hellings PW, Bachert C. Role of Staphylococcal Superantigens in Airway Disease. *Int Arch Allergy Immunol.* 2013;161(4):304-314. doi:10.1159/000350329
457. Lin H, Li H, Cho H-J, et al. Air-liquid interface (ALI) culture of human bronchial epithelial cell monolayers as an in-vitro model for airway drug transport studies. *J Pharm Sci.* 2007;96(2):341-350. doi:10.1002/jps.20803
458. Otto M. *Staphylococcus aureus* toxins. *Curr Opin Microbiol.* 2014;17:32-37. doi:10.1016/j.mib.2013.11.004
459. Bhakdi S, Tranum-Jensen J. Alpha-toxin of *Staphylococcus aureus*. *Microbiol Rev.* 1991;55(4):733-751.
460. Hermann I, R ath S, Ziesemer S, et al. *Staphylococcus aureus* Hemolysin A Disrupts Cell-Matrix Adhesions in Human Airway Epithelial Cells. *Am J Respir Cell Mol Biol.* 2014;52(1):14-24. doi:10.1165/rcmb.2014-0082OC
461. Gierok P, Harms M, Richter E, et al. *Staphylococcus aureus* Alpha-Toxin Mediates General and Cell Type-Specific Changes in Metabolite Concentrations of Immortalized Human Airway Epithelial Cells. Otto M, ed. *PLoS One.* 2014;9(4):e94818. doi:10.1371/journal.pone.0094818
462. Ou J, Wang J, Xu Y, et al. *Staphylococcus aureus* superantigens are associated with chronic rhinosinusitis with nasal polyps: a meta-analysis. *Eur Arch Otorhinolaryngol.* 2014;271(10):2729-2736. doi:10.1007/s00405-014-2955-0

463. Shupp JW. Identification of a Transcytosis Epitope on Staphylococcal Enterotoxins. *Infect Immun.* 2002;70(4):2178-2186. doi:10.1128/IAI.70.4.2178-2186.2002
464. Edwards LA, O'Neill C, Furman MA, et al. Enterotoxin-producing staphylococci cause intestinal inflammation by a combination of direct epithelial cytopathy and superantigen-mediated T-cell activation. *Inflamm Bowel Dis.* 2011;18(4):624-640.
465. Lu D, Wörmann ME, Zhang X, Schneewind O, Gründling A, Freemont PS. Structure-based mechanism of lipoteichoic acid synthesis by *Staphylococcus aureus* LtaS. *Proc Natl Acad Sci.* 2009;106(5):1584-1589.
466. Kang S-S, Sim J-R, Yun C-H, Han SH. Lipoteichoic acids as a major virulence factor causing inflammatory responses via Toll-like receptor 2. *Arch Pharm Res.* 2016;39(11):1519-1529. doi:10.1007/s12272-016-0804-y
467. Cheung AL, Projan SJ. Cloning and sequencing of sarA of *Staphylococcus aureus*, a gene required for the expression of agr. *J Bacteriol.* 1994;176(13):4168-4172.
468. Reyes D, Andrey DO, Monod A, Kelley WL, Zhang G, Cheung AL. Coordinated Regulation by AgrA, SarA, and SarR To Control agr Expression in *Staphylococcus aureus*. *J Bacteriol.* 2011;193(21):6020-6031. doi:10.1128/JB.05436-11
469. Ziebandt A-K, Becher D, Ohlsen K, Hacker J, Hecker M, Engelmann S. The influence of agr and σ_B in growth phase dependent regulation of virulence factors in *Staphylococcus aureus*. *PROTEOMICS.* 2004;4(10):3034-3047. doi:10.1002/pmic.200400937
470. Fu Y, Zhou E, Liu Z, et al. *Staphylococcus aureus* and *Escherichia coli* elicit different innate immune responses from bovine mammary epithelial cells. *Vet Immunol Immunopathol.* 2013;155(4):245-252. doi:10.1016/j.vetimm.2013.08.003
471. Lacey KA, Leech JM, Lalor SJ, McCormack N, Geoghegan JA, McLoughlin RM. The *Staphylococcus aureus* Cell Wall-Anchored Protein Clumping Factor A Is an Important T Cell Antigen. *Infect Immun.* 2017;85(12). doi:10.1128/IAI.00549-17
472. Schwabe M, Notermans S, Boot R, Tatini SR, Krämer J. Inactivation of staphylococcal enterotoxins by heat and reactivation by high pH treatment. *Int J Food Microbiol.* 1990;10(1):33-42.
473. Fung DY, Steinberg DH, Miller RD, Kurantnick MJ, Murphy TF. Thermal inactivation of staphylococcal enterotoxins B and C. *Appl Microbiol.* 1973;26(6):938-942.
474. Momen-Heravi F, Balaj L, Alian S, et al. Current methods for the isolation of extracellular vesicles. *Biol Chem.* 2013;394(10). doi:10.1515/hsz-2013-0141
475. Witwer KW, Buzás EI, Bemis LT, et al. Standardization of sample collection, isolation and analysis methods in extracellular vesicle research. *J Extracell Vesicles.* 2013;2(1):20360. doi:10.3402/jev.v2i0.20360
476. Hong S-W, Kim M-R, Lee E-Y, et al. Extracellular vesicles derived from *Staphylococcus aureus* induce atopic dermatitis-like skin inflammation: S.

- aureus EV in atopic dermatitis. *Allergy*. 2011;66(3):351-359. doi:10.1111/j.1398-9995.2010.02483.x
477. Lee J, Lee E-Y, Kim S-H, et al. Staphylococcus aureus Extracellular Vesicles Carry Biologically Active β -Lactamase. *Antimicrob Agents Chemother*. 2013;57(6):2589-2595. doi:10.1128/AAC.00522-12
 478. Hong S-W, Choi E-B, Min T-K, et al. An Important Role of α -Hemolysin in Extracellular Vesicles on the Development of Atopic Dermatitis Induced by Staphylococcus aureus. *Horsburgh MJ, ed. PLoS One*. 2014;9(7):e100499. doi:10.1371/journal.pone.0100499
 479. Ishihama Y, Oda Y, Tabata T, et al. Exponentially Modified Protein Abundance Index (emPAI) for Estimation of Absolute Protein Amount in Proteomics by the Number of Sequenced Peptides per Protein. *Mol Cell Proteomics*. 2005;4(9):1265-1272. doi:10.1074/mcp.M500061-MCP200
 480. Sousa S, Lecuit M, Cossart P. Microbial strategies to target, cross or disrupt epithelia. *Curr Opin Cell Biol*. 2005;17(5):489-498. doi:10.1016/j.ceb.2005.08.013
 481. Feazel LM, Robertson CE, Ramakrishnan VR, Frank DN. Microbiome complexity and Staphylococcus aureus in chronic rhinosinusitis. *The Laryngoscope*. 2012;122(2):467-472. doi:10.1002/lary.22398
 482. Jervis-Bardy J, Wormald P-J. Microbiological outcomes following mupirocin nasal washes for symptomatic, Staphylococcus aureus-positive chronic rhinosinusitis following endoscopic sinus surgery. *Int Forum Allergy Rhinol*. 2012;2(2):111-115. doi:10.1002/alr.20106
 483. Kolar SL, Antonio Ibarra J, Rivera FE, et al. Extracellular proteases are key mediators of Staphylococcus aureus virulence via the global modulation of virulence-determinant stability. *MicrobiologyOpen*. 2013;2(1):18-34. doi:10.1002/mbo3.55
 484. Dubin G. Extracellular proteases of Staphylococcus spp. *Biol Chem*. 2002;383(7-8):1075-1086.
 485. Nishifuji K, Sugai M, Amagai M. Staphylococcal exfoliative toxins: "Molecular scissors" of bacteria that attack the cutaneous defense barrier in mammals. *J Dermatol Sci*. 2008;49(1):21-31. doi:10.1016/j.jdermsci.2007.05.007
 486. Cantero D, Cooksley C, Jardeleza C, et al. A human nasal explant model to study Staphylococcus aureus biofilm in vitro. *Int Forum Allergy Rhinol*. 2013;3(7):556-562. doi:10.1002/alr.21146
 487. Arvidson S, Holme T, Lindholm B. Studies on extracellular proteolytic enzymes from Staphylococcus aureus: I. Purification and characterization of one neutral and one alkaline protease. *Biochim Biophys Acta BBA-Enzymol*. 1973;302(1):135-148.
 488. Arvidson S. Studies on extracellular proteolytic enzymes from Staphylococcus aureus: II. Isolation and characterization of an EDTA-sensitive protease. *Biochim Biophys Acta BBA-Enzymol*. 1973;302(1):149-157.
 489. Sabat AJ, Wladyka B, Kosowska-Shick K, et al. Polymorphism, genetic exchange and intragenic recombination of the aureolysin gene among

- Staphylococcus aureus strains. *BMC Microbiol.* 2008;8(1):129. doi:10.1186/1471-2180-8-129
490. Vath GM, Earhart CA, Rago JV, et al. The structure of the superantigen exfoliative toxin A suggests a novel regulation as a serine protease. *Biochemistry (Mosc).* 1997;36(7):1559-1566.
491. Cavarelli J, Prévost G, Bourguet W, et al. The structure of *Staphylococcus aureus* epidermolytic toxin A, an atypic serine protease, at 1.7 Å resolution. *Structure.* 1997;5(6):813-824.
492. Popowicz GM, Dubin G, Stec-Niemczyk J, et al. Functional and Structural Characterization of Spl Proteases from *Staphylococcus aureus*. *J Mol Biol.* 2006;358(1):270-279. doi:10.1016/j.jmb.2006.01.098
493. Önerci TM. *Nasal Physiology and Pathophysiology of Nasal Disorders.* Springer; 2013.
494. Ramanathanjr M, Lane A. Innate immunity of the sinonasal cavity and its role in chronic rhinosinusitis. *Otolaryngol Head Neck Surg.* 2007;136(3):348-356. doi:10.1016/j.otohns.2006.11.011
495. Shikani AH, Sidhaye VK, Basaraba RJ, et al. Mucosal expression of aquaporin 5 and epithelial barrier proteins in chronic rhinosinusitis with and without nasal polyps. *Am J Otolaryngol.* December 2013. doi:10.1016/j.amjoto.2013.11.011
496. Runswick S, Mitchell T, Davies P, Robinson C, Garrod DR. Pollen proteolytic enzymes degrade tight junctions. *Respirology.* 2007;12(6):834-842. doi:10.1111/j.1440-1843.2007.01175.x
497. Rejman J, Di Gioia S, Bragonzi A, Conese M. *Pseudomonas aeruginosa* Infection Destroys the Barrier Function of Lung Epithelium and Enhances Polyplex-Mediated Transfection. *Hum Gene Ther.* 2007;18(7):642-652. doi:10.1089/hum.2006.192
498. Wan H, Winton HL, Soeller C, et al. Der p 1 facilitates transepithelial allergen delivery by disruption of tight junctions. *J Clin Invest.* 1999;104(1):123-133.
499. Wan H, Winton HL, Soeller C, et al. The transmembrane protein occludin of epithelial tight junctions is a functional target for serine peptidases from faecal pellets of *Dermatophagoides pteronyssinus*. *Clin Exp Allergy.* 2001;31(2):279-294.
500. Wan H, Winton HL, Soeller C, et al. Quantitative structural and biochemical analyses of tight junction dynamics following exposure of epithelial cells to house dust mite allergen Der p 1. *Clin Exp Allergy.* 2000;30(5):685-698.
501. Sørensen SB, Sørensen TL, Breddam K. Fragmentation of proteins by *S. aureus* strain V8 protease. *FEBS Lett.* 1991;294(3):195-197.
502. The UniProt Consortium. UniProt: a hub for protein information. *Nucleic Acids Res.* 2015;43(D1):D204-D212. doi:10.1093/nar/gku989
503. Scheller J, Chalaris A, Schmidt-Arras D, Rose-John S. The pro- and anti-inflammatory properties of the cytokine interleukin-6. *Biochim Biophys Acta BBA - Mol Cell Res.* 2011;1813(5):878-888. doi:10.1016/j.bbamcr.2011.01.034
504. Dienz O, Rud JG, Eaton SM, et al. Essential role of IL-6 in protection against H1N1 influenza virus by promoting neutrophil survival in the lung. *Mucosal Immunol.* 2012;5(3):258-266. doi:10.1038/mi.2012.2

505. Dann SM, Spehlmann ME, Hammond DC, et al. IL-6-Dependent Mucosal Protection Prevents Establishment of a Microbial Niche for Attaching/Effacing Lesion-Forming Enteric Bacterial Pathogens. *J Immunol*. 2008;180(10):6816-6826. doi:10.4049/jimmunol.180.10.6816
506. Ramsay AJ, Husband AJ, Ramshaw IA, et al. The role of interleukin-6 in mucosal IgA antibody responses in vivo. *Science*. 1994;264(5158):561-563.
507. Jusko M, Potempa J, Kantyka T, et al. Staphylococcal Proteases Aid in Evasion of the Human Complement System. *J Innate Immun*. 2014;6(1):31-46. doi:10.1159/000351458
508. Prasad AS. Effects of zinc deficiency on Th1 and Th2 cytokine shifts. *J Infect Dis*. 2000;182(Supplement 1):S62-S68.
509. Lansdown ABG, Mirastschijski U, Stubbs N, Scanlon E, Ågren MS. Zinc in wound healing: Theoretical, experimental, and clinical aspects. *Wound Repair Regen*. 2007;15(1):2-16. doi:10.1111/j.1524-475X.2006.00179.x
510. Turner JR. Intestinal mucosal barrier function in health and disease. *Nat Rev Immunol*. 2009;9(11):799-809. doi:10.1038/nri2653
511. Hopkins C, Gillett S, Slack R, Lund VJ, Browne JP. Psychometric validity of the 22-item Sinonasal Outcome Test. *Clin Otolaryngol*. 2009;34(5):447-454.
512. Truong-Tran AQ, Grosser D, Ruffin RE, Murgia C, Zalewski PD. Apoptosis in the normal and inflamed airway epithelium: role of zinc in epithelial protection and procaspase-3 regulation. *Biochem Pharmacol*. 2003;66(8):1459-1468. doi:10.1016/S0006-2952(03)00498-2
513. Murgia C, Grosser D, Truong-Tran AQ, et al. Apical Localization of Zinc Transporter ZnT4 in Human Airway Epithelial Cells and Its Loss in a Murine Model of Allergic Airway Inflammation. *Nutrients*. 2011;3(12):910-928. doi:10.3390/nu3110910
514. Skrovanek S. Zinc and gastrointestinal disease. *World J Gastrointest Pathophysiol*. 2014;5(4):496. doi:10.4291/wjgp.v5.i4.496
515. Roselli M, Finamore A, Garaguso I, Britti MS, Mengheri E. Zinc oxide protects cultured enterocytes from the damage induced by *Escherichia coli*. *J Nutr*. 2003;133(12):4077-4082.
516. Bao B, Prasad AS, Beck FWJ, Godmere M. Zinc modulates mRNA levels of cytokines. *Am J Physiol - Endocrinol Metab*. 2003;285(5):E1095-E1102. doi:10.1152/ajpendo.00545.2002
517. Cheng N-L. The Effect of Zinc on Cytokine Release and Signal Transduction in Airway Epithelial Cells (Doctoral Thesis). The University of Alabama at Birmingham. Alabama. 2009.
518. Lang C, Murgia C, Leong M, et al. Anti-inflammatory effects of zinc and alterations in zinc transporter mRNA in mouse models of allergic inflammation. *AJP Lung Cell Mol Physiol*. 2006;292(2):L577-L584. doi:10.1152/ajplung.00280.2006
519. Eide DJ. The zip family of zinc transporters. In: *Zinc Finger Proteins*. Springer; 2005:261-264.

520. Jenkitkasemwong S, Wang C-Y, Mackenzie B, Knutson MD. Physiologic implications of metal-ion transport by ZIP14 and ZIP8. *BioMetals*. 2012;25(4):643-655. doi:10.1007/s10534-012-9526-x
521. Murgia C, Lang CJ, Truong-Tran AQ, et al. Zinc and its specific transporters as potential targets in airway disease. *Curr Drug Targets*. 2006;7(5):607-627.
522. Thirumoorthy N, Sunder AS, Kumar KM, Ganesh GNK, Chatterjee M, others. A review of metallothionein isoforms and their role in pathophysiology. *World J Surg Oncol*. 2011;9(1):1.
523. Sewell AK, Jensen LT, Erickson JC, Palmiter RD, Winge DR. Bioactivity of Metallothionein-3 Correlates with Its Novel. beta. Domain Sequence Rather Than Metal Binding Properties. *Biochemistry (Mosc)*. 1995;34(14):4740-4747.
524. Wood AJ, Fraser JD, Swift S, Patterson-Emanuelson EA, Amirapu S, Douglas RG. Intramucosal bacterial microcolonies exist in chronic rhinosinusitis without inducing a local immune response. *Am J Rhinol Allergy*. 2012;26(4):265-270.
525. Komisar JL, Small-Harris S, Tseng J. Localization of binding sites of staphylococcal enterotoxin B (SEB), a superantigen, for HLA-DR by inhibition with synthetic peptides of SEB. *Infect Immun*. 1994;62(11):4775-4780.
526. Balaban N, Rasooly A. Staphylococcal enterotoxins. *Int J Food Microbiol*. 2000;61(1):1-10.
527. Thelestam M. Membrane damage by staphylococcal α -toxin to different types of cultured mammalian cell. *Biochim Biophys Acta BBA-Mol Cell Res*. 1983;762(4):481-488.
528. Wilke GA, Wardenburg JB. Role of a disintegrin and metalloprotease 10 in *Staphylococcus aureus* -hemolysin-mediated cellular injury. *Proc Natl Acad Sci*. 2010;107(30):13473-13478. doi:10.1073/pnas.1001815107
529. Van Crombruggen K, Holtappels G, De Ruyck N, Derycke L, Tomassen P, Bachert C. RAGE processing in chronic airway conditions: Involvement of *Staphylococcus aureus* and ECP. *J Allergy Clin Immunol*. 2012;129(6):1515-1521.e8. doi:10.1016/j.jaci.2012.02.021
530. Jeppesen DK, Hvam ML, Primdahl-Bengtson B, et al. Comparative analysis of discrete exosome fractions obtained by differential centrifugation. *J Extracell Vesicles*. 2014;3(0). doi:10.3402/jev.v3.25011
531. Klimentová J, Stulík J. Methods of isolation and purification of outer membrane vesicles from gram-negative bacteria. *Microbiol Res*. 2015;170:1-9. doi:10.1016/j.micres.2014.09.006
532. Maune S, Rath NF, Gorogh T, Steinert R. [Genetic disposition to chronic polypoid sinusitis and alpha 1-proteinase inhibitor deficiency types]. *HNO*. 1995;43(9):537-539.
533. Portenko GM. Alpha 1-antitrypsin phenotypes in healthy persons and patients with polypous rhinosinusitis. *Vestn Otorinolaringol*. 1989;(3):24.
534. Kilty SJ, Bossé Y, Cormier C, Endam LM, Desrosiers MY. Polymorphisms in the SERPINA1 (Alpha-1-Antitrypsin) gene are associated with severe chronic rhinosinusitis unresponsive to medical therapy. *Am J Rhinol Allergy*. 2010;24(1):4-9. doi:10.2500/ajra.2010.24.3429

535. Calander A-M, Dubin G, Potempa J, Tarkowski A. Staphylococcus aureus infection triggers production of neutralizing, V8 protease-specific antibodies. *Pathog Dis.* 2008;52(2):267-272.
536. Holtfreter S, Nguyen TTH, Wertheim H, et al. Human Immune Proteome in Experimental Colonization with Staphylococcus aureus. *Clin Vaccine Immunol.* 2009;16(11):1607-1614. doi:10.1128/CVI.00263-09
537. Proctor RA, Mosher DF, Olbrantz PJ. Fibronectin binding to Staphylococcus aureus. *J Biol Chem.* 1982;257(24):14788-14794.
538. Drapeau GR. [38] Protease from Staphylococcus aureus. In: *Methods in Enzymology.* Vol 45. Elsevier; 1976:469-475.
539. Balaban NP, Mardanov AM, Sharipova MR, et al. Isolation and characterization of glutamyl endopeptidase 2 from Bacillus intermedius 3-19. *Biochem Mosc.* 2003;68(11):1217-1224.
540. Grim KP, San Francisco B, Radin JN, et al. The Metallophore Staphylopine Enables Staphylococcus aureus To Compete with the Host for Zinc and Overcome Nutritional Immunity. Torres VJ, ed. *mBio.* 2017;8(5):e01281-17. doi:10.1128/mBio.01281-17